

Bangor University

DOCTOR OF PHILOSOPHY

Cobalt(III), Copper(II), and Nickel(II) coordination compounds as cations in Polyborate Chemistry

Altahan, Mohammed

Award date:
2017

Awarding institution:
Bangor University

[Link to publication](#)

General rights

Copyright and moral rights for the publications made accessible in the public portal are retained by the authors and/or other copyright owners and it is a condition of accessing publications that users recognise and abide by the legal requirements associated with these rights.

- Users may download and print one copy of any publication from the public portal for the purpose of private study or research.
- You may not further distribute the material or use it for any profit-making activity or commercial gain
- You may freely distribute the URL identifying the publication in the public portal ?

Take down policy

If you believe that this document breaches copyright please contact us providing details, and we will remove access to the work immediately and investigate your claim.

COBALT(III), COPPER(II), AND
NICKEL(II) COORDINATION
COMPOUNDS AS CATIONS IN
POLYBORATE CHEMISTRY



A THESIS SUBMITTED

BY

MOHAMMED ABDULREDHA ALTAHAN

IN ACCORDANCE WITH THE REQUIREMENTS FOR THE
DOCTOR OF PHILOSOPHY

SCHOOL OF CHEMISTRY

BANGOR UNIVERSITY

July 2017

Declaration and Consent

Details of the Work

I hereby agree to deposit the following item in the digital repository maintained by Bangor University and/or in any other repository authorized for use by Bangor University.

Author Name:

Title:

.....
.....

Supervisor/Department:

Funding body (if any):

Qualification/Degree obtained:

This item is a product of my own research endeavours and is covered by the agreement below in which the item is referred to as “the Work”. It is identical in content to that deposited in the Library, subject to point 4 below.

Non-exclusive Rights

Rights granted to the digital repository through this agreement are entirely non-exclusive. I am free to publish the Work in its present version or future versions elsewhere.

I agree that Bangor University may electronically store, copy or translate the Work to any approved medium or format for the purpose of future preservation and accessibility. Bangor University is not under any obligation to reproduce or display the Work in the same formats or resolutions in which it was originally deposited.

Bangor University Digital Repository

I understand that work deposited in the digital repository will be accessible to a wide variety of people and institutions, including automated agents and search engines via the World Wide Web.

I understand that once the Work is deposited, the item and its metadata may be incorporated into public access catalogues or services, national databases of electronic theses

and dissertations such as the British Library's EThOS or any service provided by the National Library of Wales.

I understand that the Work may be made available via the National Library of Wales Online Electronic Theses Service under the declared terms and conditions of use

(<http://www.llgc.org.uk/index.php?id=4676>). I agree that as part of this service the National Library of Wales may electronically store, copy or convert the Work to any approved medium or format for the purpose of future preservation and accessibility. The National Library of Wales is not under any obligation to reproduce or display the Work in the same formats or resolutions in which it was originally deposited.

Statement 1:

This work has not previously been accepted in substance for any degree and is not being concurrently submitted in candidature for any degree unless as agreed by the University for approved dual awards.

Signed (candidate)

Date

Statement 2:

This thesis is the result of my own investigations, except where otherwise stated. Where correction services have been used, the extent and nature of the correction is clearly marked in a footnote(s).

All other sources are acknowledged by footnotes and/or a bibliography.

Signed (candidate)

Date

Statement 3:

I hereby give consent for my thesis, if accepted, to be available for photocopying, for inter-library loan and for electronic storage (subject to any constraints as defined in statement 4), and for the title and summary to be made available to outside organisations.

Signed (candidate)

Date

NB: Candidates on whose behalf a bar on access has been approved by the Academic Registry should use the following version of **Statement 3:**

Statement 3 (bar):

I hereby give consent for my thesis, if accepted, to be available for photocopying, for inter-library loans and for electronic storage (subject to any constraints as defined in statement 4), after expiry of a bar on access.

Signed (candidate)

Date

Statement 4:

Choose **one** of the following options

a) I agree to deposit an electronic copy of my thesis (the Work) in the Bangor University (BU) Institutional Digital Repository, the British Library ETHOS system, and/or in any other repository authorized for use by Bangor University and where necessary have gained the required permissions for the use of third party material.	
b) I agree to deposit an electronic copy of my thesis (the Work) in the Bangor University (BU) Institutional Digital Repository, the British Library ETHOS system, and/or in any other repository authorized for use by Bangor University when the approved bar on access has been lifted.	
c) I agree to submit my thesis (the Work) electronically via Bangor University's e-submission system, however I opt-out of the electronic deposit to the Bangor University (BU) Institutional Digital Repository, the British Library ETHOS system, and/or in any other repository authorized for use by Bangor University, due to lack of permissions for use of third party material.	

Options B should only be used if a bar on access has been approved by the University.

In addition to the above I also agree to the following:

1. That I am the author or have the authority of the author(s) to make this agreement and do hereby give Bangor University the right to make available the Work in the way described above.
2. That the electronic copy of the Work deposited in the digital repository and covered by this agreement, is identical in content to the paper copy of the Work deposited in the Bangor University Library, subject to point 4 below.
3. That I have exercised reasonable care to ensure that the Work is original and, to the best of my knowledge, does not breach any laws – including those relating to defamation, libel and copyright.
4. That I have, in instances where the intellectual property of other authors or copyright holders is included in the Work, and where appropriate, gained explicit permission for

the inclusion of that material in the Work, and in the electronic form of the Work as accessed through the open access digital repository, or that I have identified and removed that material for which adequate and appropriate permission has not been obtained and which will be inaccessible via the digital repository.

5. That Bangor University does not hold any obligation to take legal action on behalf of the Depositor, or other rights holders, in the event of a breach of intellectual property rights, or any other right, in the material deposited.
6. That I will indemnify and keep indemnified Bangor University and the National Library of Wales from and against any loss, liability, claim or damage, including without limitation any related legal fees and court costs (on a full indemnity bases), related to any breach by myself of any term of this agreement.

Signature:

Date :

Abstract

This thesis describes the synthesis and characterization of a number of polyborate compounds containing transition metal complex cations; most of these compounds contain 6-membered B₃O₃ boroxole rings within their structures.

A total of twenty-six transition metal complex polyborate salts are reported: one contains the triborate monoanion, [B₃O₃(OH)₄]⁻, three contain the tetraborate dianion [B₄O₅(OH)₄]²⁻, twelve contain the pentaborate anion, [B₅O₆(OH)₄]⁻, three contain the hexaborate dianion, [B₆O₇(OH)₆]²⁻ and five contain heptaborate anions (three of which are [B₇O₉(OH)₅]²⁻, and two are [B₇O₉(OH)₆]³⁻). Additionally, two compounds contain two isolated polyborate anion species (octaborate dianion [B₈O₁₀(OH)₆]²⁻ with pentaborate anion [B₅O₆(OH)₄]⁻, and triborate anion [B₃O₃(OH)₄]⁻ with [B₅O₆(OH)₄]⁻). The crystal structures of fifteen salts containing these polyborate anions are reported: [Co(en)₃][B₅O₆(OH)₄][B₈O₁₀(OH)₆]²⁻·5H₂O (**6**), [Co(NH₃)₆]₂[B₄O₅(OH)₄]₃·11H₂O (**9**), *s-fac*-[Co(dien)₂][B₇O₉(OH)₆]³⁻·9H₂O (**11**), [Co(diNOsar)]₂[B₃O₃(OH)₄]⁻Cl₅·4.75H₂O (**12**), [Cu(en)₂][B₅O₆(OH)₄]₂·2H₂O (**20**), [Cu(pn)₂{B₅O₆(OH)₄}]₂[B₅O₆(OH)₄]⁻·4H₂O (**22**), [Cu(TMEDA){B₆O₇(OH)₆}]₂·6H₂O (**23**), [Cu(dac)₂(H₂O)]₂[Cu(dac)₂][B₇O₉(OH)₅]²⁻·4H₂O (**24**), [Cu(*N,N*-dmen)₂(H₂O)]₂[B₅O₆(OH)₄]₂·3H₂O (**27**), [Cu(*N,N*-dmen){B₆O₇(OH)₆}]₂·4H₂O (**28**), [Ni(en){B₆O₇(OH)₆}(H₂O)₂]₂·H₂O (**37**), [Ni(AEN)]₂[B₅O₆(OH)₄]⁻·H₂O (**38**), [Ni(dac)₂(H₂O)₂][Ni(dac)₂][B₇O₉(OH)₅]²⁻·4H₂O (**39**), [Ni(hn)₂][B₅O₆(OH)₄]₂ (**40**), and *s-fac*-[Ni(dien)₂][B₅O₆(OH)₄]₂ (**41**). All the synthesized compounds reported were characterized using spectroscopic (IR, multi-element NMR) and analytical (melting point, elemental analysis, magnetic susceptibility, thermal analysis, powder X-ray diffraction) techniques.

The solid-state structures of transition metal complex polyborate salts all display multiple cation-anion H-bond interactions and these undoubtedly play a major role in the energetics of engineering these structures. For example, in compound [Co(NH₃)₆]₂[B₄O₅(OH)₄]₃·11H₂O (**9**), fourteen of the 18 amino hydrogen atoms of the [Co(NH₃)₆]³⁺ cation are involved in secondary coordination to anions *via* H-bonds.

Two unique polyborate anions, [B₈O₁₀(OH)₆]²⁻ and [B₇O₉(OH)₆]³⁻ have been prepared and characterized in [Co(en)₃][B₅O₆(OH)₄][B₈O₁₀(OH)₆]²⁻·5H₂O (**6**) and *s-fac*-[Co(dien)₂][B₇O₉(OH)₆]³⁻·9H₂O (**11**), respectively.

The reaction of transition metal complex cations with boric acid in different ratios produced polyborate compounds with different polyborate anions *e.g.* reaction of $[\text{Cu}(\text{en})_2]^{2+}$ with boric acid in 1:10 and 1:5 ratios produce polyborate compounds with pentaborate(1-) and tetraborate(2-) anions, respectively.

New polyborate anion structural architectures are identified in this thesis: (i) the pentaborate(1-) anion in $[\text{Cu}(\text{pn})_2\{\text{B}_5\text{O}_6(\text{OH})_4\}][\text{B}_5\text{O}_6(\text{OH})_4]\cdot 4\text{H}_2\text{O}$ (**22**) acts as a monodentate ligand coordinated to the Cu(II) cation, (ii) the hexaborate(2-) anion in $[\text{Cu}(\text{TMEDA})\{\text{B}_6\text{O}_7(\text{OH})_6\}]\cdot 6\text{H}_2\text{O}$ (**23**) and $[\text{Cu}(\text{N,N-dmen})\{\text{B}_6\text{O}_7(\text{OH})_6\}]\cdot 4\text{H}_2\text{O}$ (**28**) coordinates as a tridentate ligand with the Cu(II) cations, and (iii) the hexaborate(2-) anion in $[\text{Ni}(\text{en})\{\text{B}_6\text{O}_7(\text{OH})_6\}(\text{H}_2\text{O})_2]\cdot \text{H}_2\text{O}$ (**37**) coordinates as a bidentate ligand with the Ni(II) cation. This is the first time that such coordination mode (i) and (iii) have been observed.

Acknowledgements

I wish to offer my sincerest thanks to my PhD supervisor, Prof. Mike Beckett for his continued support, guidance and encouragement throughout the course of this study. I would also like to thank my research committee, Dr Leigh Fôn Jones, Prof. Bela Paizs, and Prof. Mark S. Baird, for their constructive feedback and guidance over the duration of my project. Thanks, must also be given to my personal tutor Dr Andrew Davies for his assistance.

I would like to give a big thank you to all the technical staff at the School of Chemistry for their assistance and friendship throughout the project, Mr Gwynfor Davies, Mr Glynne Evans, Dr David Hughes, Mr Nicholas Welsby, and Mr Denis Williams.

Thanks, must also be extended to Dr Peter Horton and Simon Coles (National Crystallographic Service, Southampton) for obtaining and solving the crystallographic data. A special thank you to Dr Ian Butler for his great help and support.

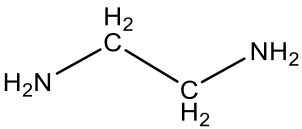
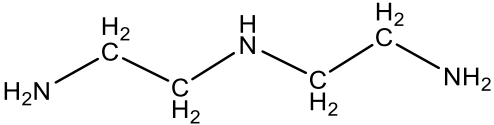
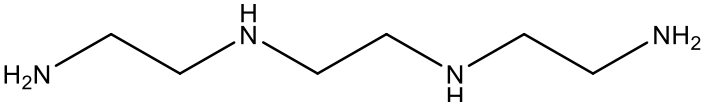
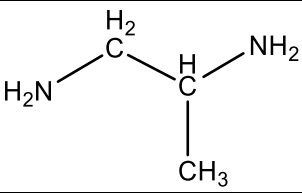
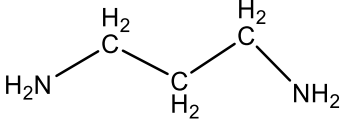
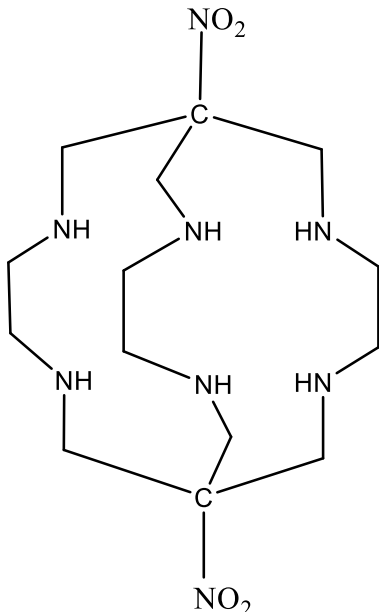
Thanks also to all the administrative staff within the School of Chemistry for all that they have done for me over the duration of my time at Bangor University.

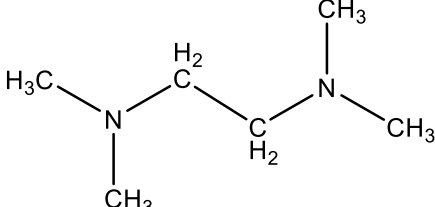
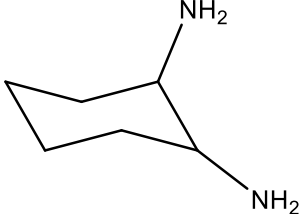
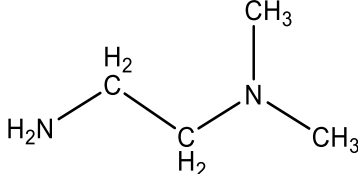
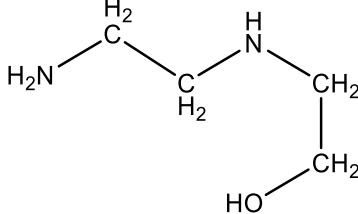
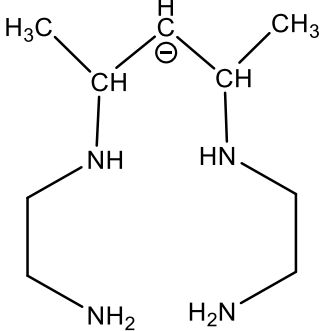
Thanks to Dr Charlotte Jones, Dr Mohammed Alqhatani, Mr Mohammed Al-mashhadani, Mr Omar Thanon, Miss Mari Slater-Parry, Mr Sean Baxter, Miss Verity Piercy and Dr Srikanth Kommanaboyina for their support, friendship and constructive discussion.

I gratefully acknowledge the financial support provided by ministry of higher education and scientific research in Iraq and Thi-Qar University with great and infinite love to my first and last home Iraq, and without which this study would not have been possible. Thanks also to Dr. Hassan Al-Alak (Iraqi cultural attache'), Laith Mashkour and all the staff within the Iraqi cultural attache'-London for all that they have done for me over the duration of my study.

Finally, I would like to express my deepest gratitude for the relentless support, patience, love, and encouragement provided by my family: my wife Nagham is my heart and my children Rafal, Samer, Mohanad, and Mira are my soul.

The structures and abbreviations of ligands employed in this thesis

Name	abbreviation	Structure
Ethylenediamine	en	
Diethylenetriamine	Dien	
Triethylenetetramine	Trien	
1,2-Diaminopropane	Pn	
1,3-Diaminopropane	tn	
1,8-Dinitro-3,6,10,13,16,19-hexaazabicyclo-(6.6.6)icosan	diNOsar	

N,N,N',N'-tetramethyl ethylenediamine	TEDA	
1,2-diaminocyclohexane	dach	
N,N-dimethylethylenediamine	N,N-dmen	
N-(2-hydroxyethyl)ethylenediamine	hn	
2,4-dimethyl-1-(3-azapropyl)-1,5,8-triazaocta-2,4-dienato	AEN	

Abbreviations

Compound name	Formula	Abbreviation
Ethylenediamine	C ₂ H ₈ N ₂	en
Diethylenetriamine	C ₄ H ₁₃ N ₃	Dien
Triethylenetetramine	C ₆ H ₁₈ N ₄	trien
1,2-Diaminopropane	C ₃ H ₁₀ N ₂	pn
1,3-Diaminopropane	C ₃ H ₁₀ N ₂	tn
1,8-Dinitro-3,6,10,13,16,19-hexaazabicyclo-(6.6.6)icosan	C ₁₄ H ₃₀ N ₈ O ₄	diNOsar
N,N,N',N'-tetramethyl ethylenediamine	C ₆ H ₁₆ N ₂	TEDA
1,2-diaminocyclohexane	C ₆ H ₁₄ N ₂	dach
N,N-dimethylethylenediamine	C ₄ H ₁₂ N ₂	N,N-dmen
N-(2-hydroxyethyl)ethylenediamine	C ₄ H ₁₂ N ₂ O	hn
2,4-dimethyl-1-(3-azapropyl)-1,5,8-triazaocta-2,4-dienato	C ₉ H ₂₁ N ₄ ⁻	AEN
Protonated ethylenediamine	C ₂ H ₁₀ N ₂ ²⁺	H ₂ en
Tris(2-aminoethyl)amine	C ₆ H ₁₈ N ₄	TREN
Piperazine	C ₄ H ₁₀ N ₂	Pip
Acetate	C ₂ H ₃ O ₂ ⁻	OAc
N,N,N,N'-Tetrakis-(2-aminoethyl)-1,2-ethandiamine	C ₁₀ H ₂₈ N ₆	-
1,4,8,11-Tetraazacyclotetradecane	C ₁₀ H ₂₄ N ₄	Cyclam
1,10-Phenanthroline	C ₁₂ H ₈ N ₂	PHEN
N,N-Dimethylacetamide	C ₄ H ₉ NO	DMAc
N-Methyl-2-pyrrolidine	C ₅ H ₉ NO	NMP
Pyridine	C ₅ H ₅ N	py
1-Cyanopiperazinium	C ₅ H ₁₁ N ₃ ⁺	-
Piprazinium	C ₄ H ₁₂ N ₂ ²⁺	-

Contents

Declaration and consent.....	i
Abstract.....	vi
Acknowledgements.....	viii
The structures and abbreviations of ligands employed in this thesis.....	ix
Abbreviations.....	xi
Contents.....	xii
List of figures.....	xviii
List of tables.....	xxvi
Chapter One: Introduction.....	1
1.1 Introduction.....	2
1.2 Aim of study.....	2
1.3 Coordination compounds.....	3
1.3.1 Coordination number and coordination geometry.....	3
1.3.2 Isomerism in transition-metal complexes.....	5
1.4 Boron and boron-oxygen compounds.....	8
1.4.1 General background of boron.....	8
1.4.2 Boron-oxygen compounds.....	9
1.5 Experimental techniques used to study borate chemistry.....	18
1.6 Nuclear magnetic resonance spectroscopy (NMR).....	21
1.6.1 Introduction.....	21
1.6.2 Nuclear spin (<i>I</i>).....	21
1.6.3 Natural abundance.....	22
1.6.4 The NMR experiment.....	23

1.6.5 Relaxation.....	23
1.6.6 The chemical shift (δ).....	24
1.7 NMR applied to polyborate species.....	24
Chapter Two: Polyborate salts containing cationic cobalt(III) complexes.....	26
2.1 Introduction.....	27
2.2 Aims.....	27
2.3 Result and discussion.....	28
2.3.1 Synthesis of cobalt(III) complex chloride.....	28
2.3.2 Preparation of cobalt(III) complex polyborate salts.....	28
2.3.3 Characterisation of cobalt(III) complex polyborate salts.....	29
2.3.4 Thermal properties of cobalt(III) complex polyborate salts.....	33
2.3.5 Structural characterisation of cobalt(III) complex polyborate salts.....	36
2.3.5.1 Structural characterisation of $[\text{Co}(\text{en})_3][\text{B}_5\text{O}_6(\text{OH})_4][\text{B}_8\text{O}_{10}(\text{OH})_6]\cdot 5\text{H}_2\text{O}$ (6).....	36
2.3.5.2 Structural characterisation of $[\text{Co}(\text{NH}_3)_6]_2[\text{B}_4\text{O}_5(\text{OH})_4]_3\cdot 11\text{H}_2\text{O}$ (9).....	44
2.3.5.3 Structural characterisation of $[\text{Co}(\text{dien})_2][\text{B}_7\text{O}_9(\text{OH})_6]\cdot 9\text{H}_2\text{O}$ (11).....	52
2.3.5.4 Structural characterisation of $[\text{Co}(\text{diNOsar})_2][\text{B}_3\text{O}_3(\text{OH})_4]\text{Cl}_5\cdot 4.75\text{H}_2\text{O}$ (12).....	58
2.4 Conclusion and summary.....	64
Chapter Three: Copper(II) complex polyborates.....	65
3.1 Introduction.....	66
3.2 Aims.....	66
3.3 Result and discussion.....	67
3.3.1 Synthesis of copper(II) complexes.....	67
3.3.2 Preparation of copper(II) complex polyborate compounds.....	68
3.3.3 Characterization of copper(II) complex polyborate compounds.....	68
3.3.4 Thermal properties of copper(II) complex polyborate compounds.....	71

3.3.5 Structural characterisation of copper(II) complex polyborate compounds.....	75
3.3.5.1 Structural characterisation of [Cu(en) ₂][B ₅ O ₆ (OH) ₄] ₂ ·2H ₂ O (20).....	75
3.3.5.2 Structural characterisation of [Cu(pn) ₂ {B ₅ O ₆ (OH) ₄ }] ₂ [B ₅ O ₆ (OH) ₄] ₂ ·4H ₂ O (22)...	80
3.3.5.3 Structural characterisation of [Cu(TMEDA){B ₆ O ₇ (OH) ₆ }]·6H ₂ O (23)	86
3.3.5.4 Structural characterisation of [Cu(dac) ₂ (H ₂ O) ₂][Cu(dac) ₂][B ₇ O ₉ (OH) ₅] ₂ ·3H ₂ O (24).....	91
3.3.5.5 Structural characterisation of [Cu(<i>N,N</i> -dmen) ₂ (H ₂ O)][B ₅ O ₆ (OH) ₄] ₂ ·3H ₂ O(27)	96
3.3.5.6 Structural characterisation of [Cu(<i>N,N</i> -dmen){B ₆ O ₇ (OH) ₆ }]·4H ₂ O (28).....	102
3.4 Conclusion and summary.....	107
Chapter Four: Nickel(II) complex polyborate salts.....	109
4.1 Introduction.....	110
4.2 Aims.....	110
4.3 Result and discussion.....	110
4.3.1 Synthesis of nickel(II) complex compounds.....	110
4.3.2 Preparation of nickel(II) complex polyborate compounds.....	111
4.3.3 Characterisation of nickel(II) complex polyborate compounds.....	112
4.3.4 Thermal properties of nickel(II) complex polyborate compounds.....	115
4.3.5 Structural characterisation of nickel(II) complex polyborate compounds.....	117
4.3.5.1 Structural characterisation of [Ni(en){B ₆ O ₇ (OH) ₆ }(H ₂ O) ₂]·H ₂ O (37).....	117
4.3.5.2 Structural characterisation of [Ni(EAN)][B ₅ O ₆ (OH) ₄].H ₂ O (38).....	124
4.3.5.3 Structural characterisation of [Ni(dac) ₂ (H ₂ O) ₂][Ni(dac) ₂][B ₇ O ₉ (OH) ₅] ₂ ·4H ₂ O (39).....	128
4.3.5.4 Structural characterisation of [Ni(hn) ₂][B ₅ O ₆ (OH) ₄] ₂ (40).....	133

4.3.5.5 Structural characterisation of $[\text{Ni}(\text{dien})_2][\text{B}_5\text{O}_6(\text{OH})_4]_2$ (41)	137
4.4 Conclusion and summary	142
Chapter Five: General conclusion and future studies	143
5.1 General conclusion	144
5.2 Future work	145
Chapter Six: Experimental	146
6.1 Material analysis.....	147
6.2 Preparation of cobalt(III) complexes.....	147
6.2.1 Preparation of $[\text{Co}(\text{en})_3]\text{Cl}_3 \cdot 2\text{H}_2\text{O}$ (1).....	147
6.2.2 Preparation of $[\text{Co}(\text{NH}_3)_6]\text{Cl}_3$ (2).....	148
6.2.3 Preparation of $[\text{Co}(\text{dien})_2]\text{Cl}_3 \cdot 2\text{H}_2\text{O}$ (3).....	149
6.2.4 Preparation of $[\text{Co}(\text{diNOsar})]\text{Cl}_3$ (4).....	149
6.2.5 Preparation of $[\text{Co}(\text{pn})_3]\text{Cl}_3$ (5).....	150
6.3 Preparation of cobalt(III) complex polyborate salts.....	150
6.3.1 Preparation of $[\text{Co}(\text{en})_3][\text{B}_5\text{O}_6(\text{OH})_4][\text{B}_8\text{O}_{10}(\text{OH})_6] \cdot 5\text{H}_2\text{O}$ (6).....	150
6.3.2 Preparation of $[\text{Co}(\text{en})_3][\text{B}_5\text{O}_6(\text{OH})_4]_2\text{Cl} \cdot 3\text{H}_2\text{O}$ (7).....	151
6.3.3 Preparation of $[\text{Co}(\text{en})_3][\text{B}_7\text{O}_9(\text{OH})_6] \cdot 6\text{H}_2\text{O}$ (8).....	151
6.3.4 Preparation of $[\text{Co}(\text{NH}_3)_6]_2[\text{B}_4\text{O}_5(\text{OH})_4]_3 \cdot 11\text{H}_2\text{O}$ (9).....	152
6.3.5 Preparation of $[\text{Co}(\text{NH}_3)_6][\text{B}_7\text{O}_9(\text{OH})_5]\text{Cl} \cdot 5\text{H}_2\text{O}$ (10).....	152
6.3.6 Preparation of $[\text{Co}(\text{dien})_2][\text{B}_7\text{O}_9(\text{OH})_6] \cdot 9\text{H}_2\text{O}$ (11).....	153
6.3.7 Preparation of $[\text{Co}(\text{diNOsar})]_2[\text{B}_3\text{O}_3(\text{OH})_4]\text{Cl}_5 \cdot 4.75\text{H}_2\text{O}$ (12).....	153
6.3.8 Preparation of $[\text{Co}(\text{diNOsar})][\text{B}_5\text{O}_6(\text{OH})_4]_2\text{Cl} \cdot 3\text{H}_2\text{O}$ (13).....	154
6.3.9 Preparation of $[\text{Co}(\text{pn})_3][\text{B}_5\text{O}_6(\text{OH})_4]_2\text{Cl} \cdot 3\text{H}_2\text{O}$ (14).....	154
6.4 Preparation of copper(II) complexes.....	155

6.4.1 Preparation of [Cu(en) ₂]SO ₄ (15).....	155
6.4.2 Preparation of [Cu(pn) ₂]SO ₄ (16).....	155
6.4.3 Preparation of [Cu(dac) ₂ (H ₂ O) ₂]Cl ₂ (17).....	156
6.4.4 Preparation of [Cu(tn) ₂]SO ₄ ·0.5H ₂ O (18).....	156
6.4.5 [Cu(<i>N,N</i> -dmen) ₂]Cl ₂ (19).....	156
6.5 Preparation of copper(II) complex polyborate salts.....	157
6.5.1 Preparation of [Cu(en) ₂][B ₅ O ₆ (OH) ₄] ₂ ·2H ₂ O (20).....	157
6.5.2 Preparation of [Cu(en) ₂][B ₄ O ₅ (OH) ₄]·2B(OH) ₃ (21).....	157
6.5.3 Preparation of [Cu(pn) ₂ {B ₅ O ₆ (OH) ₄ }][B ₅ O ₆ (OH) ₄]·4H ₂ O (22).....	158
6.5.4 Preparation of [Cu(TMEDA){B ₆ O ₇ (OH) ₆ }]·6H ₂ O (23).....	158
6.5.5 Preparation of [Cu(dac) ₂ (H ₂ O) ₂][Cu(dac) ₂][B ₇ O ₉ (OH) ₅] ₂ ·4H ₂ O (24).....	159
6.5.6 Preparation of [Cu(tn) ₂][B ₅ O ₆ (OH) ₄][B ₃ O ₃ (OH) ₄]·2B(OH) ₃ ·2H ₂ O (25)	160
6.5.7 Preparation of [Cu(tn) ₂][B ₄ O ₅ (OH) ₄]·B(OH) ₃ ·6H ₂ O (26).....	160
6.5.8 [Cu(<i>N,N</i> -dmen) ₂ (H ₂ O)][B ₅ O ₆ (OH) ₄] ₂ ·3H ₂ O (27).....	161
6.5.9 [Cu(<i>N,N</i> -dmen){B ₆ O ₇ (OH) ₆ }]·4H ₂ O (28).....	161
6.6 Preparation of nickel(II) complexes.....	162
6.6.1 Preparation of [Ni(en) ₃]Cl ₂ ·2H ₂ O (29).....	162
6.6.2 Preparation of [Ni(AEN)]Cl·H ₂ O (30).....	162
6.6.3 Preparation of [Ni(<i>trans</i> -dac) ₂ (H ₂ O) ₂]Cl ₂ (31).....	163
6.6.4 Preparation of [Ni(hn) ₂]Cl ₂ (32).....	163
6.6.5 Preparation of [Ni(dien) ₂]Cl ₂ ·H ₂ O (33).....	163
6.6.6 Preparation of [Ni(pn) ₃]Cl ₂ ·2H ₂ O (34).....	164
6.6.7 Preparation of [Ni ₂ (trien) ₃]Cl ₄ ·2H ₂ O (35).....	164
6.7 Preparation of nickel(II) complex polyborate salts.....	165
6.7.1 Preparation of [Ni(en) ₃] [B ₅ O ₆ (OH) ₄] ₂ ·2H ₂ O (36).....	165
6.7.2 Preparation of [Ni(en){B ₆ O ₇ (OH) ₆ }(H ₂ O) ₂]·H ₂ O (37).....	165

6.7.3 Preparation of [Ni(AEN)] [B ₅ O ₆ (OH) ₄]·H ₂ O (38).....	166
6.7.4 Preparation of [Ni(dac) ₂ (H ₂ O) ₂][Ni(dac) ₂][B ₇ O ₉ (OH) ₅] ₂ ·4H ₂ O (39).....	167
6.7.5 Preparation of [Ni(hn) ₂][B ₅ O ₆ (OH) ₄] ₂ (40).....	167
6.7.6 Preparation of <i>s-fac</i> -[Ni(dien) ₂][B ₅ O ₆ (OH) ₄] ₂ (41).....	168
6.7.7 Preparation of [Ni(pn) ₃][B ₅ O ₆ (OH) ₄] ₂ ·C ₂ H ₅ OH·5H ₂ O (42).....	168
6.7.8 Preparation of [Ni ₂ (trien) ₃][B ₅ O ₆ (OH) ₄] ₂ Cl ₂ ·CH ₃ OH·6H ₂ O (43).....	169
References.....	170
Appendix I.....	177

List of Figures

Figure	Caption	Page
1.1	The common shapes of 4-coordinate metal complexes (A and B) and 6-coordinate metal complexes (C), M = metal, L = ligand.	4
1.2	Jahn-Teller distortion due to unequal occupancy of the degenerate orbitals.	4
1.3	<i>cis</i> - and <i>trans</i> -isomers of square planar geometry.	5
1.4	Facial and meridional isomers of octahedral MA ₃ X ₃ complexes.	5
1.5	The three geometrical isomers of [Co(dien) ₂] ³⁺ .	6
1.6	Left handed Λ isomer and right handed Δ isomer.	7
1.7	The λ and δ configurations in tris(ethylenediamine)cobalt(III).	7
1.8	Variation in the distribution of boron species with solution pH at 25 °C. Total boron concentration is 0.4 M.	10
1.9	Two common modes of polymerization for boroxyl rings in infinite chain borates.	15
1.10	Possible electronic transition of the octahedral d ³ transition-metal complexes.	19
1.11	Energy levels for a nucleus with spin quantum number, S = 1/2.	21
2.1	Diagram showing the protons of propylene diamine ligand and the adopted numbering scheme in compound 14 .	31
2.2	An illustration of the second mass-loss process in thermal decomposition of polyborate anions.	34
2.3	TGA diagram for the thermal decomposition of cobalt(III) complex polyborate salts 6-9 .	35

2.4	TGA diagram for the thermal decomposition of cobalt(III) complex polyborate salts 10-14 .	36
2.5	Diagram showing the structure and numbering scheme for 6 . Colour code (used throughout this chapter): deep blue (Co), blue (N), red (O), pink (B), dark grey (C) and light grey (H).	37
2.6	Structure of the octaborate(2-) anion present in the crystals of 6 (A) and isomeric $[B_8O_{10}(OH)_6]^{2-}$ anion (B), and polymeric $[B_8O_{11}(OH)_4]^{2-}$ anion (C).	39
2.7	Diagram showing the H-bond acceptor sites and their numbers in the octaborate(2-) anions.	40
2.8	Pentaborate(1-) anion $R_2^2(8)$ H-bond motif connections in 6 . Dashed blue lines represent H-bonds.	42
2.9	Octaborate(2-) anion $R_2^2(8)$ H-bond motif connections in 6 .	42
2.10	Diagram showing a 'plane' of polyborate anions (viewed along the <i>b</i> direction of the unit cell) and water molecule with $[Co(en)_3]^{3+}$ cations in 6 .	43
2.11	The connection of $[Co(en)_3]^{3+}$ cation with pentaborate(1-) anions and water molecules in 6 .	44
2.12	Diagram showing numbering scheme for 9 .	45
2.13	Diagram labelling the oxygen atom H-bond acceptor sites in the tetraborate(2-) anions.	47
2.14	H-bond interactions of tetraborate(2-) anion (A) to another anions in 9 . Dashed blue lines represent H-bonds.	48
2.15	The H-bond interactions of the tetraborate(2-) anion (B) to another anions in 9 .	48
2.16	The H-bond interactions of the tetraborate(2-) anion (C) to another anions in 9 .	49

2.17	Tetraborate(2-) anions and water molecules layer structure (viewed along the <i>a</i> direction of the unit cell) of 9 .	51
2.18	The H-bond interactions of [Co(NH ₃) ₆] ³⁺ (A) and (B) cations with tetraborate(2-) anions and water molecules in 9 .	52
2.19	Diagram showing numbering scheme for 11 .	53
2.20	The two isomeric [B ₇ O ₉ (OH) ₅] ²⁻ anions (A) and (B) and the structure of the heptaborate(3-) anion (C) present in the crystals of 11 .	54
2.21	Diagram showing atomic numbering for the heptaborate(3-) anions in 11 .	55
2.22	H-bond interactions between the heptaborate(3-) anions in 11 . Dashed blue lines represent H-bonds.	56
2.23	Supramolecular structure involving heptaborate(3-) anions and [Co(Dien) ₂] ³⁺ cations (viewed along the <i>c</i> direction of the unit cell) in 11 .	57
2.24	The H-bond connections of [Co(dien) ₂] ³⁺ with heptaborate(3-) anions and water molecule in 11 .	57
2.25	Diagram showing numbering scheme for 12 .	58
2.26	Atomic numbering for the sites of the triborate(1-) anions as found in 12 .	60
2.27	The triborate(1-) anions and water molecules layer structure (viewed along the <i>c</i> direction of the unit cell) of 12 . Dashed blue lines represent H-bonds.	61
2.28	The H-bond connections of [Co(diNOsar)] ³⁺ with triborate(1-) anions and chloride ions in 12 .	62
2.29	Triborate(1-) anions are arranged in planes linked together by H-bonds (dashed blue lines) from H ₂ O molecules. The [Co(diNOsar)] ³⁺ cations fill the cavities and link to the triborate(1-) anions by further H-bonds (viewed along the <i>c</i> direction of the unit cell) in 12 .	63

3.1	TGA diagram for the thermal decomposition of copper(II) complex polyborate compounds 20-23 .	73
3.2	TGA diagram for the thermal decomposition of copper(II) complex polyborate compounds 24-26 .	74
3.3	TGA diagram for the thermal decomposition of copper(II) complex polyborate compounds 27-28 .	74
3.4	Diagram showing the complex cation $[\text{Cu}(\text{en})_2]^{2+}$, pentaborate(1-) anion and water molecule in 20 and the adopted numbering scheme. Colour code (used throughout this chapter): Brown (Cu), Blue (N), Red (O), Pink (B), Grey (C) and white (H).	75
3.5	Diagram showing the H-bond acceptor sites and their numbers in the pentaborate(1-) anions.	77
3.6	View of a plane of pentaborate(1-) anions (viewed along the <i>c</i> direction of the unit cell) in 20 . Dashed blue lines represent H-bonds.	78
3.7	The two $R_2^2(8)$ and $R_2^2(12)$ H-bond motif connections in 20 .	79
3.8	Diagram showing a 'plane' of polyborate anions (viewed along the <i>c</i> direction of the unit cell) and water molecule with $[\text{Cu}(\text{en})_2]^{2+}$ cations in 20 .	80
3.9	Diagram showing the numbering scheme of 22 .	81
3.10	H-bonded $[\text{B}_5\text{O}_6(\text{OH})_4]^-$ network for 22 . Dashed blue lines represent H-bonds.	84
3.11	The $R_2^2(8)$ connections between free and coordinate pentaborate(1-) anions in 22 .	85
3.12	A diagram shows the structure of 22 viewed along the <i>c</i> axes. The polyborate are arranged in a plane and 'cavities' are filled by the cation $[\text{Cu}(\text{pn})_2\{\text{B}_5\text{O}_6(\text{OH})_4\}]^+$ and water molecules.	85

3.13	Diagram showing the numbering scheme of 23 .	86
3.14	Diagram showing oxygen labelling and the H-bond acceptor sites for the hexaborate(2-) anions in 23 .	89
3.15	The $R_2^2(8)$ interactions between $[\text{Cu}(\text{TMEDA})\{\text{B}_6\text{O}_7(\text{OH})_6\}]$ molecules in 23 .	90
3.16	Diagram showing a 'plane' of $[\text{Cu}(\text{TMEDA})\{\text{B}_6\text{O}_7(\text{OH})_6\}]$ (viewed along the <i>c</i> direction of the unit cell) and water molecules in 23 .	90
3.17	Diagram showing the complex cations and heptaborate(2-) anion in 24 . The water molecules containing O22 are in octahedral positions around Cu2 (bonds not shown in the diagram).	92
3.18	Diagram showing the H-bond acceptor sites of the heptaborate(2-) anions in 24 .	94
3.19	The reciprocal connection (viewed along the <i>c</i> direction of the unit cell) in 24 .	95
3.20	The two $R_2^2(8)$ and $R_2^2(12)$ H-bond motif connections in 24 .	95
3.21	The $R_2^2(8)$ interaction in between the heptaborate(2-) anion and $[\text{Cu}(\text{dach})_2]^{2+}$ cation in 24 .	96
3.22	Diagram showing the complex cation, pentaborate anions and water molecules in 27 and the adopted numbering scheme.	98
3.23	The two $R_2^2(8)$ H-bond motif connections and $R_3^3(16)$ interaction in 27 .	99
3.24	The four $R_2^2(8)$ H-bond motif connections between pentaborate(1-) anions in 27 .	100
3.25	Extended H-bonded $[\text{B}_5\text{O}_6(\text{OH})_4]^-$ plane (viewed along the <i>b</i> direction of the unit cell) for 27 .	101

3.26	Diagram showing a 'plane' of polyborate anions (viewed along the <i>b</i> direction of the unit cell) with $[\text{Cu}(\text{N},\text{N-dmen})_2(\text{H}_2\text{O})]^{2+}$ and H_2O molecules shown in the 'cavities' in 27 .	101
3.27	The H-bond connections of $[\text{Cu}(\text{N},\text{N-dmen})_2(\text{H}_2\text{O})]^{2+}$ cation in 27 .	102
3.28	Diagram showing the numbering scheme of 28 .	103
3.29	The reciprocal $R_2^2(8)$ and reciprocal $R_2^2(16)$ interactions in 28 .	106
3.30	The two $R_2^2(10)$ interactions in 28 . Dashed blue lines represent H-bonds.	106
4.1	TGA diagram for the thermal decomposition of nickel(II) complex polyborate compounds 36-39 .	116
4.2	TGA diagram for the thermal decomposition of nickel(II) complex polyborate compounds 40-43 .	117
4.3	Diagram showing the 37 and the adopted numbering scheme. Colour code (used throughout this chapter): green (Ni), blue (N), red (O), pink (B), dark grey (C) and light grey (H).	118
4.4	One of the two reciprocal $R_2^2(8)$ interactions in 37 . Dashed blue lines represent H-bonds.	121
4.5	One of the five reciprocal $R_2^2(12)$ interactions in 37 .	121
4.6	The reciprocal $R_2^2(16)$ H-bond interaction in 37 . Dashed blue lines represent H-bonds.	122
4.7	One of the two $C(8)$ connections in 37 .	122
4.8	The dimer connection in 37 .	123
4.9	Diagram showing a 'plane' of $[\text{Ni}(\text{H}_2\text{O})_2(\text{en})\{\text{B}_6\text{O}_7(\text{OH})_6\}]$ (viewed along the <i>a</i> direction of the unit cell) and water molecule in 37 .	123
4.10	Diagram showing the complex cation, pentaborate anion and water molecule in 38 and the adopted numbering scheme.	124

4.11	The three $R_2^2(8)$ H-bond motif connections in 38 . Dashed blue lines represent H-bonds.	127
4.12	Diagram showing a 'plane' of polyborate anions (viewed along <i>a</i>) and water molecule with $[\text{Ni}(\text{EAN})]^+$ cations in 38 .	127
4.13	Diagram showing the complex cation, heptaborate(2-) anion and water molecule in 39 and the adopted numbering scheme.	138
4.14	The four H-bond donor interactions of each heptaborate(2-) anion in 39 .	130
4.15	The $R_2^2(8)$ and $R_2^2(12)$ connections between heptaborate anions.	132
4.16	A plane of heptaborate anions and $[\text{Ni}(\text{DACH})_2(\text{H}_2\text{O})_2]^{2+}$ and $[\text{Ni}(\text{DACH})_2]^{2+}$ cations in plane H-bond interactions in 39 .	132
4.17	Diagram showing the complex cation and pentaborate(1-) anion in 40 and the adopted numbering scheme.	133
4.18	The $R_2^2(8)$ and $R_2^2(12)$ connections between two layers of pentaborate(1-) ion ribbons in 40 .	135
4.19	H-bonded $[\text{B}_5\text{O}_6(\text{OH})_4]^-$ network for 40 view perpendicular to the large channels (viewed along the <i>a</i> direction of the unit cell).	136
4.20	A plane of pentaborate(1-) anions and $[\text{Ni}(\text{hn})_2]^{2+}$ cations in plane of H-bond interactions in 40 (viewed along the <i>a</i> direction of the unit cell).	137
4.21	Diagram showing the complex cation and pentaborate(1-) anion in 41 and the adopted numbering scheme.	138
4.22	H-bonded $[\text{B}_5\text{O}_6(\text{OH})_4]^-$ network for 41 view perpendicular to the large channels (viewed along the <i>a</i> direction of the unit cell).	140
4.23	The $R_2^2(8)$ and $R_2^2(12)$ connections between two layers of pentaborate(1-) ion ribbons in 41 .	141
4.24	A plane of pentaborate(1-) anions and $[\text{Ni}(\text{dien})_2]^{2+}$ cations in plane of H-	141

	bond interactions in 41 (viewed along the a direction of the unit cell).	
--	---	--

List of Tables

Table	Caption	Page
1.1	Known polyborate anion species.	10
1.2	The average O-CN with fraction of B _(tet) units of polyborate anions	16
1.3	Magnetic resonance properties of selected atomic nuclei.	23
2.1	Yields of cobalt(III) complex polyborate salts.	29
2.2	Mass and molar susceptibility of cobalt(III) complexes and their polyborate salts at 24 °C.	29
2.3	CHN analysis of cobalt(III) complex polyborate salts.	30
2.4	¹ H, ¹³ C, and ¹¹ B NMR data for compounds 6-14 .	32
2.5	Observed frequencies of FT-IR spectra of the new polyborate salts 6-14 .	33
2.6	The mass loss steps of the new polyborate salts 6-14 .	34
2.7	Crystal data and structure refinement of 6 .	37
2.8	H-bond interactions in 6 .	41
2.9	Crystal data and structure refinement of 9 .	45
2.10	H-bond interactions in 9 .	49
2.11	Crystal data and structure refinement of 11 .	52
2.12	H-bond interactions in 11 .	56
2.13	Crystal data and structure refinement of 12 .	59
2.14	H-bond interactions in 12 .	60

3.1	Yields and formula of copper(II) complex polyborate compounds.	68
3.2	Magnetic properties of copper(II) complexes and their polyborate compounds at 24 °C.	69
3.3	CHN analysis of copper(II) complex polyborate compounds.	69
3.4	The chemical shift (δ) of ^{11}B -NMR spectra of copper(II) complex polyborate compounds (20-28).	70
3.5	The explanation of FT-IR spectra of copper(II) complex polyborate compounds (20-28).	71
3.6	The mass loss steps of copper(II) polyborate compounds 20-28 .	72
3.7	Crystallographic data and structure refinement of 20 .	75
3.8	H-bonds [\AA and $^\circ$] in 20 .	77
3.9	Crystal data and structure refinement details of 22 .	80
3.10	H-bonds [\AA and $^\circ$] in 22 .	83
3.11	Crystal data and structure refinement details of 23 .	86
3.12	H-bonds [\AA and $^\circ$] in 23 .	89
3.13	Crystal data and structure refinement details of 24 .	91
3.14	H-bonds [\AA and $^\circ$] in 24 .	94
3.15	Crystal data and structure refinement of 27 .	96
3.16	H-bonds [\AA and $^\circ$] of 27 .	99
3.17	Crystal data and structure refinement details of 28 .	103
3.18	H-bonds [\AA and $^\circ$] in 28 .	105
4.1	Yields and formula of nickel(II) complex polyborate compounds.	112

4.2	Magnetic properties of nickel(II) complexes and their polyborate compounds at 24 °C.	112
4.3	CHN analysis of nickel(II) complex polyborate compounds.	113
4.4	The chemical shift (δ) of ^{11}B NMR spectra of nickel(II) complex polyborate compounds.	114
4.5	The explanation of FT-IR spectra of nickel(II) complex polyborate compounds.	114
4.6	TGA data for nickel(II) polyborate compounds 36-43 .	115
4.7	Crystal data and structure refinement of 37 .	118
4.8	H-bonds [\AA and $^\circ$] in 37 .	120
4.9	Crystal data and structure refinement of 38 .	125
4.10	H-bonds [\AA and $^\circ$] of 38 .	126
4.11	Crystal data and structure refinement of 39 .	129
4.12	H-bond interactions [\AA and $^\circ$] in 39 .	131
4.13	Crystal data and structure refinement of 40 .	133
4.14	H-bonds [\AA and $^\circ$] in 40 .	134
4.15	Crystal data and structure refinement of 41 .	138
4.16	H-bonds [\AA and $^\circ$] in 41 .	139

Chapter One

Introduction

1.1 Introduction

This introductory chapter reviews aspects of inorganic chemistry pertinent to this thesis. The introduction has been divided into three main parts. Firstly, there is a review of the basic concepts of coordination compounds (i.e. complexes, coordination numbers and isomerism). Secondly, there is a review focused on boron oxygen compounds. Here, polyborate anion structures are discussed in more detail and a brief description of the anions present in known polyborate salts are included. Finally, there is a review of the experimental techniques used in this thesis to characterize the polyborate compounds and this includes a more detailed discussion of NMR spectroscopy.

1.2 Aim of study

Borates with alkali metals, alkaline earth metals, main group metals, rare earths, transition metals and non-metal cations have been widely studied and explored.¹ It is well known that certain polyborate anions *e.g.* $[\text{B}_9\text{O}_{12}(\text{OH})_6]^{3-}$, $[\text{B}_{15}\text{O}_{20}(\text{OH})_8]^{3-}$ have only been observed partnered by specific cations.^{2,3} $\text{B}(\text{OH})_3$ in basic aqueous solution exists as a dynamic combinatorial library of a variety of polyborate anions and cations can self-assemble (crystal engineer) solid-state polyborate structures by crystallization from this aqueous solution. However, many of these polyborates contain the isolated pentaborate(1-) anion and this is believed to be for the reasons set out in the following two paragraphs.

Each pentaborate(1-) anion has four H-bond donor sites and ten H-bond acceptor sites and all 4 H-bond sites are always used as H-bond donor to other pentaborate anions and form supramolecular 3D frameworks.⁴ Structurally, pentaborates are best described as supramolecular networks of H-bonded anions, with cations occupying the 'cavities' within the network. However, with pentaborate(1-) anions, these lattices can expand (within limits) with cation size. A common structure motif in all pentaborate compounds is reciprocal $\text{R}_2^2(8)$ H-bonds at α sites and this interaction is particularly strong.⁵ When 'innocent' cations are present these anion-anion H-bond interactions dominate the self-assembly energetics of the pentaborate salts.

Cation-anion H-bond interactions in the solid state can play a very important role in engineering structures of the polyborate compounds and may break up the dominance of anion-anion interactions found in pentaborates, *e.g.* $[\text{H}_2\text{en}]_2[\text{B}_4\text{O}_5(\text{OH})_4][\text{B}_7\text{O}_9(\text{OH})_5] \cdot 3\text{H}_2\text{O}$, isolated heptaborate(2-) and tetraborate(2-) anions (rather than pentaborate(1-) anion) are observed with

non-metal cation $[\text{H}_2\text{en}]^{2+}$. Here all twelve amino H-atoms of the two $[\text{H}_2\text{en}]^{2+}$ cations are involved in H-bonds.⁶

The first main aim of the research covered within this thesis is to synthesize and structurally characterize new polyborate anions with sterically demanding and / or highly charged cations, *i.e.* transition metal coordination complex cations. Polyborate salts are formed by self-assembly reactions from boric acid templated by the cations. We have investigated whether the transition metal complex cation structure directly affects the structure of the polyborate anions and if so, how the transition metal complex influences that structure. This is to be achieved by examination of solid-state structures as determined by XRD studies.

The second aim is to investigate the physical properties of the new synthesized transition metal complex polyborate compounds. Magnetic properties and thermal properties are to be reported, along with spectroscopic (IR, NMR, and UV) data.

1.3 Coordination compounds

1.3.1 Coordination number and coordination geometry

The principle feature of the geometrical structures of complex compounds (coordination number) were first determined by the Swiss chemist Alfred Werner in 1893.⁷ The coordination number of the central metal atom is defined as the total number of atoms, ions, or molecules that are bonded to the central element or ion. The coordination number can vary from two to as many as fifteen,⁸ but four and six are by far the most commonly observed coordination numbers.

Two common structures are possible for 4-coordinate metal complexes, tetrahedral (T_d) and square-planar (D_{4h}). The tetrahedral structure is mainly observed for most 4-coordinate non-transition metal complexes, also it is commonly found for 4-coordinate transition metal complexes. Square-planar geometry is commonly found for complexes of 2nd and 3rd transition metal series with d^8 electronic configuration: Rh^+ , Pd^{2+} , Ir^+ , Pt^{2+} , and Au^{3+} . The octahedral geometry is the most commonly observed shape for the 6-coordinate transition metal complexes (Figure 1.1).

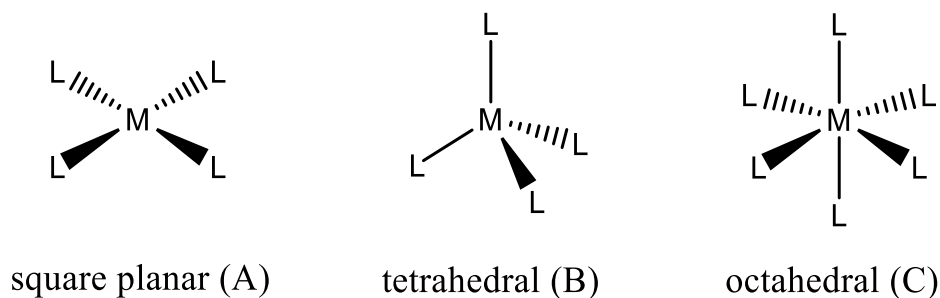


Figure 1.1 The common shapes of 4-coordinate metal complexes (A and B) and 6-coordinate metal complexes (C), M = metal, L = ligand.

In some octahedral cases distortions are observed due to unequal occupancy of degenerate orbitals in the idealized undistorted geometry. This distortion will lead to a system of lower energy and lower symmetry where the two axial bonds can be longer or shorter than those of the equatorial bonds. This geometry change is called the Jahn-Teller distortion (Figure 1.2). It is usually important when an odd number of electrons occupy the E_g level, and mostly arises in complexes with the electronic configurations high spin d^4 , low spin d^7 , and d^9 . Jahn-Teller distortion also occurs when there is a degeneracy due to electrons in the T_{2g} level, such as configuration d^1 and d^2 . In this case the effect is usually much less pronounced since the electrons occupies T_{2g} orbitals, which do not point directly at the ligands.⁹⁻¹²

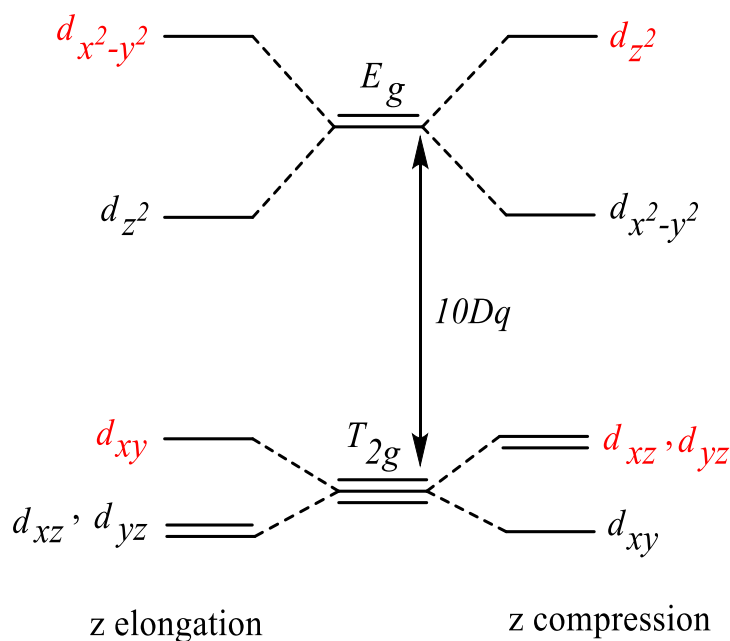


Figure 1.2 Jahn-Teller distortion due to unequal occupancy of the degenerate orbitals.

1.3.2 Isomerism in transition metal complexes

The isomerism in coordination chemistry is classified into two main categories: structural isomers and stereoisomers. Stereoisomers are compounds which have the same chemical formula and the atoms are joined together in the same arrangement, but there is a different spatial arrangement of these atoms. Stereoisomers can be subdivided into geometric isomers and optical isomers.

Geometrical isomers are possible for both octahedral and square-planar geometries. For square-planar MA_2X_2 complexes (A and X are monodentate ligands) there are two possible isomers: *cis*- and *trans*-. In the *trans*-isomer, the identical ligands are opposite to each other (180°), while in the *cis*- isomer these ligands are adjacent to each other (90°) (Figure 1.3). A similar situation applies to octahedral MA_2X_4 complexes.

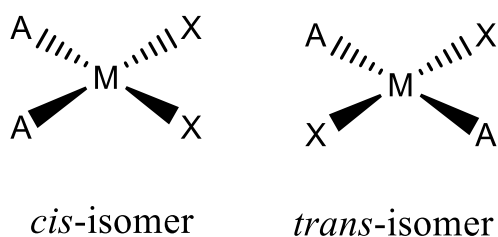


Figure 1.3 *cis*- and *trans*-isomers of square-planar geometry.

For octahedral MA_3X_3 complexes two isomers are possible: facial (*fac*) and meridional (*mer*). The facial isomers have each set of three identical groups occupying one face of the eight octahedral faces, while the meridional isomer has each set of the three identical groups occupying a plane passing through the central metal atom (Figure 1.4).

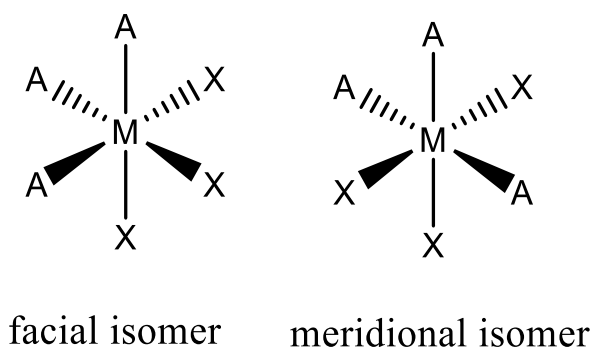


Figure 1.4 Facial and meridional isomers of octahedral MA_3X_3 complexes.

Complexes of $[MA_2]$ formula (where A is a tridentate ligand) also can show geometrical isomerism, for example $[Co(dien)_2]^{3+}$,¹³ where is diethylenetriamine (dien) shows three geometric isomers. These geometries can be designated as facial when three amino groups of the same diethylenetriamine ligands occupy one face or meridional when the three amino groups of the same diethylenetriamine occupy a plane passing through cobalt atom. In addition, there are two facial isomers which are conveniently labelled *s* (symmetric) and *u* (un-symmetric); these labels arise from whether or not the complex has a centre of symmetry, i (Figure 1.5).¹³⁻¹⁵

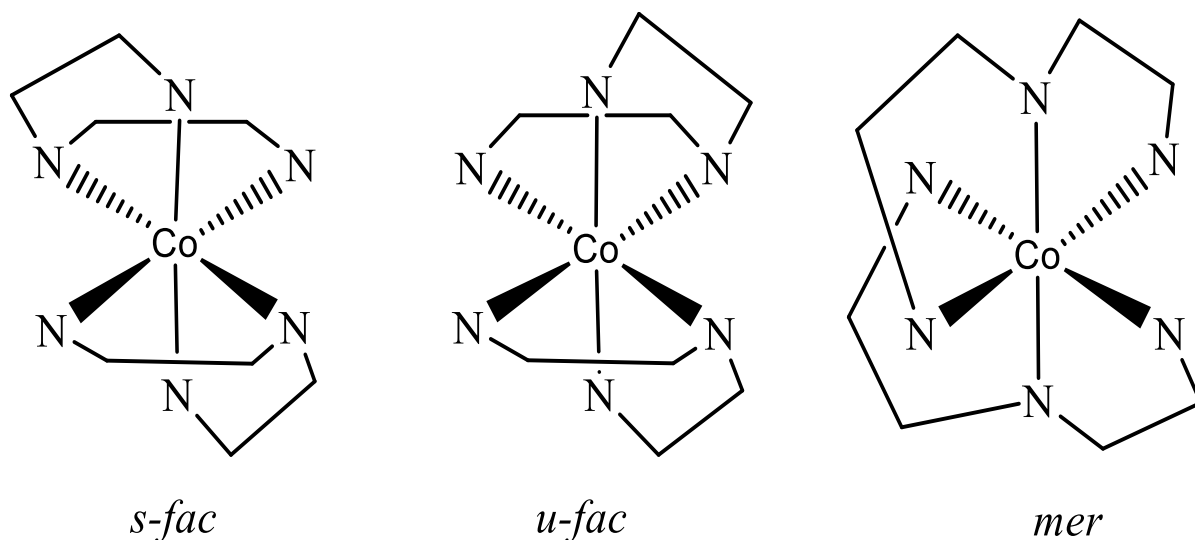


Figure 1.5 The three geometrical isomers of $[Co(dien)_2]^{3+}$.

Optical isomers are isomers that are non-superimposable mirror image of one another. The optical isomers are optically active compounds and they rotate plane-polarized light in opposite directions.

The absolute configuration of optical isomers has been denoted by various methods such as S or R, and Δ or Λ . Complexes with three bidentate ligands be designated by a symbol Λ , which is used as a prefix to describe a left-handed propeller twist, and Δ is used for a right-handed twist of the three bidentate ligands (Figure 1.6).

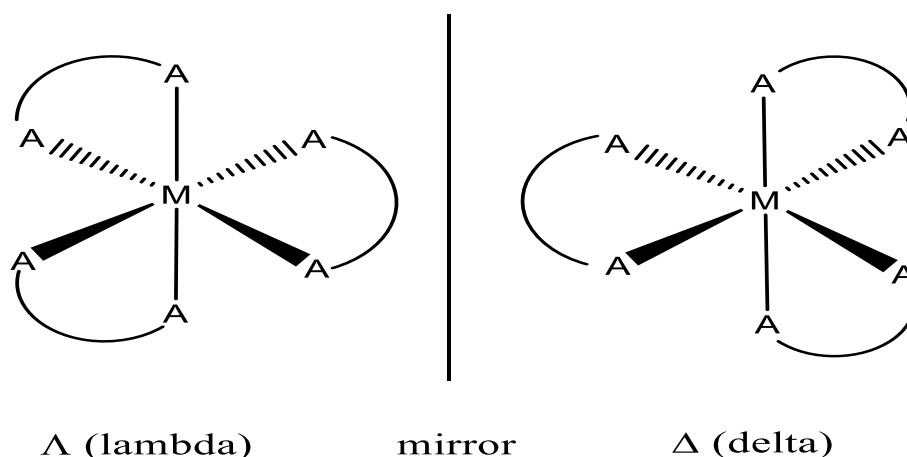


Figure 1.6 Left handed Λ isomer and right handed Δ isomer.

In 1959 Corey and Bailar first applied the principle of conformation analysis to the stereochemistry of coordination complexes.¹⁶ They recognized that the chelation of ethylenediamine with a transition metal ion formed a ring with many possible stereochemical forms. In tris(ethylenediamine)cobalt(III) complex the coordination of three bidentate ligands to a cobalt(III) ion forms three twisting five membered chelate rings. The hydrogen atoms on adjacent atoms of the twisting rings are in a staggered conformation and these hydrogen atoms will be approximately equatorial or axial to the plane of the central transition metal ion and the two nitrogen atoms of the bidentate ligand. The conformation of the five-membered rings can be designated as δ or λ (Figure 1.7).

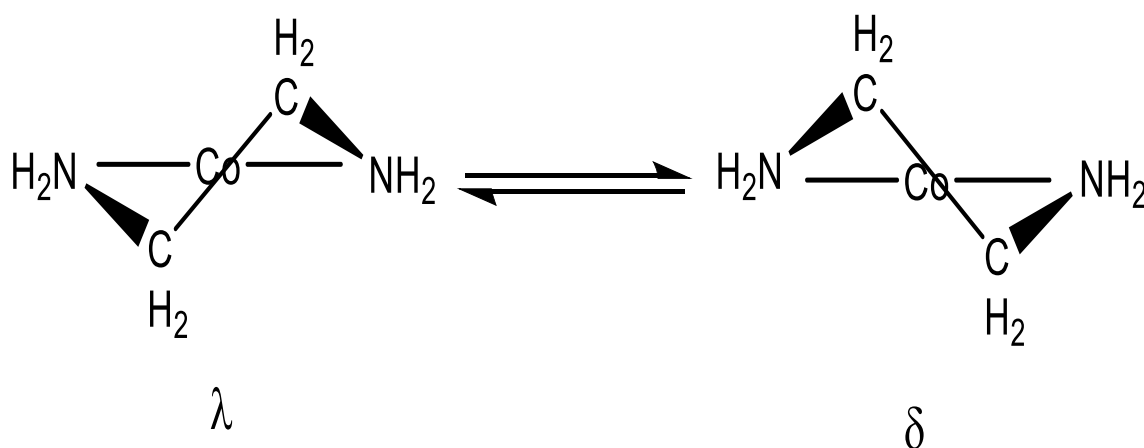


Figure 1.7 The λ and δ configurations in tris(ethylenediamine)cobalt(III).

1.4 Boron and boron-oxygen compounds

1.4.1 General background of boron¹⁷

The element boron can be defined as the chemical element with atomic number 5 and symbol B. Boron compounds have been known for thousands of years, while the element boron was believed to have been discovered independently in 1808 by Sir Humphry Davy (1778-1829 an English chemist), Louis Jaques Thenard (1777-1857 a French chemist) and Joseph Louis Gay Lussac (1778-1850 a French chemist and physicist). The isolation of boron was accomplished by the reaction of boric acid with potassium. Sir Humphrey Davy originally named this element boracium due to it being derived from boracic acid. The origin of the name boron is derived from a combination of the names boracium and carbon. Boron is a dark brown powder which is extremely hard but brittle. At room temperature, it is a poor electrical conductor, but at high temperature it is a good conductor. It is classified as a "metalloid" element because it has the properties of metallic and non-metallic elements. Boron occurs as boric acid $B(OH)_3$ and in polyboric acid salts, and is never found free in nature.¹⁷

Boron is one of the most extensively studied elements. This is due to its diverse industrial applications, and its chemically unique behavior.¹⁸ Growing evidence from many experiments indicate that boron is an essential trace element for the human body. The many beneficial actions of boron include bone growth and maintenance,¹⁹ reduction of the risk for some cancers, inflammation and oxidative stress modulation,²⁰ improved brain function, hormone facilitation, immune response,²¹ and a decrease in the risk of arthritis. Boron's bioactivity is primarily due to formation of borate esters with a ribose sugar moiety, such as oxidized nicotinamide adenine dinucleotide and *S*-adenosylmethionine. This has led to a proposal that 1 mg/day human boron intake may help peoples to live better and longer.¹⁹

Boron is in the oxidation state of +3 in its most familiar compounds such as halides, nitrides, oxides, and sulphides. The main classes of boron compounds are boranes, borides, organoboron compounds and borates. The simplest borane has the chemical formula B_2H_6 . Borides are compounds produced from a combination of boron with a more electropositive element such as titanium, *e.g.* titanium boride (TiB_2). Organoboron compounds are a large class of organic derivatives of borane BH_3 *e.g.* trialkyl boranes.²² Borates represent a major division of boron compounds where boron is bonded to oxygen and is part of a borate ester or an oxyanion group.

1.4.2 Boron-Oxygen compounds

Boron-oxygen compounds (borates) represent a major class of boron compounds and these have attracted a great deal of attention. Many papers relating to borate minerals have been published and recently many synthetic novel borate compounds have greatly contributed to the diverse literature of solid-state borate chemistry. This steady interest is due to their intriguing variety of crystal architectures and their potential applications in many different fields *e.g.* in mineralogy,²³⁻²⁷ nonlinear optical behavior,²⁸⁻³¹ photoluminescence,^{32,33} and industry applications such as agricultural micronutrients.^{34,35}

A specially developed process in glass manufacture has led to the production of a glass (*e.g.* Pyrex) with very high heat and chemical attack resistances.^{36,37} Borate compounds are essential components in modern life with applications²³⁻³⁷ such as biocidal materials (wood preservatives), glass (display panels and insulation as fibre glass), cross linking (oil recovery chemical and adhesive), fire retardants (for wood and plastic), anticorrosion (water treatment and automotive fluids), cleaning agents (industrial detergent and consumer), metal processors (fluxes of steel and other metals), chemical source of boron (borohydride fuels), and nuclear and spectroscopic application (cooling water and control rods). The great variety of application of borate compounds result from the flexible coordination modes of the boron atom: four-fold coordination (BO_4^- , tetrahedral) or three-fold coordination (BO_3 , triangular). The BO_3 and BO_4^- sub units can further link together *via* sharing common oxygen atoms to produce isolated rings and cages, or polymerize to produce infinite chains, sheets, and network leading to a rich structural chemistry.^{38,39}

The most important species in aqueous solution of boric acid are $\text{B}(\text{OH})_3$ and $\text{B}(\text{OH})_4^-$ units:



According to the equilibrium constant, the main species in solution at low pH are $\text{B}(\text{OH})_3$ units and the dominant species at high pH are $\text{B}(\text{OH})_4^-$ units. However, in practice the speciation of borate ions in aqueous solution is more complex, particularly in the pH range 5-12 (Figure 1.8). The population of polyborate anion species in solution varying according to: pH, concentration, and temperature. The known isolated (as opposed polymeric) polyborate anions, prior to writing the thesis, are described in Table 1.1.

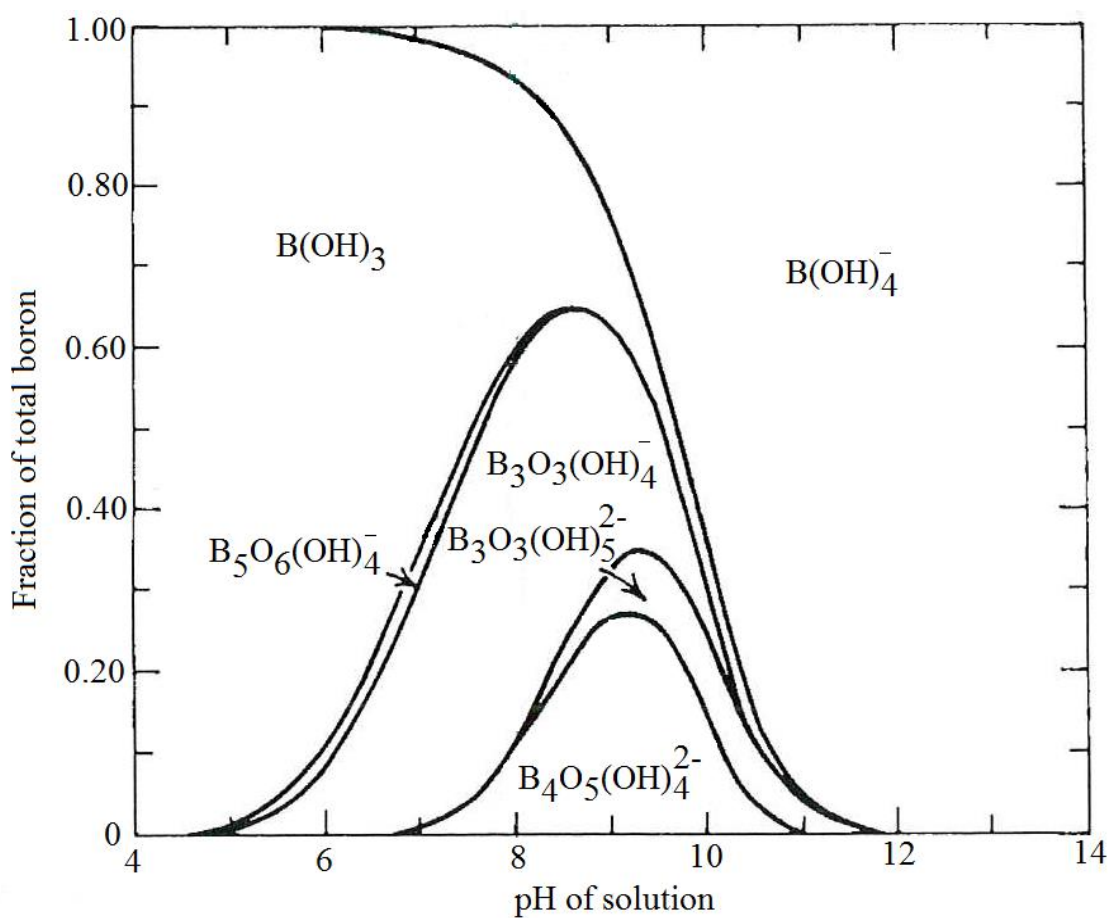
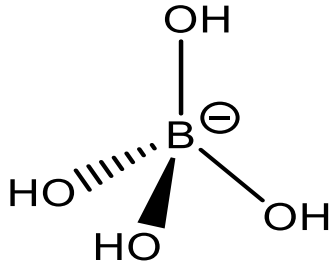
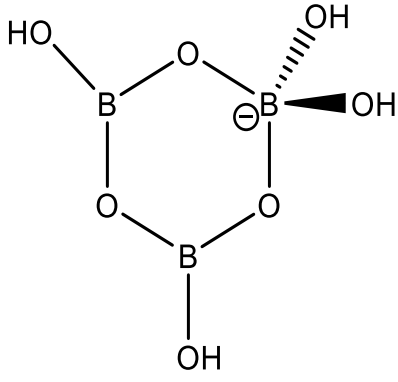
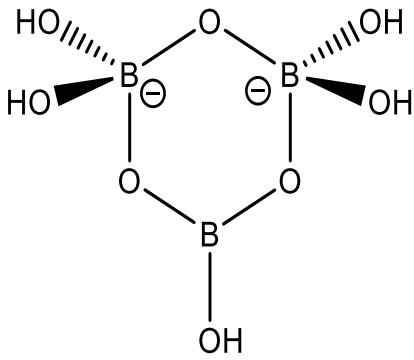
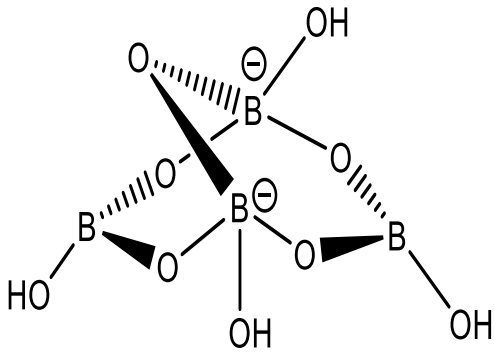
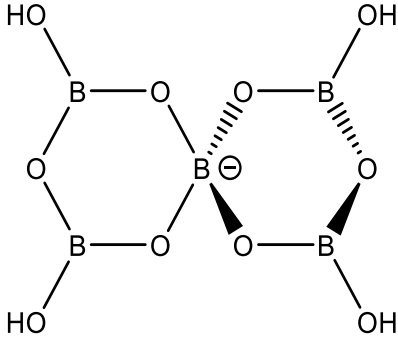
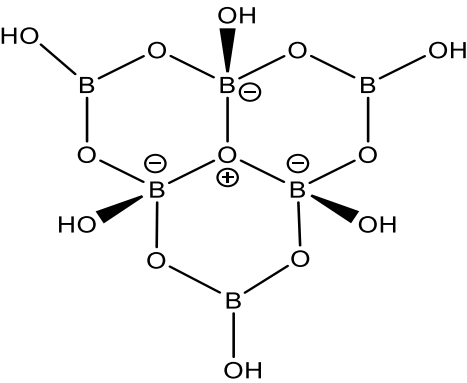
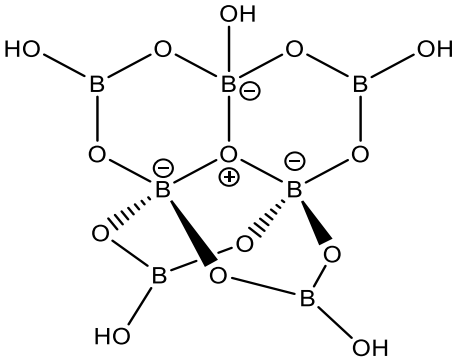
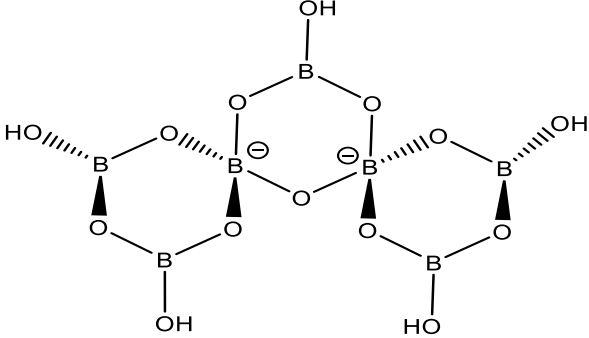


Figure 1.8 Variation in the distribution of boron species with solution pH at 25 °C. Total boron concentration is 0.4 M.⁴⁰

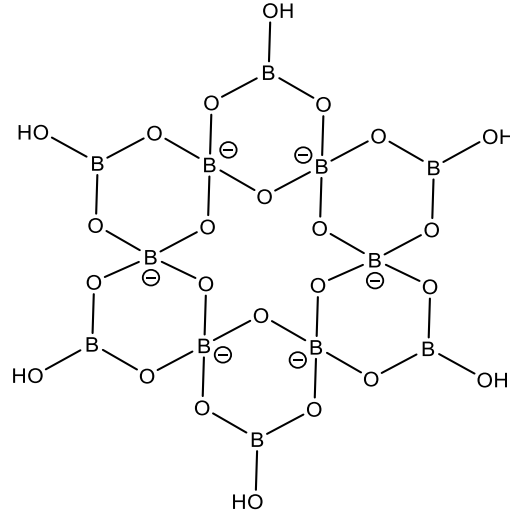
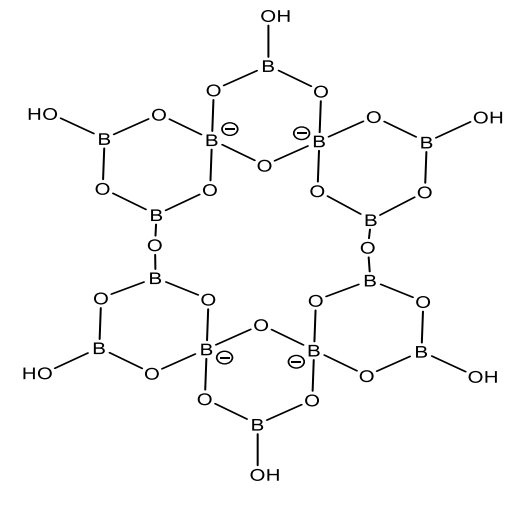
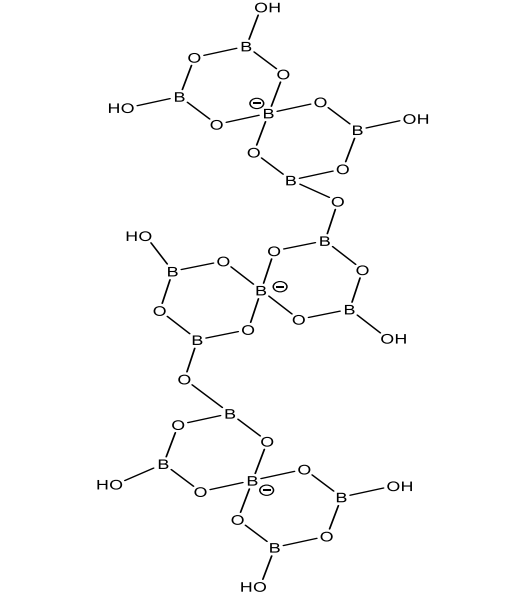
Table 1.1 Known isolated polyborate anion species.

Polyborate anion	Formula	Structure
Triangular borate unit	$B(OH)_3$	$ \begin{array}{c} OH \\ \\ B \\ / \quad \backslash \\ HO \quad OH \end{array} $

Tetrahedral borate unit	$B(OH)_4^-$	
Triborate(1-) anion	$[B_3O_3(OH)_4]^-$	
Triborate(2-) anion	$[B_3O_3(OH)_5]^{2-}$	
Tetraborate(2-) anion	$[B_4O_5(OH)_4]^{2-}$	

<p>Pentaborate(1-) anion</p>	$[B_5O_6(OH)_4]^-$	
<p>Hexaborate(2-) anion</p>	$[B_6O_7(OH)_6]^{2-}$	
<p>Heptaborate(2-) anion</p>	$[B_7O_9(OH)_5]^{2-}$	
<p>Heptaborate(2-) anion</p>	$[B_7O_9(OH)_5]^{2-}$	

Octaborate(2-) anion	$[\text{B}_8\text{O}_{10}(\text{OH})_6]^{2-}$	
Nonaborate(3-)	$[\text{B}_9\text{O}_{12}(\text{OH})_6]^{3-}$	
Dodecaborate(4-) anion	$[\text{B}_{12}\text{O}_{16}(\text{OH})_8]^{4-}$	

<p>Dodecaborate(6-)</p> <p>Anion</p>	$[B_{12}O_{18}(OH)_6]^{6-}$	
<p>Tetradecaborate(4-)</p> <p>Anion</p>	$[B_{14}O_{20}(OH)_6]^{4-}$	
<p>Pentadecaborate(3-)</p> <p>Anion</p>	$[B_{15}O_{20}(OH)_8]^{3-}$	

The structural units in Table 1.1 are referred to as hydrated borates due to the presence of B-OH groups and the absence of B-O⁻ groups. Many hydrated borates also contain interstitial water molecules and these compounds are referred to as hydroxy hydrated. The hydrated borate units can condense together into larger isolated clusters or infinite polyborate chains or networks. Boroxyl rings are common in polyborate structures and there are two primary modes connecting them. One mode involves the sharing of tetrahedral boron (Figure 1.9 A), such as in Na₂[B₄O₆(OH)₂]₂·3H₂O. The other mode of connection involves sharing exocyclic oxygen (Figure 1.9 B), such as Ca[B₃O₄(OH)₃]₂·H₂O.

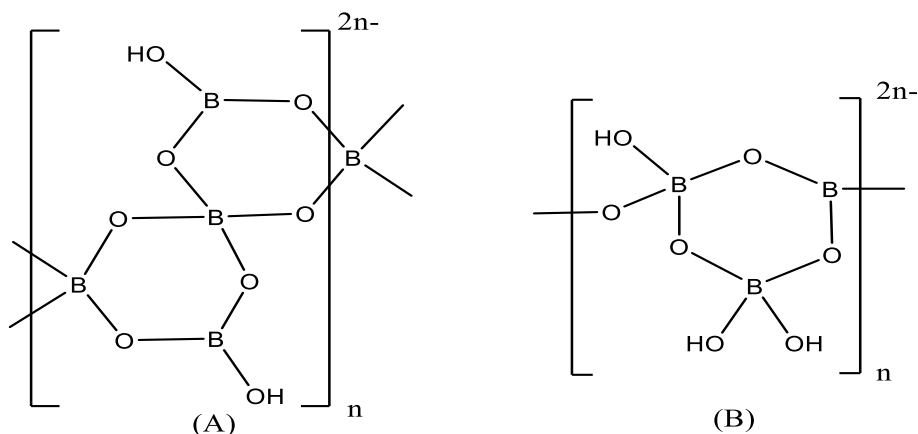


Figure 1.9 Two common modes of polymerization for boroxyl rings in infinite chain borates.

The polyborate anions are partnered by cations to form salts. These different cations can be classified into three main kinds: metal, non-metal, and transition metal complexes.

Over recent decades, many hydrated borate compounds have been prepared with a variety of main group metals, alkali metals, alkaline earth metals.^{38,39,41-68}

The metal cations are spherical and mostly accept electron density from oxygen atoms of hydrated borate units, with the metal cation acting as a Lewis acid. The acidity of the cationic metal unit should be very close to the basicity of the anionic hydrated borate unit to promote the formation of a stable metal borate compound.⁶⁹ The polyborate anions with a higher fraction of B₍₄₎ units are associated with higher average oxygen coordination numbers and higher average basicity (Table 1.2).

Table 1.2 The average O-CN with fraction of B₍₄₎ units of polyborate anions.⁷⁰

Isolated borate anion	Fraction B ₍₄₎	Formula	Average O-CN
[B(OH) ₄] ⁻	1.00	Ca[B(OH) ₄] ₂	4.0
[B ₄ O ₅ (OH) ₄] ²⁻	0.50	Na ₂ [B ₄ O ₅ (OH) ₄](H ₂ O) ₈	3.8
[B ₅ O ₆ (OH) ₄] ⁻	0.20	K(H ₂ O) ₂ [B ₅ O ₆ (OH) ₄]	3.2
[B ₅ O ₆ (OH) ₄] ⁻	0.20	Na[B ₅ O ₆ (OH) ₄](H ₂ O) ₃	3.0
[B ₁₅ O ₃₀ (OH) ₈] ³⁻	0.20	(NH ₄) ₃ [B ₁₅ O ₃₀ (OH) ₈](H ₂ O) ₄	2.8

In general, hydrated borate structural units with high Lewis basicity are commonly found in compounds partnered with metal cations of high Lewis acidity, while hydrated borate units with low Lewis basicity are often found with less Lewis acidic metal cation units or non-metal cations.

The second kind of cation is a non-metal cation derived from an organic base. The non-metal cation borate compounds have been studied far less than metal borate compounds. [NH₄][B₅O₆(OH)₄] \cdot 2H₂O, a mineral which is also synthetically available, was the first non-metal pentaborate compound to be prepared. Related non-metal cation containing quaternary ammonium cations were first prepared in 1959 with a resurgence of interest in the 1990's. In recent years these compounds of non-metal cations have attracted a great deal of attention^{2-5,28,69,71-109} due to their potential uses as non-linear optical (NLO) materials and their ability to act as a thermal precursors to new porous materials with many other applications.^{4,110}

Non-metal cations may interact with the borate structural units through hydrogen bonds rather than by direct coordination with borate oxygen units as in metal borates. Non-metal cations are mainly found as protonated Bronsted bases (mostly nitrogen containing bases). Non-metal cations exhibit a degree of Bronsted acidity and may be present as cations only over a given solution pH range. The variety of borate units with which a stable product can be produced are also dependent on the Bronsted acidity of non-metal cations. Hydrogen bonding is one of the most important factors that plays an important role in the stability and physical properties of non-metal borate materials.

More recently a new research area has been rapidly developing with the inclusion of transition metal complex cations in polyborate compounds.¹ Due to their interesting coordination chemistry and attractive physical properties, a great variety of structural chemistry is possible. However, these transition metal complex cation polyborate compounds have been less explored than metal and non-metal borate compounds. Compounds templated by

cobalt(III), cobalt(II), zinc(II), nickel(II), manganese(II), cadmium(II), silver(I) and copper(II) transition metal complexes have been reported.¹ At the time of writing this thesis the following list is exhaustive for isolated hydrated species: [Co₂(trien)₃][B₅O₆(OH)₄]₄, [Co(dien)₂][B₅O₆(OH)₄]₂, [B₅O₇Co(OH)₃(TREN)],¹¹¹ [Zn(dien)₂][B₅O₆(OH)₄]₂, [B₅O₇(OH)₃Zn(TREN)],¹¹² [Ni(C₄H₁₀N₂)(en)₂][B₅O₆(OH)₄]₂,¹¹³ [Zn(OAc)trien][B₅O₆(OH)₄],¹¹³ [Mn(C₁₀H₂₈N₆)]₂[B₅O₆(OH)₄]₂,¹¹⁴ [Ni(en)₃][B₅O₆(OH)₄]₂·2H₂O, [Co(en)₃][B₄O₅(OH)₄]Cl·3H₂O,¹¹⁵ [Cu(en)₂][B₇O₁₃H₃],¹¹⁶ [Co(en)₃][B₅O₆(OH)₄]₂·2H₂O,¹¹⁷ Na[V₁₂B₁₆O₅₀(OH)₇(en)₂(enH₂)₆(enH)₂(OH)(H₂O)₁₉],¹¹⁸ [Zn(B₄O₈H₂)(pn)]·H₂O, [Zn(B₅O₁₀H₃)(C₁₀H₂₄N₄)]·H₂O, [Zn(B₄O₈H₂)(pn)], [Zn₂(B₈O₁₅H₂)(pn)₂],¹¹⁹ [Co(en)₃][B₂P₃O₁₁(OH)₂],¹²⁰ [Co(pn)₃][B₅O₆(OH)₄]₂·H₂O, [Ni(pn)₃][B₅O₆(OH)₄]₂·H₂O,¹²¹ [Cu(PHEN)₂(OAc)][B₅O₆(OH)₄]·C₄H₉NO,¹²² [Cu(en)₂(C₅H₉NO)][B₅O₆(OH)₄]₂·C₅H₉NO,¹²³ [Cd(trien)(OAc)][B₅O₆(OH)₄],¹²⁴ [Ag(py)₂]₂[B₁₀O₁₄(OH)₄],¹²⁵ Co[B₆O₇(OH)₃{O(CH₂)₂NH₂}]₃, [Ni[B₆O₇(OH)₃{O(CH₂)₂NH₂}]₃],¹²⁶ [Cd(Dien)₂][B₅O₆(OH)₄]₂, [Cd(en)₃][B₅O₆(OH)₄]₂·2H₂O,¹²⁷ [Zn(pn)0.5(pn')0.5{B₄O₆(OH)₂}]·H₂O,¹²⁸ K₇{(BO₃)Zn(B₁₂O₁₈(OH)₆)}·H₂O,¹²⁹ [Zn(dien)₂][{Al(OH)}{B₅O₉F}],¹³⁰ [Cu(en)₂B(OH)₃][B₅O₅(OH)₇],¹³¹ Li₂Pb₂CuB₄O₁₀,¹³² Zn₈[(BO₃)₃O₂(OH)₃]¹³³ K₇[(BO₃)Mn{B₁₂O₁₈(OH)₆}]·H₂O,¹³⁴ (C₅H₁₁N₃)[Co{B₆O₇(OH)₆}]₂·4H₂O,¹³⁵ [Ni(en)₃][B₅O₆(OH)₄][OAc],¹³⁶ [Cu(en)₂][B₄O₅(OH)₄]·2B(OH)₃, 2{Cu(en)₂B(OH)₃H₂O[B₄O₅(OH)₄]}·H₂O, and {Cu(H₂O)₂[B₄O₅(OH)₄]₂}(μ-H₂O){Ag(en)₂}·(μ-H₂O){Na(H₂O)₂}.¹³⁷

Hydrated borates templated by transition metal complex cations are also favourable candidates for the preparation of open network materials. A few transition metal complex cation pentaborate salts have previously been isolated with interstitial moieties such as H₂O,¹¹⁷ CH₃CO₂⁻,¹³⁶ H₃BO₃,¹³⁷ and chloride,¹¹⁵ and a few transition metal complex cations with polyborate anion such as tetraborate,^{115,119,128,132} hexaborate,¹²⁶ heptaborate,^{138,116} octaborate,¹³⁹ decaborate¹²⁵ and dodecaborate^{129,134} have been previously prepared.

Transition metal complex cations can possess a range of chemical sizes and structural shapes, they also possess unique spatial configurations, different charges and flexibilities, and the possibility of many hydrogen bonding interactions. These properties may stabilize and develop unusual polyborate system, producing good opportunities to explore polyborate structural units and determine structure stability relationship.

1.5 Experimental techniques used to study borate chemistry

The new polyborate species presented in this thesis have been characterized by several techniques. X-ray crystallography (EPSPC National Crystallography Service at the University of Southampton) is essential to this study but new compounds have also been characterized by a range of other techniques. These include p-XRD, spectroscopic analysis (FT-IR, NMR, UV/Vis), magnetic susceptibility and thermal analysis (TGA/DSC). NMR is a useful technique for the study of polyborate anions and this is discussed fully in Section 1.6.

Polyborate anions usually contain both tetrahedral and trigonal planar boron centres, with B-O stretches particularly strong in IR spectra. IR stretching frequencies have been assigned by Li and coworkers¹⁴⁰ as follows: 1450-1300 cm^{-1} -asymmetrical $\text{B}_{(3)}\text{-O}$, 1150-1000 cm^{-1} asymmetrical $\text{B}_{(4)}\text{-O}$, 960-890 cm^{-1} symmetrical $\text{B}_{(3)}\text{-O}$, and 890-740 cm^{-1} symmetrical $\text{B}_{(4)}\text{-O}$.

Another useful technique for the study of transition metal borate complexes is by thermogravimetric analysis/differential scanning calorimetry (TGA/DSC). This is a thermal analysis method that is used to detect changing physical and chemical properties of material as measured by weight loss and heat exchange as the sample is heated at a uniform rate. The thermogravimetric analysis of hydrated transition metal borate complexes generally shows three mass loss steps.¹²⁴ The first mass loss step is observed between 50 and 190 °C, which belongs to the loss of interstitial water molecules. The second mass loss step is observed between 200 and 290°C and this is attributed to the condensation of polyborate ions with removal of water from borate ions. The third mass loss step is observed between 300 and 800°C, and they are related to oxygenolysis of ligands in the coordination sphere.

Elemental analysis also provides useful information on the stoichiometric composition of the transition metal complex borate compound. p-XRD can be used to confirm the crystallinity and homogeneity of a solid sample. Transition metal complexes are amenable to further study by UV/Vis spectroscopy and by magnetic susceptibility measurements.

Generally, transition metal complexes show absorption bands in the ultraviolet-visible spectral region. These absorption bands are related to charge transfer transitions (CT), and d-d transitions. Charge transfer transitions may be attributed to MLCT or LMCT transitions and they are intense absorptions. The d-d transitions appear as weak absorptions in the ultraviolet region or visible region (Figure 1.10). UV/Vis spectra are characterized by absorption maximum (λ_{max}) and extinction coefficient (ϵ).¹⁴¹

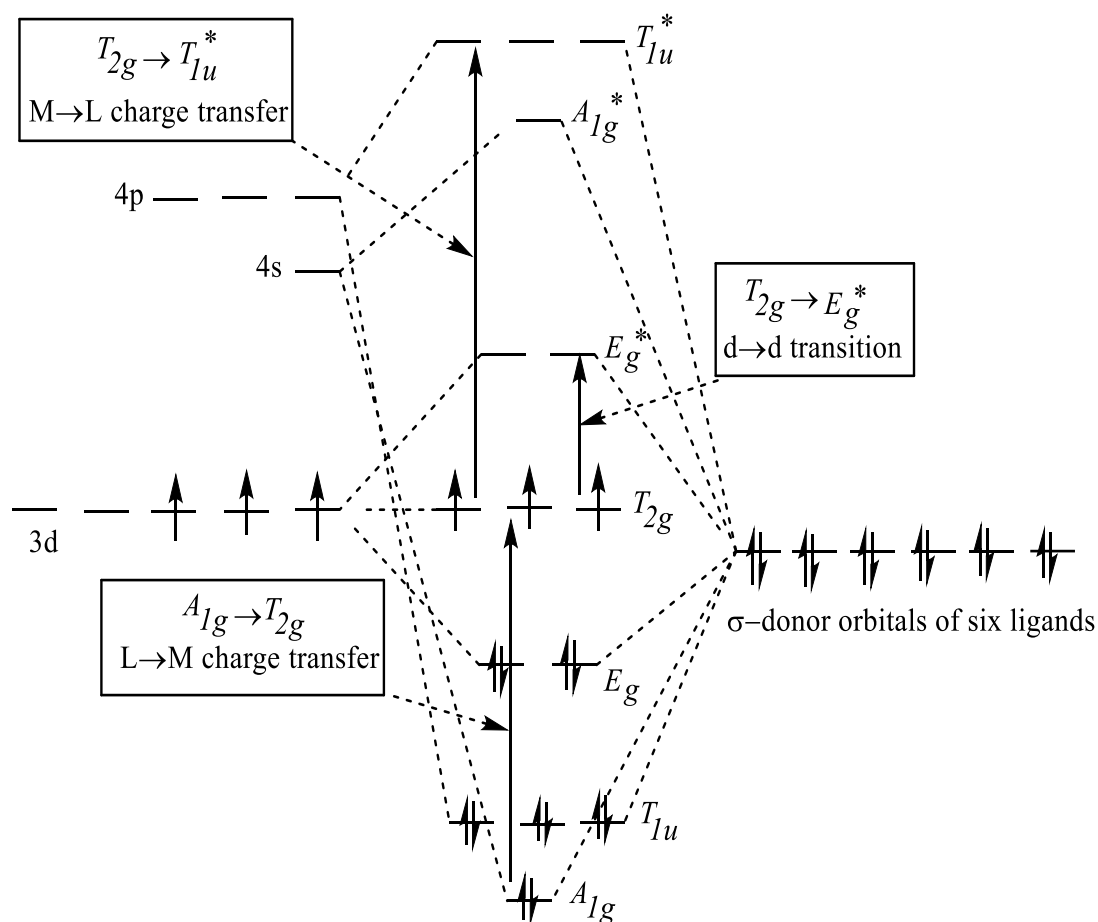


Figure 1.10 Possible electronic transition of the octahedral d^3 transition metal complexes.

Magnetic susceptibility measurements of transition metal complexes can be used to characterize their magnetic properties. Magnetic susceptibility measurements offer a source of information about the number of unpaired electrons. All transition metal complexes can be classified into one of three classes: those repelled by magnetic field (diamagnetic), those attracted to a magnetic field (paramagnetic), and the last class is ferromagnetic. The magnetic properties of paramagnetic and diamagnetic materials may only be observed in the presence of applied external magnetic field, while magnetic properties of ferromagnetic materials can be measured even after the external field is removed. The magnetic susceptibility can be defined as the ratio of the intensity of induced magnetism in a material to intensity of applied field.

The mass susceptibility, $\chi_{g(\text{observed})}$, as obtained using Johnson-Matthey balance, is calculated using Eq. 1.2. Where C = calibration constant of the balance, ℓ = length of the sample in cm, m = mass of the sample in grams, R = reading value for tube with sample. Generally, if

the sample is paramagnetic R is a large positive value, if the sample is diamagnetic R is a small negative value, and R_0 = value for tube and is generally small and negative. Mass susceptibility ($\chi_{g(\text{observed})}$) is converted to molar susceptibility ($\chi_{m(\text{observed})}$) by multiplying by formula mass (Eq. 1.3).

$$\chi_{g(\text{observed})} = \frac{C\ell(R - R_0)}{10^9 m} \quad (\text{Eq. 1.2})$$

$$\chi_{m(\text{observed})} = \chi_{g(\text{observed})} \times \text{MWt} \quad (\text{Eq. 1.3})$$

In general, if $\chi_{m(\text{observed})}$ value is positive and with a value of *ca.* 10^{-4} cgs units the compound is paramagnetic and if the $\chi_{m(\text{observed})}$ is negative the complex is diamagnetic. $\chi_{m(\text{observed})}$ needs to be corrected for diamagnetism since this is observed in all matter and the molar susceptibility $\chi_{m(\text{para})}$ is the sum of paramagnetic (caused by unpaired electrons) and diamagnetic terms (Eq. 1.4) (MWt is the molecular weight of the substance). From $\chi_{m(\text{para})}$ we can calculate the effective magnetic moment (μ_{eff}) (Eq. 1.6). We can then compare experimental value of μ_{eff} with the value obtained from 'spin-only' formula (Eq. 1.7) where n is the number of unpaired electrons.¹⁴²

$$\chi_{m(\text{para})} = \chi_{m(\text{observed})} - \chi_{m(\text{dia})} \quad (\text{Eq. 1.4})$$

$$\chi_{m(\text{dia})} \approx - \frac{\text{MWt}}{2} \cdot 10^{-6} \quad (\text{Eq. 1.5})$$

$$\mu_{\text{eff}} = 2.828 \times (\chi_{m(\text{para})} \times T)^{1/2} \quad (\text{Eq. 1.6})$$

$$\mu_{\text{eff}} = [n(n + 2)]^{1/2} \quad (\text{Eq. 1.7})$$

1.6 Nuclear magnetic resonance spectroscopy (NMR)

1.6.1 Introduction

The rapid progress in chemical analysis during the second half of the twentieth century has been mainly related to the development of nuclear magnetic resonance spectroscopy. NMR spectroscopy is one of the most powerful and theoretically complex analytical techniques. It is one of the few analytical techniques that does not require chemical processing and the chemical sample is neither destroyed nor consumed during the analysis. In 1946 Bloch *et al.*¹⁴³ and Purcell *et al.*¹⁴⁴ independently discovered NMR spectroscopy using liquid and solid samples, respectively. A brief overview of the some of the key concepts of nuclear magnetic resonance spectroscopy is now given with particular references to ¹H, ¹³C, and ¹¹B nuclei since these are the NMR spectra most commonly encountered in this thesis.

1.6.2 Nuclear spin (*I*)¹⁴⁵

Nuclei that have either an odd number of neutrons or protons (or both) possess a nuclear spin. *I* is the nuclear spin quantum number, and its values can be ½, 3/2...etc. Nuclei with nuclear spin quantum number values greater than zero are termed nuclear magnetic resonance active. Nuclei with an even number of both protons and neutrons have *I* = 0, and they are termed as NMR silent.

The NMR spectroscopy active nucleus with a spin of *I* possess (2*I* + 1) possible orientations in a magnetic field (*B*). For example, a hydrogen nucleus of spin *I* = 1/2 will have two possible orientations, *M_s* = ±½ (Figure 1.11).

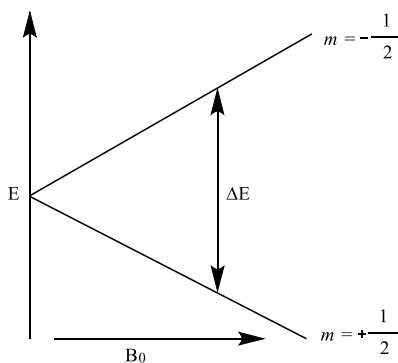


Figure 1.11 Energy levels for a nucleus with spin quantum number, *S* = 1/2.

In the absence of a magnetic field, all the spin states are of equal energy, however when an external magnetic field is applied then the spins states are no longer of equal energy. The lower energy level will contain slightly more nuclei than the higher energy level as described in the Boltzmann distribution law.

The NMR phenomenon occurs when nuclei aligned with the applied external magnetic field (B_0) are induced to absorb an identified amount of energy equal to the energy difference between the spin states involved and change their spin orientation ($\Delta m_I = \pm 1$). The energy difference is a function of the applied magnetic field B_0 (Figure 1.11), and it also depends on the particular nucleus involved. Each nucleus has a specific gyromagnetic ratio (γ) which is constant for a particular nucleus and determines the energy dependence on the applied magnetic field (Eq. 1.8 and Eq. 1.9).

$$\Delta E \propto \gamma B_0 \quad (\text{Eq. 1.8})$$

$$\Delta E = h/2\pi \gamma B_0 \quad (\text{Eq. 1.9})$$

1.6.3 Natural abundance

The vast majority of the elements have at least one nucleus that is NMR active. Taking carbon as an example, it has an average atomic mass of 12.01 and atomic number of six. With six neutrons and six protons the nucleus of carbon-12 would have $I = 0$ and hence be NMR inactive. Carbon however also has the isotope carbon-13. The spin of carbon-13 is $1/2$ and hence is NMR active. The amount of carbon-13 in existence is referred to as its natural abundance. The natural abundance of an NMR active nuclei is a significant factor in the receptivity of the nucleus. The magnetic resonance properties of selected atomic nuclei are listed in Table 1.3.

Table 1.3 Magnetic resonance properties of selected atomic nuclei.¹⁴⁵

Nucleus	Spin	Natural abundance (%)	Magnetogyric ratio $\gamma \times 10^{-8}$ (rad S ⁻¹ T ⁻¹)	Nucleus	Spin	Natural abundance (%)	Magnetogyric ratio $\gamma \times 10^{-8}$ (rad S ⁻¹ T ⁻¹)
¹³ C	1/2	1.108	0.6728	¹⁴ N	1	99.63	0.1933
¹ H	1/2	99.99	2.6752	¹⁵ N	1/2	0.365	-0.2711
² H	1	0.015	0.4107	¹⁹ F	1/2	100	2.516
¹¹ B	3/2	81.17	0.8583	²⁹ Si	1/2	4.70	-0.531
¹⁰ B	3	18.83	0.2875	³¹ P	1/2	100	1.082

¹⁰B and ¹¹B are both NMR active with natural abundance 19.9 and 80.1% respectively. Both nuclei have overall spins of more than 1/2 and they are termed quadrupolar.¹⁴⁶ In general, ¹¹B is preferred to ¹⁰B nuclei in NMR spectroscopy due to its higher natural abundance, sensitivity, and lower quadrupole moment. However, the rapid relaxation times and higher sensitivity of ¹¹B nuclei generally leads to well defined, but broad, signals in NMR spectra.

1.6.4 The NMR experiment¹⁴⁵

A short pulse of radiofrequency (*ca.* 20 μ s) irradiates the chemical sample which causes an excitation and promotion of nuclei from a ground state to an excited state ($\Delta m_I = \pm 1$). Some of the energy gain is re-emitted when the excited nuclei fall back down into the original energy level. This process is called the free induction decay (FID), which is recorded at times ranging from milliseconds to seconds, depending on the nuclei used and is called the acquisition time (t_{aq}). The whole process of t_{aq} is repeated many times, so as to improve the signal to noise ratio in the spectrum and the resulting free induction decays are added together. When the FID undergoes Fourier transformation (FT), a spectrum is obtained.

1.6.5 Relaxation¹⁴⁷

The excited nuclei in a NMR sample experiment may relax back to the thermal equilibrium by dispersion of their gained excited energy. There are two pathways to describe the mechanism of the nuclei relaxation in the NMR experiment.

- (1) **Spin-lattice relaxation mechanism:** the spin lattice relaxation time, T_1 , corresponds to an exchange energy between nuclear spin system and neighbouring molecules (the lattice).
- (2) **Spin-spin relaxation mechanism:** the spin-spin relaxation time, T_2 , which results from an exchange of energy between the individual spins in the system.

1.6.6 The chemical shift (δ)

The chemical shift of a nucleus is the resonant frequency of a nucleus relative to a chemical standard in a magnetic field, therefore according to the local chemical environment, different nuclei in a molecule resonate at different frequencies. Tetramethylsilane (TMS) is used as an external standard reference for ^1H , ^{13}C , and ^{29}Si NMR spectroscopy, while boron trifluoride diethyl etherate, $\text{BF}_3 \cdot \text{OEt}_2$, is used as an external reference for ^{11}B -NMR.¹⁴⁸

The chemical shift for a particular signal is given in part per million (ppm). The chemical shift of most ^1H NMR signals are observed between +0 and +10 ppm (normally between -20 and +30 ppm), the chemical shift of ^{13}C NMR signals are observed between -20 and +200 ppm, while the total chemical shift range of ^{11}B NMR also covers about +200 ppm.

There are many factors that affect the chemical shift of boron such as quadrupolar effects and the coordination number of boron.¹⁴⁶ The coordination number of boron is an important factor that affects the chemical shift, so the chemical shift of a tetrahedral boron sp^3 species are shifted more up field (+20 to -128 ppm) than a trigonal boron sp^2 species (+92 to -8 ppm), this shifted can be attributed to increase the electron density around the tetrahedral boron centre, which causes an increase in the nuclear shielding, so there is an associated upfield shift compared to three-coordinate species.

1.7 NMR applied to polyborate species

One method for analysing and studying borate compounds is NMR spectroscopy of the ^{11}B nucleus. The individual borate species may possess diagnostic chemical shifts which are easily identifiable.

The chemical shift regions of pure trigonal $\text{B}(\text{OH})_3$ and tetrahedral $[\text{B}(\text{OH})_4]^-$ units appear at +19.48 ppm and +2.48 ppm, respectively.¹⁴⁹ The structural information on borate anions in solution is complicated due to the equilibria of borate anions in solutions.^{150,151} The ^{11}B -NMR spectrum of a concentration solution of hydrated potassium pentaborate, $\text{K}[\text{B}_5\text{O}_6(\text{OH})_4] \cdot 2\text{H}_2\text{O}$ shows three peaks at +18, +13, and +1 ppm which are attributed to $\text{B}(\text{OH})_3/[\text{B}(\text{OH})_4]^-$, $[\text{B}_3\text{O}_3(\text{OH})_4]^-$, and $[\text{B}_5\text{O}_6(\text{OH})_4]^-$, respectively. These signals are concentration dependent. According to Salentine,¹⁴⁹ approximately 90% of a solid pentaborate salt dissociates in solution by hydrolysis to give $\text{B}(\text{OH})_3$, $[\text{B}(\text{OH})_4]^-$, and $[\text{B}_3\text{O}_3(\text{OH})_4]^-$ species. The resonance at +18 ppm is due to $\text{B}(\text{OH})_3/[\text{B}(\text{OH})_4]^-$ ion. The signal at +13 ppm belongs to the triborate ion $[\text{B}_3\text{O}_3(\text{OH})_4]^-$. The resonance at +1 ppm arises from the $[\text{B}_5\text{O}_6(\text{OH})_4]^-$ ion. This

signal is assigned to the 4-coordinate B centre and the 3-coordinate B centres are not observed due to exchange/relaxation effects.

In dilute NMR samples, where the polyborates are absent, only a single peak is observed due to $B(OH)_3/[B(OH)_4]^-$ exchange. The chemical shift of this peak can be predicted by using Eq. 1.10, which can be derived from Salentine observations. Where $\delta_{tet.}$ is the chemical shift of tetrahedral $[B(OH)_4]^-$ (+2.48 ppm), while δ_{tri} is the chemical shift of trigonal $B(OH)_3$ (+19.48 ppm), and $\delta_{obs.}$ is the observed chemical shift of the borate sample. By rearrangement of Eq. 1.10, the boron:base ratio in dilute NMR sample can be calculated by using Eq. 1.11 and Eq. 1.12.

$$\delta_{obs.} = \delta_{tet.} + \left(\frac{\text{No. of B atoms} - \text{Charge of anion}}{\text{No. of B atoms}} \right) \cdot (\delta_{tri.} - \delta_{tet.}) \quad (\text{Eq. 1.10})$$

$$B: base = \frac{1}{1 - \left(\frac{\delta_{obs.} - \delta_{tet.}}{\delta_{tri.} - \delta_{tet.}} \right)} \quad (\text{Eq. 1.11})$$

$$B: base = \frac{17.00}{19.48 - \delta_{obs.}} \quad (\text{Eq. 1.12})$$

Chapter Two

Polyborate salts containing cationic cobalt(III) complexes

The work presented within this chapter has been published in the following journal articles:

M.A. Altahan, M.A. Beckett, S.J. Coles, P.N. Horton, *Inorg. Chem.*, 2015, **52**, 412-414.

M.A. Altahan, M.A. Beckett, S.J. Coles, P.N. Horton, *Inorg. Chem. Commun.*, 2015, **59**, 95-98.

M.A. Altahan, M.A. Beckett, S.J. Coles, P.N. Horton, *phosphorus, Sulfur, and Silicon*, 2016, **191**, 572-575.

2.1 Introduction

The chemistry of polyborate anions partnered with cobalt complexes shows great structural diversity. Salts containing isolated polyborate anions with cobalt complex cations are known in the literature: $[\text{Co}(\text{dien})_2][\text{B}_5\text{O}_6(\text{OH})_4]_2$,^{111,152} $[\text{Co}_2(\text{trien})_3][\text{B}_5\text{O}_6(\text{OH})_4]_4$,¹¹¹ $[\text{Co}(\text{en})_3][\text{B}_4\text{O}_5(\text{OH})_4]\text{Cl}\cdot 3\text{H}_2\text{O}$,¹¹⁵ $[\text{Co}(\text{en})_3][\text{B}_5\text{O}_6(\text{OH})_4]_2\cdot 2\text{H}_2\text{O}$,¹¹⁷ $[\text{Co}(\text{en})_3][\text{B}_2\text{P}_3\text{O}_{11}(\text{OH})_2]$,¹²⁰ and $[\text{Co}(\text{pn})_3][\text{B}_5\text{O}_6(\text{OH})_4]_2\cdot \text{H}_2\text{O}$.¹²¹ Complexes of cobalt are also known in which the polyborate anion is formally within the first coordination sphere of the metal centre. These is illustrated with the anionic complexes $\text{Rb}_2[\text{Co}\{\text{B}_6\text{O}_7(\text{OH})_6\}_2]$,¹⁵³ $(\text{C}_4\text{H}_{12}\text{N}_2)[\text{Co}\{\text{B}_6\text{O}_7(\text{OH})_6\}_2]\cdot 6\text{H}_2\text{O}$ ¹⁵⁴ and $(\text{C}_5\text{H}_{11}\text{N}_3)[\text{Co}\{\text{B}_6\text{O}_7(\text{OH})_6\}_2]\cdot 4\text{H}_2\text{O}$,¹³⁵ all of which a coordinated tridentate $[\text{B}_6\text{O}_7(\text{OH})_6]^{2-}$ ligand. This coordination mode is also observed in the neutral complex, $[\text{Co}\{\text{B}_6\text{O}_7(\text{OH})_3\}\{\text{O}(\text{CH}_2)_2\text{NH}_3\}_3]$,¹²⁶ whilst the neutral complex $[\{\text{B}_5\text{O}_7(\text{OH})_3\}\text{Co}(\text{TREN})]$, (TREN = tris(2-aminoethyl)amine)¹¹¹ has the $[\text{B}_5\text{O}_7(\text{OH})_3]^{2-}$ ligand coordinated in a mono dentate manner *via* an anionic (deprotonated) oxygen centre of a pentaborate(2-) anion.

In this chapter, we report the synthesis and characterisation of nine new polyborate salts of cobalt(III) complex cations. These salts all contain isolated polyborate anions. Four of the salts have been characterized by single-crystal XRD studies and *s-fac*- $[\text{Co}(\text{dien})_2][\text{B}_7\text{O}_9(\text{OH})_6]\cdot 9\text{H}_2\text{O}$ ¹³⁸ and $[\text{Co}(\text{en})_3][\text{B}_8\text{O}_{10}(\text{OH})_6][\text{B}_5\text{O}_6(\text{OH})_4]\cdot 5\text{H}_2\text{O}$ ¹³⁹ show previously unobserved heptaborate(3-) and octaborate(2-) anions, respectively.

2.2 Aims

The primary aim of this research area was to synthesize novel polyborate anions, using a strategy of templating such species using sterically demanding and/or highly charged cations. A set of cationic cobalt(III) coordination complexes of ethylenediamine (en), 1,8-dinitro-3,6,10,13,16,19-hexaazabicyclo-(6.6.6)icosane (diNOsar), 1,2-diaminopropane (pn), NH_3 , and diethylenetriamine (dien) ligands were prepared to template polyborate salt formation. The cobalt(III) complex cations were chosen due to their high charge and their potential to form many donor H-bond interactions in their coordination sphere. Since these interactions play an important role in the formation of the three-dimensional supramolecular frameworks in polyborate salts.

The secondary aim is to evaluate the structure directing effects associated with the cobalt(III) complex cations seen in the solid-state supramolecular structures.

2.3 Result and discussion

2.3.1 Synthesis of cobalt(III) complex chlorides

The known cobalt(III) complexes $[\text{Co}(\text{en})_3]\text{Cl}_3 \cdot 2\text{H}_2\text{O}$ (**1**),¹⁵⁵ $[\text{Co}(\text{NH}_3)_6]\text{Cl}_3$ (**2**),¹⁵⁶ $[\text{Co}(\text{dien})_2]\text{Cl}_3 \cdot 2\text{H}_2\text{O}$ (**3**),¹³ $[\text{Co}(\text{diNOsar})]\text{Cl}_3$ (**4**),¹⁵⁷ and $[\text{Co}(\text{pn})_3]\text{Cl}_3$ (**5**),¹⁵⁸ of ethylenediamine (en), NH_3 , diethylenetriamine (dien), 1,8-dinitro-3,6,10,13,16,19-hexaazabicyclo-(6.6.6)icosane (diNOsar), and 1,2-diaminopropane (pn) ligands were all prepared by standard literature methods. Physical properties of the prepared complexes were all in accord with literature data.

Compounds **1-5** were all prepared as their chloride salts and it was therefore necessary to convert these chloride salts to the corresponding hydroxide salts before reaction with boric acid. The hydroxide salts were prepared by ion exchange using Dowex 550A (OH^- form) from the chloride salts in aqueous solution. It was assumed that the hydroxide complex salts were formed in quantitative yields by the ion exchange reaction. The experiment details are explained in Chapter 6.

2.3.2 Preparation of cobalt(III) complex polyborate salts

A series of cobalt(III) complex polyborate salts **6-14** have been prepared as crystalline solids from cobalt(III) complex hydroxides. Boric acid was added in the ratios of 1:5, 1:7, 1:10, and 1:15 to the hydroxide solutions. The solutions were then stirred, concentrated using a rotary evaporator and cooled to yield polyborate salts as solid crude products (**6-14**). The crude products were isolated by filtration and dried.

Crystals suitable for single-crystal X-ray diffraction studies of the cobalt(III) complex polyborate salts were prepared by recrystallization of the crude products by dissolving them in distilled water. The recrystallized products were isolated by slow evaporation from aqueous solution or by vapour diffusion from aqueous solution using ethanol. The recrystallized yields of the cobalt(III) complex polyborate salts (**6-14**) and their formula are shown in Table 2.1.

Table 2.1 Yields of cobalt(III) complex polyborate salts.

Compound	Formula	% Yield
6	[Co(en) ₃][B ₅ O ₆ (OH) ₄][B ₈ O ₁₀ (OH) ₆]·5H ₂ O	41
7	[Co(en) ₃][B ₅ O ₆ (OH) ₄] ₂ Cl·3H ₂ O	57
8	[Co(en) ₃][B ₇ O ₉ (OH) ₆]·6H ₂ O	45
9	[Co(NH ₃) ₆] ₂ [B ₄ O ₅ (OH) ₄] ₃ ·11H ₂ O	41
10	[Co(NH ₃) ₆][B ₇ O ₉ (OH) ₅]Cl·5H ₂ O	36
11	<i>s-fac</i> -[Co(dien) ₂][B ₇ O ₉ (OH) ₆]·9H ₂ O	35
12	[Co(diNOsar)] ₂ [B ₃ O ₃ (OH) ₄] ₂ Cl ₅ ·4.75H ₂ O	10
13	[Co(diNOsar)][B ₅ O ₆ (OH) ₄] ₂ Cl·3H ₂ O	54
14	[Co(pn) ₃][B ₅ O ₆ (OH) ₄] ₂ Cl·3H ₂ O	50

2.3.3 Characterisation of cobalt(III) complex polyborate salts

The magnetic properties of the cobalt(III) complex starting materials and their polyborate salts were measured at room temperature using a Johnson Matthey electronic balance with mercury tetrathiocyanatocobaltate(II) as a calibrant. The mass susceptibility and molar susceptibility of compounds **1-14** are shown in Table 2.2. The cobalt(III) complexes and their polyborate salts are all diamagnetic and there is no diagnostic change in magnetic properties between the starting cobalt(III) complex chlorides and their polyborate salts. The cobalt(III) complexes are all low-spin d⁶, and the magnetic susceptibility values are comparable to literature data on typical cobalt(III) complexes.¹⁵⁹

Table 2.2 Mass and molar susceptibility of cobalt(III) complexes and their polyborate salts at 24 °C.

Comp.	Mass susceptibility χ_g (cm ³ .g ⁻¹)	Molar susceptibility χ_m (cm ³ .mol. ⁻¹)	Comp.	Mass susceptibility χ_g (cm ³ .g ⁻¹)	Molar susceptibility χ_m (cm ³ .mol. ⁻¹)
1	-0.40 × 10 ⁻⁶	-155 × 10 ⁻⁶	8	-0.38 × 10 ⁻⁶	-255 × 10 ⁻⁶
2	-0.46 × 10 ⁻⁶	-123 × 10 ⁻⁶	9	-0.30 × 10 ⁻⁶	-330 × 10 ⁻⁶
3	-0.20 × 10 ⁻⁶	-83 × 10 ⁻⁶	10	-0.06 × 10 ⁻⁶	-37 × 10 ⁻⁶
4	-0.32 × 10 ⁻⁶	-167 × 10 ⁻⁶	11	-0.16 × 10 ⁻⁶	-120 × 10 ⁻⁶
5	-0.34 × 10 ⁻⁶	-133 × 10 ⁻⁶	12	-0.02 × 10 ⁻⁶	-25 × 10 ⁻⁶
6	-0.11 × 10 ⁻⁶	-101 × 10 ⁻⁶	13	-0.05 × 10 ⁻⁶	-50 × 10 ⁻⁶
7	-0.30 × 10 ⁻⁶	-230 × 10 ⁻⁶	14	-0.25 × 10 ⁻⁶	-200 × 10 ⁻⁶

Elemental analysis of the new cobalt(III) complex polyborate salts were consistent with their formulation. The elemental analysis data of the new polyborate salts (**6-14**) are shown in Table 2.3.

Table 2.3 CHN analysis of cobalt(III) complex polyborate salts.

Compound	Calculated (%)			Experimental (%)		
	C	H	N	C	H	N
6	8.0	4.9	9.4	8.2	5.0	9.6
7	9.4	5.0	11.0	9.7	4.8	10.5
8	10.8	6.4	12.3	10.7	6.3	12.6
9	-	6.4	15.4	-	6.5	15.4
10	-	5.6	14.2	-	5.6	14.1
11	12.8	6.7	11.2	13.4	7.2	11.1
12	26.4	5.8	17.5	25.6	6.5	16.7
13	18.4	5.1	12.3	18.3	5.0	12.4
14	13.4	6.5	10.4	13.6	6.3	10.4

NMR (^1H , ^{13}C , ^{11}B) data for compounds **6-14** are shown in Table 2.4. ^{11}B NMR of the cobalt(III) complex polyborate salts showed that all the pentaborate salts **7**, **13**, and **14** contained the expected three signals associated with an equilibrium mixture at ~ 18 ppm (due to $\text{B}(\text{OH})_3/\text{B}(\text{OH})_4^-$), ~ 13 ppm {due to $[\text{B}_3\text{O}_3(\text{OH})_4]^-$ }, and at ~ 1.3 ppm {due to the 4-coordinate B centre of the $[\text{B}_5\text{O}_6(\text{OH})_4]^-$ } or a single signal at $\sim +16.0$.¹⁴⁹⁻¹⁵¹ ^{11}B NMR spectra of the triborate (**12**), tetraborate (**9**), heptaborate (**8**, **10**, and **11**) salts are noticeably different from the spectra observed in the pentaborate salts with only one (averaged and exchanging) signal observed. The octaborate salt (**6**) shows two peaks at $+16.5$ and $+13.4$ ppm.

^1H NMR analysis of compounds **6-8** showed two signals at 2.7 ppm (due to protons of the en ligands) and at 4.8 ppm (due to exchanging $\text{BOH}/\text{NH}_2/\text{H}_2\text{O}$ protons). These spectra are consistent with previously reported data.¹⁶⁰ Compound **11** displayed two broad multiplets at 3.0 and 3.2 ppm (due to the methylene groups of the dien ligands) and an additional signal at 4.8 ppm (due to exchanging $\text{BOH}/\text{NH}_2/\text{H}_2\text{O}$ protons). The relative intensities of peaks in the CH_2 region were 1:3. The *s-fac* arrangement of the diethylenetriamine ligands gives rise to prochiral ethylene carbon centres and four inequivalent hydrogen atom sites and three of which overlap in the high field signal. The data we have found for **11** is in agreement with that reported for *s-fac*- $[\text{Co}(\text{dien})_2]\text{Cl}_2(\text{Bz})\cdot\text{H}_2\text{O}$ ¹⁶¹ and comparable with literature data.^{138,161} Compounds **12** and **13** showed two overlapping quartets, associated with the AB pattern of the en and cap methylene groups. In addition, they show one signal assigned to exchanging $\text{BOH}/\text{NH}_2/\text{H}_2\text{O}$ protons. ^1H NMR data of **12** and **13** are all in accord with previously reported data of $[\text{Co}(\text{diNOsar})]\text{Cl}_3$.^{157,162} The resonances assigned to protons H_1 and H_2 of **14** occurring at 3.0 ppm and 2.9 ppm, respectively are distinguishable (Figure 2.1). The H_1 resonance is a multiplet due to spin-coupling with H_2 , H_3 and methyl group protons of each 1,2-diaminopropane ligand,

while H₂ appears as a doublet of doublets arising from coupling with H₁ and H₃. The signal associated with H₃ occurs at 2.5 ppm and consist of a doublet of doublets due to coupling with H₁ and H₂. Methyl group protons appear as a doublet at 1.3 ppm due to coupling with H₁ and an additional resonance at 4.8 ppm attributed to exchanging BOH/NH₂/H₂O protons. The ¹H NMR data of compound **14** is compatible with that previously reported for [Co(pn)₃]Cl₃.¹⁶⁰

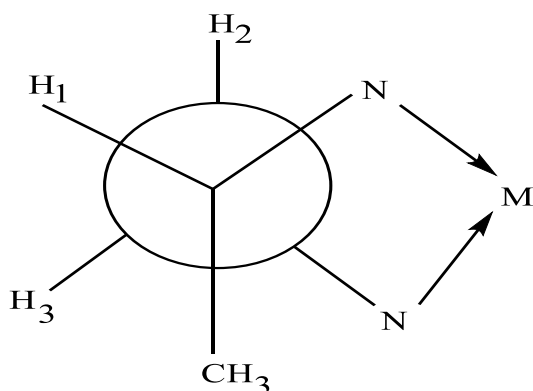


Figure **2.1** Diagram showing the protons of propylene diamine ligand and the adopted numbering scheme in compound **14**.

¹³C NMR spectra of compounds **6-8** show only one peak for each complex in a range consistent with coordinated ethylenediamine ligand.¹⁶⁰ Compound **11** displayed two signals for the dien ligand. These signals are consistent with literature data.^{138,161} Three signals are observed in **12** and **13** at ~51 ppm (due to methylene groups of the ethylenediamine ring residues), ~55 ppm (due to methylene groups of the capping units), and a signal at ~87 ppm (due to the tertiary carbon of the caps). These signals are in agreement with literature data.^{157,162} Compound **14** shows three signals at 16.5 ppm (due to carbon methyl –CH₃ group), 49.9 ppm (belonging to the carbon methylene –CH₂ group), and a signal at 53.9 ppm (due to carbon CH group). The ¹³C NMR spectrum of compound **14** is consistent with literature data.¹⁶⁰

Table 2.4 ^1H , ^{13}C , and ^{11}B NMR data for compounds **6-14**.

Comp.	^{11}B /ppm	^1H /ppm	$^{13}\text{C}\{^1\text{H}\}$ /ppm
6	16.5 (85%), 13.4 (15%)	2.7 (m, 12H, CH_2 of en), 4.8 (s, 32H, exchanging $\text{BOH}/\text{NH}_2/\text{H}_2\text{O}$ protons)	44.5 (CH_2 groups of the en)
7	17.4 (59%), 12.9 (33%), 1.2 (8%)	2.7 (m, 12H, CH_2 of en), 4.8 (s, 26H, exchanging $\text{BOH}/\text{NH}_2/\text{H}_2\text{O}$ protons)	44.3 (CH_2 groups of the en)
8	13.0	2.7 (m, 12H, CH_2 of en), 4.8 (s, 30H, exchanging $\text{BOH}/\text{NH}_2/\text{H}_2\text{O}$ protons)	44.2 (CH_2 groups of the en)
9	10.4	4.8 (s, 70H, exchanging $\text{BOH}/\text{NH}_3/\text{H}_2\text{O}$ protons)	-
10	13.4	4.8 (s, 33H, exchanging $\text{BOH}/\text{NH}_3/\text{H}_2\text{O}$ protons)	-
11	12.3	3.0 (m, 12H, CH_2), 3.2 (m, 4H, CH_2), 4.8 (s, 34H, exchanging $\text{BOH}/\text{NH}/\text{NH}_2/\text{H}_2\text{O}$ protons)	43.3 (CH_2 groups of the dien connect to NH_2), 55.0 (CH_2 groups of the dien connect to NH)
12	16.2	3.3, 3.9 (AB doublet of doublet, 12H, $J = 12$ Hz, CH_2 Caps), 2.9, 3.5 (complex AA'BB' coupling pattern, 12H, CH_2 of en), 4.8 (s, 25.5H, exchanging $\text{BOH}/\text{NH}/\text{H}_2\text{O}$ protons)	51.4 (CH_2 groups of the en), 55.1 (CH_2 groups of the capping units), 87.9 (tertiary C- NO_2 of the caps)
13	15.9	3.4, 3.9 (AB doublet of doublet, 12H, $J = 12$ Hz, CH_2 Caps), 3.0, 3.6 (complex AA'BB' coupling pattern, 12H, $J = 8$ Hz, CH_2 of en), 4.8 (s, 16H, exchanging $\text{BOH}/\text{NH}/\text{H}_2\text{O}$ protons)	51.3 (CH_2 groups of the en), 55 (CH_2 groups of the capping units), 87.8 (tertiary C- NO_2 of the caps)
14	16.6 (56%), 13.0 (33%), 1.3 (11%)	1.3 (m, 9H, CH_3 of pn), 2.5 (t, 3H, $J = 13.2$ Hz, $J = 26.4$ Hz, C_b of CH_2 of pn), 2.9 (m, 3H, H_a of CH_2 of pn), 3.0 (m, 3H, CH of pn), and 4.8 (s, 26H, exchanging $\text{BOH}/\text{NH}_2/\text{H}_2\text{O}$ protons)	16.5 (CH_3 of pn), 49.9 (CH of pn), 53.9 (CH_2 of pn)

The FT-IR spectra and their tentative assignment for the new polyborate salts **6-14** are shown in Table 2.5. Infra-red spectroscopic investigation confirmed the formation of polyborate anions within the cobalt(III) salts. The FT-IR data of compounds **6-14** have been assigned by comparison with assignment (data of Jun *et al.*)¹⁴⁰ for related polyborate anions.

Table 2.5 Selected frequencies of FT-IR spectra of the new polyborate salts **6-14**.

Comp.	$\nu(\text{O-H}),$ $\nu(\text{N-H})$	ν (C-H)	ν_{as} (B ₍₃₎ -O)	δ (B-O-H)	ν_{as} (B ₍₄₎ -O)	ν_{s} (B ₍₃₎ -O)	ν_{s} (B ₍₄₎ -O)	γ (B ₍₃₎ -O)
6	3461(s), 3265(s), 3149(s)	2960(w)	1394(s), 1324(s)	1170(s)	1059(s), 1033(m)	939(s)	779(m)	710(w)
7	3267(s), 3167(s)	2945(w)	1409(s), 1302(s)	1154(m)	1057(m), 1007(m)	916(m)	895(m), 785(m)	709(m)
8	3413(s), 3253(s)	2926(w), 2855(w)	1385(s), 1322(s)	1162(m)	1058(s), 1005(s)	930(m)	825(w), 757(w)	702(w)
9	3400(s), 3308(s)	-	1421(s), 1384(s)	1190(s)	1015(s)	995(s), 943(m)	809(m)	704(w)
10	3477(s), 3407(s), 3320(s)	-	1440(s), 1401(m)	1164(m)	1114(s), 1037(s)	954(m)	852(m), 800(m)	767(w)
11	3432(s), 3201(s), 3095(s)	2950(m)	1415(s), 1385(s)	1134(m)	1084(s), 1047(s)	932(m)	861(m), 750(w)	656(w)
12	3552(s), 3475(s), 3413(s), 3236(m)	2866(m)	1432(m), 1343(m)	1134(w)	1076(m), 1018(w)	988(w), 952(w)	847(w), 812(w)	620(m)
13	3437(s), 3025(s)	2859(s)	1447(s), 1348(s)	1100(m)	1078(m)	925(m)	810(m)	696(w)
14	3437(s), 3249(m)	2925(m)	1435(s), 1352(s)	1238(w)	1091(m), 1023(m)	925(m)	780(w)	692(w)

s = strong, m = middle, w = weak, B₍₃₎ = three coordinate boron, B₍₄₎ = four coordinate boron, ν = stretching frequency, ν_{s} = symmetrical stretching frequency, ν_{as} = asymmetrical stretching frequency, δ = bending frequency.

2.3.4 Thermal properties of cobalt(III) complex polyborate salts

Thermal gravimetric analysis (TGA) and differential scanning calorimetry (DSC) analysis were used to investigate the thermal properties of the new cobalt(III) complex polyborate salts. Samples were heated in an alumina (Al₂O₃) crucible at a temperature ramp rate of 10 °C / min between 25-800 °C under a flow air (100 mL / min.). The thermal decomposition stages of compounds **6-14** are detailed in Table 2.6. Hydrated transition metal complex polyborate salts undergo three mass-loss steps to form anhydrous transition metal borates.¹²⁴ The first mass loss step is due to the loss of interstitial water molecules and the temperature at which this happens varies from compound to compound but is generally complete by 180 °C. The release of these water molecules is associated with an endothermic peak in the DSC trace. The second mass loss step is due to dehydration of the isolated polyborate anions, by the formation of B-O-B bonds and polymeric polyborate anions (Figure 2.2). The temperature at which this step happens again varies from compound to compound but it is generally complete by 280 °C. The release of water molecules from polyborate anions is

also associated with an endothermic peak in the DSC trace. The last mass-loss step again varies from compound to compound and the reaction is generally complete by 800 °C. This reaction relates to the oxidation of the organic ligands around the transition metal of the cation along with elimination of any remaining water molecules. The oxidation of the cation is associated with a corresponding exothermic peak in the DSC trace.

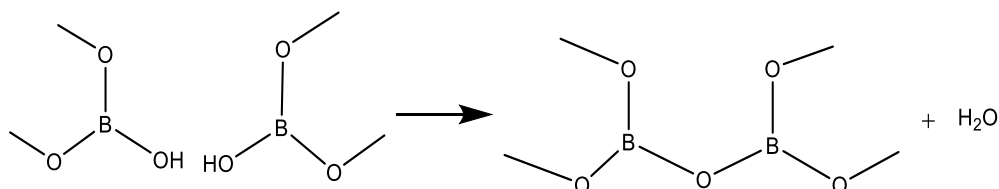


Figure 2.2 An illustration of the second mass-loss process in thermal decomposition of polyborate anions.

Table 2.6 The mass loss steps of the new polyborate salts 6-14.*

Comp.	Step No.	The thermal reactions	Temp. range °C	Expt. (%)	Calc. (%)
6	1	$[\text{Co}(\text{en})_3][\text{B}_5\text{O}_6(\text{OH})_4][\text{B}_8\text{O}_{10}(\text{OH})_6] \cdot 5\text{H}_2\text{O} \rightarrow [\text{Co}(\text{en})_3][\text{B}_5\text{O}_6(\text{OH})_4][\text{B}_8\text{O}_{10}(\text{OH})_6] + 5\text{H}_2\text{O}$	100-150	9.7	10.1
	2	$[\text{Co}(\text{en})_3][\text{B}_5\text{O}_6(\text{OH})_4][\text{B}_8\text{O}_{10}(\text{OH})_6] \rightarrow [\text{Co}(\text{en})_3][\text{B}_{13}\text{O}_{21}] + 5\text{H}_2\text{O}$	150-250	20.5	20.1
	3	$[\text{Co}(\text{en})_3][\text{B}_{13}\text{O}_{21}] + \text{excess O}_2 \rightarrow \text{CoB}_{13}\text{O}_{21} + \text{volatile oxidation products}$	250-800	41.0	40.3
		Residue $\text{CoB}_{13}\text{O}_{21}$		59.0	59.7
7	1	$[\text{Co}(\text{en})_3][\text{B}_5\text{O}_6(\text{OH})_4]_2\text{Cl} \cdot 3\text{H}_2\text{O} \rightarrow [\text{Co}(\text{en})_3][\text{B}_5\text{O}_6(\text{OH})_4]_2\text{Cl} + 3\text{H}_2\text{O}$	100-180	7.8	7.1
	2	$[\text{Co}(\text{en})_3][\text{B}_5\text{O}_6(\text{OH})_4]_2\text{Cl} \rightarrow [\text{Co}(\text{en})_3][\text{B}_{10}\text{O}_{16}]\text{Cl} + 4\text{H}_2\text{O}$	180-280	17.7	16.5
	3	$[\text{Co}(\text{en})_3][\text{B}_{10}\text{O}_{16}]\text{Cl} + \text{excess O}_2 \rightarrow \text{CoB}_{10}\text{O}_{16}\text{Cl} + \text{volatile oxidation products}$	280-800	40.0	40.1
		Residue $\text{CoB}_{10}\text{O}_{16}\text{Cl}$		60.0	59.9
8	1	$[\text{Co}(\text{en})_3][\text{B}_7\text{O}_9(\text{OH})_6] \cdot 6\text{H}_2\text{O} \rightarrow [\text{Co}(\text{en})_3][\text{B}_7\text{O}_9(\text{OH})_6] + 6\text{H}_2\text{O}$	70-180	15.0	16.1
	2	$[\text{Co}(\text{en})_3][\text{B}_7\text{O}_9(\text{OH})_6] \rightarrow [\text{Co}(\text{en})_3][\text{B}_7\text{O}_{12}] + 3\text{H}_2\text{O}$	180-280	23.2	24.1
	3	$[\text{Co}(\text{en})_3][\text{B}_7\text{O}_{12}] + \text{excess O}_2 \rightarrow \text{CoB}_7\text{O}_{12} + \text{volatile oxidation products}$	280-800	49.8	51.2
		Residue $\text{CoB}_7\text{O}_{12}$		50.2	48.8
9	1	$[\text{Co}(\text{NH}_3)_6]_2[\text{B}_4\text{O}_5(\text{OH})_4]_3 \cdot 11\text{H}_2\text{O} \rightarrow [\text{Co}(\text{NH}_3)_6]_2[\text{B}_4\text{O}_5(\text{OH})_4]_3 + 11\text{H}_2\text{O}$	70-170	17.8	18.1
	2	$[\text{Co}(\text{NH}_3)_6]_2[\text{B}_4\text{O}_5(\text{OH})_4]_3 + \text{excess O}_2 \rightarrow \text{Co}_2\text{B}_{12}\text{O}_{21} + \text{volatile oxidation products}$	170-350	46.5	46.7
		Residue $\text{Co}_2\text{B}_{12}\text{O}_{21}$		53.5	53.3
10	1	$[\text{Co}(\text{NH}_3)_6][\text{B}_7\text{O}_9(\text{OH})_5]\text{Cl} \cdot 5\text{H}_2\text{O} \rightarrow [\text{Co}(\text{NH}_3)_6][\text{B}_7\text{O}_9(\text{OH})_5]\text{Cl} + 5\text{H}_2\text{O}$	70-180	14.3	15.2
	2	$[\text{Co}(\text{NH}_3)_6][\text{B}_7\text{O}_9(\text{OH})_5]\text{Cl} + \text{excess O}_2 \rightarrow \text{CoB}_7\text{O}_{11.5}\text{Cl} + \text{volatile oxidation products}$	180-370	40.9	40.2
		Residue $\text{CoB}_7\text{O}_{11.5}\text{Cl}$		59.1	59.8
11	1	$[\text{Co}(\text{dien})_2][\text{B}_7\text{O}_9(\text{OH})_6] \cdot 9\text{H}_2\text{O} \rightarrow [\text{Co}(\text{dien})_2][\text{B}_7\text{O}_9(\text{OH})_6] + 9\text{H}_2\text{O}$	70-200	19.5	21.7
	2	$[\text{Co}(\text{dien})_2][\text{B}_7\text{O}_9(\text{OH})_6] \rightarrow [\text{Co}(\text{dien})_2][\text{B}_7\text{O}_{12}] + 3\text{H}_2\text{O}$	200-280	28.4	28.9
	3	$[\text{Co}(\text{dien})_2][\text{B}_7\text{O}_{12}] + \text{excess O}_2 \rightarrow \text{CoB}_7\text{O}_{12} + \text{volatile oxidation products}$	280-800	56.9	56.6
		Residue $\text{CoB}_7\text{O}_{12}$		43.1	43.5
12	1	$[\text{Co}(\text{diNOSar})_2]_2[\text{B}_3\text{O}_3(\text{OH})_4]\text{Cl}_5 \cdot 4.75\text{H}_2\text{O} \rightarrow [\text{Co}(\text{diNOSar})_2]_2[\text{B}_3\text{O}_3(\text{OH})_4]\text{Cl}_5 + 4.75\text{H}_2\text{O}$	70-150	7.8	6.7
	2	$[\text{Co}(\text{diNOSar})_2]_2[\text{B}_3\text{O}_3(\text{OH})_4]\text{Cl}_5 \rightarrow [\text{Co}(\text{diNOSar})_2]_2[\text{B}_3\text{O}_5]\text{Cl}_5 + 2\text{H}_2\text{O}$	150-250	11.0	9.5

	3	$[\text{Co}(\text{diNOsar})_2][\text{B}_3\text{O}_5]\text{Cl}_5 + \text{excess O}_2 \rightarrow \text{Co}_2\text{B}_3\text{O}_5\text{Cl}_5 + \text{volatile oxidation products}$	250-800	68.8	68.1
		Residue $\text{Co}_2\text{B}_3\text{O}_5\text{Cl}_5$		31.3	31.9
13	1	$[\text{Co}(\text{diNOsar})][\text{B}_5\text{O}_6(\text{OH})_4]_2\text{Cl}\cdot 3\text{H}_2\text{O} \rightarrow [\text{Co}(\text{diNOsar})][\text{B}_5\text{O}_6(\text{OH})_4]_2\text{Cl} + 3\text{H}_2\text{O}$	70-150	7.9	7.9
	2	$[\text{Co}(\text{diNOsar})][\text{B}_5\text{O}_6(\text{OH})_4]_2\text{Cl} \rightarrow [\text{Co}(\text{diNOsar})][\text{B}_{10}\text{O}_{16}]\text{Cl} + 4\text{H}_2\text{O}$	150-250	15.0	15.7
	3	$[\text{Co}(\text{diNOsar})][\text{B}_{10}\text{O}_{16}]\text{Cl} + \text{excess O}_2 \rightarrow \text{CoB}_{10}\text{O}_{16}\text{Cl} + \text{volatile oxidation products}$	250-800	59.1	59.1
		Residue $\text{CoB}_{10}\text{O}_{16}\text{Cl}$		40.9	40.9
14	1	$[\text{Co}(\text{pn})_3][\text{B}_5\text{O}_6(\text{OH})_4]_2\text{Cl}\cdot 3\text{H}_2\text{O} \rightarrow [\text{Co}(\text{pn})_3][\text{B}_5\text{O}_6(\text{OH})_4]_2\text{Cl} + 3\text{H}_2\text{O}$	70-160	7.2	6.7
	2	$[\text{Co}(\text{pn})_3][\text{B}_5\text{O}_6(\text{OH})_4]_2\text{Cl} \rightarrow [\text{Co}(\text{pn})_3][\text{B}_{10}\text{O}_{16}]\text{Cl} + 4\text{H}_2\text{O}$	160-250	16.0	15.6
	3	$[\text{Co}(\text{pn})_3][\text{B}_{10}\text{O}_{16}]\text{Cl} + \text{excess O}_2 \rightarrow \text{CoB}_{10}\text{O}_{16}\text{Cl} + \text{volatile oxidation products}$	250-800	44.8	43.2
		$\text{CoB}_{10}\text{O}_{16}\text{Cl}$		55.2	56.8

* Calculated values and experimental values are given as totals relative to 100%, and include the process described and earlier mass loss process.

The new polyborate compounds **6-8**, **11-14** followed the expected three step path of decomposition, with observed mass losses in agreement with calculated values. Compound **9** and **10** showed two mass-loss steps rather than three associated with the dehydration of the polyborate anions and the oxidation of the ammonia ligands occurring in one step rather than two (Figure 2.3 and Figure 2.4). The thermal behaviour of the cobalt(III) complex polyborate salts were in accord with published data describing thermal decomposition of transition metal complex cations containing polyborate anions.^{115,127}

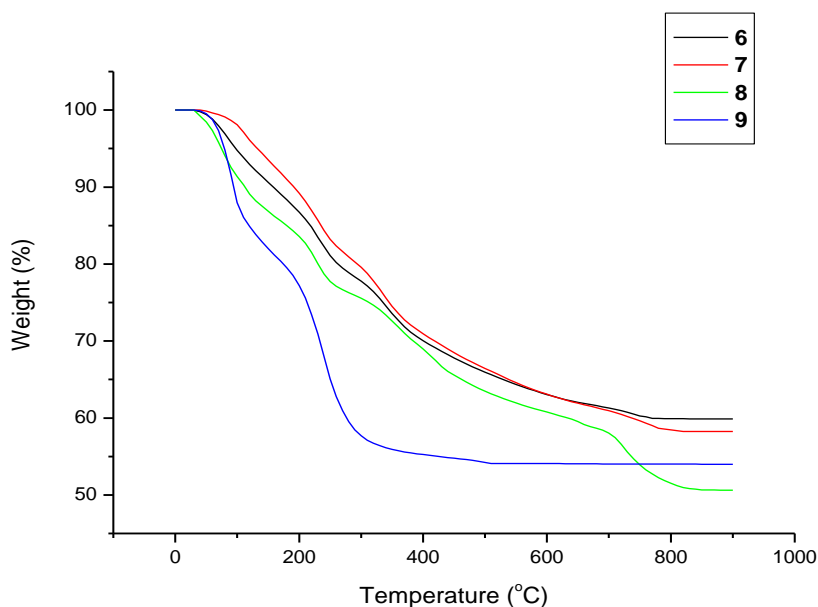


Figure 2.3 TGA diagram for the thermal decomposition of cobalt(III) complex polyborate salts **6-9**.

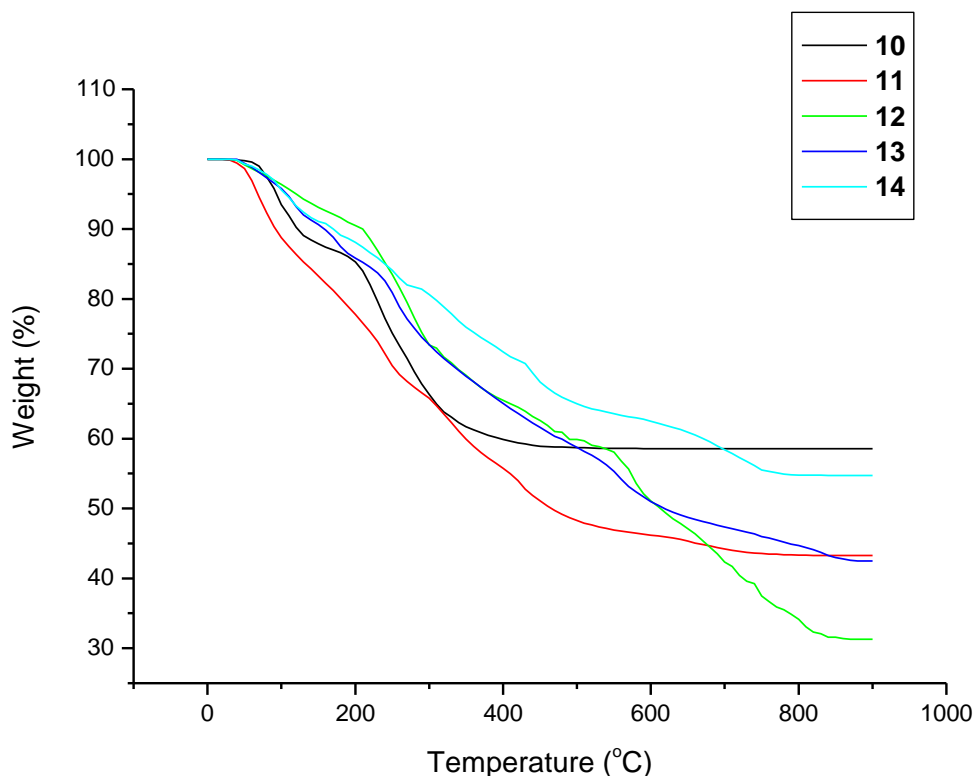


Figure 2.4 TGA diagram for the thermal decomposition of cobalt(III) complex polyborate salts **10-14**.

2.3.5 Structural characterisation of cobalt(III) complex polyborate salts

2.3.5.1 Structural characterisation of $[\text{Co}(\text{en})_3][\text{B}_5\text{O}_6(\text{OH})_4][\text{B}_8\text{O}_{10}(\text{OH})_6] \cdot 5\text{H}_2\text{O}$ (6**)**

Crystals of **6** are triclinic, $P\bar{1}$ and contain two $[\text{Co}(\text{en})_3][\text{B}_5\text{O}_6(\text{OH})_4][\text{B}_8\text{O}_{10}(\text{OH})_6] \cdot 5\text{H}_2\text{O}$ formula units in the asymmetric unit cell. It is an ionic compound with one transition metal complex cation $[\text{Co}(\text{en})_3]^{3+}$ partnered with one $[\text{B}_5\text{O}_6(\text{OH})_4]^-$ and one $[\text{B}_8\text{O}_{10}(\text{OH})_6]^{2-}$ anion and five interstitial water molecules (Figure 2.5). Crystallographic data are shown in Table 2.7. The ligands of tris(ethylenediamine)cobalt(III) moiety are disordered over two positions with *s.o.f.* in the ratio 0.87 and 0.13.

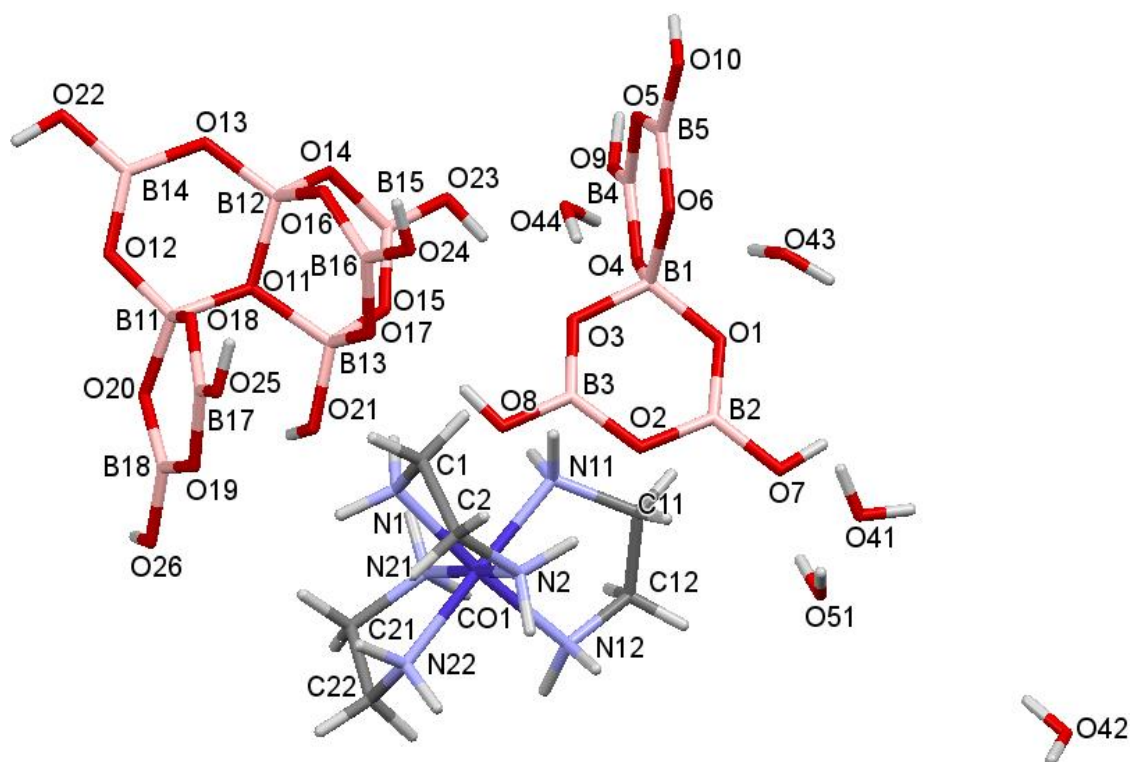


Figure 2.5 Diagram showing the structure and numbering scheme for **6**. Colour code (used throughout this chapter): deep blue (Co), blue (N), red (O), pink (B), dark grey (C) and light grey (H).

Table 2.7 Crystal data and structure refinement of **6**.

Empirical formula	C ₆ H ₄₄ B ₁₃ N ₆ O ₃₁ Co	
Formula weight	895.93	
Temperature	100(2) K	
Wavelength	0.71075 Å	
Crystal system	Triclinic	
Space group	<i>P</i> -1	
Unit cell dimensions	<i>a</i> = 11.2993(8) Å <i>b</i> = 11.5139(8) Å <i>c</i> = 13.7574(10) Å	α = 88.272(4)° β = 76.220(4)° γ = 88.984(4)°
Volume	1737.4(2) Å ³	
<i>Z</i>	2	
Density (calculated)	1.713 mg / m ³	
Absorption coefficient	0.612 mm ⁻¹	
<i>F</i> (000)	924	
Crystal	Cut Blade; Orange	
Crystal size	0.050 × 0.050 × 0.010 mm ³	
θ range for data collection	3.050 – 27.483°	
Index ranges	-14 ≤ <i>h</i> ≤ 12, -14 ≤ <i>k</i> ≤ 14, -17 ≤ <i>l</i> ≤ 17	
Reflections collected	27217	
Independent reflections	7900 [<i>R</i> _{int} = 0.0491]	
Completeness to θ = 25.242°	99.7%	
Absorption correction	Semi-empirical from equivalents	

Max. and min. transmission	1.000 and 0.785
Refinement method	Full-matrix least-squares on F^2
Data / restraints / parameters	7900 / 164 / 588
Goodness-of-fit on F^2	1.043
Final R indices [$F^2 > 2\sigma(F^2)$]	$RI = 0.0463$, $wR2 = 0.1182$
R indices (all data)	$RI = 0.0645$, $wR2 = 0.1280$
Extinction coefficient	n/a
Largest diff. peak and hole	1.281 and $-0.781 \text{ e } \text{Å}^{-3}$
Radiation source (wavelength)	Mo-K α (0.71073 Å)

Special details: The Co(en)₃ moiety was modelled as disordered over two positions with the lesser component left isotropic. Various geometrical restraints (SAME) were also employed.

The crystallographic data revealed that **6** was composed of two different isolated polyborate species: [B₅O₆(OH)₄]⁻ and [B₈O₁₀(OH)₆]²⁻. The pentaborate(1-) anion is well known but the [B₈O₁₀(OH)₆]²⁻ anion present in this complex has never been previously observed. Their structures and their associated numbering schemes are shown in Figure 2.5. The [B₅O₆(OH)₄]⁻ anion is frequently observed in polyborate chemistry with interstitial moieties such as H₂O,¹¹⁵ pyridine,¹¹⁷ B(OH)₃,¹²² and chloride,¹³¹ but it has never been observed previously co-crystallized with another polyborate anion. The observation of two different polyborates in one compound is rare, with only one known example, [H₂en]₂[B₄O₅(OH)₄][B₇O₉(OH)₅] \cdot 3H₂O,⁶ which contains both the [B₄O₅(OH)₄]²⁻ and [B₇O₉(OH)₅]²⁻ anions. Cobalt(III) centred coordination complexes as cations with polyborate anions are very rare, with only one known compound: [Co(en)₃][B₄O₅(OH)₄]Cl \cdot 3H₂O.¹¹⁵

The isolated octaborate [B₈O₁₀(OH)₆]²⁻ anion in **6** (Figure 2.6 (A)) is an isomer of another isolated [B₈O₁₀(OH)₆]²⁻ anion (Figure 2.6 (B)), which was reported in 2006.⁹⁸ In 2007 a related polymeric [B₈O₁₁(OH)₄]²⁻ anion,⁹³ consisting of a chain of boroxole (B₃O₃) rings connected by oxo bridges with pendant pentaborate moieties (Figure 2.6 (C)) was reported.

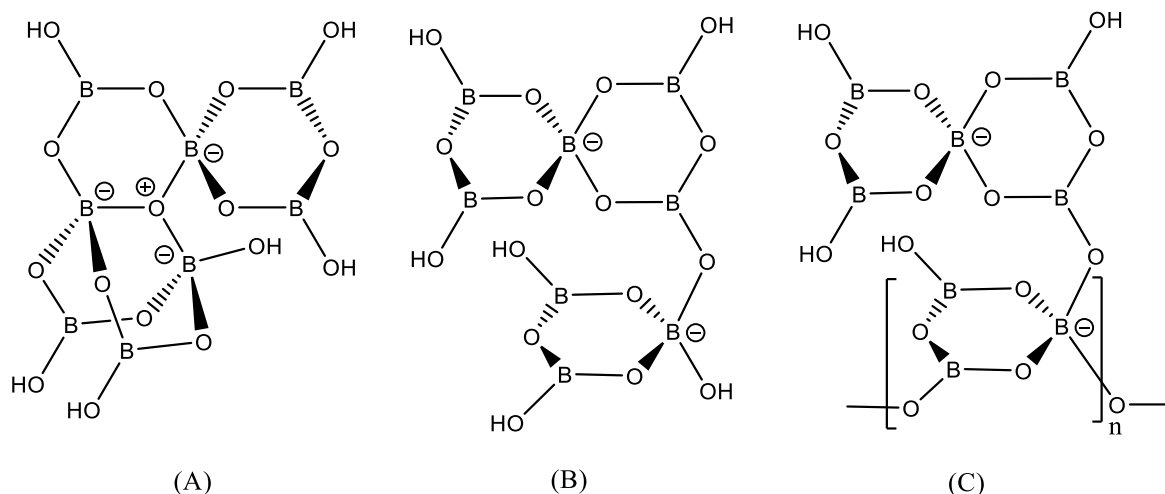


Figure 2.6 Structure of the octaborate(2-) anion present in the crystals of **6** (A) and isomeric $[\text{B}_8\text{O}_{10}(\text{OH})_6]^{2-}$ anion (B),⁹⁸ and polymeric $[\text{B}_8\text{O}_{11}(\text{OH})_4]^{2-}$ anion (C).⁹³

The octaborate(2-) anion observed in **6** possesses several interesting structural features including a 3-coordinate formally positively charged oxygen (O11) centre. This O11 is connected to three 4-coordinate boron centres (B11, B12, B13) and is the main fused connection point between three (six membered) boroxole rings. The octaborate(2-) anion in **6** consists of 4 rings. These four rings are non-planar. The octaborate(2-) anion offers many opportunities to partake in H-bond interactions. The OH groups provide six potential H-bond donor sites which are also capable of accepting H-bond interactions, and a further ten B-O-B units which are potential H-bond acceptor sites. The octaborate(2-) anion is comprised of three 4-coordinate sp^3 boron centres, five 3-coordinate sp^2 boron centres, 10 bridging oxygen atoms, and six exo-OH groups.

The B-O distances to the 4-coordinate tetrahedral B11 centre range from 1.439(4) to 1.554(3) Å [av. 1.477 Å] with those to B12 and B13 ranging from 1.443(3) to 1.543(3) Å [av. 1.481 Å], and 1.423(3) to 1.565(3) Å [av. 1.479 Å], respectively. O11, with a formal positive charge, is bound to all three 4-coordinate boron centres and has the three longest B-O bonds in the anion [av. 1.554 Å]. Coordination about O11 is pyramidal, and is situated 0.357 Å above the plane containing B11, B12, and B13 and with the sum of its B-O-B angles 344.54°. This deviation from planarity is greater than that previously observed in $[\text{H}_3\text{N}(\text{CH}_2)_7\text{NH}_3][\text{B}_7\text{O}_9(\text{OH})_5] \cdot \text{H}_2\text{O}$, $[\text{cyclo-C}_6\text{H}_{11}\text{NH}_3]_2[\text{B}_7\text{O}_9(\text{OH})_5] \cdot 3\text{H}_2\text{O} \cdot \text{B}(\text{OH})_3$, and $[\text{cyclo-C}_7\text{H}_{13}\text{NH}_3]_2[\text{B}_7\text{O}_9(\text{OH})_5] \cdot 2\text{H}_2\text{O} \cdot 2\text{B}(\text{OH})_3$.^{77,97} As a consequence of the pyramidal O11, the octaborate(2-) anion in **6** is chiral, but the solid-state structure is racemic because the

octaborate(2-) anions are arranged as centrosymmetric (enantiomeric) pairs in the crystalline lattice. B-O bonds involving trigonal boron atoms range from 1.344(4) to 1.398(4) Å and terminal OH groups are at the shorter end of the range [av. 1.375 Å], whilst B-O bonds involving ring oxygen atoms are longer [av. 1.418 Å]. Bond angles at the B11 range from 107.0(2)° to 112.2(2)°, B12 range from 107.12(19)° to 111.3(2)°, and B13 range from 105.34(19)° to 112.3(2)° consistent with sp³ hybridization. Angles at the trigonal boron centres range from 108.601(18)° to 124.1(2)° consistent with sp² hybridization. The bond lengths and bond angles of **6** are listed in Appendix I (Table 1 and Table 2). The atomic numbering for the oxygen atoms in the octaborate(2-) anion is shown in Figure 2.7.

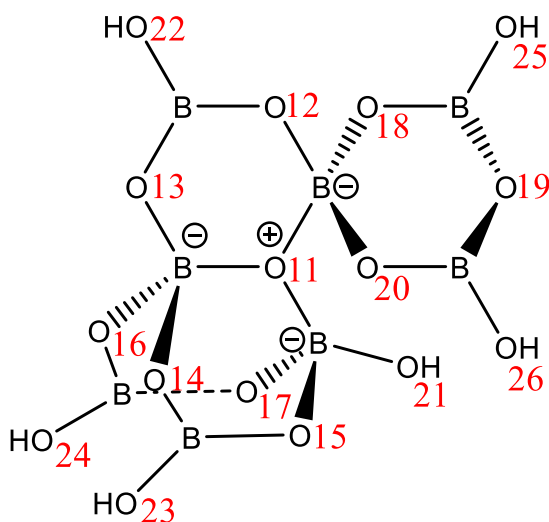


Figure 2.7 Diagram showing the H-bond acceptor sites and their numbers in the octaborate(2) anions.

The bond distances and bond angles for the pentaborate(1-) anion in **6** are within the ranges observed for previously reported structures involving isolated [B₅O₆(OH)₄]⁻ anions^{83,4,113}. The B-O distances to the 4-coordinate B1 centre range from 1.459(4) - 1.4919(4) Å [av. 1.471 Å] and are significantly longer than those involving the 3-coordinate B centres which range from 1.354(4) - 1.391(4) Å. B-O bonds involving 3-coordinate B centres and terminal OH groups are at the shorter end of the range [av. 1.362 Å] whilst B-O bonds involving oxygen atoms distal (O2, O5) to the 4-coordinate B1 centre are at the longer end of the range [av. 1.382 Å]. Bond angles at B1 range from 107.1(2)° - 112.4(2)°, and angles at the other ring

atoms range from 116.1(2)° - 122.6(2)° for B centres consistent with sp³ and sp² hybridization, respectively, Appendix I (Table 1 and Table 2).

There are ten potential H-bond acceptor sites on the [B₅O₆(OH)₄]⁻ anion, and all, with the exception of O2 and O4, are acceptors. Each pentaborate(1-) anion has H-bonds to three cations, three H₂O and two octaborate(2-) anions. The H-bonds data are shown Table 2.8.

Table 2.8 H-bond interactions in 6.

<i>D-H...A</i>	<i>d(D...A)</i>	<i>D-H...A</i>	<i>d(D...A)</i>
N1-H1C...O17	2.939(3)	O8-H8...O15	2.686(3)
N1-H1D...O19	3.330(3)	O9-H9...O51 ^{vi}	2.670(4)
N1-H1D...O42 ⁱ	2.999(3)	O10-H10...O41 ^{vi}	2.733(3)
N2-H2C...O14 ⁱⁱ	3.088(3)	O21-H21...O20 ^{vii}	3.010(3)
N2-H2D...O10 ⁱⁱⁱ	2.945(3)	O22-H22...O1 ⁱ	2.813(3)
N6-H6D...O17	2.96(2)	O23-H23...O3	2.830(3)
N11-H11C...O8	3.040(3)	O24-H24...O18 ^{viii}	2.738(3)
N11-H11D...O43 ⁱⁱⁱ	3.006(3)	O25-H25...O16 ^{viii}	2.705(3)
N12-H12C...O23 ⁱⁱ	2.982(3)	O26-H26...O11 ^{vii}	2.853(3)
N12-H12D...O9 ^{iv}	2.882(3)	O41-H41A...O25 ^v	3.095(4)
N16-H16D...O8	2.761(16)	O41-H41B...O44 ⁱⁱⁱ	2.745(4)
N21-H21C...O8	3.082(3)	O42-H42A...O22 ^{ix}	2.753(3)
N21-H21C...O21	2.992(3)	O42-H42B...O19 ^v	2.805(3)
N21-H21D...O4 ^{iv}	3.259(3)	O43-H43A...O6	2.959(3)
N22-H22C...O14 ⁱⁱ	2.972(3)	O43-H43B...O24 ⁱⁱⁱ	2.856(3)
N22-H22D...O42 ⁱ	2.956(3)	O44-H44A...O6	3.149(3)
N26-H26C...O19	3.304(17)	O44-H44B...O43 ⁱⁱⁱ	2.935(3)
N26-H26D...O21	2.761(17)	O51-H51A...O7	2.656(4)
O7-H7...O12 ^v	2.672(3)	O51-H51B...O41	3.124(5)

(i) x,y,z-1 (ii) x+1,y,z (iii) -x+1,-y,-z+1 (iv) -x+1,-y+1,-z+1 (v) x,y,z+1 (vi) x-1,y,z
(vii) -x+1,-y+1,-z (viii) -x+1,-y,-z (xi) x+1,y,z+1

Christ and Clark¹⁶³ and Heller²⁷ proposed a crystal chemical classification scheme. According to it, the shorthand notification of [B₅O₆(OH)₄]⁻ and [B₈O₁₀(OH)₆]²⁻ are [5:4Δ + 1T] and [8:5Δ + 3T], respectively. In 1990 a nomenclature system was devised by Etter¹⁶⁴ to describe H-bond connections between sets of molecules according to the nature of the donors and acceptors involved in the H-bond. This system indicates whether the motif is cyclic or linear, and finite or infinite. The designators R (ring), C (chain), and D (dimer) are used to denote intermolecular H-bonds, while S refers intramolecular H-bonds. These designators are followed by two numbers *e.g.* R₂²(8) and a further number in parenthesis. The subscript number

is the number of donor sites in the motif and the superscript is the number of acceptor sites in the motif, whilst the number in parenthesis signifies the number of atoms in the repeating motif.

All six donor sites on octaborate(2-) anion are involved in $R_2^2(8)$ interactions with neighbouring polyborates: two to pentaborates and four to octaborates. Details of the H-bonding interactions are given in Table 2.8. These interactions are illustrated in Figure 2.8 and 2.9.

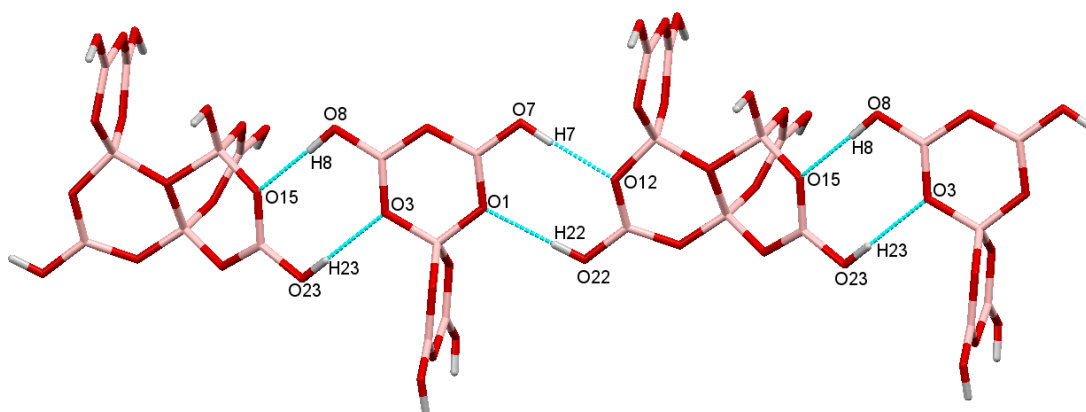


Figure 2.8 Pentaborate(1-) anion $R_2^2(8)$ H-bond motif connections in **6**. Dashed blue lines represent H-bonds.

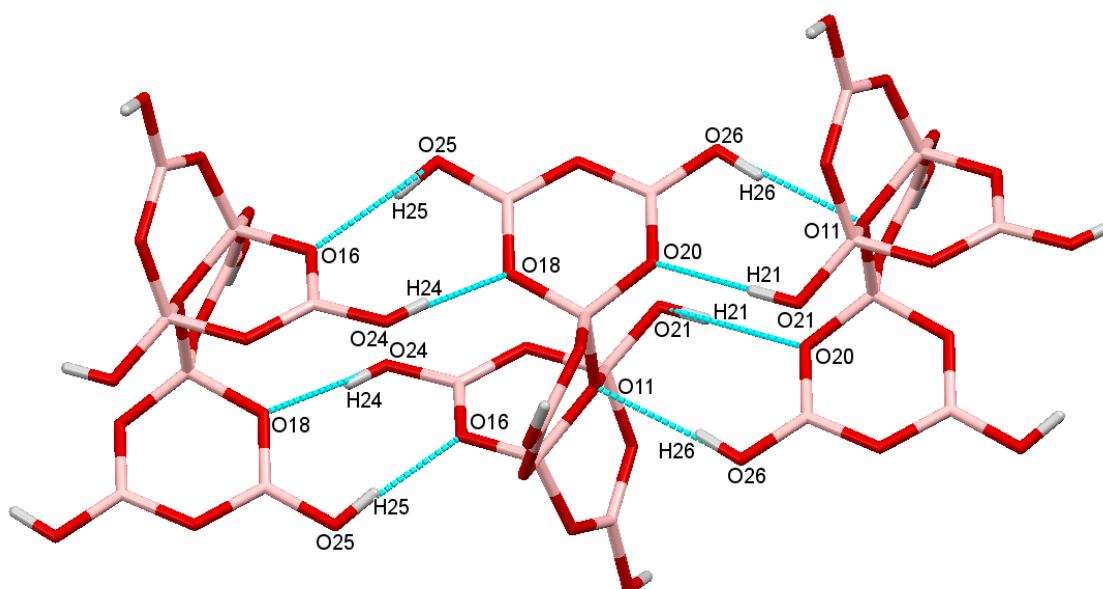


Figure 2.9 Four octaborate(2-) anion - octaborate(2-) anion $R_2^2(8)$ H-bond motif connections in **6**.

O11, the 3-coordinate O atom in the octaborate(2-) anions, effectively becomes 4-coordinate in **6** because it accepts a H-bond from O26-H26. This interaction is approximately linear (173.2°), with $d(D\cdots A)$ and $d(H\cdots A)$ distances of 2.853(3) and 2.02 Å, respectively. The $R_2^2(8)$ interaction involving O11 is unusual in that the heavy (BO) $R_2^2(8)$ atoms are nonplanar (half-chair) with the 3-coordinate O centre (O11) out of the plane by 0.98 Å. As a further consequence of these H-bonding interactions, there is an intramolecular O20 \cdots O21 distance of 2.823 Å. These structural aspects have not been observed in polyborates before.

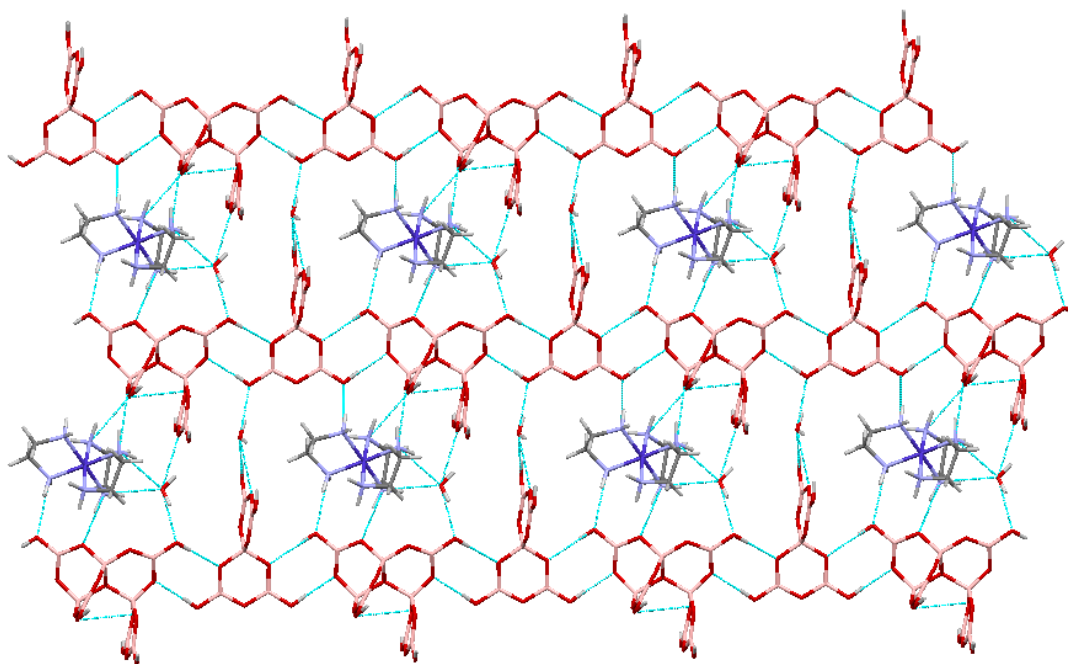


Figure **2.10** Diagram showing a 'plane' of polyborate anions (viewed along the *b* direction of the unit cell) and water molecule with $[Co(en)_3]^{3+}$ cations in **6**.

The $[Co(en)_3]^{3+}$ cations, $[B_5O_6(OH)_4]^-$ anions, $[B_8O_{10}(OH)_6]^{2-}$ anions, and H_2O molecules of crystallization of **6** are connected through a complex series of H-bond interactions, with the anion network templated by the cations. According to Figure **2.10** the supramolecular layered structure of **6** shows that the $[Co(en)_3]^{3+}$ cations connect the octaborate(2-) and pentaborate(1-) anion ribbons by H-bond interactions, forming a three dimensional network. The $[Co(en)_3]^{3+}$ cations are situated in the cavities arising within the supramolecular $[B_8O_{10}(OH)_6]^{2-} / [B_5O_6(OH)_4]^-$ framework.

Ten of the twelve amino hydrogen atoms of the $[\text{Co}(\text{en})_3]^{3+}$ cations are involved as H-bond donors to their neighbouring polyborate anions and water molecules. Each $[\text{Co}(\text{en})_3]^{3+}$ cation is H-bonded to three $[\text{B}_5\text{O}_6(\text{OH})_4]^-$ anions, two $[\text{B}_8\text{O}_{10}(\text{OH})_6]^{2-}$ anions and two water molecules in the secondary coordination shell. Details of H-bond interactions are given in Table 2.8. The connections of $[\text{Co}(\text{en})_3]^{3+}$ cation to $[\text{B}_5\text{O}_6(\text{OH})_4]^-$ anions are $\text{N}2\text{-H}2\text{D}\cdots\text{O}10^*$, $\text{N}11\text{-H}11\text{D}\cdots\text{O}8^*$, and $\text{N}12\text{-H}12\text{D}\cdots\text{O}9^*$ (where * represents a neighbouring molecule). The connections of cation to octaborate(2-) anions are $\text{N}1\text{-H}1\text{C}\cdots\text{O}17^*$, $\text{N}21\text{-H}21\cdots\text{O}21^*$, $\text{N}12\text{-H}12\text{C}\cdots\text{O}23^*$, and $\text{N}22\text{-H}22\text{C}\cdots\text{O}14^*$. The connections of cation to water molecules are $\text{N}11\text{-H}11\text{D}\cdots\text{O}43^*$, $\text{N}1\text{-H}1\text{D}\cdots\text{O}42^*$, and $\text{N}22\text{-H}22\cdots\text{O}42^*$. Nine of the ten H-bond interactions are illustrated in Figure 2.11.

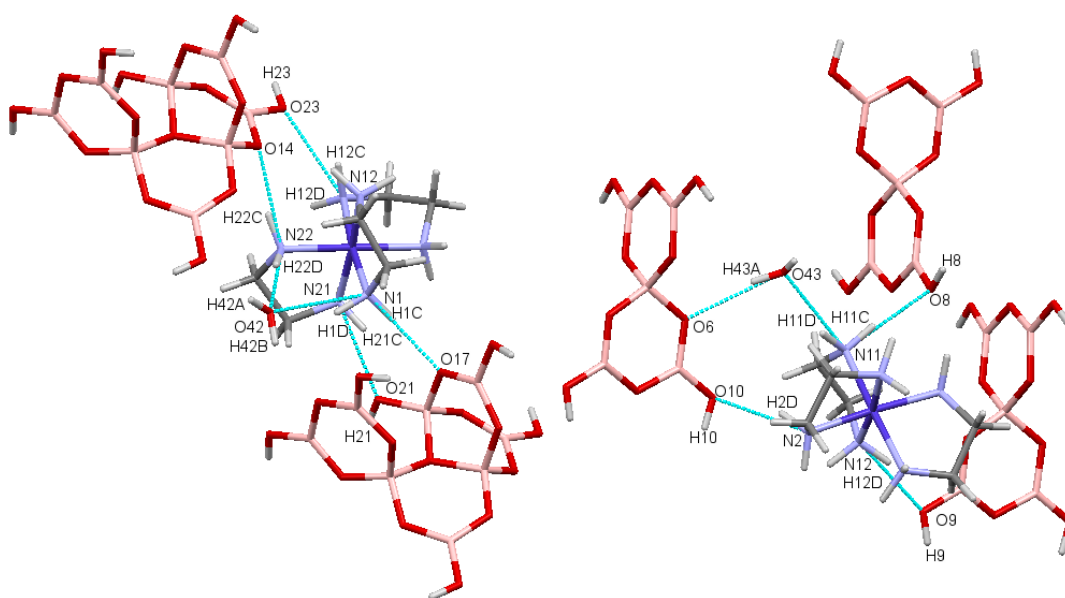


Figure 2.11 The connection of $[\text{Co}(\text{en})_3]^{3+}$ cation with pentaborate(1-) anions, water molecules, and octaborate(2-) anions in **6**.

2.3.5.2 Structural characterisation of $[\text{Co}(\text{NH}_3)_6]_2[\text{B}_4\text{O}_5(\text{OH})_4]_3 \cdot 11\text{H}_2\text{O}$ (**9**)

Crystallographic data of **9** are shown in Table 2.9. The crystals of **9** are monoclinic, $P2_1/c$ and **9** is an ionic compound with two $[\text{Co}(\text{NH}_3)_6]^{3+}$ cations (A and B) partnered with three $[\text{B}_4\text{O}_5(\text{OH})_4]^{2-}$ anions (A, B, and C) and eleven interstitial water molecules (Figure 2.12). The structure unit of **9** in Figure 2.12 shows that there are three transition metal cations, but two of them are bisected by an internal plane of symmetry and there for equate to one cation in unit cell.

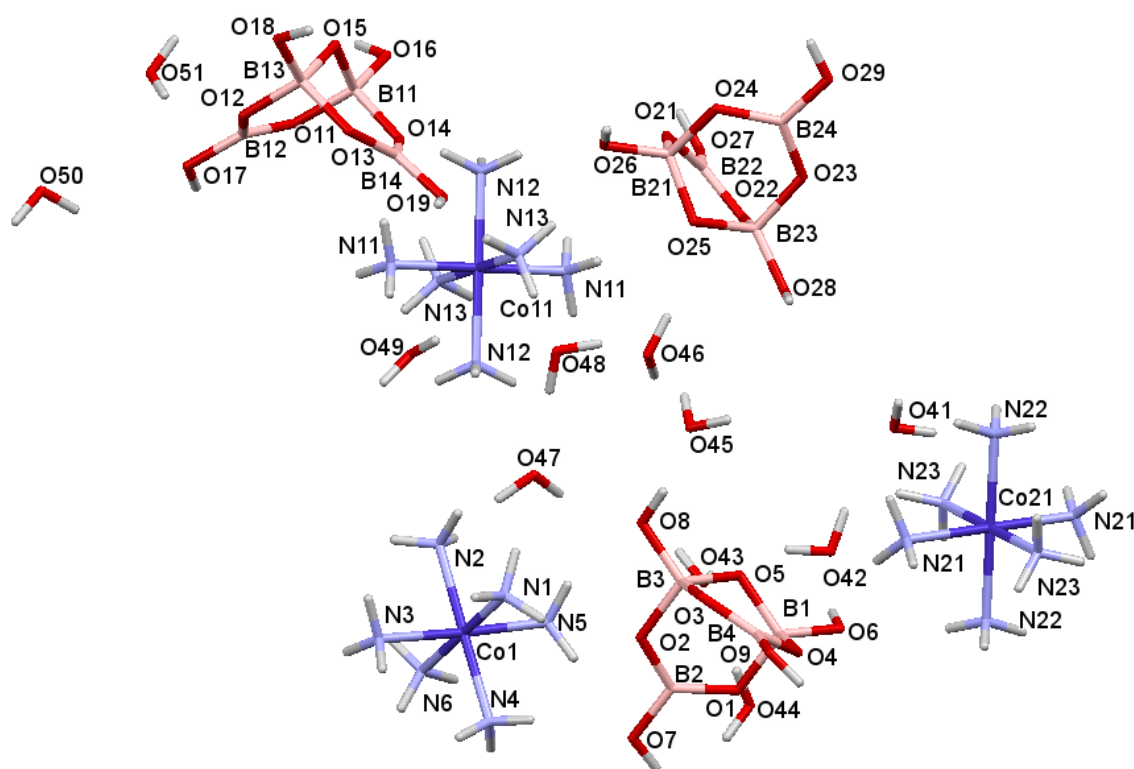


Figure 2.12 Diagram showing the structure and numbering scheme for **9**.

Table 2.9 Crystal data and structure refinement of **9**.

Empirical formula	$B_{12}H_7O_{12}N_{12}O_{38}Co_2$	
Formula weight	1094.26	
Temperature	100(2) K	
Wavelength	0.71075 Å	
Crystal system	Monoclinic	
Space group	$P2_1/c$	
Unit cell dimensions	$a = 21.8873(15)$ Å	$\alpha = 90^\circ$
	$b = 8.8674(5)$ Å	$\beta = 101.2910(10)^\circ$
	$c = 21.6637(15)$ Å	$\gamma = 90^\circ$
Volume	$4123.2(5)$ Å ³	
Z	4	
Density (calculated)	1.763 Mg / m ³	
Absorption coefficient	0.933 mm ⁻¹	
$F(000)$	2288	
Crystal	Plate; Light Orange	
Crystal size	$0.210 \times 0.040 \times 0.020$ mm ³	
θ range for data collection	$2.951 - 27.483^\circ$	
Index ranges	$-28 \leq h \leq 28, -9 \leq k \leq 11, -28 \leq l \leq 28$	
Reflections collected	53472	
Independent reflections	9431 [$R_{int} = 0.0492$]	
Completeness to $\theta = 25.242^\circ$	99.8%	
Absorption correction	Semi-empirical from equivalents	
Max. and min. transmission	1.000 and 0.752	

Refinement method	Full-matrix least-squares on F^2
Data / restraints / parameters	9431 / 36 / 670
Goodness-of-fit on F^2	1.034
Final R indices [$F^2 > 2\sigma(F^2)$]	$RI = 0.0296$, $wR2 = 0.0756$
R indices (all data)	$RI = 0.0356$, $wR2 = 0.0793$
Extinction coefficient	n/a
Largest diff. peak and hole	0.468 and $-0.593 \text{ e } \text{\AA}^{-3}$
Radiation source (wavelength)	Mo-K α (0.71073 \AA)

The transition metal in each $[\text{Co}(\text{NH}_3)_6]^{3+}$ cation is octahedrally coordinated by six nitrogen atoms from six monodentate (ammonia) ligands, with Co-N bond lengths in the range of 1.9625(14) - 1.9820(14) \AA . The bond length and bond angles in **9** are listed in Appendix I (Table 3 and Table 4).

The isolated $[\text{B}_4\text{O}_5(\text{OH})_4]^{2-}$ anion in **9** is well known. The shorthand designation, according to Christ and Clark¹⁶³ and Heller²⁷ schemes, for $[\text{B}_4\text{O}_5(\text{OH})_4]^{2-}$ anion is 4:2 Δ + 2T. Bond lengths and bond angles of the tetraborate(2-) anion in **9** are in agreement with published data of transition metal complex cationic tetraborates,¹¹⁵ metal cationic tetraborates,¹⁶⁵ and non-metal cationic tetraborates.^{84,101,102,115} The structure of the isolated $[\text{B}_4\text{O}_5(\text{OH})_4]^{2-}$ anion consists of two 3-coordinate boron centres $\{\text{BO}_2(\text{OH})\}$ and two 4-coordinate boron centres $\{\text{BO}_3(\text{OH})\}$ linked by common oxygen atoms, forming a double six-membered ring with two boron and one oxygen atoms in common. Each tetraborate(2-) anion has four potential H-bond donor sites which are also capable of accepting H-bond interactions, and five additional potential H-bond acceptor sites. The four chemically non-equivalent oxygen sites are labelled α , β , δ , and ϵ by using a similar nomenclature system to that previously described (Figure 2.13).^{98,77} The three tetraborate(2-) anions in **9** are all crystallographically independent and they here been labelled A-C. All 4 donor sites on tetraborate(2-) anions A, B, and C are involved in H-bond interactions with neighbouring polyborate anions and water molecules. The H-bond acceptor sites arising from donor H-bond sites of the three tetraborate(2-) anions A, B, and C are $\omega\alpha\omega\alpha$, $\epsilon\delta\delta\omega$, and $\alpha\alpha\alpha\omega$, respectively, where α and δ are tetraborate acceptor sites, and ω is an water acceptor site.

The gross structures of tetraborate(2-) anions A, B, and C found in **9** are all very similar. B-O bond length and O-B-O and B-O-B angles are typical of those found in tetraborate(2-) and other polyborate systems¹¹⁵ and are illustrated in detail for anion A. The B-O distances to the 4-coordinate tetrahedral B1 and B3 centres of tetraborate(2-) anion (A) range from 1.4469(19) - 1.5104(19) \AA [av. 1.4778 \AA] and these are significantly longer than those involving the 3-coordinate boron centres, which range from 1.367(2) - 1.378(2) \AA [av. 1.373 \AA]. The B-O distances involving B-OH groups are dependent on whether the boron centre is tetrahedral

(1.4469(19), 1.452(2)) or trigonal (1.372(2), 1.378(2)). The O-B-O bond angles range from 105.61(12) - 113.76(13)° for 4-coordinate centres (B1 and B3), while O-B-O bond angles for 3-coordinate centres (B2 and B4) range from 116.66(14) - 122.91(14)°.

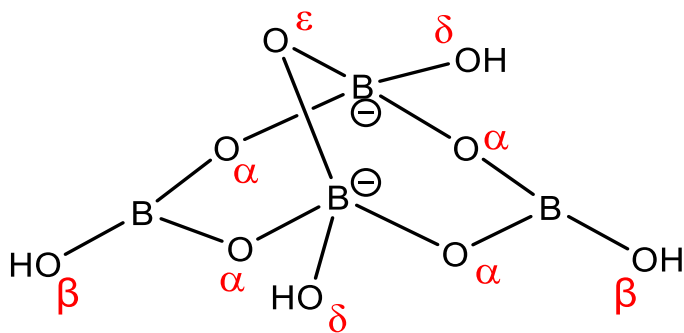


Figure **2.13** Diagram labelling the oxygen atom H-bond acceptor sites in the tetraborate(2-) anions.

The solid-state structure of **9** involves H-bonded giant supramolecular tetraborate(2-) anion structures with ‘cavities’ filled with the associated transition metal complex cations and water molecules. Table **2.10** shows H-bond interactions between tetraborate(2-) anions and the acceptor sites.

The tetraborate(2-) anion (A) has 19 acceptor H-bonds and 4 donor H-bonds with interactions to two cations, five H₂O and three tetraborate(2-) anions. A view of the supramolecular layered structure of the tetraborate(2-) anions in **9** is shown in Figure **2.14**. Details of H-bond interactions are given in Table **2.10**. Here each tetraborate(2-) anion (A) is linked to three neighbouring tetraborate(2-) anions within the plane *via* two pairwise R₂²(8) H-bond interactions O7-H7...O4*/O9*-H9*...O1 and O7*-H7*...O4/O9-H9...O1*, and one H-bond interaction O16-H16...O8*.

The tetraborate(2-) anion (B) has twenty acceptor H-bonds and four donor H-bonds with interactions to four cations, five H₂O and three tetraborate(2-) anions. A view of the H-bond interactions of the tetraborate(2-) anion (B) to another anions in **9** is shown in Figure **2.15**. Here each tetraborate(2-) anion (B) is linked to three neighbouring tetraborate(2-) anions within the plane *via* one pairwise R₂²(8) H-bond interaction O19*-H19*...O25/O28-H28...O13* and two H-bond interactions O16*-H16*...O8 and O17*-H17*...O28.

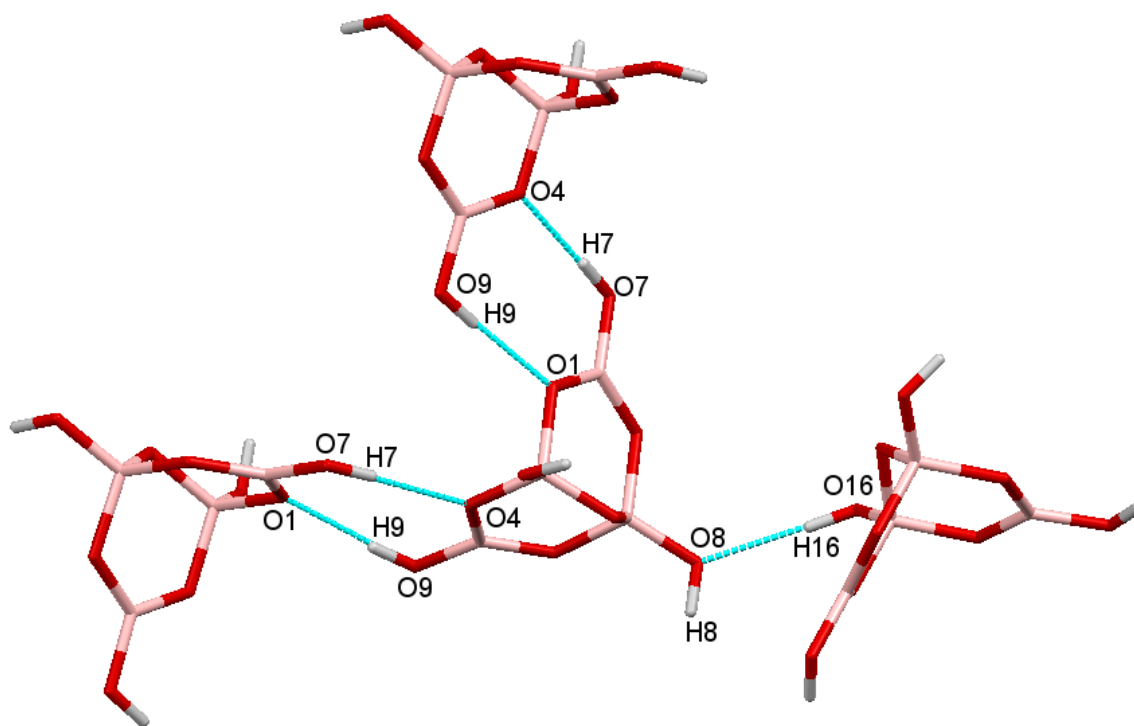


Figure 2.14 H-bond interactions of tetraborate(2-) anion (A) to other anions in **9**. Dashed blue lines represent H-bonds.

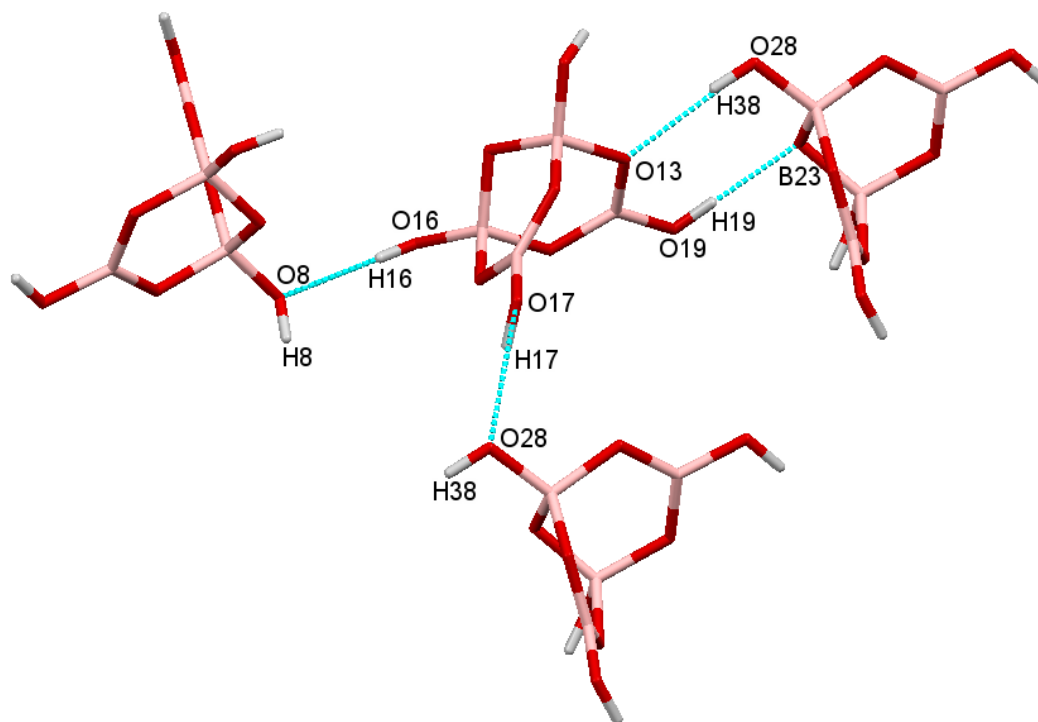


Figure 2.15 The H-bond interactions of the tetraborate(2-) anion (B) to other anions in **9**.

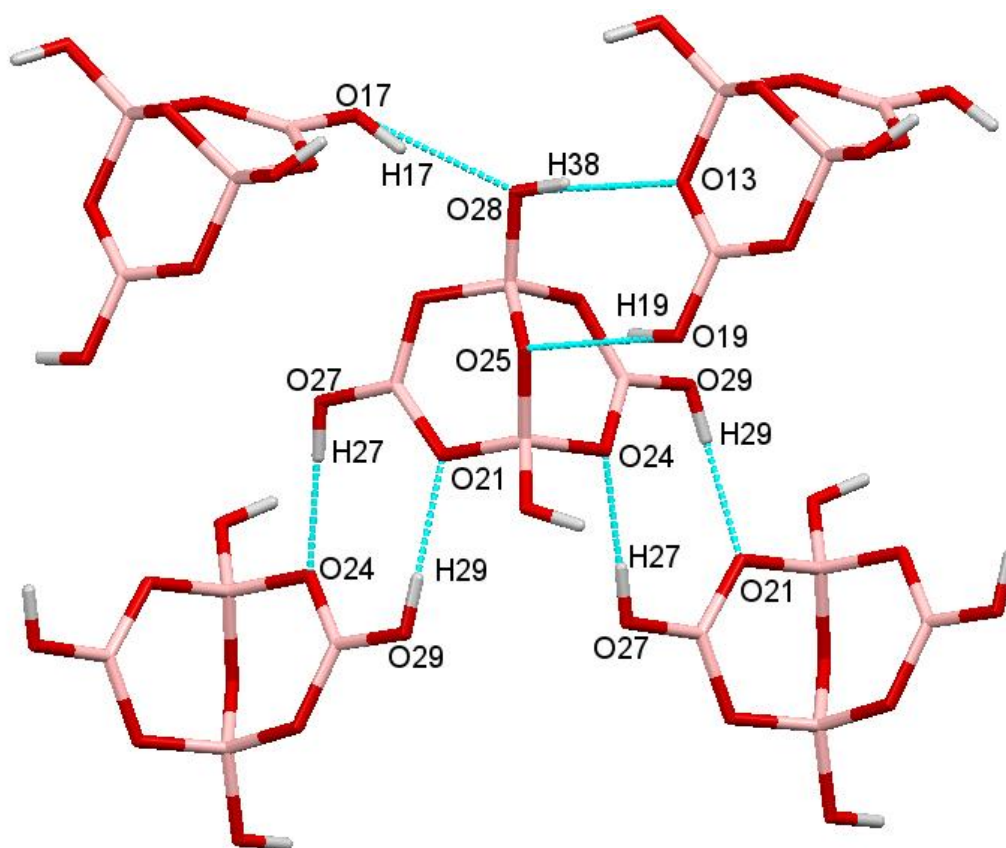


Figure **2.16** The H-bond interactions of the tetraborate(2-) anion (C) to another anions in **9**.

The tetraborate(2-) anion (C) has nineteen acceptor H-bonds and four donor H-bonds with interactions to 3 $[\text{Co}(\text{NH}_3)_6]^{3+}$ cations, 4 H_2O and 4 tetraborate(2-) anions. A view of the H-bond interactions of the tetraborate(2-) anion (C) to another anions in **9** is shown in Figure **2.16**. Here each tetraborate(2-) anion (C) is linked to four neighbouring tetraborate (2-) anions within the plane *via* three pairwise $R_2^2(8)$ H-bond interactions $\text{O}27^*-\text{H}27^*\cdots\text{O}24/\text{O}29-\text{H}29\cdots\text{O}21^*$, $\text{O}27-\text{H}27\cdots\text{O}24^*/\text{O}29^*-\text{H}29^*\cdots\text{O}21$, and $\text{O}19-\text{H}19\cdots\text{O}25^*/\text{O}28^*-\text{H}28^*\cdots\text{O}13$ and one further H-bond interaction $\text{O}17-\text{H}17\cdots\text{O}28^*$.

Table **2.10** H-bond interactions in **9**.

<i>D-H</i> ⋯ <i>A</i>	<i>d(D</i> ⋯ <i>A)</i>	<i>D-H</i> ⋯ <i>A</i>	<i>d(D</i> ⋯ <i>A)</i>
N1-H1A⋯O23 ⁱⁱⁱ	2.9753(17)	O6-H6⋯O42	3.0923(18)
N1-H1B⋯O16 ⁱ	2.9562(16)	O7-H7⋯O4 ^{xi}	2.7485(16)
N1-H1C⋯O2	2.9791(18)	O8-H8⋯O45	2.8547(16)
N2-H2A⋯O27 ^{iv}	2.9665(18)	O9-H9⋯O1 ^{xii}	2.6793(17)
N2-H2B⋯O45 ^v	3.0054(18)	O16-H16⋯O8 ⁱ	2.8588(16)
N2-H2C⋯O16 ⁱ	3.1682(18)	O17-H17⋯O28 ⁱ	2.6623(16)

N3–H3A...O12 ^{vi}	3.0282(17)	O18–H18...O51 ^{xiii}	2.7891(17)
N3–H3A...O13 ^{vi}	3.4351(17)	O19–H19...O25 ^{ix}	2.7127(16)
N3–H3B...O22 ^{iv}	3.3117(18)	O26–H26...O48 ^{ix}	2.8033(17)
N3–H3C...O29 ⁱⁱⁱ	3.0984(18)	O27–H27...O24 ^{xiv}	2.6741(17)
N4–H4A...O12 ^{vi}	2.9027(17)	O28–H38...O13 ^{ix}	2.8640(15)
N4–H4B...O7	3.0027(18)	O29–H29...O21 ^{xv}	2.7320(16)
N4–H4C...O41 ^{iv}	2.9773(19)	O41–H41A...O6 ^{viii}	3.2218(18)
N5–H5A...O9 ^v	2.9558(19)	O41–H41A...O9 ^x	3.0760(17)
N5–H5B...O15 ⁱ	3.1928(16)	O41–H41A...O44 ^{viii}	3.2461(19)
N5–H5B...O16 ⁱ	3.2525(18)	O41–H41B...O50 ⁱ	2.8990(19)
N5–H5C...O3 ^v	3.1265(17)	O42–H42A...O41	2.8505(19)
N5–H5C...O45 ^v	3.1750(18)	O42–H42B...O43	2.7612(18)
N6–H6A...O17 ^{vi}	3.0189(17)	O43–H43A...O5	2.7988(16)
N6–H6B...O3 ^v	2.9152(17)	O43–H43B...O15 ⁱ	2.6911(17)
N6–H6C...O22 ^{iv}	3.0346(18)	O44–H44A...O1 ^{xi}	3.2872(17)
N6–H6C...O47 ^v	3.325(2)	O44–H44A...O4 ^{xi}	3.2883(16)
N11–H11A...O14 ⁱ	2.9759(18)	O44–H44B...O43	2.8477(18)
N11–H11B...O25	3.3539(17)	O45–H45A...O46	2.7471(18)
N11–H11B...O46	3.1938(19)	O45–H45B...O13 ^{ix}	3.1573(16)
N11–H11C...O49 ⁱ	2.9746(19)	O45–H45B...O15 ^{ix}	2.8330(16)
N12–H12A...O14	3.1682(18)	O46–H46A...O11 ⁱ	2.8237(17)
N12–H12A...O16	3.2138(19)	O46–H46B...O25	2.8927(16)
N12–H12B...O49 ⁱ	3.1934(19)	O46–H46B...O28	3.1978(16)
N12–H12C...O26	3.0560(18)	O47–H47A...O22 ⁱⁱⁱ	3.1089(18)
N13–H13A...O26 ⁱ	2.8709(17)	O47–H47A...O23 ⁱⁱⁱ	2.9462(17)
N13–H13B...O19 ⁱ	3.0535(19)	O47–H47B...O8	2.7520(18)
N13–H13C...O48 ⁱ	2.9930(19)	O48–H48A...O47	2.7637(19)
N21–H21A...O18 ^{vii}	2.9976(19)	O48–H48B...O45	3.1823(19)
N21–H21B...O4 ⁱⁱ	3.1948(17)	O49–H49A...O21 ⁱⁱⁱ	3.3296(17)
N21–H21B...O6 ⁱⁱ	3.2251(18)	O49–H49A...O27 ⁱ	3.2093(18)
N21–H21C...O44 ^{viii}	2.9933(19)	O49–H49B...O24 ^{ix}	3.1630(18)
N22–H22A...O18 ^{ix}	2.9444(18)	O49–H49B...O48	3.081(2)
N22–H22B...O7(x)	3.1569(17)	O50–H50A...O2 ^{vi}	2.9117(16)
N22–H22C...O6 ⁱⁱ	3.0986(18)	O50–H50B...O28 ⁱ	3.0279(18)
N23–H23A...O51 ⁱ	3.0078(19)	O51–H51A...O5 ⁱ	2.6918(15)
N23–H23B...O42 ^{viii}	2.964(2)	O51–H51B...O17	3.0070(17)
N23–H23C...O44 ^{viii}	3.1008(18)		

(i) $-x+1, -y+1, -z+1$ (ii) $-x, -y+2, -z+1$ (iii) $x, -y+3/2, z-1/2$ (iv) $x, -y+1/2, z-1/2$ (v) $x, y-1, z$ (vi) $-x+1, y-1/2, -z+1/2$ (vii) $x-1, y, z$ (viii) $-x, -y+1, -z+1$ (ix) $-x+1, -y+2, -z+1$ (x) $x, -y+3/2, z+1/2$ (xi) $-x, y-1/2, -z+1/2$ (xii) $-x, y+1/2, -z+1/2$ (xiii) $x, y+1, z$ (xiv) $-x+1, y-1/2, -z+3/2$ (xv) $-x+1, y+1/2, -z+3/2$

The tetraborate(2-) anions form a ribbon structure and these ribbons are interconnected to form a layer. A view of the ribbon / layered structure of the $[\text{B}_4\text{O}_5(\text{OH})_4]^{2-}$ anions of **9** is shown in Figure 2.17.

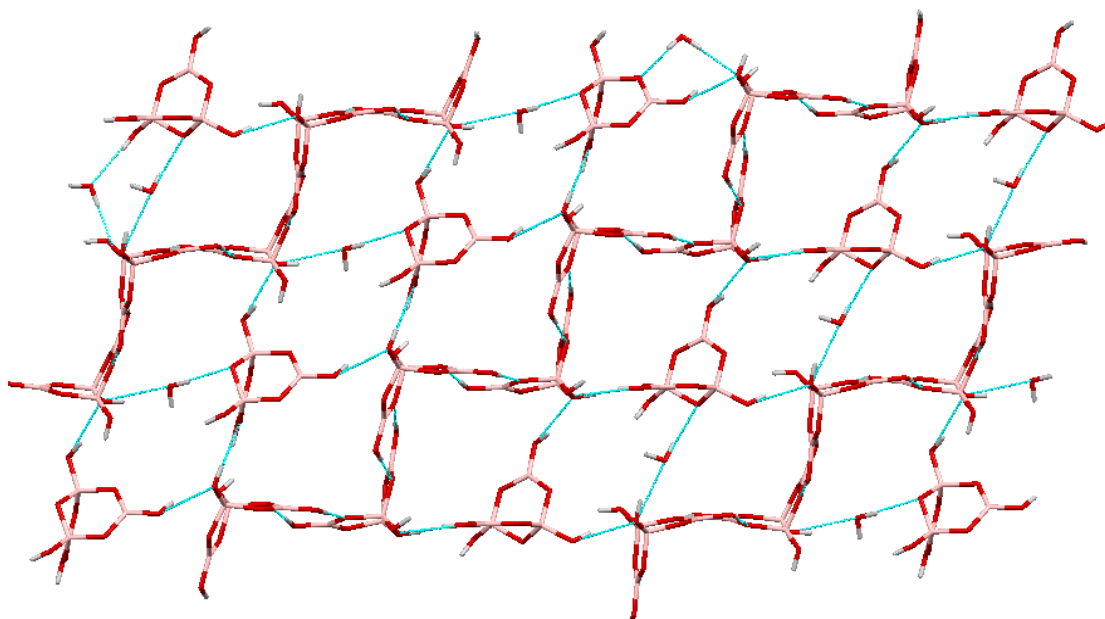


Figure **2.17** Tetraborate(2-) anions and water molecules layer structure (viewed along the *a* direction of the unit cell) of **9**.

The two $[\text{Co}(\text{NH}_3)_6]^{3+}$ cations, and eleven H_2O molecules of crystallization of **9** are connected through a complex series of H-bond interactions, with the tetraborate anion network templated by the cations. The connection of ribbon-layer shown in Figure **2.17** to the neighbouring planes is formed by further H-bond interactions, forming a three-dimensional network. Compound **9** possess two $[\text{Co}(\text{NH}_3)_6]^{3+}$ cations: A contains Co1 and B contains Co11 and Co21. These cations are involved in H-bonding to $[\text{B}_4\text{O}_5(\text{OH})_4]^{2-}$ anions as described below.

All eighteen of the amino hydrogen atoms of the $[\text{Co}(\text{NH}_3)_6]^{3+}$ (A) and (B) cations are involved as H-bond donors to their neighbouring tetraborate(2-) anions and water molecules. Cation A has H-bonds to six $[\text{B}_4\text{O}_5(\text{OH})_4]^{2-}$ anions and three H_2O molecules in its secondary coordination shell *via* twenty-two H-bond interactions. Fourteen of the twenty-two H-bond interactions are illustrated in Figure **2.18**. Cation B acts as H-bond donors to eight $[\text{B}_4\text{O}_5(\text{OH})_4]^{2-}$ anions and six H_2O molecules *via* twenty-one H-bond interactions. These are described in detail in Table **2.10**.

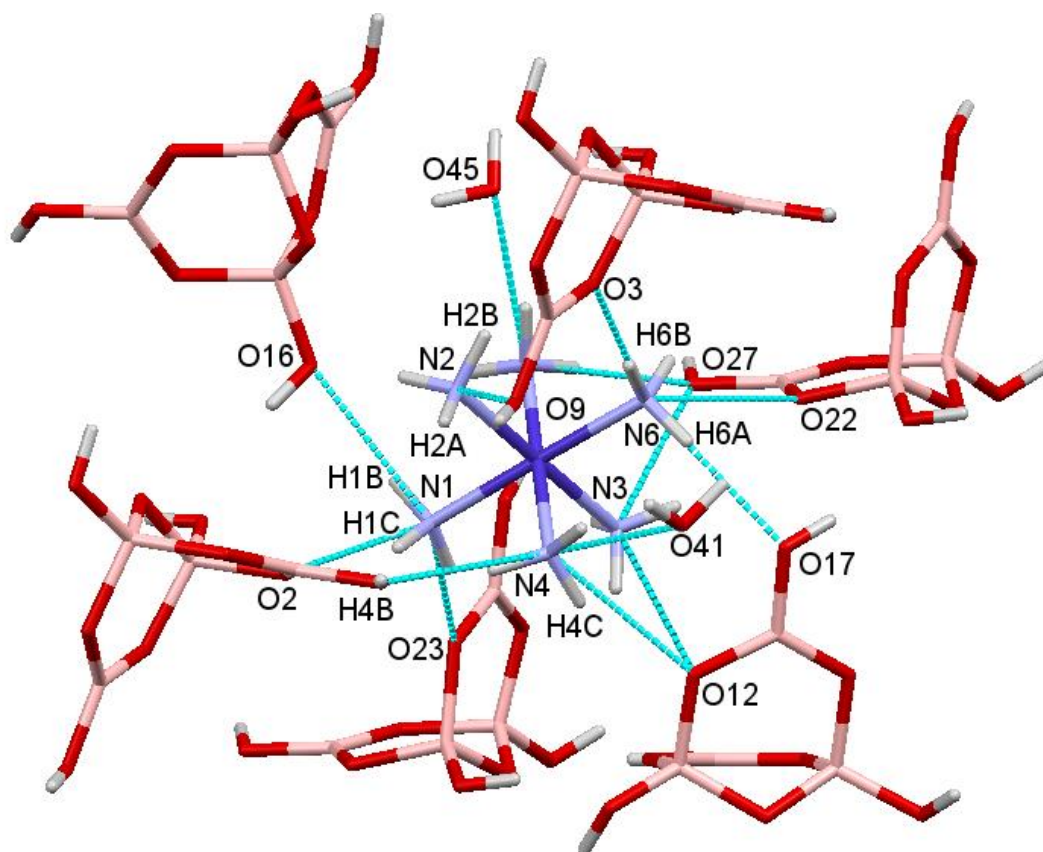


Figure **2.18** The H-bond interactions of $[\text{Co}(\text{NH}_3)_6]^{3+}$ (A) cation with tetraborate(2-) anions and water molecules in **9**.

2.3.5.3 Structural characterisation of $[\text{Co}(\text{dien})_2][\text{B}_7\text{O}_9(\text{OH})_6]\cdot 9\text{H}_2\text{O}$ (**11**)

Crystallographic data for compound **11** are shown in Table **2.11**. The crystals of **11** are triclinic, $P2_1/n$ and contain a discrete *s-fac*- $[\text{Co}(\text{dien})_2]^{3+}$ cation partnered with a unique $[\text{B}_7\text{O}_9(\text{OH})_6]^{3-}$ anion and nine water molecules of crystallization, held together by an extensive H-bond network (Figure **2.19**). Two water molecules are disordered, each over two positions, however they were successfully modelled in to a predominant form O58 (*s.o.f.* 0.819(7)) and O59 (*s.o.f.* 0.600(11)).

Table **2.11** Crystal data and structure refinement of **11**.

Empirical formula	$\text{C}_8\text{H}_{50}\text{B}_7\text{N}_6\text{O}_{24}\text{Co}$	
Formula weight	749.14	
Temperature	100(2) K	
Wavelength	0.71075 Å	
Crystal system	Monoclinic	
Space group	$P2_1/n$	
Unit cell dimensions	$a = 11.7755(3)$ Å	$\alpha = 90^\circ$
	$b = 15.3238(3)$ Å	$\beta = 96.515(3)^\circ$

	$c = 17.3965(7) \text{ \AA}$ $\gamma = 90^\circ$
Volume	$3118.85(16) \text{ \AA}^3$
Z	4
Density (calculated)	1.595 Mg / m^3
Absorption coefficient	0.651 mm^{-1}
$F(000)$	1576
Crystal	Cut Blade; Orange
Crystal size	$0.150 \times 0.080 \times 0.010 \text{ mm}^3$
θ range for data collection	$2.357 - 27.680^\circ$
Index ranges	$-15 \leq h \leq 15, -19 \leq k \leq 16, -22 \leq l \leq 19$
Reflections collected	29346
Independent reflections	7250 [$R_{int} = 0.0491$]
Completeness to $\theta = 25.242^\circ$	99.9%
Absorption correction	Semi-empirical from equivalents
Max. and min. transmission	1.000 and 0.797
Refinement method	Full-matrix least-squares on F^2
Data / restraints / parameters	7250 / 0 / 414
Goodness-of-fit on F^2	1.008
Final R indices [$F^2 > 2\sigma(F^2)$]	$R1 = 0.0483, wR2 = 0.1159$
R indices (all data)	$R1 = 0.0711, wR2 = 0.1258$
Extinction coefficient	n/a
Largest diff. peak and hole	1.214 and $-0.801 \text{ e \AA}^{-3}$
Radiation source (wavelength)	Mo-K α (0.71073 \AA)

Special details: Two of the water molecules (labelled as O88 and O89) were modelled as disordered over two positions.

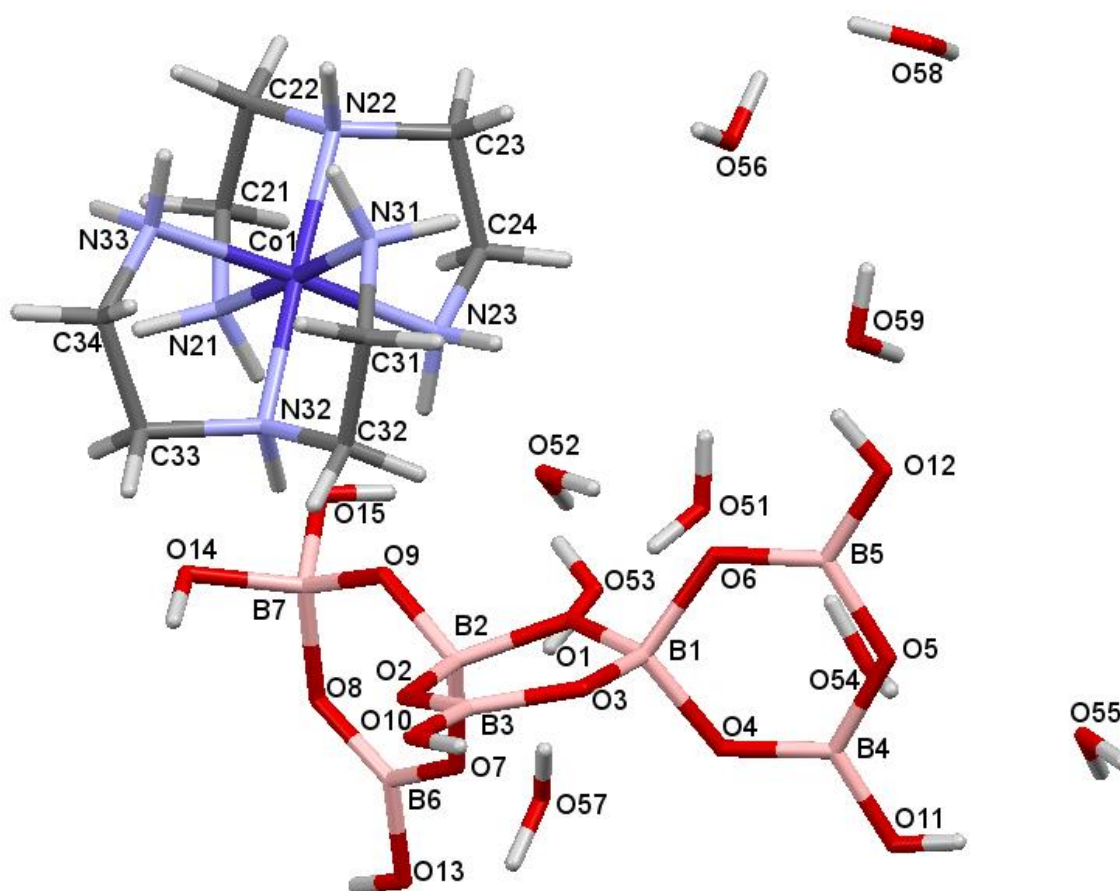


Figure 2.19 Diagram showing the structure and numbering scheme for 11.

Whilst salts containing the pentaborate(1-) anions are common, salts containing heptaborate anions are relatively rare, and are limited to two isomeric form of the heptaborate(2-) anion^{6,77,97,166} (Figure 2.20, (A) and (B)). Compound **11** contains a novel heptaborate(3-) anion, $[\text{B}_7\text{O}_9(\text{OH})_6]^{3-}$ (Figure 2.20 (C)).

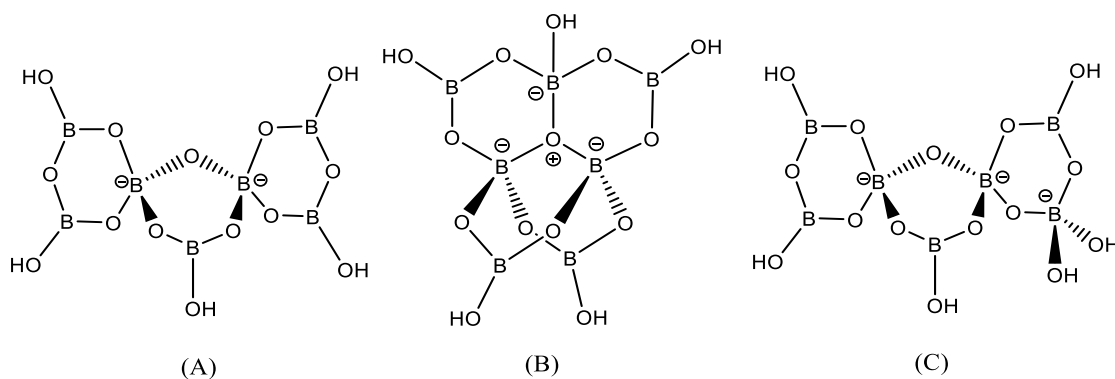


Figure 2.20 The two isomeric $[\text{B}_7\text{O}_9(\text{OH})_5]^{2-}$ anions (A) and (B) and the structure of the heptaborate(3-) anion (C) present in the crystals of **11**.

The heptaborate(3-) anion in **11** has never been previously observed in minerals or in synthetic borates. According to Christ and Clark¹⁶³ and Heller²⁷ the shorthand notation for the $[\text{B}_7\text{O}_9(\text{OH})_6]^{3-}$ anion is $[7:4\Delta + 3\text{T}]$. The atomic numbering for the oxygen and boron atoms in the heptaborate(3-) anion is shown in Figure 2.21. The heptaborate(3-) anion is comprised of three almost planar (half-chair) boroxole (B_3O_3) rings with B2, B1, and O1 lying 0.044, 0.097 and 0.155 Å out of best planes, respectively. These connect together by sharing two 4-coordinate boron centres (B1 and B2), in a similar way to that observed for one of the known isomers of $[\text{B}_7\text{O}_9(\text{OH})_5]^{2-}$ anion (Figure 2.20 (A)).⁶ However, the $[\text{B}_7\text{O}_9(\text{OH})_6]^{3-}$ anion found in **11** (Figure 2.21) has an additional 4-coordinate boron centre (B7) formed by the addition of OH^- to a 3-coordinate boron centre on a terminal boroxole ring in $[\text{B}_7\text{O}_9(\text{OH})_5]^{2-}$. In addition, there are four 3-coordinate boron (B3, B4, B5, B6) centres, with each centre connected to two oxygen atoms and one hydroxyl group. The ‘plane’ of the middle ring is perpendicular to the ‘best planes’ of the outer two rings.

Bond lengths and bond angles for the heptaborate(3-) anion found in **11** are within the ranges observed for previously reported polyborate anions, and generally not significantly different to those found in the heptaborate(2-) anion with the exception of data associated with the outer boroxole ring containing the additional hydroxyl group. The B1, B2, and B7 atoms

are 4-coordinate centres with B-O distances ranging from 1.424(3)-1.507(3) Å, 1.444(3)-1.508(4) Å, and 1.448(3)-1.516(3) Å, respectively, and angles ranging from 105.42(19)°-113.7(2)°, 104.9(2)°-111.7(2)°, and 104.40(19)-112.0(2)°, respectively. The B-O bond length and angle values of B1, B2, and B7 centres are appropriate for a distorted tetrahedral geometry. The B-O distances to the tetrahedral centres are significantly longer than those involving the 3-coordinate (B3, B4, B5, and B6) centres which range from 1.356(3)-1.371(4) Å, 1.348(3)-1.400(3) Å, 1.347(3)-1.385(3) Å, and 1.354(3)-1.366(3) Å, respectively with angles ranging from 117.5(2)°-122.9(3)°, 118.3(2)°-121.2(2)°, 116.0(2)°-123.2(2)°, and 115.(2)°-124.3(2)°, respectively. The inclusion of the addition OH group has little structural effects on other parameters within this boroxole ring, other than shortening B6-O8 [1.365(3) Å] relative to that observed in $[\text{B}_7\text{O}_9(\text{OH})_5]^{2-}$ [1.393(7) Å].⁶ These data are similar to that for $[\text{B}_3\text{O}_4(\text{OH})_4]^-$,³⁹ and with adduct formation in boroxine ring systems since O8-B6 π -bonding increases in $[\text{B}_7\text{O}_9(\text{OH})_6]^{3-}$ as the 4-coordinate B7 can no longer partake in π -bonding. This outer boroxole ring in $[\text{B}_7\text{O}_9(\text{OH})_6]^{3-}$ has a similar bond length distribution to that found in $\text{Ca}[\text{B}_3\text{O}_3(\text{OH})_5]\cdot\text{H}_2\text{O}$ (meyerhofferite) which contains a boroxole ring with two 4-coordinate boron centres.¹⁶⁷ The bond lengths and angles of **11** are listed in Appendix I (Table 5 and Table 6).

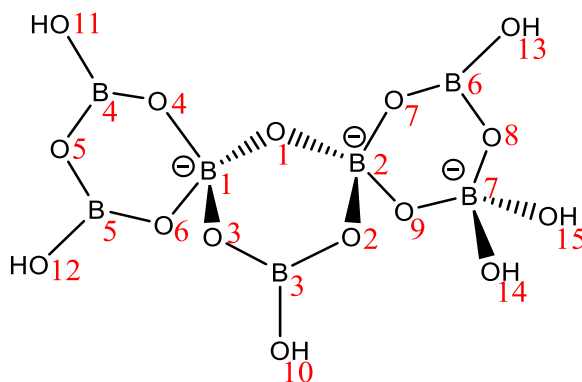


Figure 2.21 Diagram showing atomic numbering for the heptaborate(3-) anions in **11**.

Detailed inspection of Figure 2.22 shows that the ribbons of $[\text{B}_7\text{O}_9(\text{OH})_6]^{3-}$ anions are horizontally connected by C(10) chain motif interaction O11-H11 \cdots O14*. The heptaborate anion ribbons are further linked to other heptaborate anion ribbons by two pairwise $R_2^2(8)$ connections O12-H12 \cdots O8*/O13*-H13* \cdots O6 and O12*-H12* \cdots O8/O13-H13 \cdots O6*. Details of the H-bonding interactions are given in Table 2.12.

Table 2.12 H-bond interactions in **11**.

<i>D</i> -H... <i>A</i>	<i>d</i> (<i>D</i> ... <i>A</i>)	<i>D</i> -H... <i>A</i>	<i>d</i> (<i>D</i> ... <i>A</i>)
O10-H10...O57	2.787(2)	N33-H33D...O12 ^{iv}	2.915(3)
O11-H11...O14 ⁱ	2.645(2)	O51-H51A...O1	2.670(2)
O12-H12...O8 ⁱⁱ	2.767(2)	O51-H51B...O59	2.870
O13-H13...O6 ⁱⁱⁱ	2.605(2)	O51-H51B...O89	2.767
O14-H14...O58 ⁱⁱⁱ	2.825(2)	O52-H52A...O53	2.828
O14-H14...O88 ⁱⁱⁱ	2.864(2)	O52-H52B...O51	2.775
O15-H15...O52	2.787(2)	O53-H53A...O57 ^v	2.841
N21-H21C...O14	3.146(3)	O53-H53B...O3 ^v	2.872(2)
N21-H21C...O15	2.887(3)	O53-H53B...O4 ^v	3.311(2)
N21-H21D...O5 ^{iv}	2.901(3)	O54-H54A...O51	2.746
N22-H22...O4 ⁱⁱ	3.072(3)	O55-H55A...O10 ^{vi}	2.769(2)
N22-H22...O11 ⁱⁱ	3.008(3)	O55-H55B...O15 ⁱ	2.680(2)
N23-H23C...O13 ⁱⁱ	2.777(3)	O56-H56A...O55 ^{vii}	2.8333(19)
N23-H23D...O9	2.939(3)	O56-H56B...O2 ⁱⁱ	3.0806(19)
N23-H23D...O15	3.358(3)	O56-H56B...O7 ⁱⁱ	3.039(2)
N31-H31C...O7 ⁱⁱ	2.910(3)	O57-H57A...O3 ^{viii}	2.949(2)
N31-H31C...O13 ⁱⁱ	3.260(3)	O57-H57A...O6 ^{viii}	3.014(2)
N31-H31D...O4 ⁱⁱ	3.104(3)	O57-H57B...O8 ^{ix}	3.048(2)
N31-H31D...O54 ⁱⁱ	3.063(3)	O58-H58A...O54 ^{vii}	2.934(3)
N32-H32...O9	2.941(3)	O58-H58B...O2 ⁱⁱ	2.781(2)
N32-H32...O14	3.195(3)	O88-H88A...O54 ^{vii}	3.066(3)
N33-H33C...O11 ⁱⁱ	2.970(3)	O59-H59B...O56	2.748
N33-H33C...O54 ⁱⁱ	3.337(3)	O89-H89A...O56	2.307

(i) $x-1,y,z$ (ii) $-x+1/2,y+1/2,-z+1/2$ (iii) $-x+1/2,y-1/2,-z+1/2$ (iv) $x+1,y,z$ (v) $x+1/2,-y+1/2,z+1/2$
(vi) $x-1/2,-y+1/2,z+1/2$ (vii) $-x,-y+1,-z+1$ (viii) $-x,-y+1,-z$ (ix) $x-1/2,-y+1/2,z-1/2$

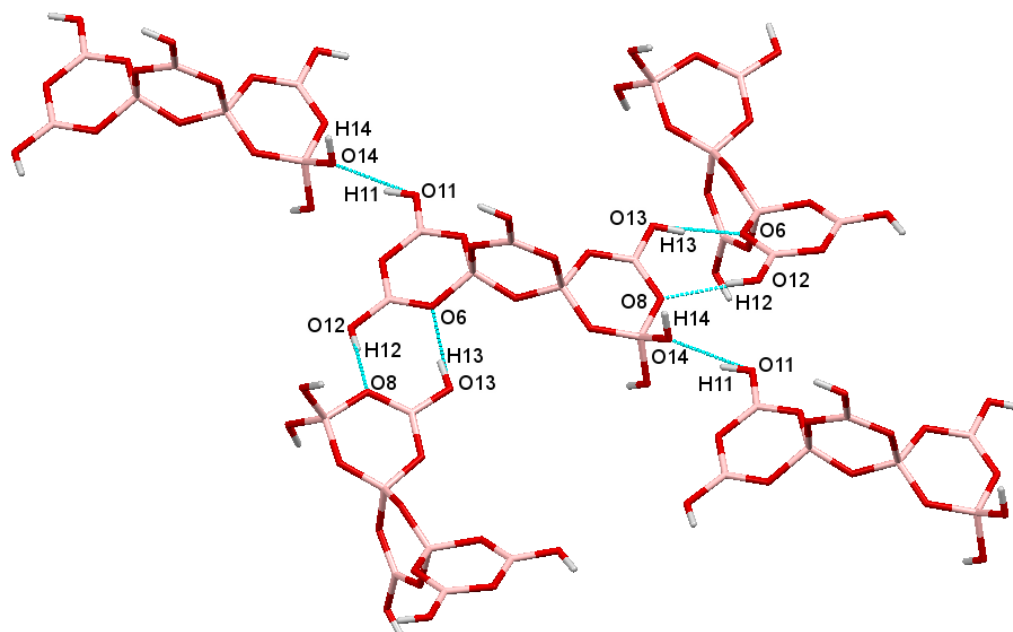


Figure 2.22 H-bond interactions between the heptaborate(3-) anions in **11**. Dashed blue lines represent H-bonds.

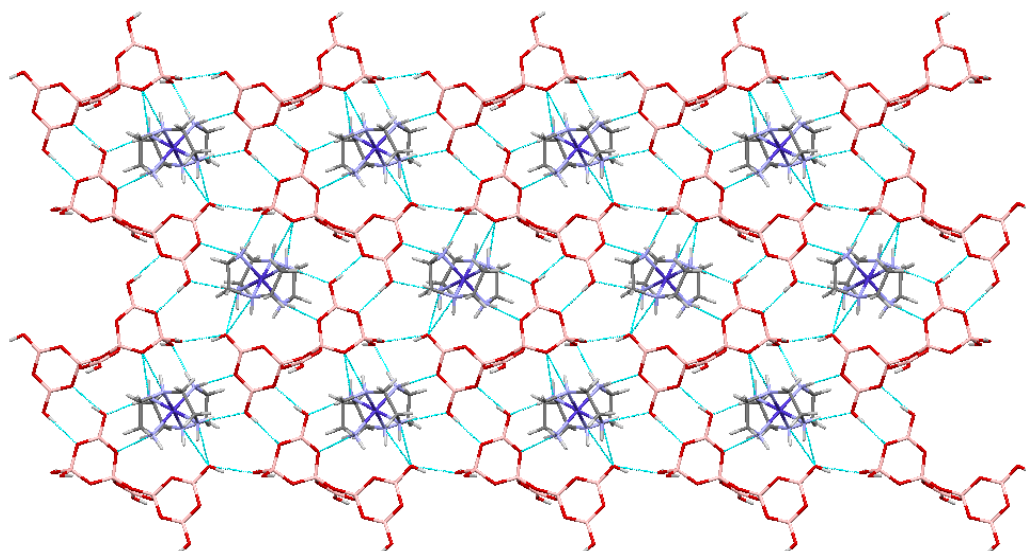


Figure 2.23 Supramolecular structure involving heptaborate(3-) anions and $[\text{Co}(\text{Dien})_2]^{3+}$ cations (viewed along the c direction of the unit cell) in **11**.

As shown in Figure 2.23 the supramolecular layered structure of **11** has the $[\text{Co}(\text{dien})_2]^{3+}$ cations connected to the heptaborate(3-) anion ribbons by additional H-bond interactions. The connection of plane shown in Figure 2.23 to the neighbouring planes is formed by further H-bond interactions, forming a three-dimensional network.

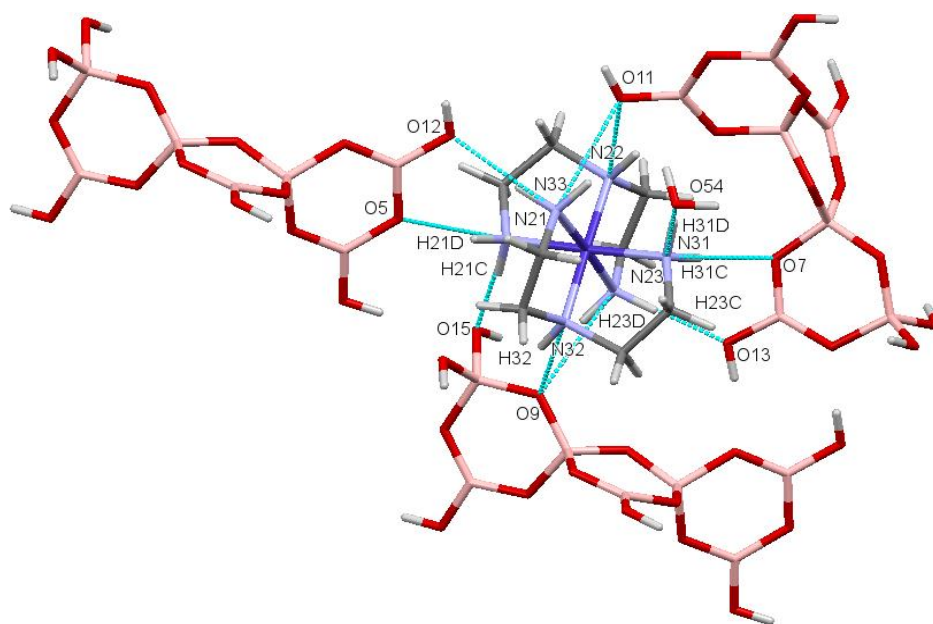


Figure 2.24 The H-bond connections of $[\text{Co}(\text{dien})_2]^{3+}$ with heptaborate(3-) anions and water molecule in **11**.

All ten of the amino hydrogen atoms of the $[\text{Co}(\text{dien})_2]^{3+}$ cations are involved as H-bond donors to three $[\text{B}_7\text{O}_9(\text{OH})_6]^{3-}$ anions and one water molecule in its secondary coordination shell. The ten H-bond interactions consist of nine H-bonds to three heptaborate(3-) anions and one H-bond connection to a one H_2O molecule (Figure 2.24). Details are in Table 2.12.

2.3.5.4 Structural characterisation of $[\text{Co}(\text{diNOsar})_2][\text{B}_3\text{O}_3(\text{OH})_4]\text{Cl}_5 \cdot 4.75\text{H}_2\text{O}$ (12)

Crystallographic data for compound **12** are listed in Table 2.13. The crystals of compound **12** are monoclinic, $P-1$ consists of two $[\text{Co}(\text{diNOsar})]^{3+}$ cations partnered with one isolated $[\text{B}_3\text{O}_3(\text{OH})_4]^-$ polyborate anion, five Cl^- anions, and 4.75 water molecules (Figure 2.25). There is one disordered water molecule that is positioned in either one of two positions, with an *s.o.f.* ratio of 0.75 / 0.25.

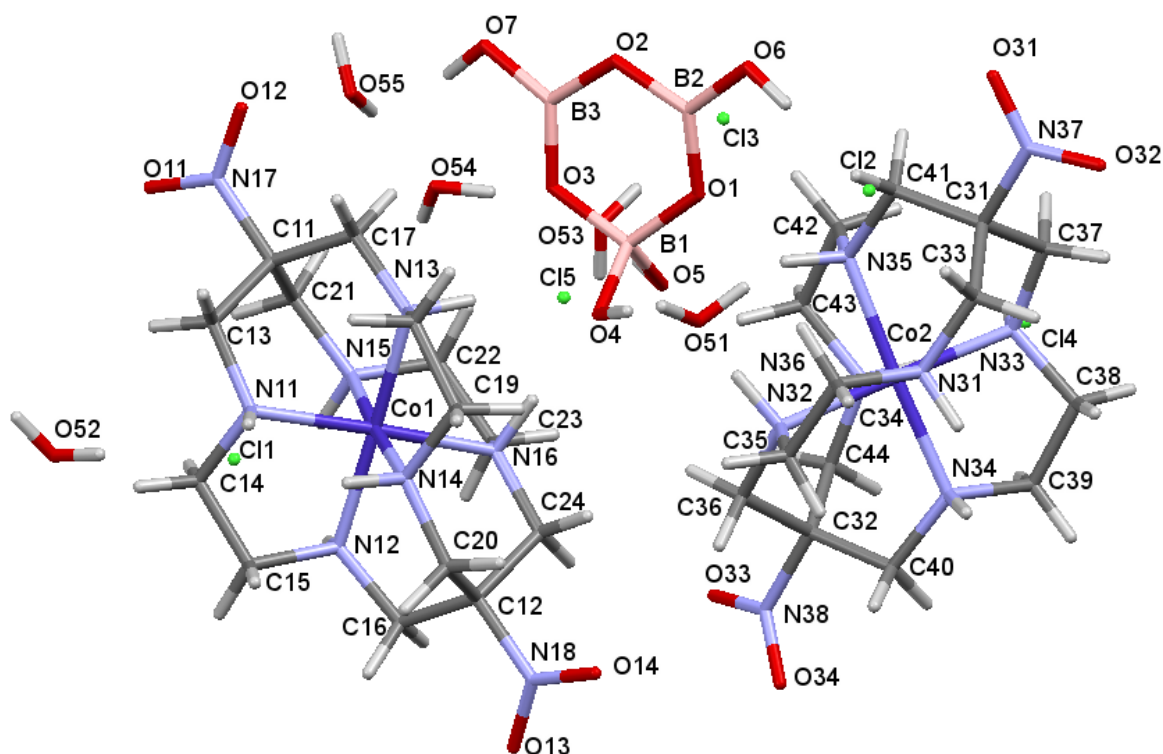


Figure 2.25 Diagram showing the structure and numbering scheme for **12**.

Table 2.13 Crystal data and structure refinement of **12**.

Empirical formula	C ₂₈ H _{73.50} B ₃ Cl ₅ N ₁₆ O _{19.75} CO ₂
Formula weight	1278.06
Temperature	100(2) K
Wavelength	0.71075 Å
Crystal system	Triclinic
Space group	<i>P</i> -1
Unit cell dimensions	$a = 9.6900(4)$ Å $\alpha = 85.079(3)^\circ$ $b = 10.0170(6)$ Å $\beta = 88.439(3)^\circ$ $c = 29.1374(7)$ Å $\gamma = 62.137(5)^\circ$
Volume	2490.9(2) Å ³
<i>Z</i>	2
Density (calculated)	1.704 Mg / m ³
Absorption coefficient	1.024 mm ⁻¹
<i>F</i> (000)	1331
Crystal	Lath; Orange
Crystal size	0.180 × 0.030 × 0.010 mm ³
θ range for data collection	2.420 – 29.944°
Index ranges	-13 ≤ <i>h</i> ≤ 12, -13 ≤ <i>k</i> ≤ 13, -38 ≤ <i>l</i> ≤ 40
Reflections collected	36914
Independent reflections	12826 [<i>R</i> _{int} = 0.0478]
Completeness to $\theta = 25.242^\circ$	99.9%
Absorption correction	Semi-empirical from equivalents
Max. and min. transmission	1.000 and 0.869
Refinement method	Full-matrix least-squares on <i>F</i> ²
Data / restraints / parameters	12826 / 0 / 668
Goodness-of-fit on <i>F</i> ²	1.023
Final <i>R</i> indices [<i>F</i> ² > 2σ(<i>F</i> ²)]	<i>R</i> 1 = 0.0485, <i>wR</i> 2 = 0.0976
<i>R</i> indices (all data)	<i>R</i> 1 = 0.0740, <i>wR</i> 2 = 0.1072
Extinction coefficient	n/a
Largest diff. peak and hole	0.881 and -0.662 e Å ⁻³
Radiation source (wavelength)	Mo-Kα (0.71073 Å)

Special details: There was disordered water for which exists either one or two molecules. Hence the given fractional formula.

The triborate(1-) anion is structurally known but rare, and a triborate(1-) anion with transition metal complex cations has never been observed before. The shorthand notification for the [B₃O₃(OH)₄]⁻ anion is 3:2Δ + 1T according to Christ and Clark¹⁶³ and Heller²⁷ schemes. As shown in Figure 2.26 the [B₃O₃(OH)₄]⁻ anion is comprised of a planar boroxole (B₃O₃) ring which contains one 4-coordinate boron centre (B1) and two 3-coordinate boron centres (B2, and B3). The B-O bonds to the 4-coordinate boron centre (B1) range from 1.466(4) - 1.471(4) Å [av. 1.468 Å] and these bond lengths are significantly longer than those involving the 3-coordinate boron centres (B2 and B3). The B-O distances to B2 and B3 centres range from 1.351(3) - 1.380(4) Å [av. 1.363 Å] and 1.347(4) - 1.386(4) Å [av. 1.363 Å], respectively. B-OH bonds involving the 4-coordinate boron centre (B1) are 1.467(3) Å and 1.468(3) Å, while B-OH bonds involving the 3-coordinate boron centres (B2 and B3) are 1.359(4) and 1.357(4)

Å, respectively. B2-O1 (1.351(3) Å) and B3-O3 (1.347(4) Å) are significantly shorter than the other B-O bonds within the boroxole rings. The boroxole ring is planar with ring angles ranging from 112.3(2) – 122.4(2)°. The smallest ring angle (O1-B1-O3) involves the 4-coordinate boron centre, whereas ring angles at O1, O2, and O3 average 121.1° and those at the 3-coordinate boron centres (B2 and B3) average 121.6°. This pattern of bond angles and bond lengths are in accord with previously reported data^{61,168–170} for this anion. The bond angles and lengths of **12** are listed in Appendix I (Table 7, and Table 8).

There are many H-bonding interactions to be found in the solid-state structure of **12**. These include H-bonds from anion to anion, cation to anion, H₂O to anion, and H₂O to H₂O. The four chemically non-equivalent oxygen sites may be designated α , α' , β , and γ (Figure 2.26) by using a similar nomenclature system to that previously described.^{98,77} This labelling system may be used to classify the H-bond interactions between different neighbouring ions and to differentiate between the available sites.

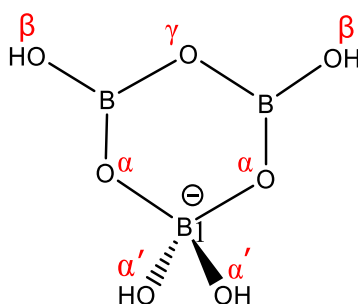


Figure 2.26 Diagram labelling the oxygen atom H-bond acceptor sites in the tetraborate(2-) anions.

The triborate(1-) anion in **12** displays four donor H-bond interactions involving three water molecules and one chloride anion acceptor sites.^{77,98} All the H-bond interactions are shown in Table 2.14.

Table 2.14 H-bond interactions in **12**.

$D-H \cdots A$	$d(D \cdots A)$	$D-H \cdots A$	$d(D \cdots A)$
O4–H4...O51	2.783(2)	N34–H34...Cl3 ⁱⁱ	3.182(2)
O5–H5...O53	2.804(2)	N35–H35...O5	2.898(3)
O6–H6...Cl2	3.082(2)	N36–H36...Cl4	3.087(2)
O7–H7...O55	2.757(3)	O51–H51A...Cl2	3.2728(19)

O7–H7...O61	2.769(3)	O51–H51B...Cl5	3.056(2)
N11–H11...Cl1	3.148(2)	O52–H52A...Cl5 ⁱⁱⁱ	3.121(3)
N12–H12...Cl5 ⁱ	3.136(2)	O52–H52B...Cl1	3.131(2)
N13–H13...O4	2.935(3)	O53–H53A...Cl2 ⁱ	3.1252(18)
N14–H14...Cl1	3.172(2)	O53–H53B...Cl3	3.1404(14)
N15–H15...Cl5 ⁱ	3.080(2)	O54–H54A...O53	2.603
N16–H16...O4	2.731(3)	O54–H54B...O6 ⁱ	2.934(2)
N31–H31...Cl3 ⁱⁱ	3.077(2)	O55–H55A...O54	2.656
N32–H32...O5	2.810(3)	O55–H55B...O51 ^{iv}	2.858(2)
N33–H33...Cl4	3.091(2)	O61–H61B...O51 ^{iv}	3.165(2)

(i) $x, y+1, z$

(ii) $x+1, y-1, z$

(iii) $-x+1, -y+1, -z$

(iv) $x-1, y+1, z$

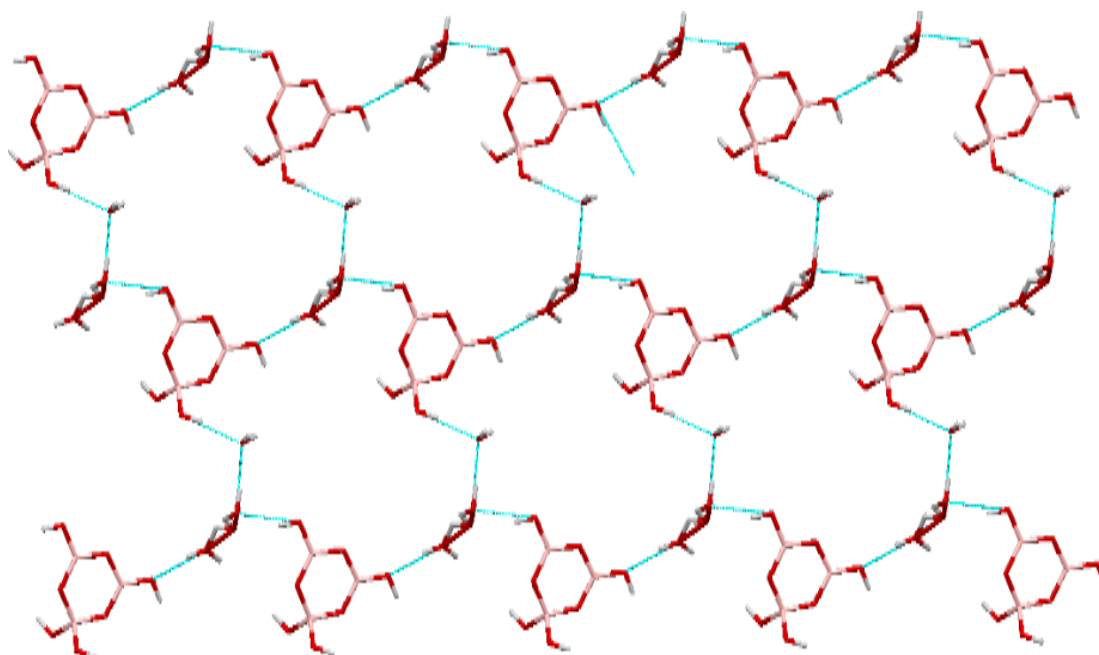


Figure 2.27 The triborate(1-) anions and water molecules layer structure (viewed along the c direction of the unit cell) of **12**. Dashed blue lines represent H-bonds.

Polyborate anions usually display multiple anion to anion H-bond interactions and these are believed⁵ to be the driving force in the synthesis of non-metal cation pentaborate(1-) salts. Anion to anion interactions were found to be present in **6**, **9** and **11**. However in **12**, triborate-triborate H-bond interactions are absent and each $[B_3O_3(OH)_4]^-$ anion is isolated from others by H_2O bridges, forming sheets (Figure 2.27). This isolation implies that the crystal structure of **12** is engineered by interactions with other components within the system. The triborate(1-) anion is able to form four donor H-bonds and has seven potential H-bond acceptor sites, and all, with the exception of α and γ -sites, are acceptors. The triborate(1-) anion accepts two H-bonds at α' -sites, and also at a β -site. The H-bonds directed at the α' -sites originate from amino

hydrogens of two $[\text{Co}(\text{diNOsar})]^{3+}$ cations in a chelating mode, as shown in Figure 2.28. These H-bond interactions are likely to be responsible for templating this salt and assembling the triborate(1-) anion. Secondary amine hydrogens of $[\text{Co}(\text{diNOsar})]^{3+}$ are known¹⁷¹ to form similar H-bond interactions *e.g.* $[\text{Co}(\text{diNOsar})][\text{S}_2\text{CN}(\text{CH}_2)_4]_3$. Details of all the H-bonding interactions are given in Table 2.14.

The $[\text{Co}(\text{diNOsar})]^{3+}$ cations, $[\text{B}_3\text{O}_3(\text{OH})_4]^-$ anions, Cl^- ions and H_2O molecules of crystallisation of compound **12** are connected through a complex series of H-bond interactions, with the anion network templated by the cations. The connection of the plane shown in Figure 2.29 to its neighbouring planes is formed by further H-bond interactions, forming a three-dimensional network

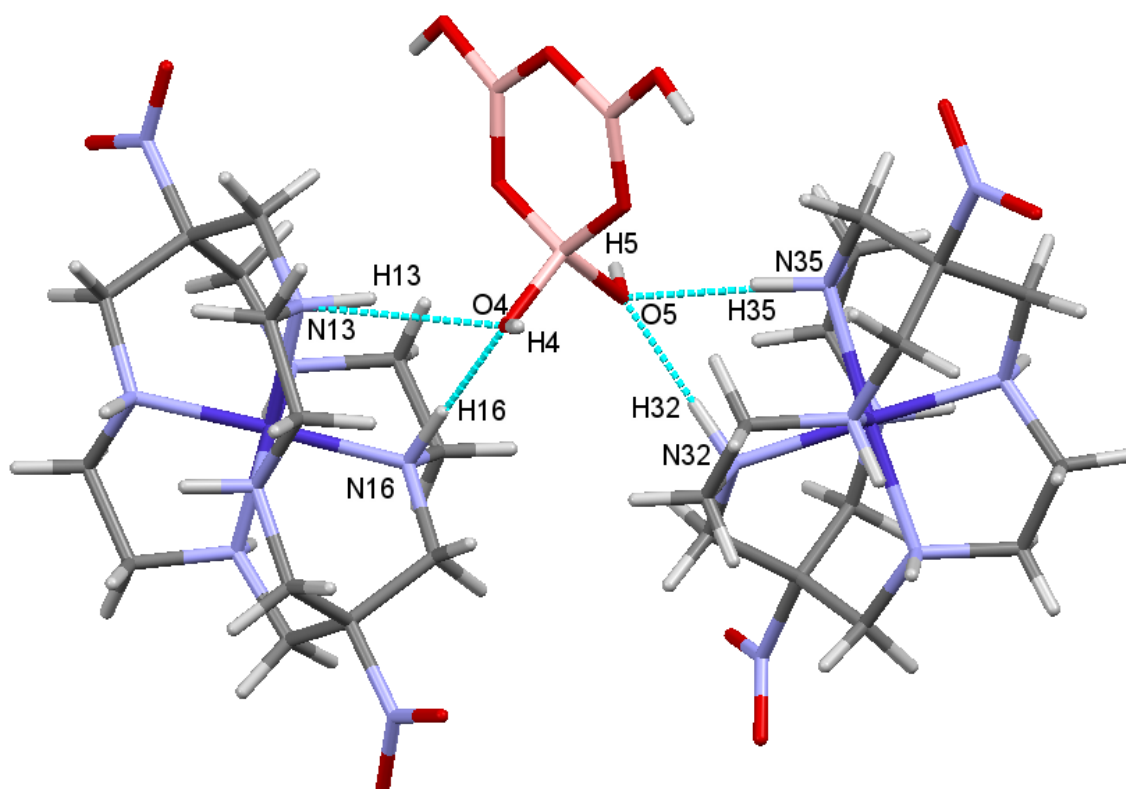


Figure 2.28 The H-bond connections of $[\text{Co}(\text{diNOsar})]^{3+}$ with triborate(1-) anions and chloride ions in **12**.

The $[\text{Co}(\text{diNOsar})]^{3+}$ cation comprises a central Co^{3+} ion surrounded by the six N donor atoms of the hexadentate neutral 1,8-dinitro-3,6,10,13,16,19-hexaazabicyclo[6.6.6]icosan

(diNOsar) ligand in a distorted octahedral environment. *Cis* and *trans* N-Co-N angles range from 86.43(9)-92.58(9)° [av. 90.06°] and 175.79(9)-178.12(10)° [av. 176.62°], respectively. The Co-N bond lengths range from 1.963(2)-1.975(2) Å, [av. 1.969 Å]. These data are not significantly different from previously reported data for this cation.¹⁷¹ According to Table 2.13 there are two [Co(diNOsar)]³⁺ cations (A and B) per unit cell. Each cation is involved in H-bonding to one [B₃O₃(OH)₄]⁻ anion and two chloride ions. Both cations interact at α' sites with the triborate(1-) anions (Figure 2.29). Full details are given in Table 2.14.

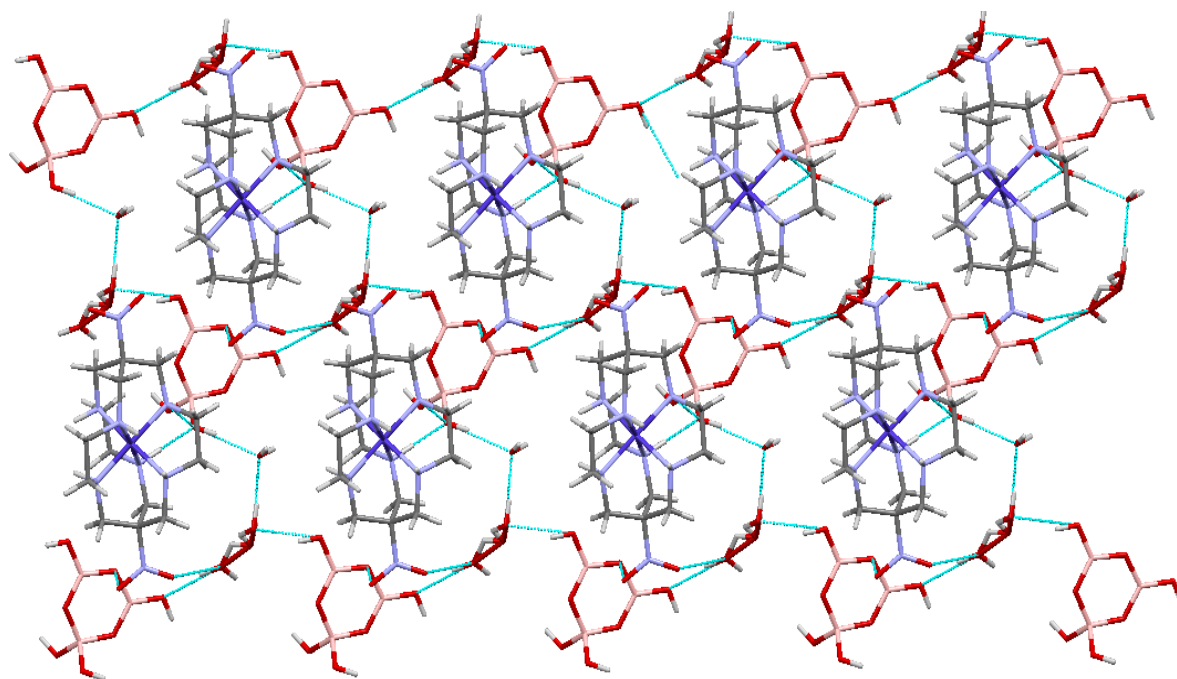


Figure 2.29 Triborate(1-) anions are arranged in planes linked together by H-bonds (dashed blue lines) from H₂O molecules. The [Co(diNOsar)]³⁺ cations fill the cavities and link to the triborate(1-) anions by further H-bonds (viewed along the *c* direction of the unit cell) in **12**.

2.4 Conclusion and summary

The synthesis of cobalt(III) complex polyborate salts by the reaction of boric acid and cobalt(III) complex hydroxide salts in varying ratios yielded polyborate salts in good yields. Nine polyborate salts have been prepared containing different polyborate anions: triborate(1-) (**12**), tetraborate(2-) (**9**), pentaborate(1-) (**6**, **7**, **13** and **14**), heptaborate(2-) (**10**), heptaborate(3-) (**8** and **11**), and octaborate(2-) (**6**) anions. Four of these salts have been characterized by single-crystal XRD studies (**6**, **9**, **11**, and **12**). Two compounds *s-fac*-[Co(dien)₂][B₇O₉(OH)₆]·9H₂O (**11**)¹³⁸ and [Co(en)₃][B₈O₁₀(OH)₆][B₅O₆(OH)₄]·5H₂O (**6**)¹³⁹ show previously unobserved heptaborate(3-) and octaborate(2-) anions, respectively.

Reaction of [Co(en)₃]³⁺ with boric acid in a 1:15 ratio produced compound **6** which contains two different polyborates anions, octaborate(2-) and pentaborate(1-), whereas the reaction in 1:10 ratio afforded two different polyborate compounds, **7** and **8**, containing pentaborate(1-) and heptaborate(3-) anions, respectively. Tetraborate(2-) salt **9** was produced as a result of the reaction [Co(NH₃)₆]³⁺ with boric acid in a 1:10 ratio, whilst heptaborate(2-) salt **10** was produced from 1:7 ratio. Reaction of [Co(diNOsar)]³⁺ in a 1:5 or 1:10 ratio yielded the triborate(1-) salt **12** or pentaborate(1-) salt **13**, respectively. The ratio of the boric acid and the complex cation reactions play a very important role in the identity of the polyborate salts formed.

The solid-state structures of **6**, **9**, **11**, and **12**, all display multiple cation-anion H-bond interactions and this undoubtedly plays a major role in the energetics of engineering these structures. For example, in compound **9**, all eighteen of the amino hydrogen atoms of the [Co(NH₃)₆]³⁺ cations are involved in secondary coordination to anions *via* H-bonds.

Chapter Three

**Copper(II) complex
polyborates**

3.1 Introduction

Copper is capable of forming a wide range of coordination compounds with different ligands in both copper(I) or copper(II) oxidation states. Copper(I) (cuprous) complexes are dominated by four coordination, while copper(II) (cupric) complexes have varying coordination numbers. The most common coordination number for copper(II) is six, but complexes with a coordination numbers of four or five are also known. The octahedral geometry of six-coordinate copper(II) complexes is generally distorted due to unequal occupation of e_g^* orbitals ($d_{x^2-y^2}$ and d_{z^2} orbitals) when the copper(II) ion with d^9 electronic configuration is subject to a Jahn-Teller effect (Section 1.3.2). The distortion (axial elongation) of copper(II) complexes has been described by the term tetragonality (T).¹⁷² It is defined as the ratio of the mean in-plane bond-length R_S^n and the mean out-of-plane bond-length R_L^n , n is the effective coordination number.

The chemistry of polyborate anions partnered with metal (*e.g.* sodium ion) or non-metal cations (*e.g.* ammonium ion) have been extensively studied.¹ In contrast reports of transition metal complex cations with polyborate anions are rare. Only a few copper(II) amine complexes have successfully formed polyborate systems, *e.g.* $[\text{Cu}(\text{C}_{12}\text{H}_8\text{N}_2)_2(\text{OAc})][\text{B}_5\text{O}_6(\text{OH})_4] \cdot \text{C}_4\text{H}_9\text{NO}$,¹²² $[\text{Cu}(\text{en})_2][\text{B}_7\text{O}_{13}\text{H}_3]_n$,¹¹⁶ $[\text{Cu}(\text{en})_2(\text{C}_5\text{H}_9\text{NO})][\text{B}_5\text{O}_6(\text{OH})_4]_2 \cdot \text{C}_5\text{H}_9\text{NO}$,¹²³ $[\text{Cu}(\text{en})_2\text{B}(\text{OH})_3][\text{B}_5\text{O}_5(\text{OH})_7]$,¹³¹ $\{[\text{Cu}(\text{H}_2\text{O})_2[\text{B}_4\text{O}_5(\text{OH})_4]_2\}(\mu\text{H}_2\text{O})\{\text{Ag}(\text{en})_2\} \cdot (\mu\text{H}_2\text{O})\{\text{Na}(\text{H}_2\text{O})_2\}$, $[\text{Cu}(\text{en})_2][\text{B}_4\text{O}_5(\text{OH})_4] \cdot 2\text{B}(\text{OH})_3$, and $[\text{Cu}(\text{en})_2\text{B}(\text{OH})_3(\text{H}_2\text{O})][\text{B}_4\text{O}_5(\text{OH})_4] \cdot 0.5\text{H}_2\text{O}$.¹³⁷ Polyborate anions associated with copper(II) complexes show considerable structural diversity. Copper(II) ions have also been found to coordinate with polyborate anions to produce anionic complex ions partnered with potassium or sodium cations. These form mixed-metal polyborate salts such as $\text{K}_5\text{H}\{\text{Cu}_4\text{O}[\text{B}_{20}\text{O}_{32}(\text{OH})_8]\} \cdot 33\text{H}_2\text{O}$ and $\text{Na}_5\text{H}[\text{Cu}_4\text{O}[\text{B}_{20}\text{O}_{32}(\text{OH})_8]\} \cdot 32\text{H}_2\text{O}$.¹⁷³

3.2 Aims

The main aim of this research was to synthesise and characterise some new copper(II) complex cation polyborate compounds. Several cationic copper(II) coordination complexes of ethylenediamine (en), *N,N,N',N'*-tetramethyl ethylenediamine (TMEDA), 1,2-diaminopropane (pn), 1,2-diaminocyclohexane (dach), *N*-(2-hydroxyethyl)ethylenediamine (hn), and *N,N*-dimethylethylenediamine (*N,N*-dmen) ligands have been prepared to template polyborate salt formation. Copper(II) complex cations have been chosen due to their potential to form many donor H-bond interactions with polyborate anions and their high steric bulk. These interactions

are believed to play an important role in the formation of the 3D supramolecular framework of the polyborate salts. In addition, the copper(II) polyborate compounds can be used to evaluate the structure directing effects in solid-state supramolecular structures associated with the copper(II) complex cations.

3.3 Result and discussion

3.3.1 Synthesis of copper(II) complexes

Previously reported copper(II) complexes; $[\text{Cu}(\text{en})_2]\text{SO}_4$ (**15**),¹⁷⁴ $[\text{Cu}(\text{pn})_2]\text{SO}_4$ (**16**),¹⁷⁵ and $[\text{Cu}(\text{dach})_2(\text{H}_2\text{O})_2]\text{Cl}_2$ (**17**),¹⁷⁶ were all prepared by standard literature methods, while $[\text{Cu}(\text{tn})_2]\text{SO}_4 \cdot 0.5\text{H}_2\text{O}$ (**18**) has been synthesised by method analogous to that described for $[\text{Cu}(\text{en})_2]\text{SO}_4$. $[\text{Cu}(\text{N,N-dmen})_2]\text{Cl}_2$ (**19**) was prepared by a procedure modified from Cui *et al.*¹⁷⁷ Physical properties of the prepared complexes were all in accordance with literature data. In general, a slight excess of ligand was added to the aqueous solutions of copper(II) sulphate or chloride salts. The solutions were stirred and then gently evaporated using a water bath. Finally, the concentrated solutions were cooled to yield the crude product. In the preparation of $[\text{Cu}(\text{en})_2]\text{SO}_4$ additional a large excess of ethylenediamine should be avoided due to formation $[\text{Cu}(\text{en})_3]\text{SO}_4$ in addition to the desired $[\text{Cu}(\text{en})_2]\text{SO}_4$.^{178,179}

The synthesised copper(II) complexes were prepared as chloride (**17** and **19**) and sulphate (**15**, **16**, and **18**) salts and it was therefore necessary to convert these salts to the corresponding hydroxide forms before reaction with boric acid (see Chapter 6 for experimental details). Copper(II) complex hydroxides were prepared using two different methods depending on the counter ion.

- i- Copper(II) hydroxide complexes were synthesised from copper(II) chloride complexes by using Dowex monosphere 550A ion exchange resin as described in Section **2.3.2**.
- ii- Copper(II) chloride complexes were converted to the hydroxide salts using stoichiometric amount of silver(I) oxide. The solution was left to stir for 30 minutes at room temperature until a precipitate of AgCl had formed.
- iii- Copper(II) sulphate complexes were converted to the hydroxide salts using stoichiometric amounts of barium hydroxide octahydrate. The mixture was rapidly stirred at room temperature for 10 minutes, then the white precipitate of barium sulphate was completely removed by filtration.

3.3.2 Preparation of copper(II) complex polyborate compounds

A series of copper(II) complex polyborate compounds **20-28** has been prepared as crystalline solids from the reaction of copper(II) complex cation hydroxides and boric acid in the ratios of 1:5 and 1:10. Seven copper(II) complex cations were used to react with boric acid. All nine compounds are new, except for **21**, which has been previously reported. A crystal structure and IR data have been reported for **21**. We now report additional data: ^{11}B NMR, p-XRD, magnetic properties, and thermal analyses.¹³⁷ We re-synthesised this compound using a new method. Spectroscopic data for **21** is discussed in the next sections and are reported in the experimental chapter.

Crystals suitable for single-crystal X-ray diffraction studies of copper(II) complex polyborate compounds were prepared by recrystallization of crude products by dissolving them in distilled water. The recrystallized products were obtained as described in Section 2.3.2. The recrystallized yields of copper(II) complex polyborate compounds and their formula are shown in Table 3.1.

Table 3.1 Yields and formula of copper(II) complex polyborate compounds.

Compound	Formula	% Yield
20	$[\text{Cu}(\text{en})_2][\text{B}_5\text{O}_6(\text{OH})_4]_2 \cdot 2\text{H}_2\text{O}$	52
21	$[\text{Cu}(\text{en})_2][\text{B}_4\text{O}_5(\text{OH})_4] \cdot 2\text{B}(\text{OH})_3$	59
22	$[\text{Cu}(\text{pn})_2\{\text{B}_5\text{O}_6(\text{OH})_4\}][\text{B}_5\text{O}_6(\text{OH})_4] \cdot 4\text{H}_2\text{O}$	56
23	$[\text{Cu}(\text{TMEDA})\{\text{B}_6\text{O}_7(\text{OH})_6\}] \cdot 6\text{H}_2\text{O}$	53
24	$[\text{Cu}(\text{dach})_2(\text{H}_2\text{O})_2][\text{Cu}(\text{dach})_2][\text{B}_7\text{O}_9(\text{OH})_5]_2 \cdot 4\text{H}_2\text{O}$	52
25	$[\text{Cu}(\text{tn})_2][\text{B}_5\text{O}_6(\text{OH})_4][\text{B}_3\text{O}_3(\text{OH})_4] \cdot 2\text{B}(\text{OH})_3 \cdot 2\text{H}_2\text{O}$	52
26	$[\text{Cu}(\text{tn})_2][\text{B}_4\text{O}_5(\text{OH})_4] \cdot \text{B}(\text{OH})_3 \cdot 6\text{H}_2\text{O}$	22
27	$[\text{Cu}(\text{N,N-dmen})_2(\text{H}_2\text{O})][\text{B}_5\text{O}_6(\text{OH})_4]_2 \cdot 3\text{H}_2\text{O}$	53
28	$[\text{Cu}(\text{N,N-dmen})\{\text{B}_6\text{O}_7(\text{OH})_6\}] \cdot 4\text{H}_2\text{O}$	41

3.3.3 Characterization of copper(II) complex polyborate compounds

The magnetic properties of the copper(II) complex starting materials and their polyborate derivatives were measured using Johnson Matthey balance. The mass susceptibility (χ_g), molar susceptibility (χ_m), diamagnetic susceptibility (χ_d), paramagnetic susceptibility (χ_p), and effective magnetic moment (μ_{eff}) of compounds **15-25**, and **27-28** are shown in Table 3.2. The copper(II) complexes and their polyborate salts were all found to be paramagnetic and did

not show any diagnostic change in magnetic properties between starting copper(II) complexes and their polyborate salts. The experimental effective magnetic moment data are close to those calculated from spin-only formula. The μ_{eff} values of Cu(II) complexes and their polyborate compounds are in agreement with literature data for Cu(II) complexes.¹⁸⁰

Table 3.2 Magnetic properties of copper(II) complexes and their polyborate compounds at 24 °C.

Compound	χ_g (cm ³ .g ⁻¹)	χ_m (cm ³ .mol ⁻¹)	χ_d	χ_p	μ_{eff} Bohr magneton	N
15	4.3×10^{-6}	1210×10^{-6}	-140×10^{-6}	1350×10^{-6}	1.79	1.05
16	4.5×10^{-6}	1380×10^{-6}	-150×10^{-6}	1530×10^{-6}	1.90	1.14
17	3.3×10^{-6}	1270×10^{-6}	-195×10^{-6}	1460×10^{-6}	1.86	1.11
18	3.7×10^{-6}	1170×10^{-6}	-158×10^{-6}	1180×10^{-6}	1.67	0.95
19	3.1×10^{-6}	960×10^{-6}	-160×10^{-6}	1110×10^{-6}	1.51	0.81
20	1.7×10^{-6}	1134×10^{-6}	-327×10^{-6}	1461×10^{-6}	1.86	1.11
21	2.0×10^{-6}	1007×10^{-6}	-249×10^{-6}	1256×10^{-6}	1.73	1.00
22	1.5×10^{-6}	1094×10^{-6}	-360×10^{-6}	1454×10^{-6}	1.85	1.10
23	2.3×10^{-6}	1320×10^{-6}	-283×10^{-6}	1603×10^{-6}	1.95	1.19
24	1.7×10^{-6}	1145×10^{-6}	-325×10^{-6}	1470×10^{-6}	1.86	1.12
25	1.8×10^{-6}	1365×10^{-6}	-369×10^{-6}	1734×10^{-6}	2.02	1.25
27	1.1×10^{-6}	820×10^{-6}	-370×10^{-6}	1200×10^{-6}	1.40	0.72
28	1.7×10^{-6}	880×10^{-6}	-250×10^{-6}	1140×10^{-6}	1.45	0.76

Elemental analysis of the copper(II) complex polyborate compounds were consistent with calculated values. The elemental analysis data of copper(II) complex polyborate compounds (**20-28**) are listed in Table 3.3.

Table 3.3 CHN analysis of copper(II) complex polyborate compounds.

Compound	Calculated (%)			Experimental (%)		
	C	H	N	C	H	N
20	7.5	4.1	8.8	7.4	4.4	8.6
21	9.6	5.2	11.2	9.7	5.4	11.4
22	10.0	5.0	7.8	10.1	5.4	7.6
23	12.7	6.1	4.9	12.8	6.2	5.0
24	22.2	6.0	8.6	22.0	6.1	8.5
25	10.1	5.4	7.6	9.8	5.2	7.6
26	12.6	6.9	9.8	12.9	6.8	9.5
27	12.8	5.4	7.5	13.0	5.3	7.3
28	9.5	5.2	5.6	9.7	5.2	5.5

NMR (^{11}B) data for compounds **20-28** are listed in Table 3.4. ^{11}B -NMR spectroscopy of copper(II) complex polyborate salts showed that pentaborate salts **20**, **22**, and **27** contained the characteristic three peaks ~ 18 ppm (due to $\text{B}(\text{OH})_3/\text{B}(\text{OH})_4^-$), ~ 13 ppm {due to $[\text{B}_3\text{O}_3(\text{OH})_4]^-$ }, and at ~ 1.3 ppm {due to the 4-coordinate boron centre of the $[\text{B}_5\text{O}_6(\text{OH})_4]^-$ } or a single signal at $\sim +16.0$ ppm.¹⁴⁹⁻¹⁵¹ ^{11}B NMR spectra of the triborate(1-) (**25**), tetraborate(2-) (**21** and **26**), hexaborate(2-) (**23** and **28**), and heptaborate(2-) (**24**) salts are quantitatively different from the spectra observed in the pentaborate salts with generally only one (averaged and exchanging) signal observed.

^1H and ^{13}C NMR spectra were not obtained. This may be attributed to paramagnetic effects of the copper(II) ion broadening the signals associated with the organic ligands which are within the primary coordination sphere of the metal. However, ^{11}B NMR spectra were obtainable since the polyborates in **20**, **21**, **24-27** are present as discrete anions, which are less influenced by the copper(II) ions. Compounds **22**, **23**, and **28** contain coordinated polyborates but the presence of ^{11}B signals of these compounds would indicate that the borate ligands are labile, and undergo the expected equilibria reactions once ligand dissociation to the aqueous solution has taken place.¹⁴⁹

Table 3.4 The chemical shift (δ) of ^{11}B -NMR spectra of copper(II) complex polyborate compounds (**20-28**).

Compound	^{11}B NMR/ppm
20	17.3 (72%), 13.4 (25%), 1.3 (2%)
21	13.9
22	16.9 (74%), 13.2 (24%), 1.5 (2%)
23	15.3
24	14.7
25	16.7
26	14.4
27	16.5
28	16.9

The FT-IR spectra assignment for the copper(II) complex polyborate compounds (**20-28**) are illustrated in Table 3.5. Infra-red data for compounds **20-28** support the formation of new polyborate compounds with copper(II) complexes and are in agreement with the reported literature data for the various proposed polyborate anions.¹⁴⁰

Table 3.5 Selected FT-IR spectroscopic data for the copper(II) complex polyborate compounds (20-28).

Comp.	$\nu(\text{O-H}),$ $\nu(\text{N-H})$	ν (C-H)	ν_{as} (B ₍₃₎ -O)	δ (B-O-H)	ν_{as} (B ₍₄₎ -O)	ν_{s} (B ₍₃₎ -O)	ν_{s} (B ₍₄₎ -O)	γ (B ₍₃₎ -O)
20	3459(bs), 3328(bs), 3282(bs)	2956(w), 2904(w)	1416(s), 1314(s)	1139(s)	1094(s), 1041(s)	927(s)	776(s)	708(s)
21	3513(bs), 3346(bs), 3252(bs)	2960(s), 2920(m)	1466(s), 1432(s)	1219(m)	1042(s), 1005(s)	943(m)	806(m), 707(m)	681(m)
22	3405(bs), 3305(bs)	2974(bs)	1423(s), 1380(s)	1120(m)	1061(s), 1019(s)	921(s)	778(s)	708(s)
23	3399(bs)	2926(w)	1469(m), 1419(s)	1133(s)	1086(s), 1037(s)	953(s)	809(s)	694(w)
24	3480(bs), 3303(bs), 3245(bs)	2931(s), 2863(m)	1467(m), 1454(s)	1183(s)	1134(s), 1059(s)	949(w)	854(s)	686(w)
25	3384(bs), 3333(bs)	2961(w)	1405(m), 1362(s)	1114(s)	1086(s), 1041(sh)	954(m)	809(s)	696(w)
26	3429(bs), 3350(bs)	2961(s)	1450(s), 1403(s)	1164(m)	1112(m), 1027(s)	933(m)	818(m), 708(w)	671(w)
27	3587(m), 3336(m)	2980(m)	1421(s), 1308(s)	1158(m)	1065(m), 1017(m)	918(m)	812(w), 776(m)	708(m)
28	3340(b), 3254(b)	2931(w), 2859(w)	1423(s), 1366(s)	1269(s)	1091(s), 1052(s)	958(m)	892(m), 859(m)	964(m)

B = broad, m = middle, s = strong, w = weak, sh = shoulder, B₍₃₎ = three coordinate boron, B₍₄₎ = four coordinate boron, ν = stretching frequency, ν_{s} = symmetrical stretching frequency, ν_{as} = asymmetrical stretching frequency, δ = bending frequency.

3.3.4 Thermal properties of copper(II) complex polyborate compounds

TGA and DSC analysis were used to investigate the thermal properties of copper(II) complex polyborate compounds. Samples were heated in an alumina (Al₂O₃) crucible at a temperature ramp rate of 10 °C / min between 25-800 °C under a flow air (100 mL / min.). The thermal decomposition stages of compounds 20-28 are illustrated in Table 3.6 and shown in Figures 3.1, 3.2, and 3.3. Previous work on hydrated transition metal complex polyborate salts has shown that they thermally lose their lattice water molecules at temperature up to 180 °C in air (*via* an endothermic process). At higher temperature (up to 280 °C), an endothermic process occurs due to dehydration of polyborate anion to afford anhydrous transition metal complex polyborate salts. Finally, at higher temperature (up to 850 °C), exothermic processes occur which are consistent with oxidation of the copper(II) complex cation ligands.

All the copper(II) complex compounds 20, 22-28 followed the expected path of decomposition, with observed mass losses agreeing with calculated values. The thermal

behaviour of the copper(II) complex polyborate compounds agreed with published data describing thermal decomposition of transition metal complex cations containing polyborate anions.^{122,123,131} Compound **21** has only two mass loss steps rather than three due to the absence of lattice water (Table 3.6) in its formation.

Table 3.6 The mass loss steps of copper(II) polyborate compounds **20-28**.*

Comp.	Step No.	The thermal reactions	Temp. Range °C	Expt. (%)	Calc. (%)
20	1	$[\text{Cu}(\text{en})_2][\text{B}_5\text{O}_6(\text{OH})_4]_2 \cdot 2\text{H}_2\text{O} \rightarrow [\text{Cu}(\text{en})_2][\text{B}_5\text{O}_6(\text{OH})_4]_2 + 2\text{H}_2\text{O}$	70-180	6.0	5.5
	2	$[\text{Cu}(\text{en})_2][\text{B}_5\text{O}_6(\text{OH})_4]_2 \rightarrow [\text{Cu}(\text{en})_2][\text{B}_{10}\text{O}_{16}] + 4\text{H}_2\text{O}$	180-280	16.0	16.5
	3	$[\text{Cu}(\text{en})_2][\text{B}_{10}\text{O}_{16}] + \text{excess O}_2 \rightarrow \text{CuB}_{10}\text{O}_{16} + \text{volatile oxidation products}$	280-600	32.9	34.9
		Residue $\text{CuB}_{10}\text{O}_{16}$		67.1	65.1
21	1	$[\text{Cu}(\text{en})_2][\text{B}_4\text{O}_5(\text{OH})_4] \cdot 2\text{H}_3\text{BO}_3 \rightarrow [\text{Cu}(\text{en})_2][\text{B}_6\text{O}_{10}] + 5\text{H}_2\text{O}$	100-200	18.9	18.1
	2	$[\text{Cu}(\text{en})_2][\text{B}_6\text{O}_{10}] + \text{excess O}_2 \rightarrow \text{CuB}_6\text{O}_{10} + \text{Volatile oxidation products}$	200-550	41.2	42.2
		Residue $\text{CuB}_6\text{O}_{10}$		58.8	57.8
22	1	$[\text{Cu}(\text{pn})_2\{\text{B}_5\text{O}_6(\text{OH})_4\}][\text{B}_5\text{O}_6(\text{OH})_4] \cdot 4\text{H}_2\text{O} \rightarrow [\text{Cu}(\text{pn})_2\{\text{B}_5\text{O}_6(\text{OH})_4\}][\text{B}_5\text{O}_6(\text{OH})_4] + 4\text{H}_2\text{O}$	70-180	9.1	10.0
	2	$[\text{Cu}(\text{pn})_2\{\text{B}_5\text{O}_6(\text{OH})_4\}][\text{B}_5\text{O}_6(\text{OH})_4] \rightarrow [\text{Cu}(\text{pn})_2][\text{B}_{10}\text{O}_{16}] + 4\text{H}_2\text{O}$	180-250	18.2	20.0
	3	$[\text{Cu}(\text{pn})_2][\text{B}_{10}\text{O}_{16}] + \text{excess O}_2 \rightarrow \text{CuB}_{10}\text{O}_{16} + \text{Volatile oxidation products}$	250-650	19.9	20.5
		Residue $\text{CuB}_{10}\text{O}_{16}$		61.9	59.4
23	1	$[\text{Cu}(\text{TMEDA})\{\text{B}_6\text{O}_7(\text{OH})_6\}] \cdot 6\text{H}_2\text{O} \rightarrow [\text{Cu}(\text{TMEDA})\{\text{B}_6\text{O}_7(\text{OH})_6\}] + 6\text{H}_2\text{O}$	70-180	19.4	19.1
	2	$[\text{Cu}(\text{TMEDA})\{\text{B}_6\text{O}_7(\text{OH})_6\}] \rightarrow [\text{Cu}(\text{TMEDA})][\text{B}_6\text{O}_{10}] + 3\text{H}_2\text{O}$	180-250	28.6	28.6
	3	$[\text{Cu}(\text{TMEDA})][\text{B}_6\text{O}_{10}] + \text{excess O}_2 \rightarrow \text{CuB}_6\text{O}_{10} + \text{Volatile oxidation products}$	250-650	48.1	49.2
		Residue $\text{CuB}_6\text{O}_{10}$		51.9	50.8
24	1	$[\text{Cu}(\text{dach})_2(\text{H}_2\text{O})_2][\text{Cu}(\text{dach})_2][\text{B}_7\text{O}_9(\text{OH})_5]_2 \cdot 4\text{H}_2\text{O} \rightarrow [\text{Cu}(\text{dach})_2]_2[\text{B}_7\text{O}_9(\text{OH})_5]_2 + 6\text{H}_2\text{O}$	70-190	9.0	8.3
	2	$[\text{Cu}(\text{dach})_2]_2[\text{B}_7\text{O}_9(\text{OH})_5]_2 \rightarrow [\text{Cu}(\text{dach})_2]_2[\text{B}_{14}\text{O}_{23}] + 5\text{H}_2\text{O}$	190-250	16.0	15.2
	3	$[\text{Cu}(\text{dach})_2]_2[\text{B}_{14}\text{O}_{23}] + \text{excess O}_2 \rightarrow \text{Cu}_2\text{B}_{14}\text{O}_{23} + \text{Volatile oxidation products}$	250-650	51.0	50.4
		Residue $\text{Cu}_2\text{B}_{14}\text{O}_{23}$		49.0	49.6
25	1	$[\text{Cu}(\text{tn})_2][\text{B}_5\text{O}_6(\text{OH})_4][\text{B}_3\text{O}_3(\text{OH})_4]_2\text{B}(\text{OH})_3 \cdot 2\text{H}_2\text{O} \rightarrow [\text{Cu}(\text{tn})_2][\text{B}_5\text{O}_6(\text{OH})_4][\text{B}_3\text{O}_3(\text{OH})_4]_2\text{B}(\text{OH})_3 + 2\text{H}_2\text{O}$	70-200	5.8	4.9
	2	$[\text{Cu}(\text{tn})_2][\text{B}_5\text{O}_6(\text{OH})_4][\text{B}_3\text{O}_3(\text{OH})_4]_2\text{B}(\text{OH})_3 \rightarrow [\text{Cu}(\text{tn})_2][\text{B}_{10}\text{O}_{16}] + 7\text{H}_2\text{O}$	200-250	21.8	21.9
	3	$[\text{Cu}(\text{tn})_2][\text{B}_{10}\text{O}_{16}] + \text{excess O}_2 \rightarrow \text{CuB}_{10}\text{O}_{16} + \text{Volatile oxidation products}$	250-850	42.5	42.1
		Residue $\text{CuB}_{10}\text{O}_{16}$		57.5	57.9
26	1	$[\text{Cu}(\text{tn})_2][\text{B}_4\text{O}_5(\text{OH})_4]\text{H}_3\text{BO}_3 \cdot 6\text{H}_2\text{O} \rightarrow [\text{Cu}(\text{tn})_2][\text{B}_4\text{O}_5(\text{OH})_4]\text{H}_3\text{BO}_3 + 6\text{H}_2\text{O}$	70-200	17.0	18.8
	2	$[\text{Cu}(\text{tn})_2][\text{B}_4\text{O}_5(\text{OH})_4]\text{H}_3\text{BO}_3 \rightarrow [\text{Cu}(\text{tn})_2][\text{B}_5\text{O}_{8.5}] + 3.5\text{H}_2\text{O}$	200-300	27.1	29.8
	3	$[\text{Cu}(\text{tn})_2][\text{B}_5\text{O}_{8.5}] + \text{excess O}_2 \rightarrow \text{CuB}_5\text{O}_{8.5} + \text{volatile oxidation products}$	300-700	55.5	55.8
		Residue $\text{CuB}_5\text{O}_{8.5}$		44.5	44.2
27	1	$[\text{Cu}(\text{N,N-dmen})_2(\text{H}_2\text{O})][(\text{B}_5\text{O}_6(\text{OH})_4)]_2 \cdot 3\text{H}_2\text{O} \rightarrow [\text{Cu}(\text{N,N-dmen})_2][(\text{B}_5\text{O}_6(\text{OH})_4)]_2 + 4\text{H}_2\text{O}$	30-90	9.8	9.6
	2	$[\text{Cu}(\text{N,N-dmen})_2][(\text{B}_5\text{O}_6(\text{OH})_4)]_2 \rightarrow [\text{Cu}(\text{N,N-dmen})_2][\text{B}_{10}\text{O}_{16}] + 4\text{H}_2\text{O}$	90-250	21.3	19.2
	3	$[\text{Cu}(\text{N,N-dmen})_2][\text{B}_{10}\text{O}_{16}] + \text{excess O}_2 \rightarrow \text{CuB}_{10}\text{O}_{16} + \text{volatile oxide product}$	250-630	45.1	42.7

		Residue CuB ₁₀ O ₁₆		54.9	57.3
28	1	[Cu(N,N-dmen){B ₆ O ₇ (OH) ₆ }]·4H ₂ O → [Cu(N,N-dmen){B ₆ O ₇ (OH) ₆ }] + 4H ₂ O	30-120	14.2	14.3
	2	[Cu(N,N-dmen){B ₆ O ₇ (OH) ₆ }] → [Cu(N,N-dmen)B ₆ O ₁₀] + 3H ₂ O	120-250	26.0	25.0
	3	[Cu(N,N-dmen)B ₆ O ₁₀] + excess O ₂ → CuB ₆ O ₁₀ + volatile oxide product	250-630	44.3	42.5
		Residue CuB ₆ O ₁₀		55.7	57.5

* Calculated values and experimental values are given as totals relative to 100% and include the process described and the earlier mass loss process.

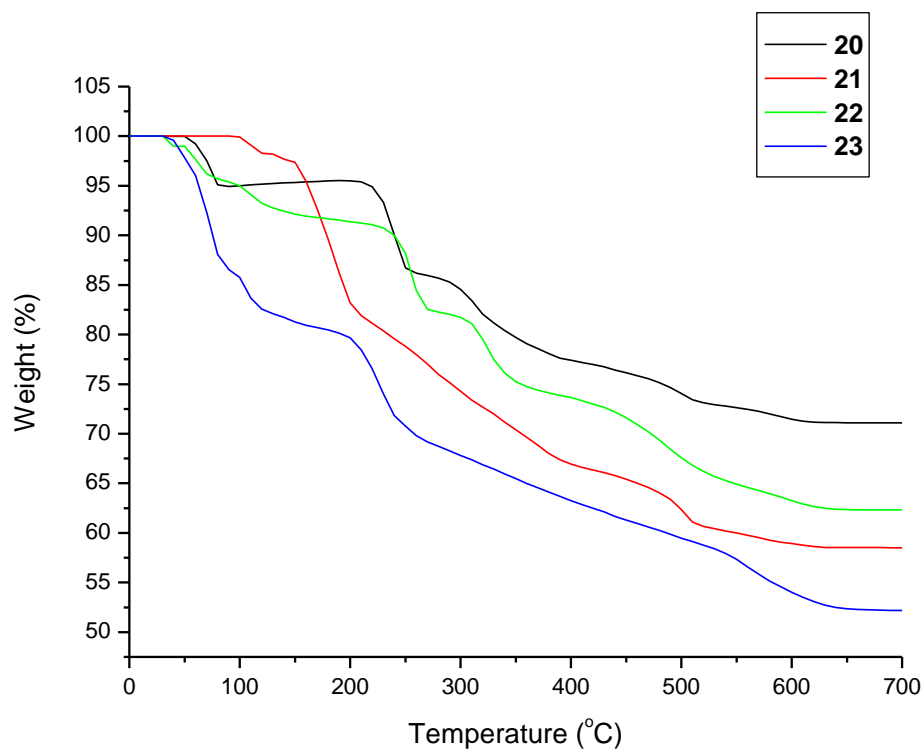


Figure 3.1 TGA diagram for the thermal decomposition of copper(II) complex polyborate compounds **20-23**.

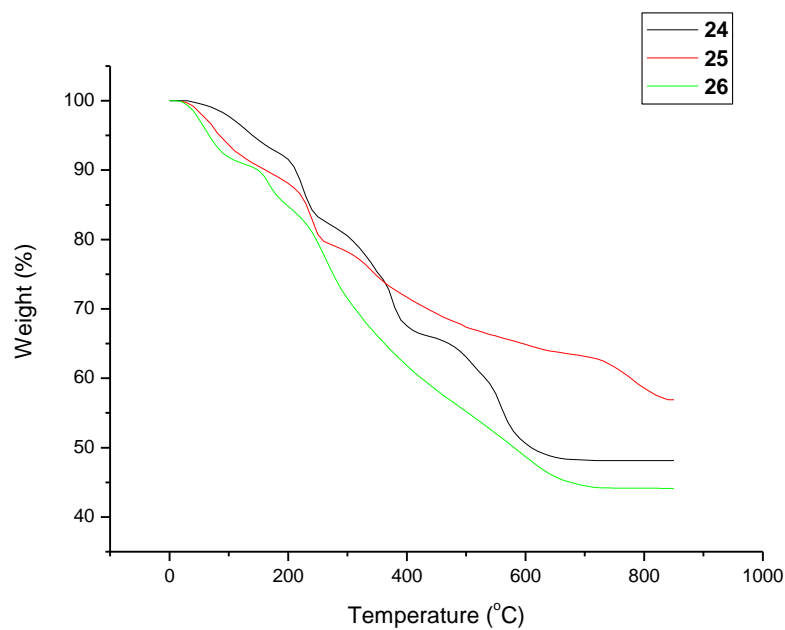


Figure 3.2 TGA diagram for the thermal decomposition of copper(II) complex polyborate compounds **24-26**.

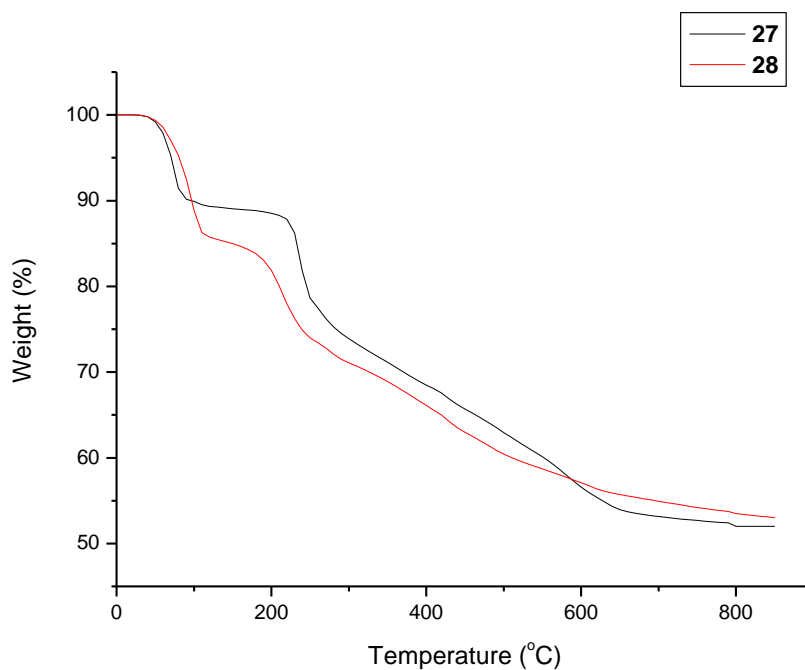


Figure 3.3 TGA diagram for the thermal decomposition of copper(II) complex polyborate compounds **27-28**.

3.3.5 Structural characterisation of copper(II) complex polyborate compounds

3.3.5.1 Structural characterisation of [Cu(en)₂][B₅O₆(OH)₄]₂·2H₂O (20)

Crystallographic data for **20** are listed in Table 3.7. The crystals of **20** are triclinic, *P*-1 contains an ionic compound with one transition metal complex cation [Cu(en)₂]²⁺ partnered with two symmetry-related [B₅O₆(OH)₄]⁻ anions and two symmetry-related water molecules as shown in Figure 3.4.

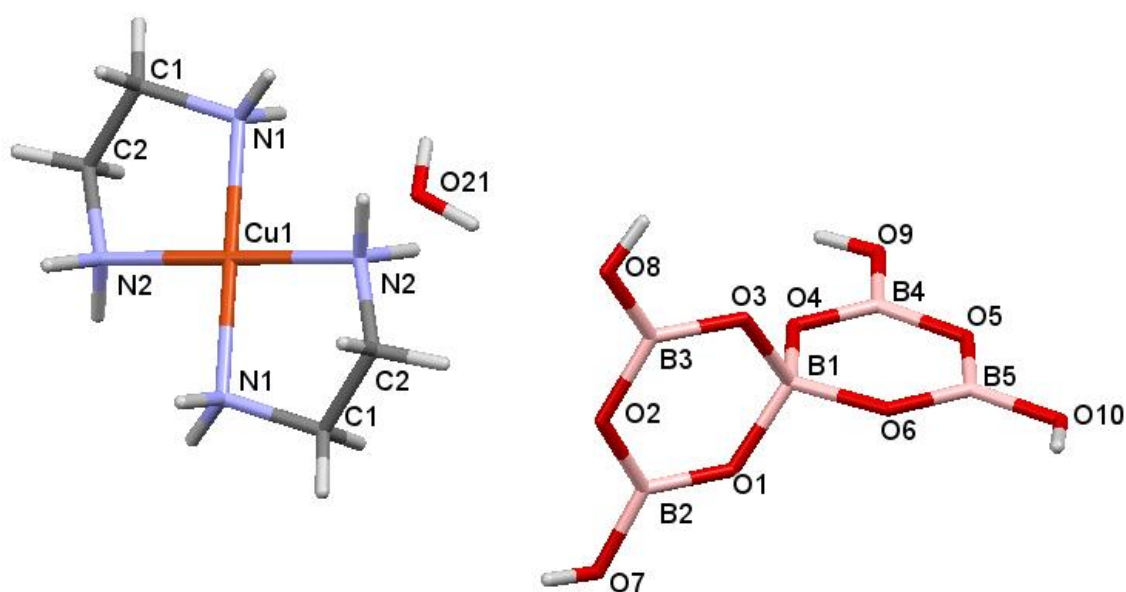


Figure 3.4 Diagram showing the complex cation [Cu(en)₂]²⁺, pentaborate(1-) anion and water molecule in **20** and the adopted numbering scheme. Colour code (used throughout this chapter): brown (Cu), blue (N), red (O), pink (B), dark grey (C) and light grey (H).

Table 3.7 Crystallographic data and structure refinement of **20**.

Empirical formula	C ₄ H ₂₈ B ₁₀ N ₄ O ₂₂ Cu	
Formula weight	655.94	
Temperature	100(2) K	
Wavelength	0.71075 Å	
Crystal system	Triclinic	
Space group	<i>P</i> -1	
Unit cell dimensions	$a = 8.0286(5) \text{ \AA}$	$\alpha = 92.867(5)^\circ$
	$b = 8.6193(5) \text{ \AA}$	$\beta = 104.567(6)^\circ$
	$c = 9.6553(7) \text{ \AA}$	$\gamma = 98.474(5)^\circ$
Volume	636.97(7) Å ³	

Z	1
Density (calculated)	1.710 Mg / m ³
Absorption coefficient	0.958 mm ⁻¹
<i>F</i> (000)	335
Crystal	Blade; Purple
Crystal size	0.180 × 0.090 × 0.030 mm ³
θ range for data collection	2.968 – 27.477°
Index ranges	-10 ≤ <i>h</i> ≤ 10, -10 ≤ <i>k</i> ≤ 11, -12 ≤ <i>l</i> ≤ 11
Reflections collected	9265
Independent reflections	2913 [<i>R</i> _{int} = 0.0341]
Completeness to $\theta = 25.242^\circ$	99.6%
Absorption correction	Semi-empirical from equivalents
Max. and min. transmission	1.000 and 0.808
Refinement method	Full-matrix least-squares on <i>F</i> ²
Data / restraints / parameters	2913 / 0 / 194
Goodness-of-fit on <i>F</i> ²	1.076
Final <i>R</i> indices [<i>F</i> ² > 2σ(<i>F</i> ²)]	<i>R</i> 1 = 0.0303, <i>wR</i> 2 = 0.0811
<i>R</i> indices (all data)	<i>R</i> 1 = 0.0337, <i>wR</i> 2 = 0.0828
Extinction coefficient	n/a
Largest diff. peak and hole	0.395 and -0.330 e Å ⁻³
Radiation source (wavelength)	Mo-Kα (0.71073 Å)

Compound **20** has Cu-N distances ranging from to 2.0044(14)-2.0195(14) Å [av. 2.0120 Å] and two pentaborate(1-) anions hydroxyl oxygen atoms (O7) at axial positions at 2.839 Å. The tetragonality (*Tⁿ*) approach of Hathaway and Hodgson,¹⁷² yields a *T* value of 0.7 which is at the low end of the range for elongated tetragonal octahedral geometry and at the high end of the range for square planar geometry. However, the axial Cu-O interactions are presumably weak, and we have formulated the [Cu(en)₂]²⁺ cation in **20** as distorted square-planar.

The pentaborate(1-) anions in **20** are structurally similar to, other transition metal complex cation pentaborate salts involving isolated [B₅O₆(OH)₄]⁻ anions.^{136,181} This also applies to non-metal cation pentaborate(1-) salts.¹ The B-O distances to the 4-coordinate B1 centre range from 1.455(2) - 1.487(2) Å [av. 1.469 Å] and are significantly longer than those involving the 3-coordinate boron centres which range from 1.356(2) - 1.393(2) Å [av. 1.373 Å]. B-O bonds involving 3-coordinate boron centres and terminal OH groups are at the shorter end of the range [av. 1.3615 Å] whilst B-O bonds involving the oxygen atoms distal (O2, O5) to the 4-coordinate B1 centre are at the longer end of the range [av. 1.3855 Å]. Bond angles at the B1 centre range from 107.74(13)° - 111.51(13)°, and angles at the other ring atoms range from 115.96(15)° - 125.52(15)° for B centres consistent with sp³ and sp² hybridization, respectively. The bond lengths and angles of **20** are listed in Appendix I (Table 9, and Table 10).

In general, each pentaborate(1-) anion has four potential H-bond donor sites (O7, O8, O9, and O10) which are also capable of accepting H-bond interactions, and six additional

potential H-bond acceptor sites with the B-O-B units. In **20** each pentaborate(1-) anion has twelve H-bond interactions (4 H-bond donors and 8 H-bond acceptors) but any H-bond interactions at O2 are absent. According to Schubert⁹⁸ the oxygen acceptor sites of pentaborate(1-) anion are labelled α , β , or γ (Figure 3.5). This labelling system have been used to classify the H-bond interactions between different neighbouring $[\text{B}_5\text{O}_6(\text{OH})_4]^-$ ions and to differentiate between the available sites.

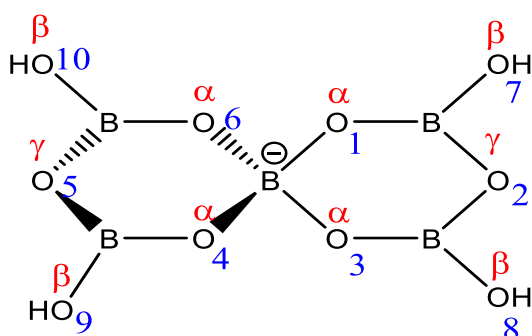


Figure 3.5 Diagram showing the H-bond acceptor sites and their numbers in the pentaborate(1-) anions.

In **20** the 4 H-bond donor sites of pentaborate(1-) anion are involved with H-bond acceptor oxygens of three different pentaborate(1-) anions ($\text{O8-H8}\cdots\text{O3}^*$, $\text{O9-H9}\cdots\text{O4}^*$ and $\text{O10-H10}\cdots\text{O3}^*$) and one water molecule ($\text{O7-H7}\cdots\text{O21}^*$). The H-bond acceptor sites arising from donor H-bond sites of the pentaborate(1-) anion can be designated as $\alpha\alpha\alpha\omega$, where ω is a water acceptor site.^{77,98} The direction of the four H atoms of the hydroxyl donor sites in the pentaborate(1-) anions of **20** are three "in" and one "out" (Figure 3.4). This is a very common structural motif.¹ All the H-bond data of **20** are given in Table 3.8.

Table 3.8 H-bonds [\AA and $^\circ$] in **20**.

$D\text{-H}\cdots A$	$d(D\cdots A)$	$D\text{-H}\cdots A$	$d(D\cdots A)$
N1-H1C \cdots O10 ⁱⁱ	3.1211(18)	O8-H8 \cdots O3 ^{vii}	2.7436(17)
N1-H1D \cdots O1 ⁱⁱⁱ	3.0289(17)	O9-H9 \cdots O4 ^{iv}	2.7595(16)
N1-H1D \cdots O4 ⁱⁱⁱ	3.4793(18)	O10-H10 \cdots O3 ^{viii}	2.9006(15)
N2-H2C \cdots O5 ^{iv}	3.0157(18)	O21-H21A \cdots O8	2.8108(18)
N2-H2D \cdots O1 ^v	2.8998(18)	O21-H21B \cdots O6 ^v	2.9334(17)
O7-H7 \cdots O21 ^{vi}	2.6936(18)		

(i) $-x, -y, -z+1$
(vi) $-x+1, -y+1, -z+1$

(ii) $x-1, y, z+1$
(vii) $-x+1, -y+1, -z$

(iii) $-x+1, -y, -z+1$
(viii) $-x+2, -y+1, -z$

(iv) $-x+1, -y, -z$

(v) $x-1, y, z$

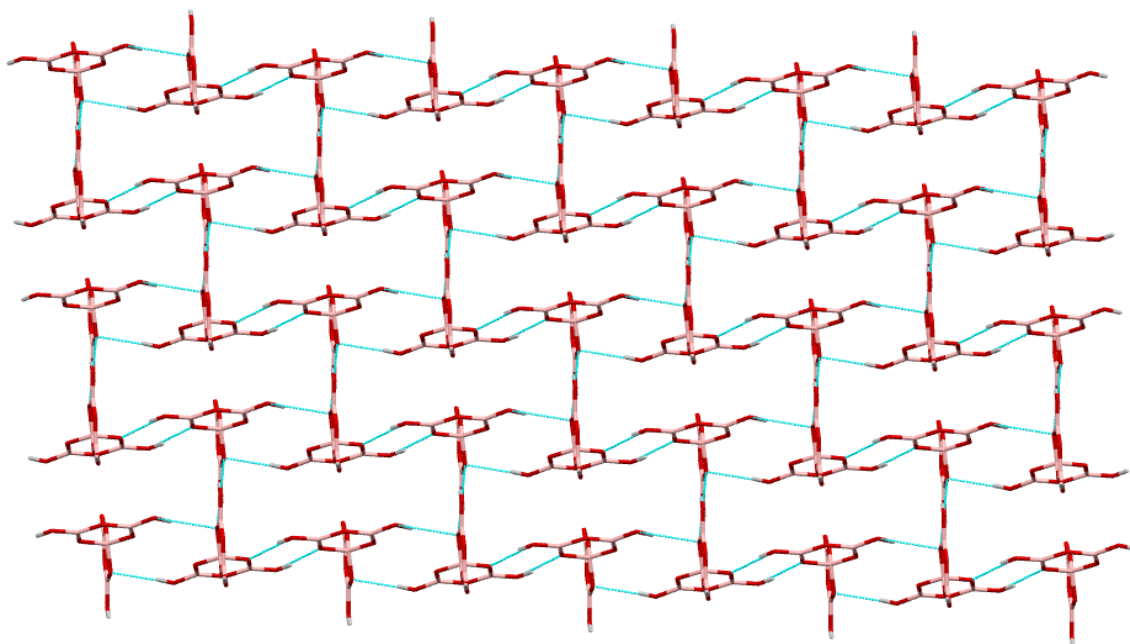


Figure 3.6 View of a plane of pentaborate(1-) anions (viewed along the *c* direction of the unit cell) in **20**. Dashed blue lines represent H-bonds.

A view of the layered structure of the $[\text{B}_5\text{O}_6(\text{OH})_4]^-$ anions of **20** is shown in Figure 3.6. Detailed inspection of Figure 3.7 shows that ribbons of $[\text{B}_5\text{O}_6(\text{OH})_4]^-$ anions are horizontally connected by two reciprocal interactions and these two interactions are composed of $\text{R}_2^2(8)$ and $\text{R}_2^2(12)$ motifs. The $\text{R}_2^2(8)$ reciprocal connection is formed between two pentaborate(1-) anions by one boroxyl (B_3O_3) ring of each pentaborate(1-) anion $\text{O9-H9}\cdots\text{O4}^*/\text{O9}^*-\text{H9}\cdots\text{O4}$ ($\text{O}\cdots\text{O}$ distance is 2.75 Å and a $\angle\text{OHO}$ angle 171.74°), while the $\text{R}_2^2(12)$ reciprocal connection is formed by unprecedented participation of both boroxyl (B_3O_3) rings of each pentaborate(1-) anion $\text{O10-H10}\cdots\text{O3}^*/\text{O10}^*-\text{H10}\cdots\text{O3}$ ($\text{O}\cdots\text{O}$ distance is 2.9 Å, and a $\angle\text{OHO}$ angle 145.48°). The boroxyl (B_3O_3) rings of the pentaborate(1-) anion ribbons are crosslinked to other pentaborate(1-) anion ribbons by a further $\text{R}_2^2(8)$ reciprocal $\beta\rightarrow\alpha$ interaction which $\text{O8-H8}\cdots\text{O3}^*/\text{O8}^*-\text{H8}\cdots\text{O3}$ ($\text{O}\cdots\text{O}$ distance is 2.74 Å and a $\angle\text{OHO}$ angle 167.02°). The final donor hydroxyl group of each $[\text{B}_5\text{O}_6(\text{OH})_4]^-$ anion acts to crosslink the planes *via* a $\beta\rightarrow\omega$ interaction with a water molecule $\text{O7-H7}\cdots\text{O21}^*$ ($\text{O}\cdots\text{O}$ distance is 2.69 Å and a $\angle\text{OHO}$ angle 173.51°). Thus, each $[\text{B}_5\text{O}_6(\text{OH})_4]^-$ anion participates in the supramolecular architecture by 3($\beta\rightarrow\alpha$) and 1($\beta\rightarrow\omega$) H-bond interactions.

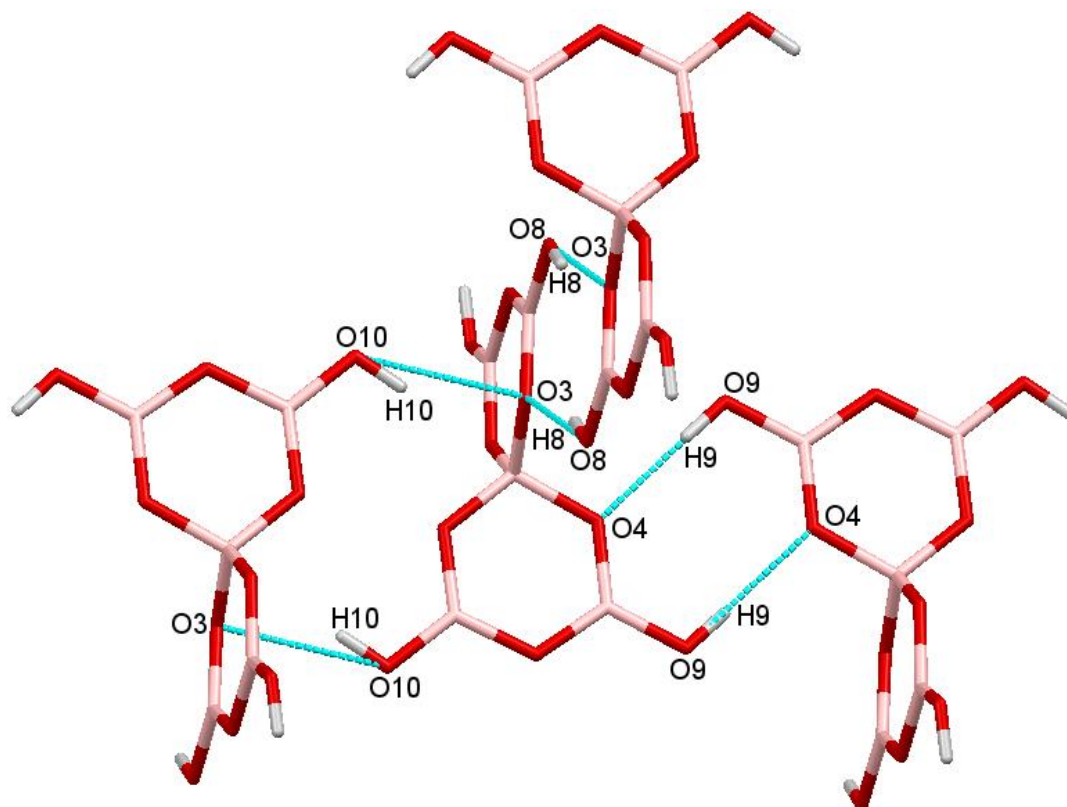


Figure 3.7 The two $R_2^2(8)$ and $R_2^2(12)$ H-bond motif connections between pentaborate(1-) anions in **20**.

The $[\text{Cu}(\text{en})_2]^{2+}$ cations, $[\text{B}_5\text{O}_6(\text{OH})_4]^-$ anions, and H_2O molecules of crystallization of **20** are connected through a complex series of H-bond interactions, with the anion network templated by the cations. Figure 3.8 shows that neighbouring planes connect *via* further H-bond interactions, forming a three-dimensional network. The $[\text{Cu}(\text{en})_2]^{2+}$ cation is included within the supramolecular framework structure, occupying the "cavities" present as shown in Figure 3.8. According to Table 3.7 there is one $[\text{Cu}(\text{en})_2]^{2+}$ cation per unit cell. This cation connects to $[\text{B}_5\text{O}_6(\text{OH})_4]^-$ ions by H-bonds. The $[\text{Cu}(\text{en})_2]^{2+}$ cation acts as a H-bond donor to two $[\text{B}_5\text{O}_6(\text{OH})_4]^-$ anions *via* three H-bond interactions involving two bifurcated H-bonds to one of the pentaborate(1-) anion $\text{N1-H1D}\cdots\text{O1}^*$ and $\text{N2-H2D}\cdots\text{O1}^*$ ($\text{N}\cdots\text{O}$ distances are 3.02 and 2.9 Å, respectively and $\angle\text{NHO}$ angles are 138.67 and 146.06°, respectively) and one H-bond to the other pentaborate(1-) anion $\text{N2-H2C}\cdots\text{O5}^*$ ($\text{N}\cdots\text{O}$ distance is 3.01 Å and $\angle\text{NHO}$ angle is 155.36°).

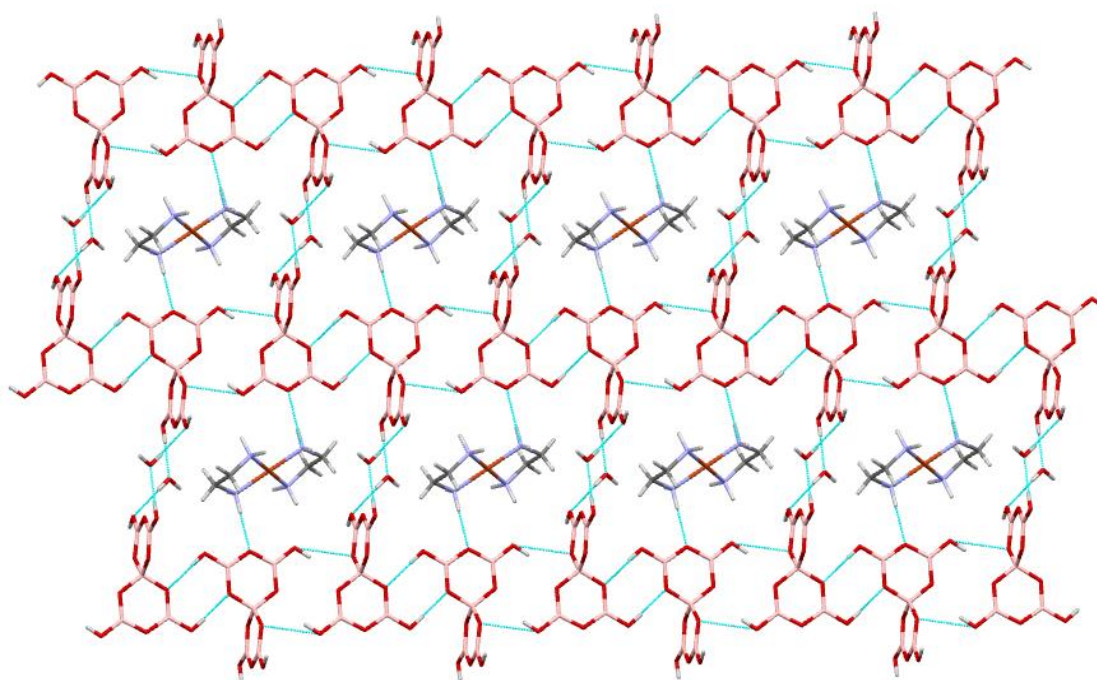


Figure 3.8 Diagram showing a 'plane' of polyborate anions (viewed along the *c* direction of the unit cell) and water molecule with $[\text{Cu}(\text{en})_2]^{2+}$ cations in **20**.

3.3.5.2 Structural characterisation of $[\text{Cu}(\text{pn})_2\{\text{B}_5\text{O}_6(\text{OH})_4\}][\text{B}_5\text{O}_6(\text{OH})_4]\cdot 4\text{H}_2\text{O}$ (**22**)

Crystallographic data of **22** compound are listed in Table 3.9. The crystals of **22** are triclinic, *P*-1 and **22** is an ionic compound with one transition metal complex cation $[\text{Cu}(\text{pn})_2\{\text{B}_5\text{O}_6(\text{OH})_4\}]^+$ partnered with a $[\text{B}_5\text{O}_6(\text{OH})_4]^-$ anion and with four water molecules as shown in Figure 3.9.

Table 3.9 Crystal data and structure refinement details of **22**.

Empirical formula	$\text{C}_6\text{H}_{36}\text{B}_{10}\text{N}_4\text{O}_{24}\text{Cu}$	
Formula weight	720.03	
Temperature	100(2) K	
Wavelength	0.71073 Å	
Crystal system	Triclinic	
Space group	<i>P</i> -1	
Unit cell dimensions	$a = 11.1860(5)$ Å	$\alpha = 72.405(5)^\circ$
	$b = 11.4551(8)$ Å	$\beta = 86.282(4)^\circ$
	$c = 12.2830(6)$ Å	$\gamma = 71.320(5)^\circ$
Volume	1420.35(15) Å ³	
<i>Z</i>	2	
Density (calculated)	1.684 Mg / m ³	

Absorption coefficient	0.872 mm ⁻¹
<i>F</i> (000)	742
Crystal	Block; Purple
Crystal size	0.230 × 0.110 × 0.050 mm ³
θ range for data collection	1.966 – 27.776°
Index ranges	-14 ≤ <i>h</i> ≤ 14, -14 ≤ <i>k</i> ≤ 13, -15 ≤ <i>l</i> ≤ 15
Reflections collected	24265
Independent reflections	6574 [<i>R</i> _{int} = 0.0178]
Completeness to $\theta = 25.242^\circ$	99.7%
Absorption correction	Semi-empirical from equivalents
Max. and min. transmission	1.000 and 0.946
Refinement method	Full-matrix least-squares on <i>F</i> ²
Data / restraints / parameters	6574 / 24 / 438
Goodness-of-fit on <i>F</i> ²	1.028
Final <i>R</i> indices [<i>F</i> ² > 2σ(<i>F</i> ²)]	<i>R</i> 1 = 0.0243, <i>wR</i> 2 = 0.0665
<i>R</i> indices (all data)	<i>R</i> 1 = 0.0252, <i>wR</i> 2 = 0.0669
Extinction coefficient	n/a
Largest diff. peak and hole	0.397 and -0.402 e Å ⁻³
Radiation source (wavelength)	Mo-Kα (0.71073 Å)

Special details: The coordinated diamines were found to be disordered over two positions resulting in the need to use various geometrical (SAME) and displacement (RIGU) restraints, with the lesser component carbon atoms left isotropic. To facilitate suitable hydrogen bonding, the nitrogen atoms were split into the two different components but constrained to be identical using the EADP and EXYZ commands.

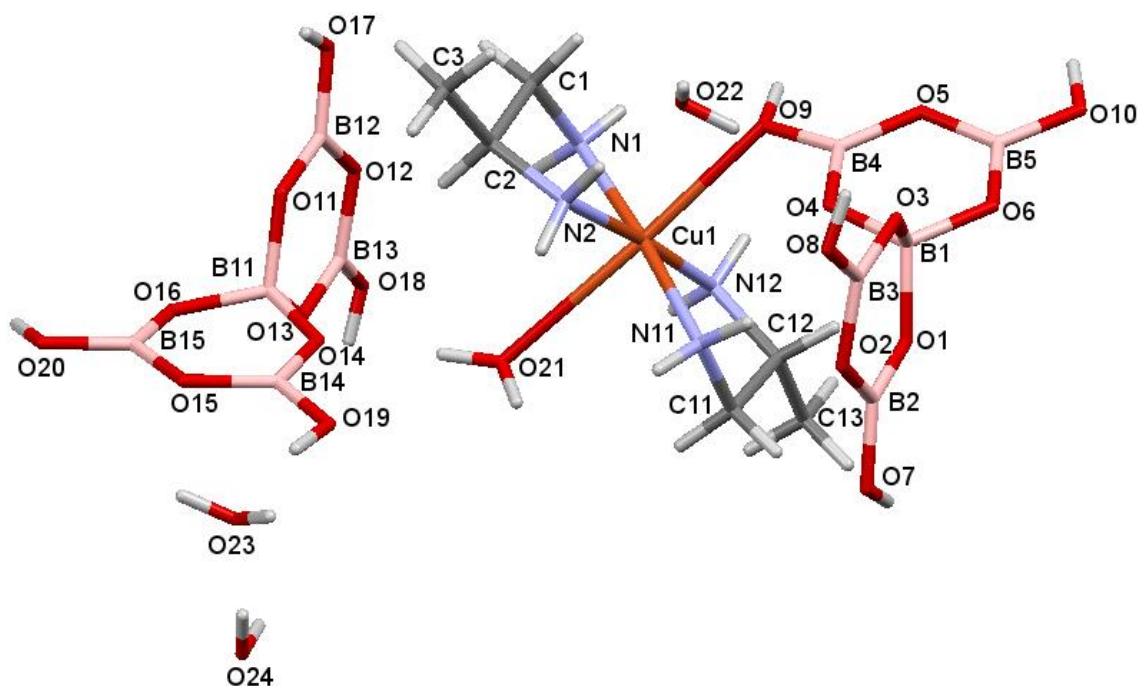


Figure 3.9 Diagram showing the structure and the numbering scheme of **22**.

The [Cu(pn)₂{B₅O₆(OH)₄}]⁺ in **22** has Cu-N distances of 1.9714(11)-2.0115(12) Å [av. 1.9936 Å] and an axial Cu-O (hydroxyl group from borate) distance of 2.490 Å shown in Figure

3.9. Although there is a sixth axially weakly coordinated H₂O ‘ligand’ at 2.785 Å, the complex is best considered as a 5-coordinate square based pyramid. This confirmed by a T^5 value of 0.8000. A τ index¹⁸² of 0.0013 for this cation supports a square-based pyramidal rather than a trigonal bipyramidal 5-coordinate geometry.

The two pentaborate(1-) anions are structurally similar and are not notably different from other transition metal complex cation pentaborate(1-) anion structure systems involving isolated [B₅O₆(OH)₄]⁻ anions.^{136,181} However, one of the two pentaborate(1-) anion is coordinated to the central metal atom copper by O9 and acts as a monodentate ligand. The coordination site of the pentaborate is from a hydroxyl oxygen atom (β) rather than from a bridging oxygen atom (α or γ). B-O bonds to the 3-coordinate boron centres for the uncoordinated pentaborate(1-) anion ranges from 1.3419(17) - 1.3848(17) Å [av. 1.3585 Å], and are not significantly different from those of the coordinated pentaborate which range from 1.3447(17) - 1.3824(17) Å [av. 1.3592 Å]. These distances are significantly shorter than those involving the 4-coordinate B11 and B1 centres of both uncoordinated and coordinated pentaborate(1-) anions, which range from 1.4474(16) to 1.4666(16) Å [av. 1.4585 Å], and from 1.4547(16) to 1.4645(15) Å [av. 1.4615 Å], respectively. B-O distances involving 3-coordinate boron centres and terminal hydroxyl groups are at the shorter end of the range from 1.3465(17) to 1.3545(16) Å [av. 1.3504 Å] for the uncoordinated pentaborate(1-) anion and from 1.3447(17) to 1.3551(16) Å [av. 1.3512 Å] for the coordinated pentaborate(1-) anion. B-O distances involving the oxygen atoms distal from the 4-coordinate boron centre for uncoordinated pentaborate(1-) anion (O12, O15) and for the coordinated pentaborate(1-) anion (O2, O5) are at the longer end of the range from 1.3692(16) to 1.3848(17) Å [av. 1.3788 Å], and from 1.3662(16) to 1.3824(17) Å [av. 1.3762 Å], respectively. Bond angles at the B11 and B1 centres range from 107.60(10) to 111.31(10), and from 107.84(10) to 111.91(10), respectively while angles at the other ring atoms are range from 116.43(12) to 122.66(12) for the uncoordinated pentaborate(1-) anion and from 116.41(11) to 122.49(12) for the coordinated pentaborate(1-) anion. The bond lengths and angles are given in Appendix I (Table 11, and Table 12).

In **22** the uncoordinated pentaborate(1-) anion has ten H-bond interactions (4 H-bond donors and six H-bond acceptors) without any connections at O12 and O15. The coordinated pentaborate(1-) anion is involved with 12 H-bond interactions (4 H-bond donors and 8 H-bond acceptors) with one coordination bond to the central (copper) metal atom. Interestingly, O5 in the γ position of the coordinated boroxyl ring has no further connections.

In **22** the 4 H-bond donor sites of the uncoordinated pentaborate(1-) anion are involved with H-bond acceptor oxygens of three different pentaborate(1-) anions (O17-H17...O1^{*}, O18-H18...O3^{*} and O20-H20...O16^{*}) and H-bond acceptor oxygen of one water molecule (O19-H19...O23^{*}). The 4 H-bond donor sites of the coordinated pentaborate(1-) anion are involved with H-bonds acceptor oxygen of three different pentaborate(1-) anions (O7-H7...O11^{*}, O8-H8...O13^{*} and O9-H9...O18^{*}), and a H-bond acceptor oxygen of one water molecule (O10-H10...O22^{*}). The H-bond acceptor sites arising from H-bond donor sites of free and coordinated pentaborate(1-) anions of **22** are $\alpha\alpha\alpha\omega$ and $\alpha\alpha\beta\omega$, respectively, where α and β are pentaborate acceptor sites, and ω is water acceptor site.^{77,98} The direction of the 4 H-bond donor sites in the free pentaborate(1-) anion are three 'in' (O17-H17, O18-H18, and O20-H20) and one 'out' (O19-H19), while the direction of the 4 H-bond donor sites of the coordinated pentaborate(1-) anion are two 'in' (O7-H7 and O8-H8) and two 'out' (O9-H9 and O10-H10) (Figure **3.9**). Details of the H-bonds interactions are listed in Table **3.10**.

Table **3.10** H-bonds [\AA and $^\circ$] in **22**.

<i>D-H...A</i>	<i>d(D...A)</i>	<i>D-H...A</i>	<i>d(D...A)</i>
N1-H1A...O24 ⁱ	3.1835(13)	O7-H7...O11 ^v	2.7538(13)
N1-H1B...O24 ⁱⁱ	3.1841(15)	O8-H8...O13 ^{vi}	2.7084(12)
N1B-H1BA...O24 ⁱ	3.1835(13)	O9-H9...O18 ^{iv}	2.6635(12)
N1B-H1BB...O24 ⁱⁱ	3.1841(15)	O10-H10...O22 ^{vii}	2.7376(18)
N2-H2A...O2 ⁱⁱⁱ	3.0483(14)	O17-H17...O1 ^{viii}	2.7638(13)
N2-H2B...O22	2.9840(13)	O18-H18...O3 ^{ix}	2.6848(12)
N2B-H2BA...O2 ⁱⁱⁱ	3.0483(14)	O19-H19...O23	2.7907(11)
N2B-H2BB...O22	2.9840(13)	O20-H20...O16(x)	2.7023(13)
N11-H11A...O4	3.0360(14)	O21-H21A...O8 ⁱⁱⁱ	2.8264(12)
N11-H11B...O8 ⁱⁱⁱ	3.1757(14)	O21-H21B...O14	2.7367(12)
N11B-H11C...O4	3.0360(14)	O23-H23A...O10 ⁱ¹	2.9141(12)
N11B-H11D...O8 ⁱⁱⁱ	3.1757(14)	O23-H23B...O6 ⁱⁱⁱ	2.8287(11)
N12-H12A...O24 ⁱⁱ	2.9242(16)	O22-H22A...O20 ^{j2}	2.7639(12)
N12-H12B...O12 ^{iv}	3.0944(14)	O22-H22B...O4	2.9367(13)
N12B-H12C...O24 ⁱⁱ	2.9242(16)	O24-H24A...O23	2.813
N2B-H12D...O12 ^{iv}	3.0944(14)	O24-H24B...O21 ⁱⁱ	2.7534(11)

(i) $x,y,z+1$ (ii) $-x+1,-y,-z+1$ (iii) $-x,-y+1,-z+1$ (iv) $-x+1,-y,-z+2$ (v) $x-1,y,z$ (vi) $x-1,y+1,z$ (vii) $-x,-y+1,-z+2$ (viii) $x+1,y,z$ (xi) $x+1,y-1,z$ (x) $-x+2,-y,-z+1$ (xi) $x+1,y,z-1$ (xii) $-x+1,-y+1,-z+1$

A view of a plane of $[\text{B}_5\text{O}_6(\text{OH})_4]^-$ anions in **22** is shown in Figure **3.10**. Within the plane a chain of uncoordinated and coordinated pentaborate(1-) anions alternate and are linked by $R_2^2(8)$ motif connections. An expanded view of the chain is shown in Figure **3.11**. The two reciprocal- α $R_2^2(8)$ connections are formed between pentaborate(1-) anions by one boroxyl

(B_3O_3) ring of both pentaborate(1-) anions. The second boroxyl (B_3O_3) ring of the uncoordinated pentaborate(1-) anion is cross linked to another uncoordinated pentaborate (1-) anion by a further reciprocal- $\alpha R_2^2(8)$ interaction. The second boroxyl ring of the coordinated pentaborate(1-) anions is linked to other chain by bridging water molecules.

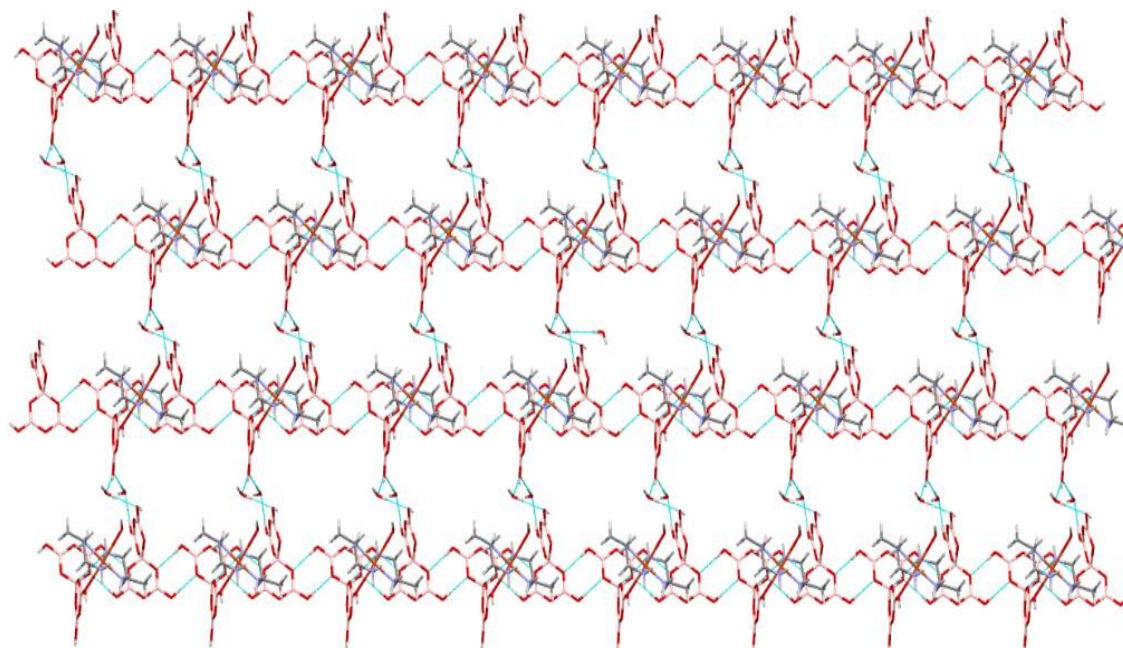


Figure **3.10** H-bonded $[B_5O_6(OH)_4]^-$ network for **22**. Dashed blue lines represent H-bonds.

The $[Cu(pn)_2\{B_5O_6(OH)_4\}H_2O]^+$ cations, $[B_5O_6(OH)_4]^-$ anions, and H_2O molecules of crystallization of **22** are connected through a complex series of H-bond interactions, with the anion network templated by the cations (Figure **3.12**).

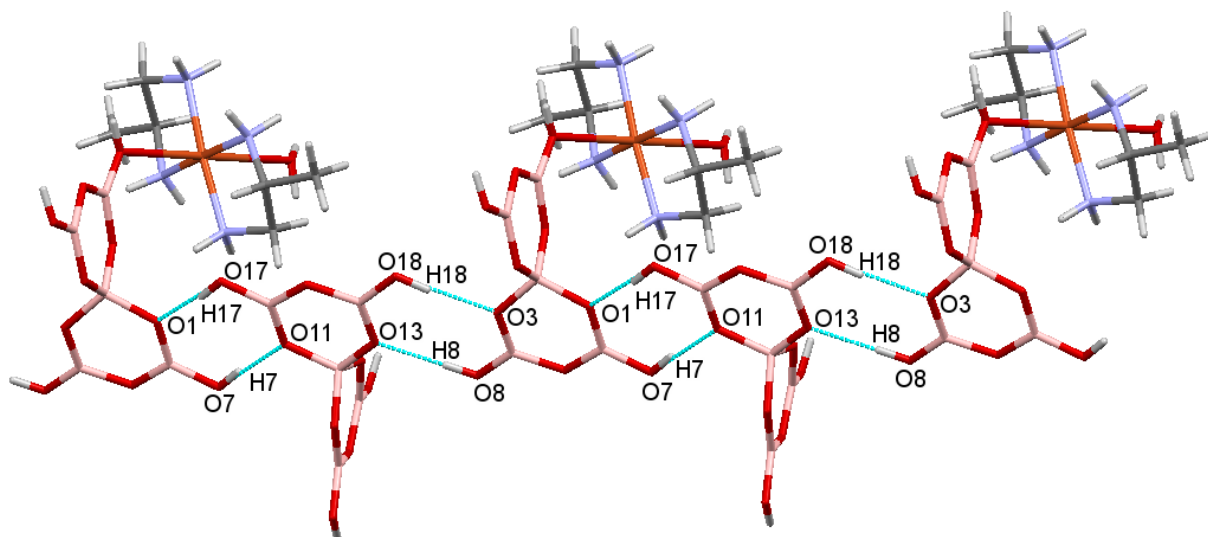


Figure **3.11** The $R_2^2(8)$ connections between free and coordinate pentaborate(1-) anions in **22**.

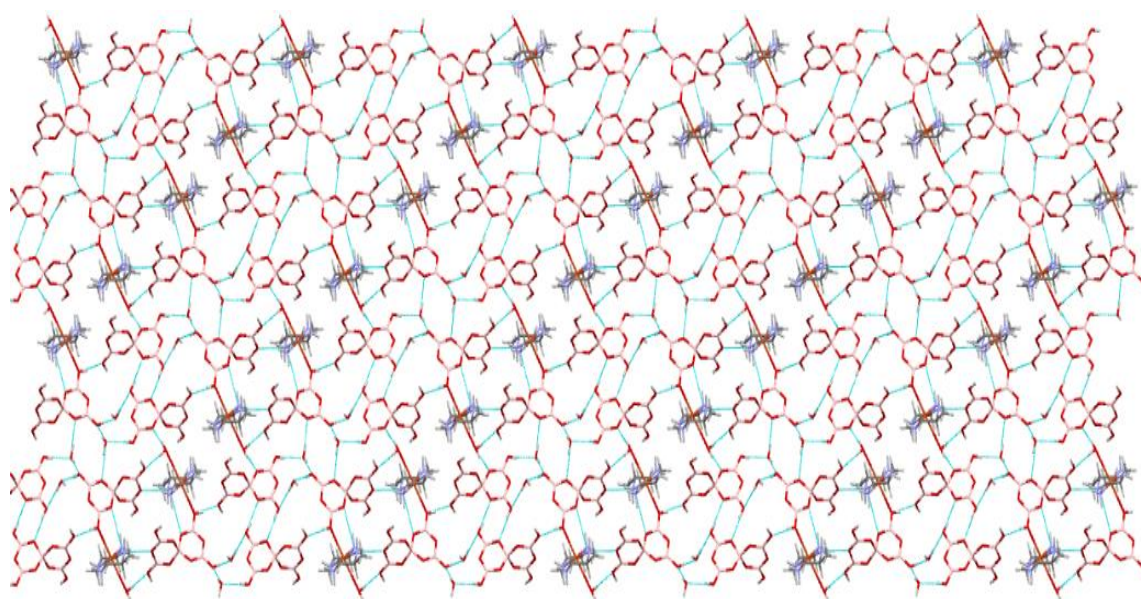


Figure **3.12** A diagram shows the structure of **22** viewed along the *c* direction of the unit cell. The polyborate groups are arranged in a plane and 'cavities' are filled by the $[\text{Cu}(\text{pn})_2\{\text{B}_5\text{O}_6(\text{OH})_4\}]^+$ cations and water molecules.

The plane shown in Figure **3.12** is connected to the neighbouring planes by further H-bond interactions, forming a three-dimensional network. The $[\text{Cu}(\text{pn})_2\{\text{B}_5\text{O}_6(\text{OH})_4\}]^+$ cation is included within the supramolecular framework structure. The cation in **22**, $[\text{Cu}(\text{pn})_2\{\text{B}_5\text{O}_6(\text{OH})_4\}]^+$, has eight amino H-atoms and which form eight donor H-bonds: four

to water molecules, three to neighbouring $\beta\gamma\gamma$ pentaborate(1-) sites and one intramolecular H-bond to the coordinated pentaborate(1-) α -site (N1H11A...O4*); details of which can be found in the legend to Figure 3.9.

3.3.5.3 Structural characterisation of [Cu(TMEDA){B₆O₇(OH)₆}]·6H₂O (**23**)

Crystallographic data for **23** are listed in Table 3.11. Crystals of **23** are monoclinic, *P*2₁/*c* and consists of a neutral transition metal complex [Cu(TMEDA){B₆O₇(OH)₆}] with six water molecules of crystallization as shown in Figure 3.13.

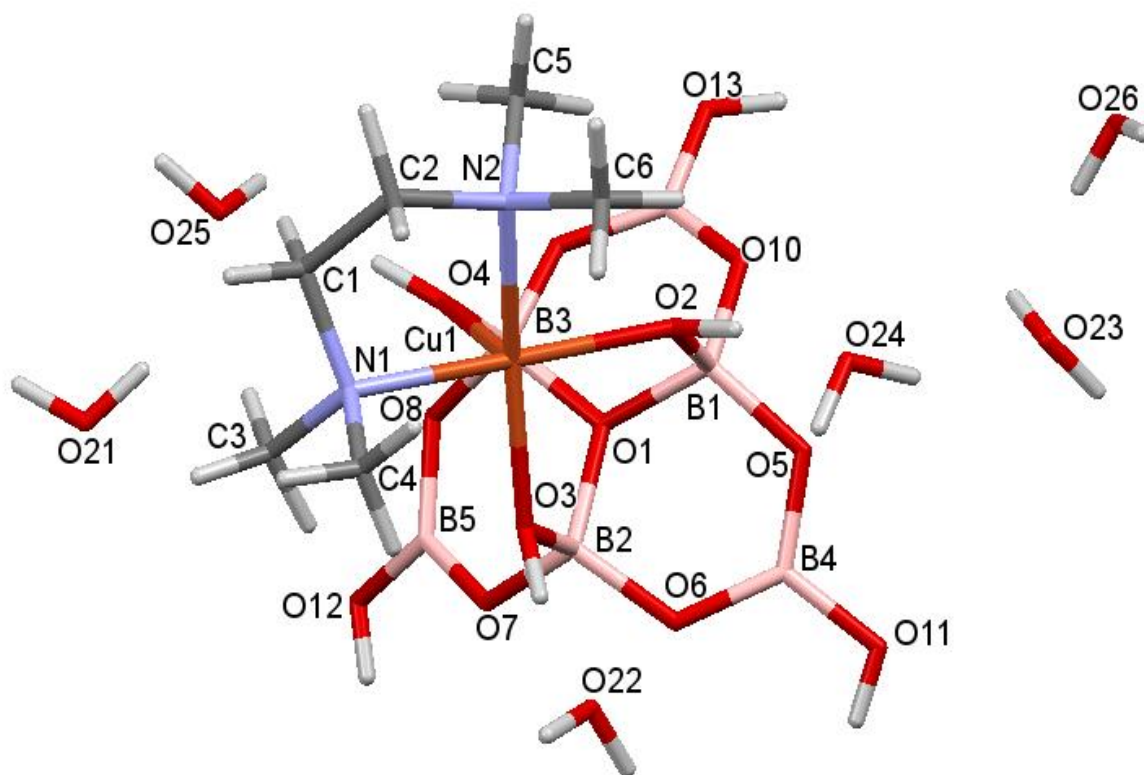


Figure 3.13 Diagram showing the structure and the numbering scheme of **23**.

Table 3.11 Crystal data and structure refinement details of **23**.

Empirical formula	C ₆ H ₃₄ B ₆ N ₂ O ₁₉ Cu
Formula weight	566.75
Temperature	100(2) K
Wavelength	0.71073 Å
Crystal system	Monoclinic

Space group	$P2_1/c$
Unit cell dimensions	$a = 15.4209(3) \text{ \AA}$ $\alpha = 90^\circ$ $b = 17.0706(3) \text{ \AA}$ $\beta = 90.861(2)^\circ$ $c = 8.88230(10) \text{ \AA}$ $\gamma = 90^\circ$
Volume	$2337.95(7) \text{ \AA}^3$
Z	4
Density (calculated)	1.610 Mg / m^3
Absorption coefficient	1.021 mm^{-1}
$F(000)$	1180
Crystal	Hexagonal Prism; Blue
Crystal size	$0.130 \times 0.080 \times 0.060 \text{ mm}^3$
θ range for data collection	$1.780 - 27.633^\circ$
Index ranges	$-19 \leq h \leq 20, -22 \leq k \leq 22, -11 \leq l \leq 11$
Reflections collected	9533
Independent reflections	9533
Completeness to $\theta = 25.242^\circ$	99.8%
Absorption correction	Semi-empirical from equivalents
Max. and min. transmission	1.000 and 0.872
Refinement method	Full-matrix least-squares on F^2
Data / restraints / parameters	9533 / 147 / 380
Goodness-of-fit on F^2	1.109
Final R indices [$F^2 > 2\sigma(F^2)$]	$RI = 0.0354, wR2 = 0.1326$
R indices (all data)	$RI = 0.0381, wR2 = 0.1405$
Extinction coefficient	n/a
Largest diff. peak and hole	0.621 and $-0.650 \text{ e \AA}^{-3}$
Radiation source (wavelength)	Mo-K α

Special details: This structure was refined as a two-component twin. Component two rotated by -179.9844° around $[1.00 \ -0.00 \ 0.00]$ (reciprocal) or $[1.00 \ -0.00 \ 0.03]$ (direct). The amine was found to be disordered and as such it resulted in the need to use various geometrical (SAME, DFIX, DANG, BUMP) and displacement (DELU, RIGU) restraints, along with a displacement (EADP) constraint.

The neutral complex in compound **23** arises from the coordination of a tridentate hexaborate(2-) $[\text{B}_6\text{O}_7(\text{OH})_6]^{2-}$ ligand to a $[\text{Cu}(\text{TMEDA})]^{2+}$ centre. The 5-coordinate copper(II) centre in **23** has a τ index of 0.02,¹⁸² consistent with a square-based pyramidal structure. The copper(II) centre has the bidentate diamine ligand within the square plane and the tridentate hexaborate(2-) anion completes the two remaining coordination sites of the square plane and the one axial site (O4). Compound **23** has Cu-N distances of $2.035(6) \text{ \AA}$ (N1) and $2.069(10) \text{ \AA}$ (N2). The Cu-O distances with the plane are $1.9802(16) \text{ \AA}$ (O2) and $1.9934(16) \text{ \AA}$ (O3), whilst the Cu-O axial distance is $2.1871(16) \text{ \AA}$ (O4).

To date, most of the synthesised and characterised borate salts have been pentaborates. In contrast, relatively fewer hexaborate(2-) anion compounds are known.^{135,153,154,183,184} The hexaborate(2-) anion has been observed as a tridentate ligand coordinated to cobalt(II)^{135,153,154} and zinc(II)¹⁸⁴ but has not been previously observed in copper(II) chemistry. The hexaborate(2-) anion in **23** acts as a tridentate ligand in to the copper(II) centre, with an average Cu-O distance

2.054 Å, while the *N,N,N',N'*-tetramethyl ethylenediamine ligand acts as a bidentate ligand. The copper(II) centre has a coordination number of five and a square base pyramidal geometry (Figure 3.13).

The hexaborate(2-) anion consist of a three fused 6-membered boroxyl rings in which three tetrahedral boron centres (B1, B2, B3) and three trigonal boron centres (B4, B5, B6). The B1, B2, and B3 centres are connected to three oxygen atoms and one hydroxyl group while B4, B5, and B6 centres are connected to two oxygen atoms and one hydroxyl group. The hexaborate(2-) anion in **23** is structurally similar to other reported transition metal complex cation hexaborates.^{135,153} The shorthand designation of the $[\text{B}_6\text{O}_7(\text{OH})_6]^{2-}$ anion is [6:3Δ + 3T] according to the Christ and Clark¹⁶³ and Heller²⁷ crystal chemical classification schemes. The B-O distances to the tetrahedral B1, B2, B3 centres are in the range of 1.436(3) - 1.513(3) Å, 1.436(3) - 1.513(3) Å, and 1.453(3) - 1.516(3) Å, respectively and these are significantly longer than those involving the trigonal B4, B5, B6 centres: The B-O distances to B4, B5, and B6 centres are in the range of 1.358(3) - 1.375(3) Å, 1.359(3) - 1.368(3) Å and 1.360(3) - 1.368(3) Å, respectively. The B-OH bonds involving tetrahedral B1, B2, and B3 centres are 1.483(3), 1.482(3), and 1.455(3) Å, respectively while the B-OH bonds involving trigonal B4, B5, and B6 centres are significantly shorter at 1.375(3), 1.368(3), and 1.368(3) Å, respectively. Bond angles at the tetrahedral centres B1, B2, and B3 range from 106.17(18)° - 112.8(18)°, 106.91(17)° - 111.15(18)°, and 105.61(16)° - 112.49(19)°, respectively while the bond angles at the trigonal B4, B5, and B6 centres range from 117.9(2)° - 123.3(2)°, 117.6(2)° - 123.2(2)°, and 118.0(2)° - 122.5(2)°, respectively. The bond lengths and angles are given in Appendix I (Table 13, and Table 14).

The four chemically non-equivalent oxygen sites of the isolated hexaborate(2-) anion are labelled A-D by using a similar nomenclature system to that previously described (Figure 3.14).^{98,77} This labelling system has been used to classify the H-bond interactions between different neighbouring $[\text{B}_6\text{O}_7(\text{OH})_6]^{2-}$ anions and to differentiate between the available sites.

In **23** the hexaborate(2-) anion has six potential H-bond donor sites (B and C) which are also capable of accepting H-bond interactions, and a further seven potential H-bond acceptor sites (A and D). The hexaborate(2-) anion has thirteen H-bond interactions (six H-bond donors and seven H-bond acceptors). In addition, there are three coordination bonds to the copper metal. The bridging O atoms (A, D; O1, O5, and O6), are not involved in further stabilizing interactions.

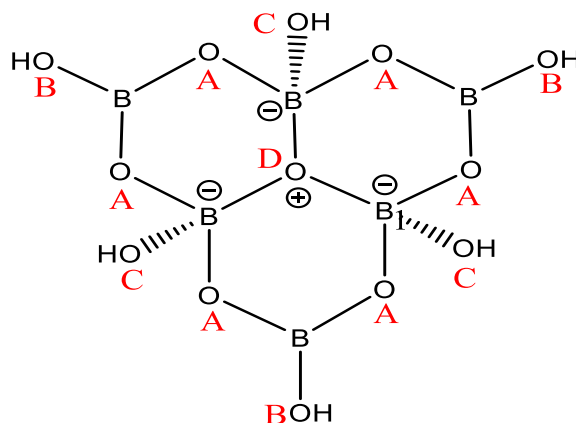


Figure 3.14 Diagram showing oxygen labelling and the H-bond acceptor sites for the hexaborate(2-) anions in **23**.

Table 3.12 H-bonds [\AA and $^\circ$] in **23**.

$D-H\cdots A$	$d(D\cdots A)$	$D-H\cdots A$	$d(D\cdots A)$
O11-H11...O22 ⁱ	2.742(2)	O24-H24B...O11 ^v	2.7320(19)
O12-H12...O6 ⁱⁱ	3.154(2)	O22-H22A...O21 ^{vi}	2.805(2)
O12-H12...O7 ⁱⁱ	2.779(2)	O22-H22B...O21 ^{vii}	2.8056(19)
O13-H13...O10 ⁱⁱⁱ	2.736(2)	O23-H23A...O13 ⁱⁱⁱ	2.7240(19)
O2-H2...O24	2.6837(17)	O23-H23B...O24 ⁱ	2.772
O3-H3...O22	2.7326(18)	O25-H25A...O26 ^{viii}	2.795(2)
O4-H4...O25	2.8679(17)	O25-H25B...O8 ^{iv}	2.9236(18)
O21-H21A...O12 ^{iv}	2.718(2)	O26-H26A...O9 ^{ix}	2.7906(19)
O21-H21B...O25	2.859	O26-H26B...O23	2.794
O24-H24A...O23	2.784		

(i) $x, -y+3/2, z-1/2$ (ii) $-x+2, -y+1, -z$ (iii) $-x+1, -y+1, -z$ (iv) $x, -y+1/2, z+1/2$ (v) $x, -y+3/2, z+1/2$
 (vi) $-x+2, y+1/2, -z+1/2$ (vii) $-x+2, -y+1, -z+1$ (viii) $-x+1, y-1/2, -z+1/2$ (ix) $-x+1, y+1/2, -z+1/2$

In **23** all six potential H-bond donor sites partake in H-bond interaction: three coordinated hydroxyl groups are H-bonded to H₂O molecules (O2-H2...O24^{*}, O3-H3...O22^{*}, O4-H4...O25^{*}) and the three uncoordinated hydroxyl groups are H-bonded to one H₂O and two hexaborates. However, **23** does not possess any amino hydrogen atoms in the TMEDA ligand, and this leads to only hexaborate(2-)-hexaborate (2-) interactions between neighbouring [Cu(TMEDA){B₆O₇(OH)₆}] units. The units are linked into infinite chains through two-reciprocal R₂²(8) interactions: O13-H13...O10^{*}/O13^{*}-H13^{*}...O10 and O12-H12...O7^{*}/O12^{*}-H12^{*}...O7 (Figure 3.15). Details of the H-bonding interactions are given in Table 3.12.

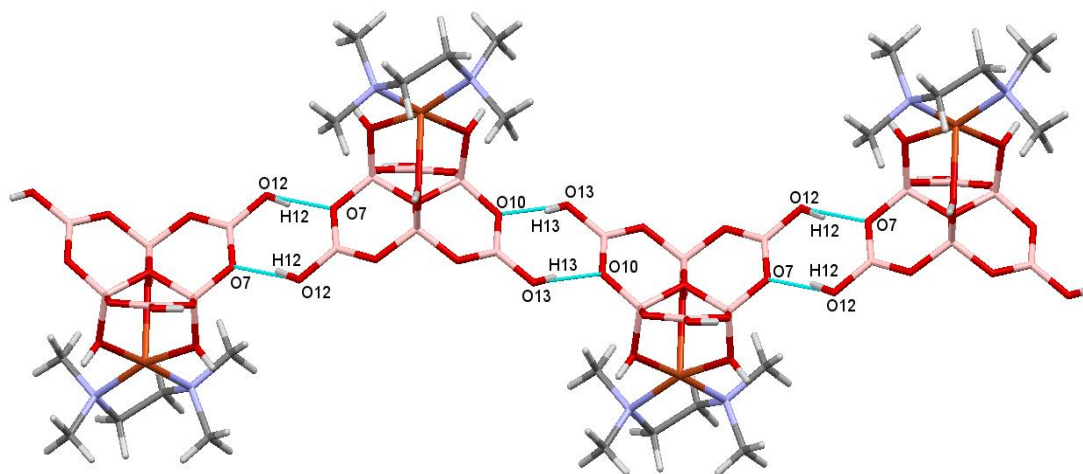


Figure 3.15 The $R_2^2(8)$ interactions between $[\text{Cu}(\text{TMEDA})\{\text{B}_6\text{O}_7(\text{OH})_6\}]$ molecules in **23**.

The $[\text{Cu}(\text{TMEDA})\{\text{B}_6\text{O}_7(\text{OH})_6\}]$ units and H_2O molecules of the **23** compound are connected through a complex series of H-bond interactions to produce planes (Figure 3.16) which are further linked to produce a three-dimension network.

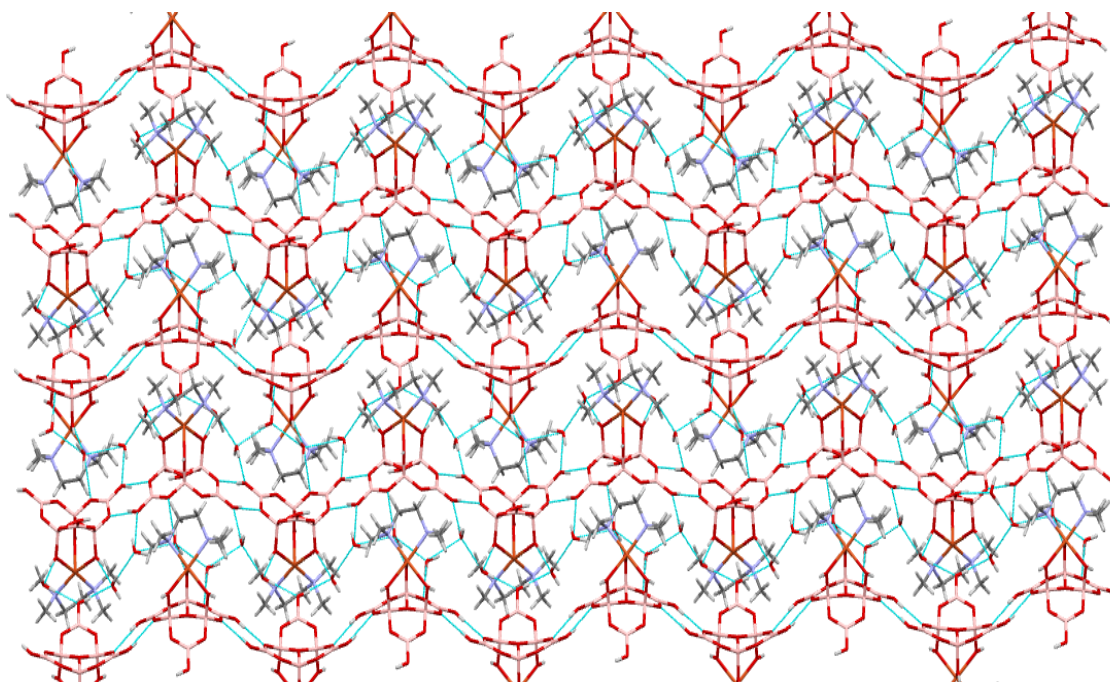


Figure 3.16 Diagram showing a 'plane' of $[\text{Cu}(\text{TMEDA})\{\text{B}_6\text{O}_7(\text{OH})_6\}]$ (viewed along the c direction of the unit cell) and water molecules in **23**.

3.3.5.4 Structural characterisation of [Cu(dach)₂(H₂O)₂][Cu(dach)₂][B₇O₉(OH)₅]₂·3H₂O (24)

Crystallographic data of **24** are listed in Table 3.13. Crystals of **24** are monoclinic, *C2/c*. Compound **24** is a salt and comprised of two copper(II) complex cations, two heptaborate (2-) anions, and four waters of crystallization.

Table 3.13 Crystal data and structure refinement details of **24**.

Empirical formula	C ₁₂ H ₃₉ B ₇ N ₄ O ₁₇ Cu
Formula weight	650.68
Temperature	100(2) K
Wavelength	0.71073 Å
Crystal system	Monoclinic
Space group	<i>C2/c</i>
Unit cell dimensions	$a = 22.4696(9)$ Å $\alpha = 90^\circ$ $b = 10.8711(3)$ Å $\beta = 108.267(4)^\circ$ $c = 23.0016(7)$ Å $\gamma = 90^\circ$
Volume	5335.4(3) Å ³
Z	8
Density (calculated)	1.620 Mg / m ³
Absorption coefficient	0.903 mm ⁻¹
<i>F</i> (000)	2712
Crystal	Blade; Purple
Crystal size	0.090 × 0.050 × 0.020 mm ³
θ range for data collection	2.175 – 27.483°
Index ranges	-28 ≤ <i>h</i> ≤ 27, -13 ≤ <i>k</i> ≤ 14, -29 ≤ <i>l</i> ≤ 29
Reflections collected	26756
Independent reflections	6106 [<i>R</i> _{int} = 0.0378]
Completeness to $\theta = 25.242^\circ$	99.9%
Absorption correction	Semi-empirical from equivalents
Max. and min. transmission	1.000 and 0.799
Refinement method	Full-matrix least-squares on <i>F</i> ²
Data / restraints / parameters	6106 / 940 / 525
Goodness-of-fit on <i>F</i> ²	1.045
Final <i>R</i> indices [<i>F</i> ² > 2σ(<i>F</i> ²)]	<i>R</i> 1 = 0.0522, <i>wR</i> 2 = 0.1330
<i>R</i> indices (all data)	<i>R</i> 1 = 0.0656, <i>wR</i> 2 = 0.1404
Extinction coefficient	n/a
Largest diff. peak and hole	1.516 and -0.557 e Å ⁻³
Radiation source (wavelength)	Mo-Kα

Special details: Both the 1,2-diaminocyclohexane ligands were successfully modelled as disordered over two positions. As such various geometrical (SAME, SADI) and displacement (RIGU, SIMU) restraints were applied.

The copper(II) complex cations in **24** each contain both the (1*S*,2*S*)-1,2-diaminocyclohexane and (1*R*,2*R*)-1,2-diaminocyclohexane ligands in a square-planar arrangement. Additionally, both cations connect to two mutually trans H₂O molecules yielding formally 6-coordinate metal cations. However, due to the Jahn-Teller effect, one cation has both

the axial Cu-O distances at a long distance of 2.836 Å. This complex is best considered as a 4-coordinate square-planar $\{T = 0.70,^{172} \text{Cu-N distances range from } 1.963(7) - 2.013(8) \text{ Å}\}$. The other cation has both axial Cu-O distances at 2.381(3) Å and designated elongated octahedron $\{T = 0.80,^{172} \text{Cu-N distances range from } 1.910(13) - 1.923(11) \text{ Å}\}$. Each cation is partnered by a $[\text{B}_7\text{O}_9(\text{OH})_5]^{2-}$ anion and an additional water of crystallization. The anions and cations are shown in Figure 3.17.

The heptaborate(2-) anion, $[\text{B}_7\text{O}_9(\text{OH})_5]^{2-}$, contains four fused 6-membered rings with three tetrahedral boron centres (B1, B2, B3) and four trigonal boron centres (B4, B5, B6, B7). The B2 and B3 centres are surrounded by four bridging oxygen atoms, while B4, B5, B6, B7 centres are connected to two bridging oxygen atoms and one hydroxyl group. B1 is unique and is connected to three bridging oxygen atoms and one hydroxyl group (Figure 3.17).

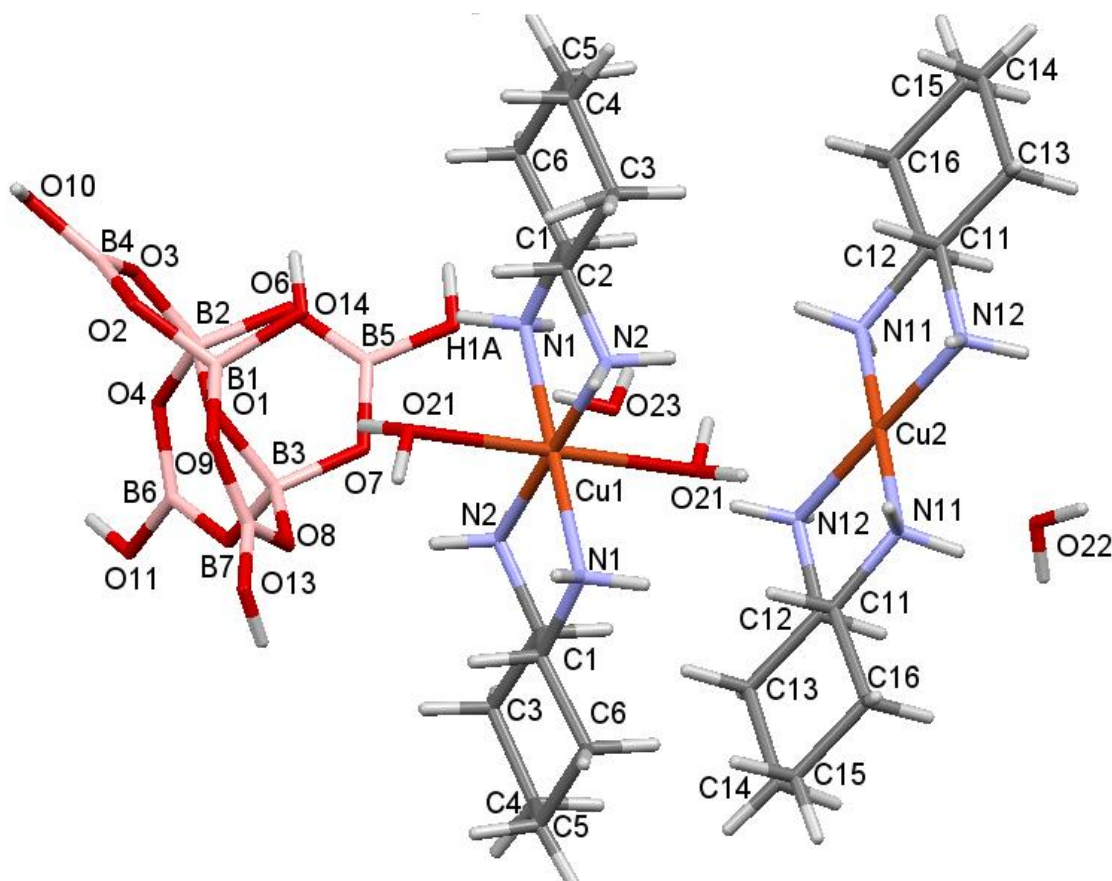


Figure 3.17 Diagram showing the complex cations and heptaborate(2-) anion in **24**. The water molecules containing O22 are in octahedral positions around Cu2 (bonds not shown in the diagram).

The structure of the heptaborate(2-) anions in **24** is essentially the same as those reported for $[\text{H}_3\text{N}(\text{CH}_2)_7\text{NH}_3][\text{B}_7\text{O}_9(\text{OH})_5] \cdot \text{H}_2\text{O}$,⁹⁷ $[\text{cyclo-C}_6\text{H}_{11}\text{NH}_3]_2[\text{B}_7\text{O}_9(\text{OH})_5] \cdot 3\text{H}_2\text{O} \cdot \text{B}(\text{OH})_3$, and $[\text{cyclo-C}_7\text{H}_{13}\text{NH}_3]_2[\text{B}_7\text{O}_9(\text{OH})_5] \cdot 2\text{H}_2\text{O} \cdot 2\text{B}(\text{OH})_3$,⁷⁷ and can be considered as a hexaborate(2-) anion condensed with an additional $\text{B}(\text{OH})_3$ molecule forming a fused tetracyclic (four boroxyl) ring system with one bridgehead (formally positively charged) 3-coordinate oxygen site, and three bridgehead (formally negatively charged) 4-coordinate boron sites. The B–O distances for the 3-coordinate boron centres range from 1.355(4) – 1.376(3) Å, and B–O distances around the 4-coordinate boron centres range from 1.436(3) – 1.471(3) Å. The O–B–O angles for the 3-coordinate boron centres range from 114.8(3) – 123.4(2)° and O–B–O angles at the 4-coordinate boron centres range from 106.0(2) – 112.1(2)° (Appendix I, Table 15, and Table 16). These distances and angles are as expected for sp^2 and sp^3 hybridized boron centres.⁶ The ring B–O–B angles range from 110.7(2) – 122.8(2)° indicating sp^2 hybridized oxygen atoms. The central three-coordinate oxygen centre is pyramidal ($349.39^\circ = \text{angles sum}$ and 0.288 Å out of the B1B2B3 plane, with B–O bond lengths [av. 1.59 Å] longer than typically expected for oxygen atoms bound to four-coordinate boron centres (~ 1.48 Å).⁷⁷ The three-coordinate oxygen centres, O1, are *transoid* relative to the OH group of B1.

In **24** the heptaborate(2-) anion has five potential H-bond donor sites which are also capable of accepting H-bond interactions, and nine further potential H-bond acceptor sites. According to Christ and Clark's¹⁶³ and Heller's²⁷ crystal chemical classification schemes, the shorthand notification of $[\text{B}_7\text{O}_9(\text{OH})_5]^{2-}$ is $[7:4\Delta + 3\text{T}]$. A labelling scheme was introduced by Beckett⁷⁷ to differentiate between the available sites of the H-bonding interactions between $[\text{B}_7\text{O}_9(\text{OH})_5]^{2-}$ anions. The seven chemically distinct O sites are labelled A–G, (Figure 3.18). By analogy with Schubert's pentaborate labelling sites A, D and E are α to 4-coordinate boron centres, whilst sites B and F are on 3-coordinate boron centres and β to 4-coordinate boron centres. Sites C and G do not have corresponding sites on pentaborate(1-) anions. All the H-bonds data are listed in Table 3.14.

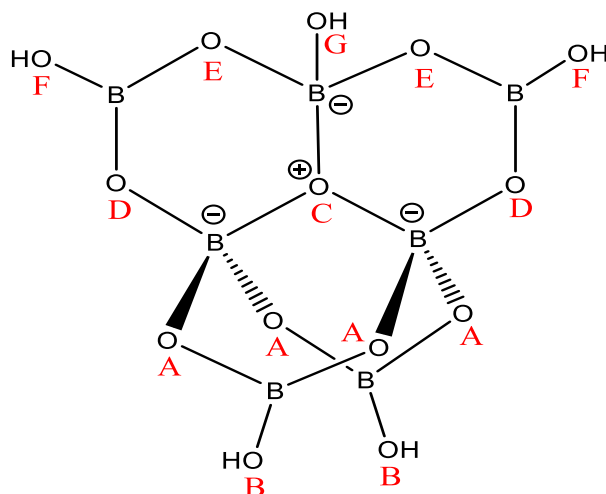


Figure 3.18 Diagram showing the H-bond acceptor sites of the heptaborate(2-) anions in **24**.

Table 3.14 H-bonds [\AA and $^\circ$] in **24**.

$D-H\cdots A$	$d(D\cdots A)$	$D-H\cdots A$	$d(D\cdots A)$
O21-H21A...O22 ⁱⁱⁱ	2.698(4)	N11B-H11C...O10 ^{iv}	3.09(2)
O21-H21B...O9	3.067(3)	N11B-H11D...O21 ⁱ	3.35(3)
O21-H21B...O14	2.996(4)	N11B-H11D...O9 ⁱ	2.99(2)
N1-H1A...O14 ⁱ	3.211(9)	N12B-H12C...O23	3.01(4)
N1-H1B...O12 ^j	3.200(6)	N12B-H12D...O13 ^v	2.93(4)
N2-H2A...O8	3.027(6)	O10-H10...O2 ^{vi}	2.724(3)
N1B-H1BA...O14 ⁱ	2.975(16)	O11-H11F...O6 ^{vii}	2.717(3)
N2B-H2BA...O7	2.971(10)	O12-H12F...O4 ^{viii}	2.740(3)
N11-H11A...O10 ^{iv}	3.027(8)	O13-H13...O5 ^{ix}	2.693(3)
N11-H11B...O9 ⁱ	3.002(9)	O22-H22A...O23 ⁱⁱ	2.775(5)
N12-H12A...O23	3.091(14)	O22-H22B...O11(x)	2.867(4)
N12-H12B...O13 ^v	2.869(15)	O23-H23A...O12	2.790(3)

(i) $-x+3/2, -y+3/2, -z+1$

(ii) $-x+1, -y+2, -z+1$

(iii) $x+1/2, y-1/2, z$

(iv) $x-1/2, -y+3/2, z-1/2$

(v) $x-1/2, y+1/2, z$

(vi) $-x+2, y, -z+3/2$

(vii) $-x+3/2, y-1/2, -z+3/2$

(viii) $-x+3/2, y+1/2, -z+3/2$

(xi) $-x+3/2, -y+1/2, -z+1$

(x) $-x+1, -y+1, -z+1$

A view of a plane of a heptaborate(2-) anions found in **24** is given in Figure 3.19. Four out of the five donor sites in **24** are involved in H-bonding to four different heptaborate(2-) anions involving a reciprocal $R_2^2(8)$ interaction $O10-H10\cdots O2^*$, a reciprocal $R_2^2(12)$ $O13-H13\cdots O5^*$, and two non-reciprocal $R_2^2(8)$ interactions $O11-H11\cdots O6^*/O12^*-H12^*\cdots O4$ and $O11^*-H11^*\cdots O6/O12-H12\cdots O4^*$ (Figure 3.20). The unique hydroxyl group (O14H14) on the 4-coordinate boron center (B1) is *transoid* to O1 and is not involved in H-bonding.

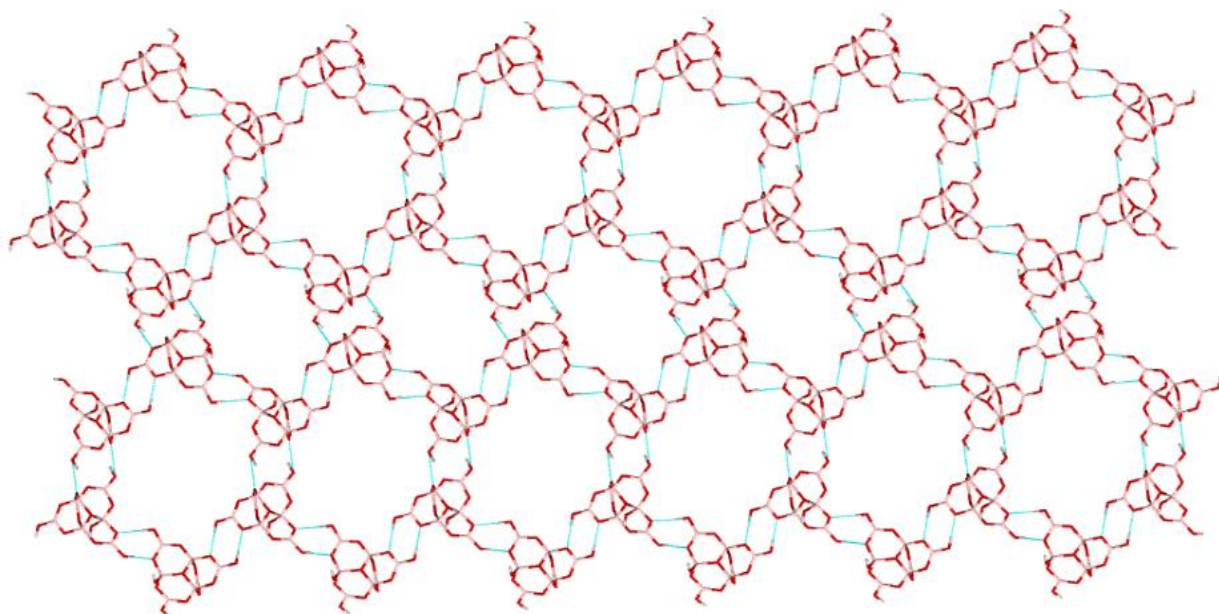


Figure 3.19 The reciprocal connection (viewed along the *c* direction of the unit cell) in **24**.

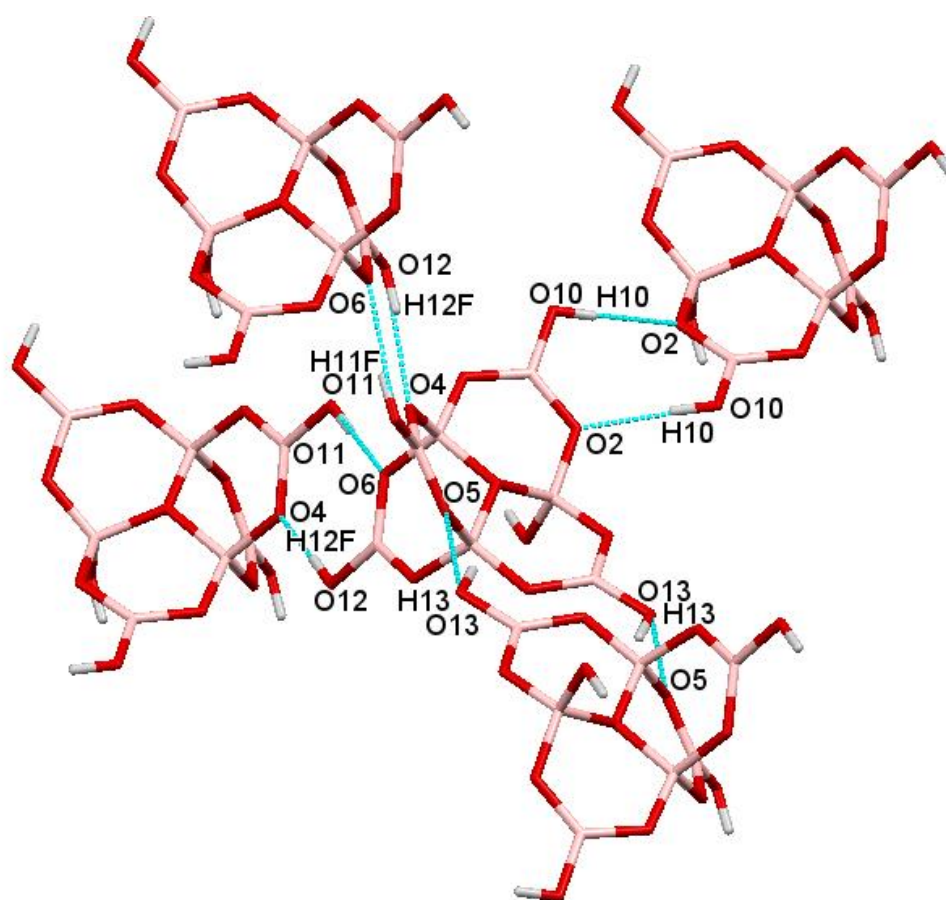


Figure 3.20 The two $R_2^2(8)$ and $R_2^2(12)$ H-bond motif connections between heptaborate(2-) anions in **24**.

The heptaborate(2-) anions are further held within the second coordination spheres of both the $[\text{Cu}(\text{dach})_2(\text{H}_2\text{O})_2]^{2+}$ and $[\text{Cu}(\text{dach})_2]^{2+}$ cations *via* H-bonds involving the amino hydrogen atoms. The $[\text{Cu}(\text{dach})_2(\text{H}_2\text{O})_2]^{2+}$ cation forms two five-point H-bond contacts with its neighbouring heptaborate(2-) anions N1-H1B \cdots O21*, N2-H2A \cdots O8*, N1-H1A \cdots O14*, O21-H21B \cdots O9*, O21-H21B \cdots O14* and this is likely to be involved in structure directing the formation of this compound from aqueous solution. Likewise a $R_2^2(8)$ interaction, where the heptaborate(2-) is a double acceptor is present for the square-planar copper(II) center (Figure 3.21).

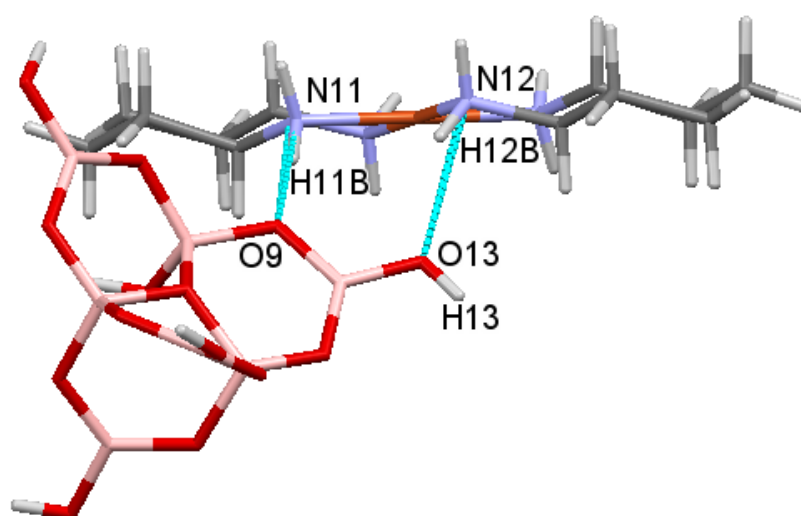


Figure 3.21 The $R_2^2(8)$ interaction in between the heptaborate(2-) anion and $[\text{Cu}(\text{dach})_2]^{2+}$ cation in **24**.

3.3.5.5 Structural characterisation of $[\text{Cu}(\text{N,N-dmen})_2(\text{H}_2\text{O})][\text{B}_5\text{O}_6(\text{OH})_4]_2 \cdot 3\text{H}_2\text{O}$ (**27**)

Crystallographic data for **27** compound are listed in Table 3.15. Crystals of **27** are triclinic, *P*-1 and **27** is an ionic compound with one transition metal complex cation $[\text{Cu}(\text{N,N-dmen})_2(\text{H}_2\text{O})]^{2+}$ partnered with two $[\text{B}_5\text{O}_6(\text{OH})_4]^-$ anions (A and B) and three water molecules of crystallization (Figure 3.22).

Table 3.15 Crystal data and structure refinement of **27**.

Empirical formula	$\text{C}_8\text{H}_{40}\text{B}_{10}\text{N}_4\text{O}_{24}\text{Cu}$
Formula weight	748.08
Temperature	100(2) K

Wavelength	0.71073 Å
Crystal system	Triclinic
Space group	<i>P</i> -1
Unit cell dimensions	$a = 11.7189(4)$ Å $\alpha = 80.468(3)^\circ$ $b = 11.7226(4)$ Å $\beta = 66.245(3)^\circ$ $c = 12.9108(4)$ Å $\gamma = 78.270(3)^\circ$
Volume	1582.49(9) Å ³
Z	2
Density (calculated)	1.57 Mg / m ³
Absorption coefficient	0.786 mm ⁻¹
Crystal	Prism; purple
Crystal size	0.210×0.150×0.110 mm ³
θ range for data collection	2.366 – 27.484°
Index ranges	$-15 \leq h \leq 14, -15 \leq k \leq 13, -16 \leq l \leq 16$
Reflections collected	26183
Independent reflections	7230 [$R_{int} = 0.0230$]
Completeness to $\theta = 25.242^\circ$	99.9%
Absorption correction	Semi-empirical from equivalents
Max. and min. transmission	1.000 and 0.868
Refinement method	Full-matrix least-squares on F^2
Data / restraints / parameters	7230 / 0 / 509
Goodness-of-fit on F^2	1.068
Final R indices [$F^2 > 2\sigma(F^2)$]	$RI = 0.0248, wR2 = 0.0657$
R indices (all data)	$RI = 0.0258, wR2 = 0.0664$
Extinction coefficient	n/a
Largest diff. peak and hole	0.336 and -0.521 e Å ⁻³
Radiation source (wavelength)	Mo-K α

The [Cu(*N,N*-dmen)₂(H₂O)]²⁺ in **27** has Cu-N distances ranging from 1.9937(11)-2.0781(11) Å with a fifth ligand (H₂O) at a distance of 2.3368(10) Å. This Cu-O distance is significantly shorter than that found in **20** and since the nearest potential oxygen donor on the other axial site is at 3.55 Å the complex is best considered as a 5-coordinate square based pyramid ($T^5 = 0.87$, τ index = 0.12).^{172,182}

The two pentaborate(1-) anions A (B1-B5) and B (B11-B15) are structurally similar to other transition metal complex polyborate structure systems involving isolated [B₅O₆(OH)₄]⁻ anions.^{136,181} The B-O distances to the 4-coordinate B1 and B11 centres range from 1.4596(15) - 1.4859(15) Å and 1.4712(15) - 1.4763(15) Å, respectively, and these are longer than those involving the trigonal boron centres of pentaborate(1-) anions A and B which range from 1.3502(16) - 1.3915(16) Å and 1.3533(16) - 1.3870(15) Å, respectively. B-O bonds involving trigonal boron atoms and terminal OH groups are at the shorter end of the range [av. 1.359 Å and av. 1.358 Å for A and B, respectively], whilst B-O bonds involving trigonal boron atoms and the distal oxygen atoms for anion A (O2 and O5) and B (O12 and O15) are at the longer end of the range [av. 1.384 Å and av. 1.385 Å, respectively]. Bond angles at the tetracoordinate B1 of anion A range from 107.69(10)° - 111.80(10)°, and angles at the other ring boron atoms

range from $115.72(11)^\circ$ - $123.72(11)^\circ$. Bond angles at the tetracoordinate B11 of anion B range from $108.17(9)^\circ$ - $110.64(9)^\circ$, and angles at the other ring boron atoms range from $115.07(11)^\circ$ - $123.78(11)^\circ$ consistent with sp^3 and sp^2 hybridisation, respectively. Specific bond lengths and bond angles of the pentaborate anion are listed in Appendix I (Table 17, and Table 18).

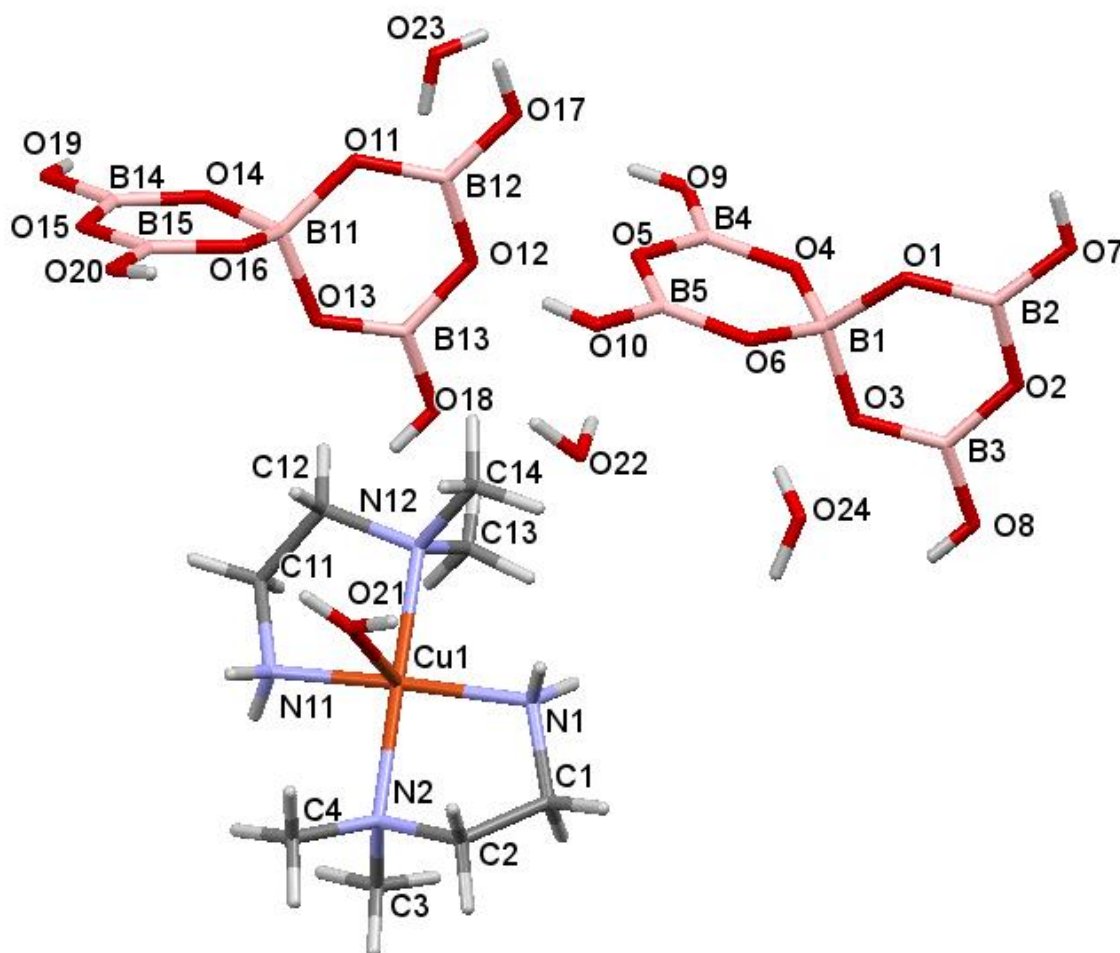


Figure 3.22 Diagram showing the complex cation, pentaborate anions and water molecules in **27** and the adopted numbering scheme.

In **27** the pentaborate(1-) anion (A) contains eleven H-bond interactions (four H-bond donors and seven H-bond acceptors) but there are no H-bond interactions at O5. The four H-bond donor sites of pentaborate(1-) anion are involved with H-bonds acceptor oxygen of four different pentaborate(1-) anions ($O9-H9\cdots O17^*$, $O10-H10\cdots O15^*$, $O8-H8\cdots O13^*$ and $O7-H7\cdots O11^*$). This may be described as $\alpha\alpha\beta\gamma$, where α , β , and γ are pentaborate acceptor sites.^{77,98} The hydrogen atoms in pentaborate (A) on the β -oxygens may be described as two 'in' and two

'out', whilst these on pentaborate (B) are four 'in'. This unusual conformation results in a $\alpha\alpha\alpha\alpha$ H-bond arrangement (O17-H17 \cdots O1^{*}, O18-H18 \cdots O3^{*}, O19-H19 \cdots O14^{*} and O20-H20 \cdots O16^{*}). All H-bonds data for **27** are listed in Table 3.16.

Table 3.16 H-bonds [\AA and $^\circ$] of **27**

<i>D-H\cdotsA</i>	<i>d(D\cdotsA)</i>	<i>D-H\cdotsA</i>	<i>d(D\cdotsA)</i>
O21-H21A-O24 ⁱ	2.7351(15)	O18-H18-O3 ⁱⁱⁱ	2.7543(13)
O21-H21B-O7 ⁱⁱ	2.8634(14)	O19-H19-O14 ^{vii}	2.6890(13)
N1-H1A-O24 ⁱ	2.9310(15)	O20-H20-O16 ^{vi}	2.7479(12)
N1-H1B-O12 ⁱⁱⁱ	3.1078(14)	O22-H22A-O10	2.8290(15)
N11-H11A-O23 ^{iv}	3.0038(16)	O22-H22B-O19 ^{vi}	2.7987(14)
N11-H11B-O2 ⁱⁱ	2.9404(14)	O23-H23A-O4 ^v	2.7606(14)
O7-H7-O11 ^v	2.7453(12)	O23-H23B-O20 ^{vi}	3.0021(15)
O8-H8-O13 ⁱⁱⁱ	2.6992(13)	O24-H24A-O3	3.2303(14)
O9-H9-O17	2.7347(13)	O24-H24A-O6	2.9429(14)
O10-H10-O15 ^{vi}	3.0075(13)	O24-H24B-O22 ⁱ	2.7119(15)
O17-H17-O1 ^v	2.6443(12)		

i = 1-x,-y,1-z; ii = 1+x,+y,-1+z; iii = 1-x,1-y,1-z; iv = 1+x,+y,+z; v = -x,1-y,1-z; vi = 1-x,1-y,-z; vii = 1-x,2-y,-z

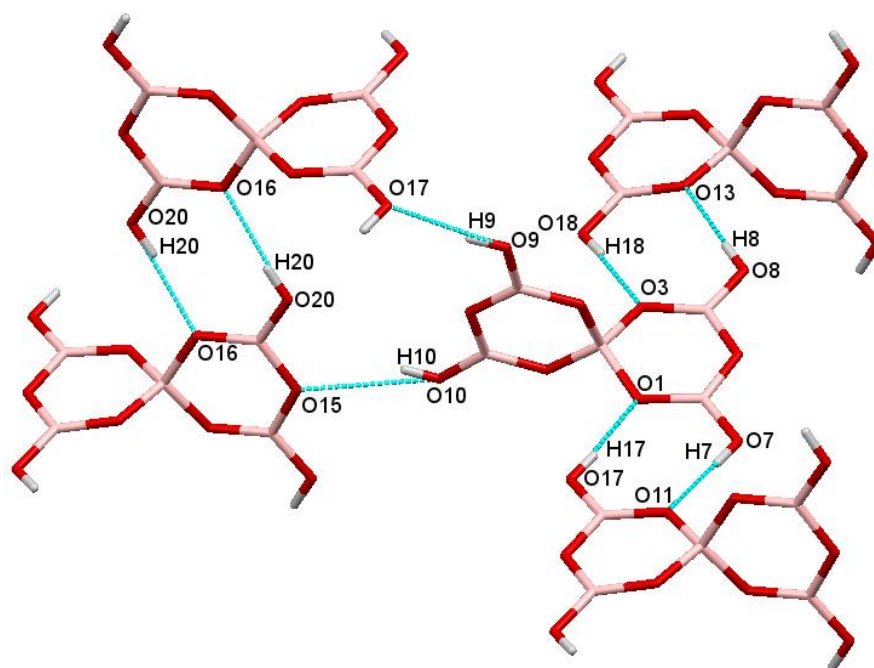


Figure 3.23 The two $R_2^2(8)$ H-bond motif connections and $R_3^3(16)$ interaction in **27**. Dashed blue lines represent H-bonds.

The pentaborate(1-) anions are linked together in a chain and a section of this chain is shown in Figure 3.23. The $[\text{B}_5\text{O}_6(\text{OH})_4]^-$ anion (A) within the chain is connected by two $\text{R}_2^2(8)$ interactions: $\text{O}8\text{-H}8\cdots\text{O}13^*/\text{O}18^*\text{-H}18^*\cdots\text{O}3$ and $\text{O}7\text{-H}7\cdots\text{O}11^*/\text{O}17^*\text{-H}17^*\cdots\text{O}1$. Each pentaborate(1-) anion (A) is further linked to another pentaborate(1-) anions by a $\text{R}_3^3(16)$ interactions. The three $\text{R}_3^3(16)$ interactions are $\text{O}9\text{-H}9\cdots\text{O}17^{**}$, $\text{O}10\text{-H}10\cdots\text{O}15^*$, and $\text{O}20^*\text{-H}20^*\cdots\text{O}16^*$.

The pentaborate(1-) anions (B) are linked by many H-bond interactions as shown in Figure 3.24. Each $[\text{B}_5\text{O}_6(\text{OH})_4]^-$ anion (B) is connected by four $\text{R}_2^2(8)$ interactions: $\text{O}17\text{-H}17\cdots\text{O}1^*/\text{O}7^*\text{-H}7^*\cdots\text{O}11$, $\text{O}18\text{-H}18\cdots\text{O}3^*/\text{O}8^*\text{-H}8^*\cdots\text{O}13$, $\text{O}19\text{-H}19\cdots\text{O}14^*/\text{O}19^*\text{-H}19^*\cdots\text{O}14$ and $\text{O}20\text{-H}20\cdots\text{O}16^*/\text{O}20^*\text{-H}20^*\cdots\text{O}16$.

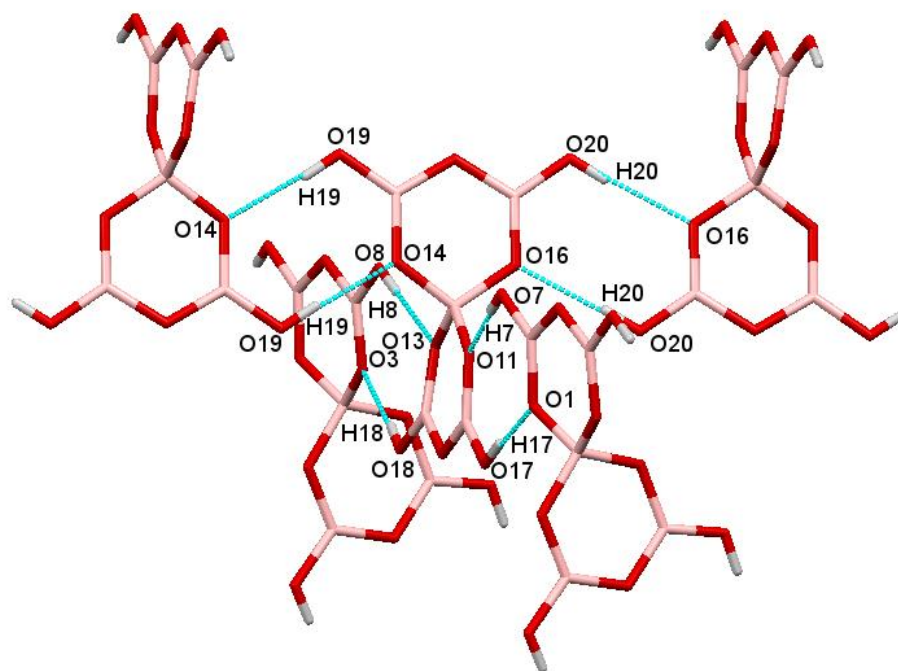


Figure 3.24 The four $\text{R}_2^2(8)$ H-bond motif connections between pentaborate(1-) anions in **27**.

A view of a plane of a pentaborate(1-) anions found in **27** is given in Figure 3.25.

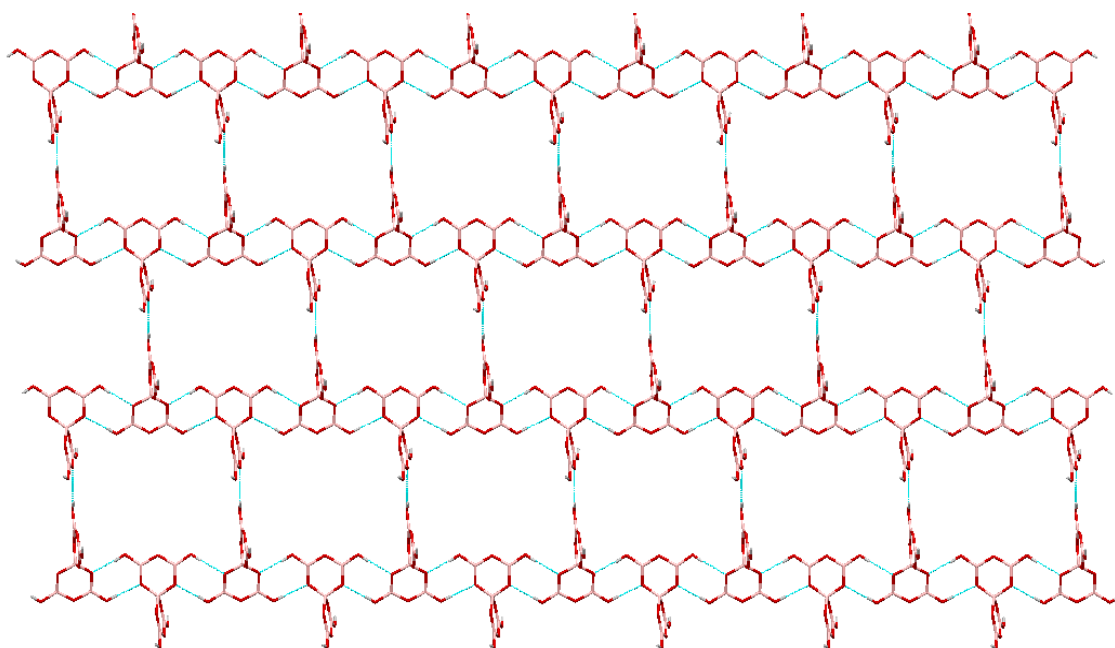


Figure 3.25 Extended H-bonded $[B_5O_6(OH)_4]$ plane (viewed along the b direction of the unit cell) for **27**.

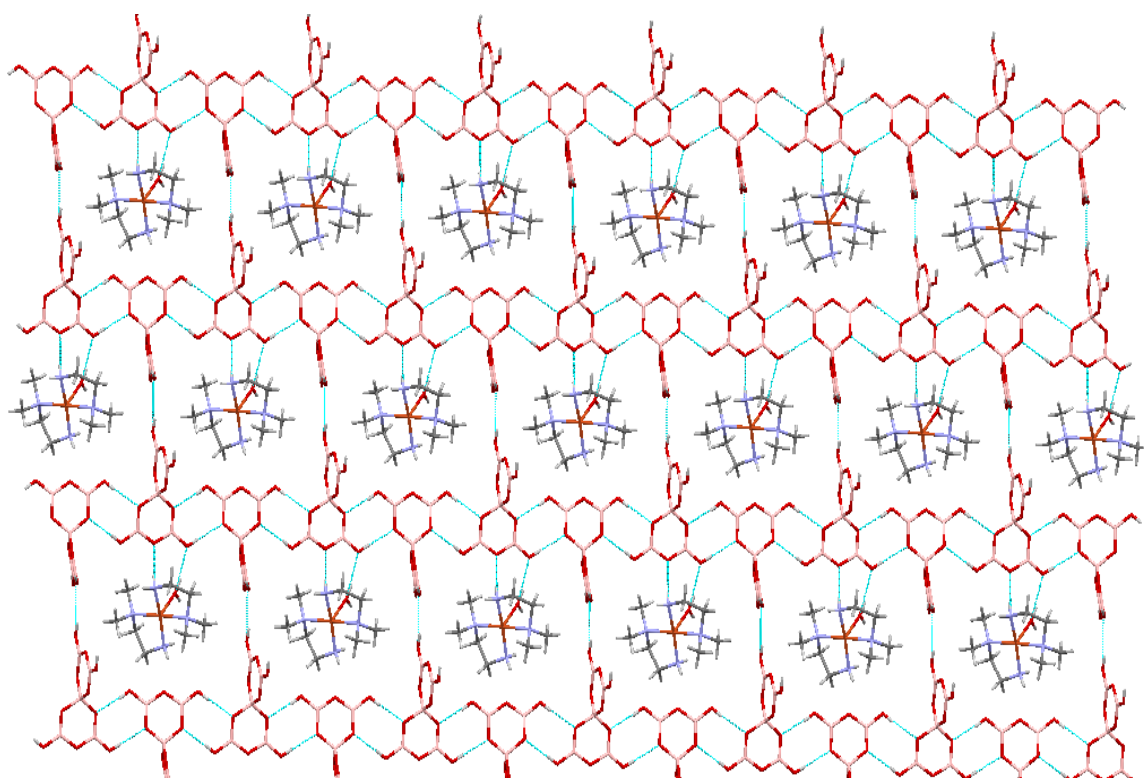


Figure 3.26 Diagram showing a 'plane' of polyborate anions (viewed along the b direction of the unit cell) with $[Cu(N,N-dmen)_2(H_2O)]^{2+}$ and H_2O molecules shown in the 'cavities' in **27**.

The solid-state structures of all transition metal complex polyborate compounds involve H-bonded supramolecular polyborate giant anions, with 'cavities' and 'channels', which can involve the transition metal complex cation. The $[\text{Cu}(\text{N},\text{N}\text{-dmen})_2(\text{H}_2\text{O})]^{2+}$ cations, $[\text{B}_5\text{O}_6(\text{OH})_4]^-$ anions, and the H_2O molecules of crystallization of **27** are connected through a complex series of H-bond interactions as shown in Figure 3.26. The connection of the plane shown in Figure 3.25 to the neighbouring planes is formed by further H-bond interactions, forming a three-dimensional network.

Each $[\text{Cu}(\text{N},\text{N}\text{-dmen})_2(\text{H}_2\text{O})]^{2+}$ cation connects to two H_2O molecules and one pentaborate(1-) anion (Figure 3.27), in the secondary coordination sphere and these units are held there by six H-bonds $\text{N1-H1A}\cdots\text{O24}^*$, $\text{N1-H1B}\cdots\text{O12}^*$, $\text{N11-H11A}\cdots\text{O23}^*$, $\text{N11-H11B}\cdots\text{O2}^*$, $\text{O21-H21A}\cdots\text{O24}^*$, and $\text{O21-H21B}\cdots\text{O7}^*$ (Table 3.16).

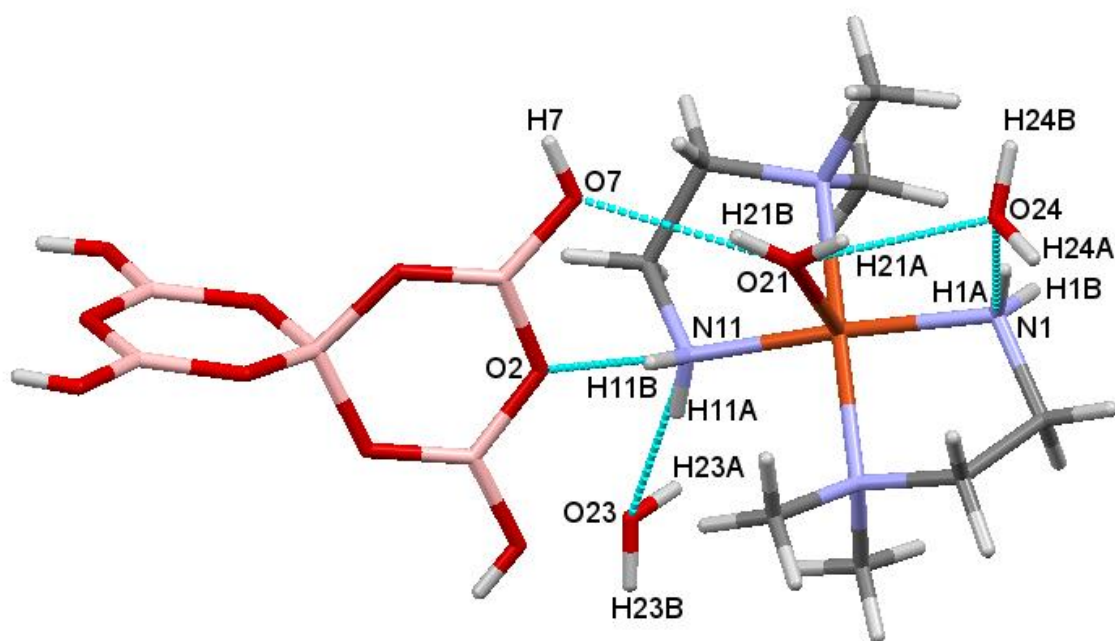


Figure 3.27 The H-bond connections of $[\text{Cu}(\text{N},\text{N}\text{-dmen})_2(\text{H}_2\text{O})]^{2+}$ cation in **27**

3.3.5.6 Structural characterisation of $[\text{Cu}(\text{N},\text{N}\text{-dmen})\{\text{B}_6\text{O}_7(\text{OH})_6\}]\cdot 4\text{H}_2\text{O}$ (28**)**

Crystallographic data for **28** are listed in Table 3.17. Crystals of **28** are monoclinic, $P2_1/n$ and consists of a neutral transition metal complex $[\text{Cu}(\text{N},\text{N}\text{-dmen})\{\text{B}_6\text{O}_7(\text{OH})_6\}]$ with four interstitial water molecules as shown in Figure 3.28.

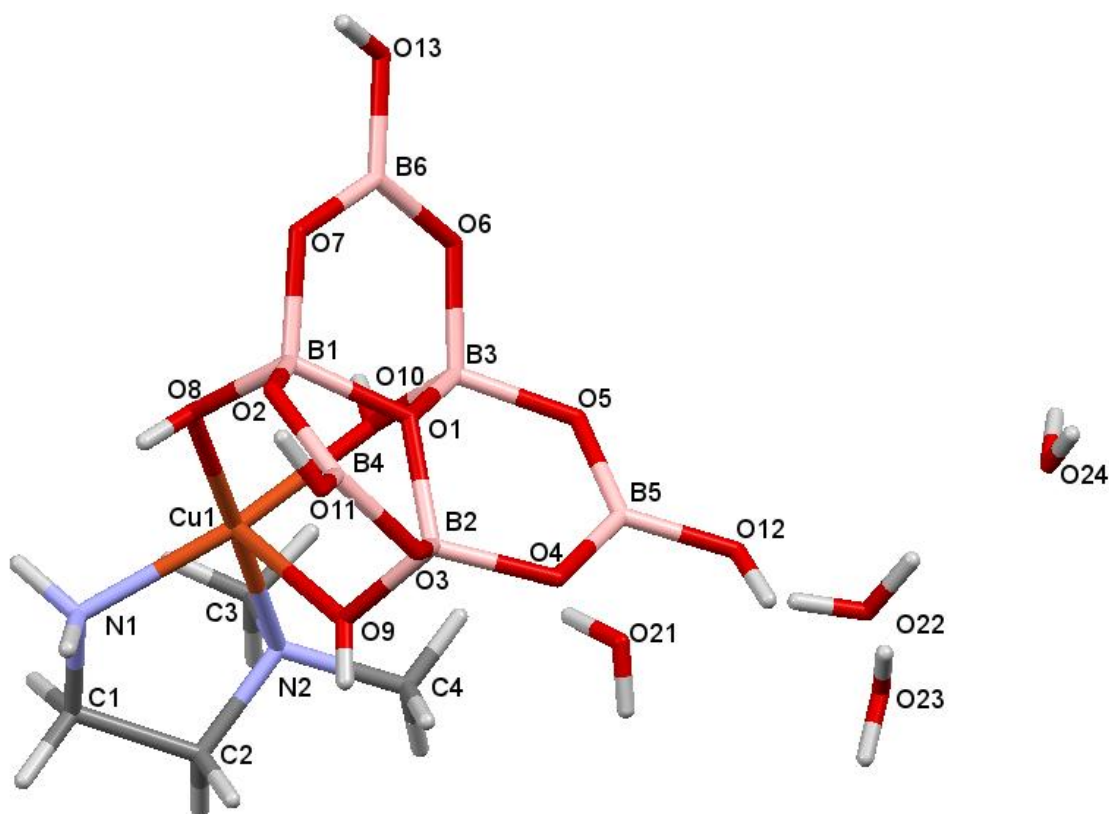


Figure 3.28 Diagram showing the structure and the numbering scheme of **28**.

Table 3.17 Crystal data and structure refinement details of **28**.

Empirical formula	$C_4H_{26}B_6N_2O_{17}Cu$	
Formula weight	502.67	
Temperature	100(2) K	
Wavelength	0.71073 Å	
Crystal system	Monoclinic	
Space group	$P2_1/n$	
Unit cell dimensions	$a = 12.75604(17)$ Å	$\alpha = 90^\circ$
	$b = 9.86582(12)$ Å	$\beta = 103.2331(14)$
	$c = 15.7331(2)$ Å	$\gamma = 90^\circ$
Volume	$1927.41(5)$ Å ³	
Z	4	
Density (calculated)	1.732 g / cm ³	
Absorption coefficient	1.219 mm ⁻¹	
Crystal	Prism; deep blue	
Crystal size	$0.110 \times 0.100 \times 0.050$ mm ³	
θ range for data collection	$2.456 - 27.480^\circ$	
Index ranges	$-16 \leq h \leq 16, -12 \leq k \leq 12, -20 \leq l \leq 20$	
Reflections collected	24614	
Independent reflections	4397 [$R_{int} = 0.0195$]	
Completeness to $\theta = 25.242^\circ$	99.9%	
Absorption correction	Semi-empirical from equivalents	
Max. and min. transmission	1.000 and 0.844	
Refinement method	Full-matrix least-squares on F^2	
Data / restraints / parameters	4397 / 12 / 337	

Goodness-of-fit on F^2	1.066
Final R indices [$F^2 > 2\sigma(F^2)$]	$RI = 0.0221$, $wR2 = 0.0597$
R indices (all data)	$RI = 0.0231$, $wR2 = 0.0604$
Extinction coefficient	n/a
Largest diff. peak and hole	0.348 and $-0.404 \text{ e } \text{Å}^{-3}$
Radiation source (wavelength)	Mo-K α

The neutral complex in compound **28** arises from the coordination of tridentate hexaborate(2-) $[\text{B}_6\text{O}_7(\text{OH})_6]^{2-}$ ligands to a cationic $[\text{Cu}(\text{L-L})]^{2+}$ centre { L-L = *N,N*-dmem }. The 5-coordinate copper(II) centre in **28** has a τ index of 0.19,¹⁸² demonstrating that its structure is best represented as square-based pyramidal structure. The slightly disordered square-based pyramidal copper(II) centre has a bidentate diamine ligand is within the square plane and the tridentate hexaborate(2-) anion completes the two remaining coordination sites of the square plane and the one axial site (O9). Compound **28** has Cu-N distances of 2.0011(11) Å (N1) and 2.0478(11) Å (N2). The square plane Cu-O distances are 2.0052(9) Å (O8) and 1.9566(9) Å (O10), whilst the Cu-O axial distance is slightly longer at 2.2481(9) Å (O9).

The hexaborate(2-) anion in **28** acts as a tridentate ligand (same as in **24**) to the copper(II) centre, with an average Cu-O distance 2.070 Å, whilst the *N,N*-dimethylethylenediamine ligand acts as a bidentate ligand. The copper(II) centre has a coordination number of five and a square based pyramidal geometry (Figure **3.28**).

The hexaborate(2-) anion consist of a three fused 6-membered boroxyl rings containing 3 tetrahedral boron centres (B1, B2, B3) and 3 trigonal boron centres (B4, B5, B6) (see Section **3.3.5.3** for more details). The hexaborate(2-) anion in **28** is structurally similar to other reported hexaborate compounds.^{135,153,154,184} The B-O distances to the tetrahedral B1, B2, B3 centres are in the range of 1.4381(16) - 1.5161(16) Å [av. 1.472 Å], 1.4437(17) - 1.5142(16) Å [av. 1.474 Å], and 1.4409(16) - 1.5199(15) Å [av. 1.470 Å], respectively and these are significantly longer than those involving the trigonal B4, B5, B6 centres: the B-O distances to B4, B5, and B6 centres are in the range of 1.3582(17) - 1.3770(17) Å [av. 1.368 Å], 1.3561(17) - 1.3750(17) Å [av. 1.368 Å], and 1.3619(17) - 1.3756(17) Å [av. 1.367 Å], respectively. The B-OH bond lengths involving tetrahedral B1, B2, and B3 centres are 1.4818(16), 1.4437(17), and 1.4674(16) Å, respectively while B-OH bond lengths involving trigonal B4, B5, and B6 centres are significantly shorter at 1.3713(17), 1.3750(17), and 1.3756(17) Å, respectively. Bond angles at the tetrahedral centres B1, B2, and B3 range from 107.95(10)° - 111.18(10)°, 106.07(10)° - 113.30(11)° and 106.25(10)° - 112.11(10)°, respectively while the bond angles at the trigonal B4, B5, and B6 centres range from 117.21(12)° - 122.97(12)°, 115.95(12)° - 123.92(12)°, and

117.20(12)[°] - 122.69(12)[°], respectively. The bond lengths and angles are given in Appendix I (Table 19, and Table 20).

In **28** the hexaborate(2-) anion has six potential H-bond donor sites which are also capable of accepting H-bond interactions, and a further seven potential H-bond acceptor sites. The hexaborate(2-) anion in **28** has fourteen H-bond interactions (six H-bond donors and eight H-bond acceptors), and three coordination to the copper (II) metal. There are no further stabilizing interactions at O1, O2, and O5.

Table 3.18 H-bonds [\AA and $^{\circ}$] in **28**.

<i>D-H...A</i>	<i>d(D...A)</i>	<i>D-H...A</i>	<i>d(D...A)</i>
O8-H8-O23 ⁱ	2.8424(13)	O22-H22A-O21	2.7745(15)
O9-H9-O22 ⁱⁱ	2.7567(14)	O22-H22B-O24	2.7061(15)
O10-H10-O12 ⁱⁱⁱ	2.6839(13)	O23-H23A-O22	2.7305(15)
O11-H11-O24 ⁱ	2.8009(14)	O23-H23B-O3 ⁱⁱ	2.8629(13)
O12-H12-O23	2.6816(14)	O21-H21A-O3	2.8478(14)
O13-H13-O2 ^{iv}	3.1168(13)	O21-H21B-O4 ²ⁱⁱ	2.8749(14)
O13-H13-O7 ^{iv}	2.8027(13)	O24-H24A-O21 ^{vi}	2.7793(15)
N1-H1A-O6 ⁱⁱⁱ	2.9064(14)	O24-H24B-O13 ^{vii}	2.8025(14)
N1-H1B-O11 ^v	3.0385(15)		

i = +x, 1+y, +z;
= 1-x, 2-y, 1-z;

ii = 1-x, 1-y, 1-z;
vi = 3/2-x, -1/2+y, 3/2-z;

iii = 3/2-x, 1/2+y, 1/2-z;
vii = 2-x, 1-y, 1-z

iv = 2-x, 2-y, 1-z; v

All six potential H-bond donor sites in the hexaborate(2-) anion in **28** are involved in donor interactions: the three coordinated hydroxyl groups H-bond to one hexaborate(2-) (from O10) and two H₂O molecules (from O8 and O9), whilst the three uncoordinated hydroxyl groups H-bond to two hexaborate(2-) anions and one H₂O molecule. Therefore each [Cu(*N,N*-dmen){B₆O₇(OH)₆}] unit has three other such units in its secondary coordination sphere, facilitated through H-bond interactions. The hexaborate(2-)-hexaborate(2-) interactions (O13-H13...O7*/O13*-H13*...O7) in **28** can be designated as reciprocal R₂²(8). The two amino hydrogens on the coordinated nitrogen of the *N,N*-dmen ligand in **28** are also both involved in H-bonding to neighbouring hexaborate(2-) anions. This results in an unusual reciprocal R₂²(16) {N1-H1B...O11*/N1*-H1B*...O11 (Figure 3.29)} motif in **28** and an unusual R₂²(10) motif in which a neighboring hexaborate(2-) is a double acceptor from donor hydrogen atoms on coordinated O10 and N1 atoms {O10*-H10*...O12/N1*-H1A*...O6; O10-H10...O12*/N1-H1A...O6* (Figure 3.30)}; both motifs includes the copper(II) center within their rings. The hexaborate(2-) anion in **28** is also linked by eight water molecules *via* eight H-bond interactions O23-H23B...O3*, O21-H21A...O3*, O21-H21B...O4*, O8*-H8*...O23, O9*-H9*...O22,

O11^{*}-H11^{*}...O24, O12^{*}-H12^{*}...O23, and O24-H24B...O13^{*}. Details of the H-bonding interactions are given in Table 3.18.

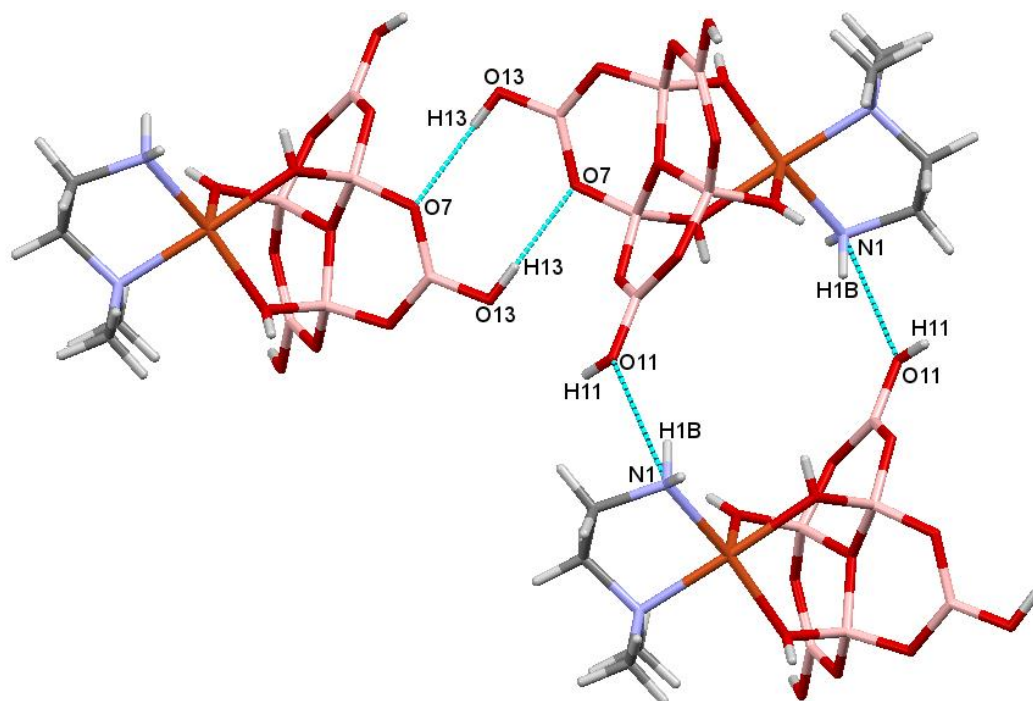


Figure 3.29 The reciprocal $R_2^2(8)$ and reciprocal $R_2^2(16)$ interactions in **28**.

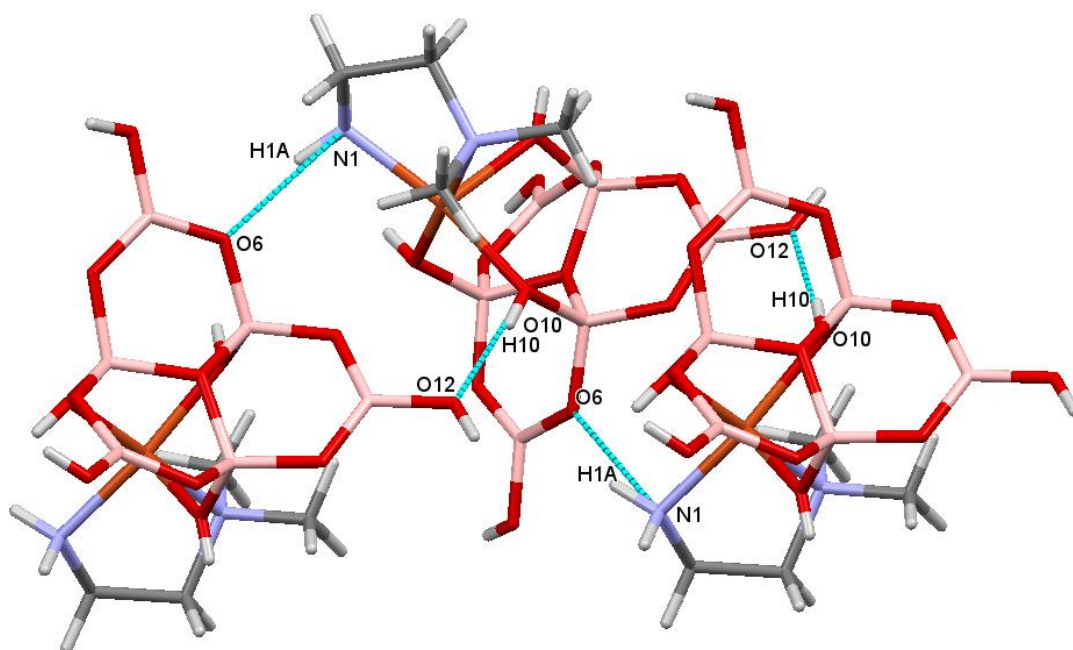


Figure 3.30 The two $R_2^2(10)$ interactions in **28**. Dashed blue lines represent H-bonds.

The $[\text{Cu}(\text{N,N-dmen})\{\text{B}_6\text{O}_7(\text{OH})_6\}]$, and H_2O molecules of **28** are connected through a complex series of H-bond interactions to produce the three-dimension network linking the hexaborates.

3.4 Conclusion and summary

The first aim of this chapter was to prepare and investigate new Cu(II) polyborate compounds. Nine polyborate compounds **20-28** containing different polyborate anions (triborate(1-), tetraborate(2-), pentaborate(1-), hexaborate(2-), and heptaborate(2-) anions have been templated in aqueous solution from boric acid using a set of sterically demanding Cu(II) complex cations. Six of these salts have been characterized by single-crystal XRD (**20**, **22-24**, **27-28**) studies.

The polyborate anions of compounds **20-28** show a number of bands in their IR spectra. The pentaborate(1-) anion of **20** shows peaks at 1094, 927, and 776 cm^{-1} , tetraborate(2-) anion in **21** has peaks at 1042, 943, and 806 cm^{-1} , hexaborate(2-) anion in **23** has peaks at 1086, 953, and 809 cm^{-1} , while the heptaborate(2-) anion in **24** has bands at 1134, 949, and 854 cm^{-1} . The higher energy bands may be assigned to asymmetric $\text{B}_{(3)}\text{-O}$ stretching whilst the lower energy peaks may be assigned to symmetric $\text{B}_{(3)}\text{-O}$ and symmetric $\text{B}_{(4)}\text{-O}$, respectively.¹⁴⁰ These peaks may become diagnostic once more compounds of those class have been prepared.

Thermal properties of the copper(II) complex polyborate compounds were analysed by thermal gravimetric analysis (TGA) and differential scanning calorimetry (DSC). The analysis of **20** and **22-28** confirmed the presence of a three-stage decomposition to give anhydrous copper(II) borates. The first mass-loss step is associated with the release of interstitial water molecules. The second stage of decomposition is due to the interionic condensation of polyborate network. The third step is related to the oxidation of the ligands of the copper(II) complex. Compound **21** showed only a two-stage decomposition profile due to the absence of interstitial water molecules.

The second aim was to evaluate the structure directing effects of copper(II) complex cations in solid-state supramolecular structures. Typical structure directing effects encountered in crystal engineering are stoichiometry, steric effects (crystal packing), and interionic interactions.

Anion-anion H-bond interactions have been shown to play a dominant role in non-metal cation pentaborate(1-) chemistry.⁵ Inspection of the crystallographic data outlined in this Chapter show that cation-anion H-bond play a dominant role in the templating of the reported solid-state structures. In particular, the polyborate anions are found within the secondary coordination shell of **20**, **24**, and **27** by amino hydrogen H-bonds and these display unusual H-bond ring interactions *e.g.* R₂²(8) involving the copper(II) centre (Figure **3.21**). In compounds **22**, **23** and **28** the polyborate anion is found within the primary coordination shell and here the hexaborate (2-) anions form 3 dative coordinate bonds to the copper(II) centres, in addition to H-bond interactions to neighbouring complexes.

Reaction of [Cu(en)₂]²⁺ with boric acid in a 1:10 ratio produced a compounds containing the pentaborate(1-) anion (**20**), while the reaction in 1:5 ratio afforded a compound containing the tetraborate(2-) anion (**21**). Reaction of [Cu(tn)₂]²⁺ in a 1:5 ratio afforded a tetraborate(2-) salt (**26**) whereas in a 1:10 ratio a compound containing two isolated polyborate anions (triborate(1-) and pentaborate(1-)) was obtained (**25**). These results show that the products obtained are also dependent upon the reaction stoichiometry.

Chapter Four

Nickel(II) complex

polyborate salts

4.1 Introduction

Over the past few years, polyborate anions with nickel(II) complex counter ions have been the focus of relatively few studies within the area of crystal engineering and supramolecular chemistry fields. Salts containing isolated polyborate anions partnered with nickel(II) complex cations are known in the literature but these are limited to $[\text{Ni}(\text{en})_2\text{pip}][\text{B}_5\text{O}_6(\text{OH})_4]_2$,¹⁸¹ $[\text{Ni}(\text{en})_3][\text{B}_5\text{O}_6(\text{OH})_4]\cdot\text{CH}_3\text{CO}_2$,¹³⁶ $[\text{Ni}(\text{en})_2(\text{C}_4\text{H}_{10}\text{N}_2)][\text{B}_5\text{O}_6(\text{OH})_4]_2$,¹¹³ and $[\text{Ni}(\text{en})_3][\text{B}_5\text{O}_6(\text{OH})_4]\cdot 2\text{H}_2\text{O}$.¹¹⁵

In this chapter we report the synthesis and characterisation of eight new polyborate compounds (seven polyborate salts of nickel(II) complex cations and one neutral nickel(II) complex containing the hexaborate(2-) anion). Five of these compounds have been characterised by single-crystal XRD studies: four of these contain either isolated pentaborate(1-) anions (three) or isolated heptaborate(2-) anion (one), and one of these, $[\text{Ni}(\text{en})\{\text{B}_6\text{O}_7(\text{OH})_6\}(\text{H}_2\text{O})_2]\cdot\text{H}_2\text{O}$, contains the $[\text{B}_6\text{O}_7(\text{OH})_6]^{2-}$ anion coordinated as a bidentate ligand *via* two hydroxyl oxygen centres of the hexaborate(2-) anion.

4.2 Aims

The aim of this research was to synthesise and characterise a new series of polyborate compounds containing nickel(II) complex cations. A series of the cationic nickel(II) coordination complexes of ethylenediamine (en), 1,2-diaminopropane (pn), 1,2-diaminocyclohexane (dach), diethylenetriamine (dien), triethylenetetramine (trien), 2,4-dimethyl-1-(3-azapropyl)-1,5,8-triazaocta-2,4-dienato (AEN) and *N*-(2-hydroxyethyl) ethylenediamine (hn) ligands were prepared to template formation of the polyborates.

Nickel(II) complex cations were chosen due to their relatively high charge, their sterically bulky structure, and their potential to form many H-bond interactions to moieties within their secondary coordination sphere.

4.3 Result and discussion

4.3.1 Synthesis of nickel(II) complex compounds

The known nickel(II) complexes: $[\text{Ni}(\text{en})_3]\text{Cl}_2\cdot 2\text{H}_2\text{O}$ (**29**),¹⁸⁵ $[\text{Ni}(\text{AEN})]\text{Cl}\cdot\text{H}_2\text{O}$ (**30**),¹⁸⁶ $[\text{Ni}(\textit{trans}\text{-dach})_2(\text{H}_2\text{O})_2]\text{Cl}_2$ (**31**),¹⁸⁷ $[\text{Ni}(\text{hn})_2]\text{Cl}_2$ (**32**),¹⁸⁸ $[\text{Ni}(\text{dien})_2]\text{Cl}_2\cdot\text{H}_2\text{O}$ (**33**),¹⁸⁹

[Ni(pn)₃]Cl₂·2H₂O (**34**),¹⁸⁵ and [Ni₂(trien)₃]Cl₄·2H₂O (**35**),¹⁹⁰ were all prepared by standard literature methods. Physical properties of the prepared complexes were all in accord with literature data.

Compounds **29-35** were all prepared as their chloride salts and it was therefore necessary to convert these chloride salts to the corresponding hydroxide salts before reaction with boric acid. The hydroxide salts were prepared as outlined in Chapter two. The experiment details are given in Chapter 6.

4.3.2 Preparation of Nickel(II) complex polyborate compounds

A series of nickel(II) complex polyborate compounds **36, 38-43** have been prepared as crystalline solids from nickel(II) complex hydroxides. Boric acid was added in a ratio of 1:10 to the hydroxide solutions. The solutions were then stirred, concentrated using a rotary evaporator and cooled to yield polyborate compounds as solid crude products (**36, 38-43**). The crude products were isolated by filtration and dried.

Compound **37** was prepared by mixing ethylenediamine, nickel(II) sulphate hexahydrate and barium hydroxide octahydrate in water. The mixture was stirred and then filtered to remove the barium sulphate which had formed. Boric acid was added to the filtrate with stirring. Followed by work up as outlined above.

Crystals suitable for single-crystal X-ray diffraction studies of the nickel(II) complex polyborate compounds were prepared by recrystallization of the crude products from distilled water. The recrystallized products were isolated by slow evaporation from aqueous solution or by vapour diffusion from aqueous solution using ethanol and/or methanol.

Seven new nickel(II) complex polyborate compounds (**37-43**) were prepared. Characterisation data reported for the previously prepared **36** is limited to ¹¹B NMR, p-XRD, and magnetic properties.¹¹⁵ This compound was re-synthesised by a new method. Spectroscopic data for this compound is discussed in the next sections and are reported in the experimental chapter. The recrystallized yields of the nickel(II) complex polyborate compounds (**36-43**) and their formula are shown in Table 4.1.

Table 4.1 Yields and formula of nickel(II) complex polyborate compounds.

Compound	Formula	% Yield
36	[Ni(en) ₃][B ₅ O ₆ (OH) ₄] ₂ ·2H ₂ O	63
37	[Ni(en){B ₆ O ₇ (OH) ₆ }(H ₂ O) ₂] ₂ ·H ₂ O	33
38	[Ni(AEN)][B ₅ O ₆ (OH) ₄] ₂ ·H ₂ O	38
39	[Ni(dach) ₂ (H ₂ O) ₂][Ni(dach) ₂][B ₇ O ₉ (OH) ₅] ₂ ·4H ₂ O	47
40	[Ni(hn) ₂][B ₅ O ₆ (OH) ₄] ₂	37
41	<i>s-fac</i> -[Ni(dien) ₂][B ₅ O ₆ (OH) ₄] ₂	34
42	[Ni(pn) ₃][B ₅ O ₆ (OH) ₄] ₂ C ₂ H ₅ OH·5H ₂ O	47
43	[Ni ₂ (trien) ₃][B ₅ O ₆ (OH) ₄] ₂ Cl ₂ ·CH ₃ OH·6H ₂ O	28

4.3.3 Characterisation of nickel(II) complex polyborate compounds

The nickel(II) complexes and their polyborate compounds are generally paramagnetic with exception of **30** and **38** which are diamagnetic. The mass susceptibility (χ_g), molar susceptibility (χ_m), diamagnetic susceptibility (χ_d), paramagnetic susceptibility (χ_p), and effective magnetic moment (μ_{eff}) of compounds **29-43** are shown in Table 4.2. There is no significant diagnostic change between the magnetic properties of the starting nickel(II) complexes and their polyborate compounds. The experimentally determined effective magnetic moment values are very close to those calculated using the ‘spin-only’ formula for square planar (**30** and **38**) or octahedral (**29, 31-37, 39-43**) complexes. The μ_{eff} values of Ni(II) complexes and their polyborate compounds are in agreement with literature data for other Ni(II) complexes.^{180,191}

Table 4.2 Magnetic properties of nickel(II) complexes and their polyborate compounds at 24 °C.

Compound	χ_g (cm ³ ·g ⁻¹)	χ_m (cm ³ ·mol ⁻¹)	χ_d	χ_p	μ_{eff} Bohr magneton	N
29	9.8×10^{-6}	3390×10^{-6}	-170×10^{-6}	3563×10^{-6}	2.91	2.08
30	-0.2×10^{-6}	-56×10^{-6}	-	-	-	-
31	7.7×10^{-6}	3040×10^{-6}	-190×10^{-6}	3237×10^{-6}	2.77	1.96
32	9.5×10^{-6}	3200×10^{-6}	-168×10^{-6}	3368×10^{-6}	2.82	2.00
33	7.9×10^{-6}	2790×10^{-6}	-177×10^{-6}	2967×10^{-6}	2.65	1.83
34	7.7×10^{-6}	3010×10^{-6}	-194×10^{-6}	3204×10^{-6}	2.76	1.94
35	3.9×10^{-6}	2906×10^{-6}	-366×10^{-6}	3269×10^{-6}	2.78	1.95
36	4.0×10^{-6}	2844×10^{-6}	-355×10^{-6}	3199×10^{-6}	2.75	1.94
37	5.7×10^{-6}	2588×10^{-6}	-225×10^{-6}	2813×10^{-6}	2.58	1.81
38	-0.4×10^{-6}	-170×10^{-6}	-	-	-	-
39	2.3×10^{-6}	3030×10^{-6}	-645×10^{-6}	3675×10^{-6}	2.95	2.11
40	4.8×10^{-6}	3430×10^{-6}	-350×10^{-6}	3780×10^{-6}	2.99	2.14

41	5.0×10^{-6}	3516×10^{-6}	-350×10^{-6}	3856×10^{-6}	3.02	2.18
42	3.3×10^{-6}	2810×10^{-6}	-426×10^{-6}	3236×10^{-6}	2.76	1.94
43	2.6×10^{-6}	3125×10^{-6}	-601×10^{-6}	3721×10^{-6}	2.97	2.12

The elemental analysis data of the new nickel(II) complex polyborate compounds (**37-43**) and the starting nickel(II) complexes (**30, 34, 35**) are listed in Table 4.3. Elemental analysis data of the nickel(II) complex polyborate compounds were consistent with their formulation.

Table 4.3 CHN analysis of nickel(II) complex polyborate compounds.

Compound	Calculated (%)			Experimental (%)		
	C	H	N	C	H	N
30	36.5	7.1	18.9	37.1	6.7	18.8
34	27.9	8.8	21.7	28.1	8.9	21.7
35	29.5	8.0	22.9	29.6	8.1	22.4
37	5.3	4.5	6.2	5.4	4.5	6.2
38	22.6	5.3	11.7	22.7	5.4	11.7
39	22.3	6.1	8.7	21.8	6.3	8.4
40	13.7	4.6	8.0	13.7	4.7	8.0
41	13.7	4.9	12.0	14.0	5.4	12.1
42	15.5	6.3	9.9	15.5	6.6	10.0
43	19.0	6.5	14.0	18.9	6.3	13.7

The chemical shift (δ) of ^{11}B NMR spectra of nickel(II) complex polyborate salts obtained in D_2O are listed in Table 4.4. ^{11}B NMR spectroscopy of nickel(II) complex polyborate compounds showed that the pentaborate salts (**40-42, 43**) contained the characteristic three peaks.¹⁴⁹⁻¹⁵¹ These peaks correspond to the $\text{B}(\text{OH})_3/\text{B}(\text{OH})_4^-$, $[\text{B}_3\text{O}_3(\text{OH})_4]^-$ and the four coordinate centre of the $[\text{B}_5\text{O}_6(\text{OH})_4]^-$ anion (for more details see Section 2.3.3), whilst the pentaborate(1-) salts **36** and **38** show two signals and only one signal, respectively. ^{11}B NMR spectra of the hexaborate (**37**) and heptaborate (**39**) compounds are quantitatively different from the spectra observed in the pentaborate salts with only one (averaged and exchanging) signal observed. The observed chemical shift for the hexaborate(2-) complex (**37**) is similar to that observed for hexaborate(2-) copper(II) complex salts (**23, 28**) described in Section 3.3.3. Likewise, the observed chemical shift for the heptaborate(2-) nickel(II) complex compound (**39**) is comparable to that of the copper(II) complex heptaborate salt (**24**) described in Section 3.3.3.

^1H and ^{13}C NMR spectra were not obtained due to the paramagnetic properties of the Ni^{2+} cations. However, compound **38** was diamagnetic and ^1H NMR: 2, 2.5, 3.2, and 4.8 ppm, ^{13}C NMR: 19.9, 43, 53.6, and 160.5 ppm. These data agree with reported literature data of the cation.¹⁸⁶

Table 4.4 The chemical shift (δ) of ^{11}B NMR spectra of nickel(II) complex polyborate compounds.

Compound	$^{11}\text{B}/\text{ppm}$
36	13.4 (16%), 16.1 (84%)
37	17.7
38	16.3
39	15.8
40	1.2 (3%), 13.4 (23%), 18.0 (74%)
41	1.5 (1%), 13.3 (13%), 17.4 (86%)
42	1.5 (2%), 13.8 (20%), 16.8 (78%)
43	1.2 (3%), 13.8 (30%), 16.5 (67%)

Infra-red spectroscopic investigation confirmed that the nickel(II) complex salts contained polyborate anions. The FT-IR data for B-O stretches for compounds **36-43** (Table 4.5) have been assigned by comparison with data of Jun *et al.*¹⁴⁰ for related polyborate anions.

Table 4.5 Selected FT-IR spectroscopic data for nickel(II) polyborate compounds.

Comp.	$\nu(\text{O-H})$, $\nu(\text{N-H})$	$\nu \text{ C-H}$	ν_{as} ($\text{B}_{(3)}\text{-O}$)	δ (B-O-H)	ν_{as} ($\text{B}_{(4)}\text{-O}$)	ν_{s} ($\text{B}_{(3)}\text{-O}$)	ν_{s} ($\text{B}_{(4)}\text{-O}$)	γ ($\text{B}_{(3)}\text{-O}$)
36	3344(s), 3297(s)	2947(w)	1407(s) 1315(s)	1168(m)	1026(s)	921(s)	851 w 775(m)	706(w)
37	3400(s), 3350(s)	2924(w), 2854(w)	1420(m), 1380(s)	1133(s)	1044(s)	955(m)	852(w), 809(s)	696(w)
38	3377(s), 3326(s)	2983(w), 2963(w)	1416(s), 1393(s)	1129(m)	1019(m)	924(s)	820(w), 778(m)	708(w)
39	3663(s), 3271(s)	2929(m), 2863(m)	1453(s), 1350(s)	1180(s)	1066(s)	948(w)	854(m), 807(m)	716(w)
40	3375(s), 3288(s)	2962(w)	1410(s), 1321(s)	1141(s)	1022(s)	919(s)	846(w), 774(s)	706(s)
41	3333(s), 3297(s)	2988(w), 2950(w)	1412(s), 1330(s)	1135(m)	1042(m)	915(s)	809(w), 774(s)	707(s)
42	3336(s), 3235(s)	2974(w)	1434(s), 1305(s)	1156(s)	1044(s)	916(s)	820(w), 777(s)	708(m)
43	3290(s), 3238(s)	2951(w)	1410(s), 1313(s)	1163(m)	1057(m)	920(s)	822(w), 773(m)	705(m)

b = broad, m = middle, s = strong, w = weak, sh = shoulder, $\text{B}_{(3)}$ = three coordinate boron, $\text{B}_{(4)}$ = four coordinate boron, ν = stretching frequency, ν_{s} = symmetrical stretching frequency, ν_{as} = asymmetrical stretching frequency, δ = bending frequency.

4.3.4 Thermal properties of nickel(II) complex polyborate compounds

TGA and DSC analysis were used to investigate the thermal properties of the nickel(II) complex polyborate compounds. Samples were heated in an alumina (Al₂O₃) crucible at a temperature ramp rate of 10 °C / min between 25-800 °C under a flow air (100 mL / min.). The thermal dissociation stages of compounds **36-43** are described in Table 4.6. The new polyborate compounds **36-39**, **42** and **43** followed the expected multi pathway step for decomposition (for more details see Section 2.3.4), with observed mass loss agreeing with the calculated values. Compounds **40** and **41** showed fewer mass-loss steps (Figure 4.1 and Figure 4.2).

All the dehydration processes are endothermic while the complex cation oxidation processes are exothermic and occur at higher temperatures. All the nickel(II) complex polyborate compounds **36-43** followed the expected path of decomposition to the residual anhydrous metal borates, with observed mass losses agreeing with calculated values. The thermal behaviour of these compounds were in accord with published data describing thermal decomposition of other related transition metal complex polyborates.¹¹³

Table 4.6 TGA data for nickel(II) polyborate compounds **36-43**.*

Comp.	Step No.	The thermal reactions	Temp. Range °C	Expt (%)	Calc. (%)
36	1	[Ni(en) ₃][B ₅ O ₆ (OH) ₄] ₂ ·2H ₂ O → [Ni(en) ₃][B ₅ O ₆ (OH) ₄] ₂ + 2H ₂ O	70-180	4.9	5.1
	2	[Ni(en) ₃][B ₅ O ₆ (OH) ₄] ₂ → [Ni(en) ₃][B ₁₀ O ₁₆] + 4H ₂ O	180-280	15.0	15.2
	3	[Ni(en) ₃][B ₁₀ O ₁₆] + excess O ₂ → NiB ₁₀ O ₁₆ + volatile oxidation products	280-800	38.1	40.6
		Residue NiB ₁₀ O ₁₆		61.9	59.4
37	1	[Ni(en){B ₆ O ₇ (OH) ₆ }(H ₂ O) ₂] ₂ ·H ₂ O → [Ni(en){B ₆ O ₇ (OH) ₆ }] + 3H ₂ O	100-180	10.8	12.0
	2	[Ni(en){B ₆ O ₇ (OH) ₆ }] → [Ni(en)][B ₆ O ₁₀]	180-280	24.3	23.9
	3	[Ni(en)][B ₆ O ₁₀] + excess O ₂ → NiB ₆ O ₁₀ + volatile oxidation products	280-700	38.6	37.2
		Residue NiB ₆ O ₁₀		61.4	62.8
38	1	[Ni(AEN)][B ₅ O ₆ (OH) ₄] ₂ ·H ₂ O → [Ni(AEN)][B ₅ O ₆ (OH) ₄] + H ₂ O	100-180	2.5	3.7
	2	[Ni(AEN)][B ₅ O ₆ (OH) ₄] → [Ni(AEN)][B ₅ O ₈] + 2H ₂ O	180-280	10.0	11.3
	3	[Ni(AEN)][B ₅ O ₈] + excess O ₂ → NiB ₅ O ₈ + volatile oxidation products	280-700	46.1	48.0
		Residue NiB ₅ O ₈		53.9	52.0
39	1	[Ni(dach) ₂ (H ₂ O) ₂][Ni(dach) ₂][B ₇ O ₉ (OH) ₅] ₂ ·4H ₂ O → [Ni(dach) ₂] ₂ [B ₇ O ₉ (OH) ₅] ₂ + 6H ₂ O	100-190	7.5	8.4
	2	[Ni(dach) ₂] ₂ [B ₇ O ₉ (OH) ₅] ₂ + 6H ₂ O → [Ni(dach) ₂] ₂ [B ₁₄ O ₂₃] + 5H ₂ O	190-270	15.0	15.3
	3	[Ni(dach) ₂] ₂ [B ₁₄ O ₂₃] + excess O ₂ → Ni ₂ B ₁₄ O ₂₃ + volatile oxidation products	270-720	48.2	50.7
		Residue Ni ₂ B ₁₄ O ₂₃		51.8	49.3
40	1	[Ni(hn) ₂][B ₅ O ₆ (OH) ₄] ₂ → [Ni(hn) ₂][B ₁₀ O ₁₆] + 4H ₂ O	230-290	10.3	10.2
	2	[Ni(hn) ₂][B ₁₀ O ₁₆] + excess O ₂ → NiB ₁₀ O ₁₆ + volatile oxidation products	290-700	37.9	39.9
		Residue NiB ₁₀ O ₁₆		62.1	60.1
41	1	[Ni(dien) ₂][B ₅ O ₆ (OH) ₄] ₂ → [Ni(dien) ₂][B ₁₀ O ₁₆] + 4H ₂ O	100-200	14.9	10.2
	2	[Ni(dien) ₂][B ₁₀ O ₁₆] + excess O ₂ → NiB ₁₀ O ₁₆ + volatile oxidation products	200-650	40.3	39.7
		Residue NiB ₁₀ O ₁₆		59.7	60.3
42	1	[Ni(pn) ₃][B ₅ O ₆ (OH) ₄] ₂ ·C ₂ H ₅ OH·5H ₂ O → [Ni(pn) ₃][B ₅ O ₆ (OH) ₄] ₂ + 5H ₂ O + C ₂ H ₅ OH	100-160	17.0	16.0

	2	$[\text{Ni}(\text{pn})_3][\text{B}_5\text{O}_6(\text{OH})_4]_2 \rightarrow [\text{Ni}(\text{pn})_3][\text{B}_{10}\text{O}_{16}] + 4\text{H}_2\text{O}$	160-260	23.4	24.3
	3	$[\text{Ni}(\text{pn})_3][\text{B}_{10}\text{O}_{16}] + \text{excess O}_2 \rightarrow \text{NiB}_{10}\text{O}_{16} + \text{volatile oxidation products}$	260-900	48.8	50.5
		Residue $\text{NiB}_{10}\text{O}_{16}$		51.2	49.5
43	1	$[\text{Ni}_2(\text{trien})_3][\text{B}_5\text{O}_6(\text{OH})_4]_2 \cdot \text{Cl}_2 \cdot \text{CH}_3\text{OH} \cdot 6\text{H}_2\text{O} \rightarrow [\text{Ni}_2(\text{trien})_3][\text{B}_5\text{O}_6(\text{OH})_4]_2 \cdot \text{Cl}_2 + \text{CH}_3\text{OH} + 6\text{H}_2\text{O}$	100-160	10.2	11.6
	2	$[\text{Ni}_2(\text{trien})_3][\text{B}_5\text{O}_6(\text{OH})_4]_2 \cdot \text{Cl}_2 \rightarrow [\text{Ni}_2(\text{trien})_3][\text{B}_{10}\text{O}_{16}] \cdot \text{Cl}_2 + 4\text{H}_2\text{O}$	160-240	17.9	17.6
	3	$[\text{Ni}_2(\text{trien})_3][\text{B}_{10}\text{O}_{16}] \cdot \text{Cl}_2 + \text{excess O}_2 \rightarrow \text{Ni}_2\text{B}_{10}\text{O}_{16}\text{Cl}_2 + \text{volatile oxidation products}$	240-700	54.9	54.1
		Residue $\text{Ni}_2\text{B}_{10}\text{O}_{16}\text{Cl}_2$		45.2	46.0

* Calculated values and experimental values are given as totals relative to 100%, and include the process described and earlier mass loss process.

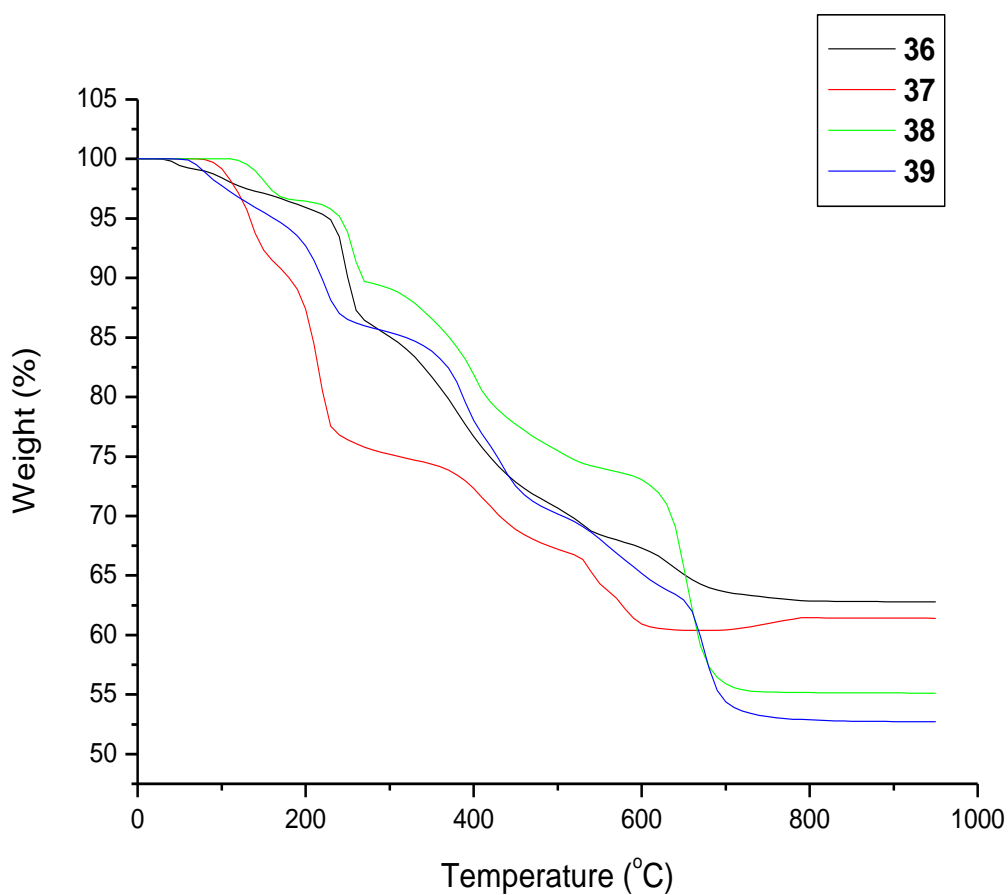


Figure 4.1 TGA diagram for the thermal decomposition of nickel(II) complex polyborate compounds **36-39**.

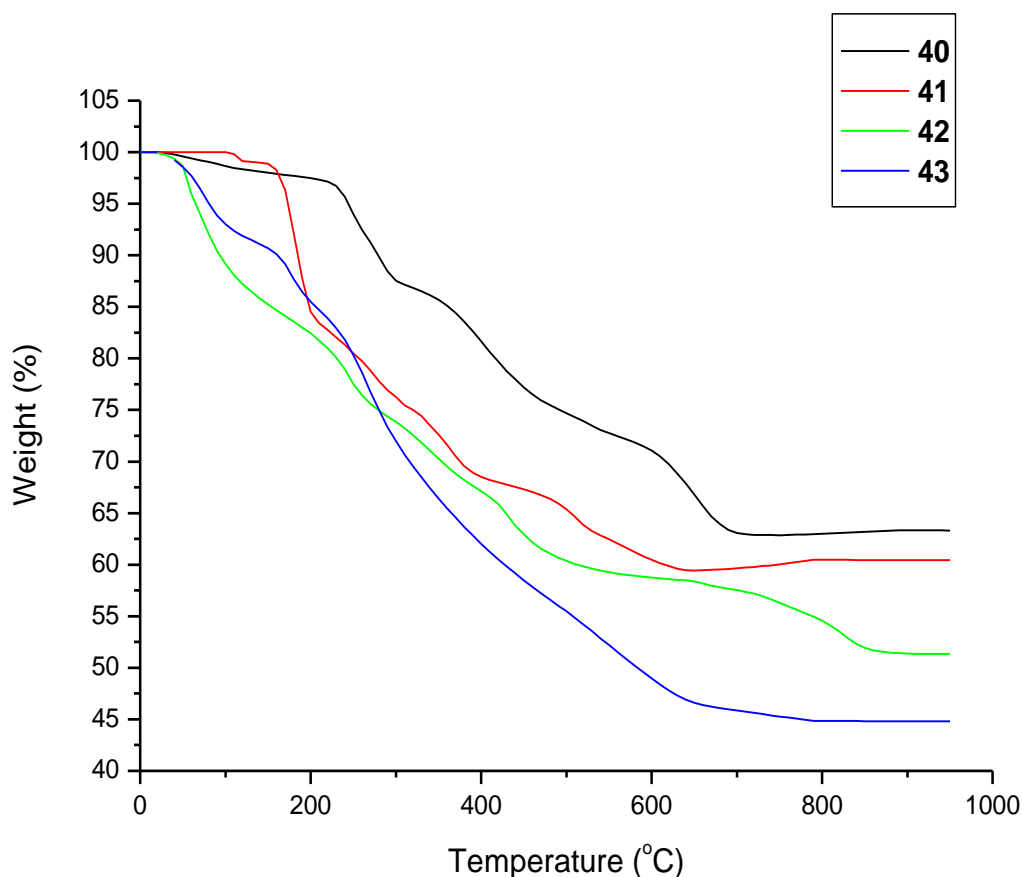


Figure 4.2 TGA diagram for the thermal decomposition of nickel(II) complex polyborate compounds **40-43**.

4.3.5 Structural characterisation of nickel(II) complex polyborate compounds

4.3.5.1 Structural characterisation of $[\text{Ni}(\text{en})\{\text{B}_6\text{O}_7(\text{OH})_6\}(\text{H}_2\text{O})_2]\cdot\text{H}_2\text{O}$ (37**)**

Crystallographic data for **37** are listed in Table 4.7. Crystals of **37** are triclinic, *P*-1 and the compound consists of an uncharged transition metal complex $[\text{Ni}(\text{H}_2\text{O})_2(\text{en})\{\text{B}_6\text{O}_7(\text{OH})_6\}]$ and one interstitial water molecule as shown in Figure 4.3.

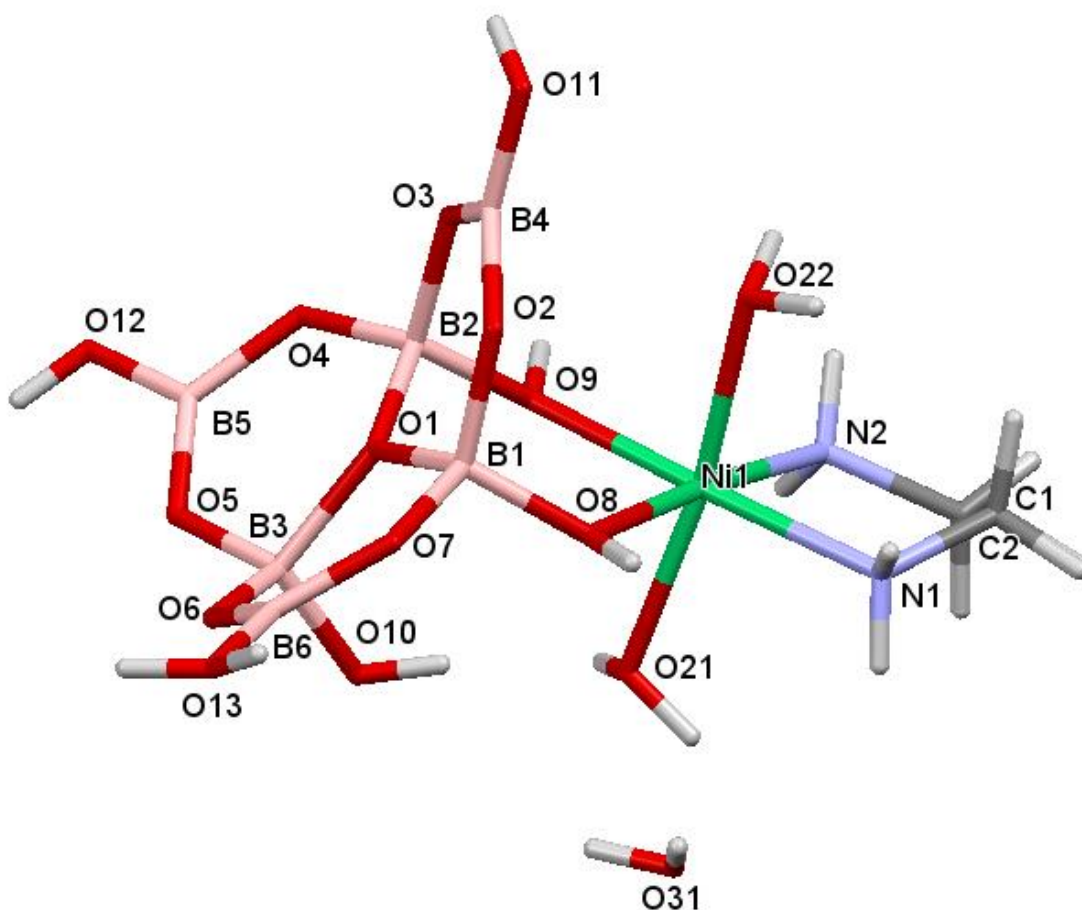


Figure 4.3 Diagram showing the **37** and the adopted numbering scheme. Colour code (used throughout this chapter): green (Ni), blue (N), red (O), pink (B), dark grey (C) and light grey (H).

Table 4.7 Crystal data and structure refinement of **37**.

Empirical formula	$C_2H_{20}B_6N_2O_{16}Ni$	
Formula weight	451.77	
Temperature	100(2) K	
Wavelength	0.71073 Å	
Crystal system	Triclinic	
Space group	$P\bar{1}$	
Unit cell dimensions	$a = 8.5116(7)$ Å	$\alpha = 89.873(5)^\circ$
	$b = 9.7946(5)$ Å	$\beta = 82.902(7)^\circ$
	$c = 9.8073(8)$ Å	$\gamma = 74.372(6)^\circ$
Volume	$780.93(10)$ Å ³	
Z	2	
Density (calculated)	1.921 Mg / m ³	
Absorption coefficient	1.333 mm ⁻¹	
Crystal	light blue, blade	
Crystal size	0.130×0.030×0.015 mm ³	
θ range for data collection	2.094 - 27.572°	
Reflections used	5320	
Independent reflections	5883	
Completeness to $\theta = 25.242^\circ$	99.9%	
Absorption correction	Semi-empirical from equivalents	

Max. and min. transmission	1.000 and 0.886
Refinement method	Full-matrix least-squares on F^2
Data / restraints / parameters	5883 / 289 / 291
Goodness-of-fit on F^2	1.027
Final R indices [$F^2 > 2\sigma(F^2)$]	$RI = 0.0682$, $wR2 = 0.1838$
R indices (all data)	$RI = 0.0745$, $wR2 = 0.1906$
Extinction coefficient	n/a
Largest diff. peak and hole	1.876 and $-0.864 \text{ e } \text{\AA}^{-3}$
Radiation source (wavelength)	Mo-K α

The majority of synthesised and characterised borate salts to date are pentaborates, whereas, fewer hexaborate(2-) anion compounds are known.^{135,153,154,183,184} The hexaborate(2-) anion in **37** acts as a bidentate ligand to the $[\text{Ni}(\text{en})(\text{H}_2\text{O})_2]^{2+}$ centre, *trans* to the bidentate ethylenediamine ligand. The nickel(II) centre has a coordination number of six and a distorted octahedral geometry (Figure 4.3), with the two remaining ligands water molecules mutually *trans*. Compound **37** has Ni-N distances of 2.086(4) Å (N1) and 2.085(4) Å (N2). The square plane Ni-O distances to hexaborate(2-) anion are 2.065(3) Å (O8) and 2.065(3) Å (O9), whilst the Ni-O axial distances to water molecules are 2.096(3) Å (O21) and 2.082(3) Å (O22).

The hexaborate(2-) anion possess three fused six-membered rings with three tetrahedral BO_4 centres and three trigonal BO_3 centres (see Section 3.3.5.3 for more details). The B-O distances to the four-coordinate tetrahedral B1, B2, B3 centres are 1.460(6) - 1.498(6) Å, 1.441(6) - 1.515(6) Å, and 1.439(6) - 1.538(6) Å, respectively, and these are significantly longer than those involving the trigonal B4, B5, B6 centres. The B-O distances to B4, B5, and B6 centres are 1.327(6) - 1.391(7) Å, 1.360(7) - 1.367(7) Å, and 1.365(6) - 1.370(7) Å, respectively. The B-OH bonds involving tetrahedral B1, B2, and B3 centres are 1.468(6), 1.470(6), and 1.455(6) Å, respectively while the B-OH bonds involving trigonal B4, B5, and B6 centres are significantly shorter at 1.327(6), 1.367(7), and 1.370(7) Å, respectively. Bond angles at the tetrahedral centres B1, B2, and B3 range from $108.9(4)^\circ$ - $111.2(4)^\circ$, $106.3(4)^\circ$ - $112.2(4)^\circ$, and $108.1(4)^\circ$ - $111.7(4)^\circ$, respectively while the bond angles at the trigonal B4, B5, and B6 centres are $118.6(4)^\circ$ - $122.1(5)^\circ$, $114.8(5)^\circ$ - $122.9(5)^\circ$, and $117.8(5)^\circ$ - $122.2(5)^\circ$, respectively. The bond lengths and angles are listed in Appendix I (Table 21, and Table 22).

In **37** the hexaborate(2-) anion has six potential H-bond donor sites and thirteen potential H-bond acceptor sites. The hexaborate(2-) anion in **37** has twenty two H-bond interactions (six H-bond donor and sixteen H-bond acceptor), and two coordination bonds to the nickel metal. Surprisingly, the potential acceptor atoms O1 and O5 are not involved in any H-bond interactions.

Table 4.8 H-bonds [\AA and $^\circ$] in **37**.

$D-H\cdots A$	$d(D\cdots A)$	$D-H\cdots A$	$d(D\cdots A)$
O8-H8 \cdots O2 ⁱ	2.786(5)	O22-H22A \cdots O4 ⁱⁱ	2.724(5)
O9-H9 \cdots O3 ⁱⁱ	2.831(5)	O22-H22B \cdots O7 ⁱ	2.744(5)
O10-H10 \cdots O8	3.227(5)	N1-H1AA \cdots O2 ⁱ	3.017(5)
O10-H10 \cdots O21	2.704(5)	N1-H1BC \cdots O7 ⁱ	3.171(5)
O11-H11 \cdots O10 ⁱⁱⁱ	2.805(5)	N1-H1BD \cdots O31B	2.993(12)
O12-H12 \cdots O6 ^{iv}	2.799(6)	N2-H2AA \cdots O10 ^{vii}	3.281(6)
O13-H13A \cdots O12 ^v	2.960(5)	N2-H2AB \cdots O4 ⁱⁱ	3.189(6)
O13-H13 \cdots O13 ^{vi}	2.684(9)	N2-H2BD \cdots O3 ⁱⁱ	2.997(5)
O21-H21A \cdots O31	2.871(9)	O31-H31A \cdots O11 ⁱ	2.715(9)
O21-H21A \cdots O31B	2.841(8)	O31-H31A \cdots O31 ^{viii}	3.01(3)
O21-H21B \cdots O5 ^{vii}	3.087(5)	O31-H31B \cdots O11 ^{ix}	2.993(13)
O21-H21B \cdots O10 ^{vii}	2.807(5)	O31B-H31C \cdots O11 ⁱ	2.812(9)

i = 1-x,1-y,1-z; ii = 1-x,2-y,1-z; iii = 1+x,+y,+z; iv = -x,2-y,2-z; v = +x,-1+y,+z; vi = -x,1-y,2-z; vii = -x,2-y,1-z; viii = -x,1-y,1-z; ix = -1+x,+y,+z

The H-bond interactions in **37** are complicated due to the presence of additional coordinated and uncoordinated water molecules and the NH centres of the ethylenediamine ligand, and H-atom disorders. These interactions may be described as eight reciprocal connections {two $R_2^2(8)$, five $R_2^2(12)$, and one unusual $R_2^2(16)$ }, two C(8) connections, and one D (dimer) interaction. The two reciprocal $R_2^2(8)$ interactions are O8-H8 \cdots O2^{*}/O8^{*}-H8^{*} \cdots O2 and O9-H9 \cdots O3^{*}/O9^{*}-H9^{*} \cdots O3. As an example, one of the two $R_2^2(8)$ interactions is illustrated in Figure 4.4. The five reciprocal $R_2^2(12)$ interactions are N1-H1AA \cdots O2^{*}/N1^{*}-H1AA^{*} \cdots O2, O22-H22B \cdots O7^{*}/O22^{*}-H22B^{*} \cdots O7, O12-H12 \cdots O6^{*}/O12^{*}-H12^{*} \cdots O6, O22-H22A \cdots O4^{*}/O22^{*}-H22A^{*} \cdots O4, and N2-H2BD \cdots O3^{*}/N2^{*}-H2BD^{*} \cdots O3, and the reciprocal $R_2^2(16)$ interaction is O21-H21B \cdots O10^{*}/O21^{*}-H21B^{*} \cdots O10. An example one of the five $R_2^2(12)$ interaction and a $R_2^2(16)$ interaction are shown in Figure 4.5 and 4.6, respectively. The two C(8) connections are O13-H13A \cdots O12^{*} and O11-H11 \cdots O10^{*} (Figure 4.7). The D interaction is O13-H13 \cdots O13^{*} (Figure 4.8).

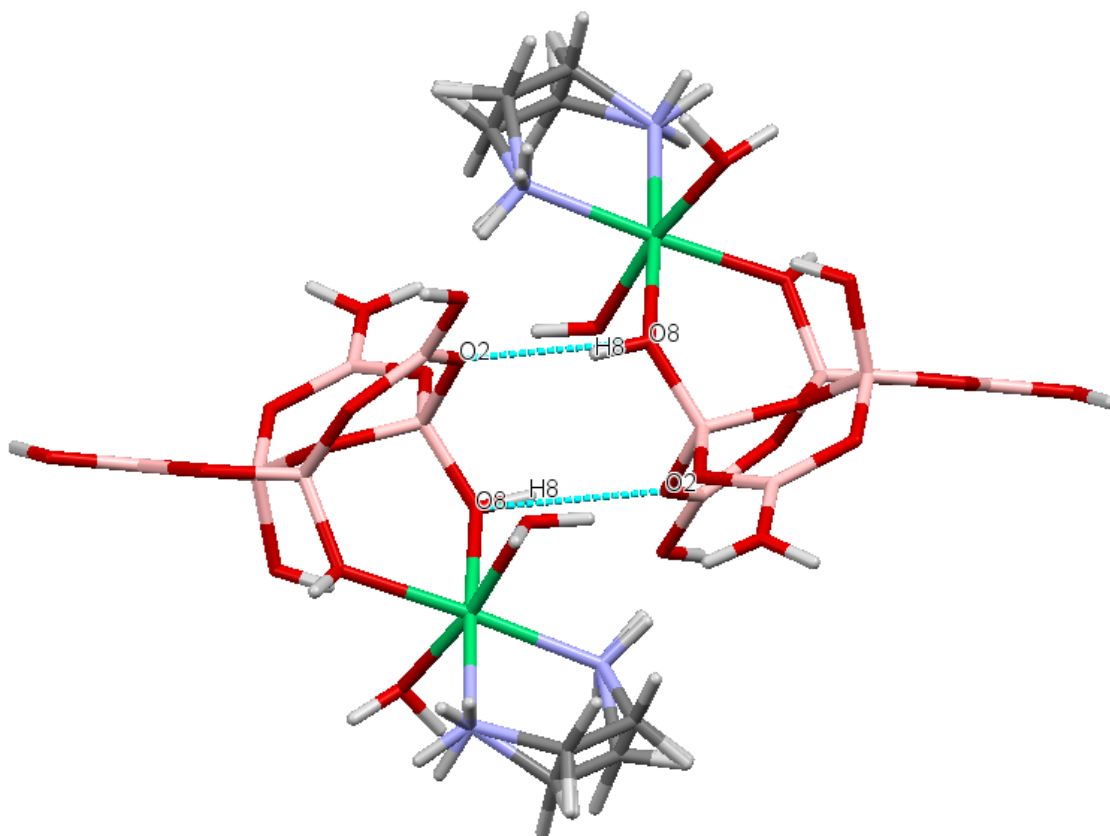


Figure 4.4 One of the two reciprocal $R_2^2(8)$ interactions in **37**. Dashed blue lines represent H-bonds.

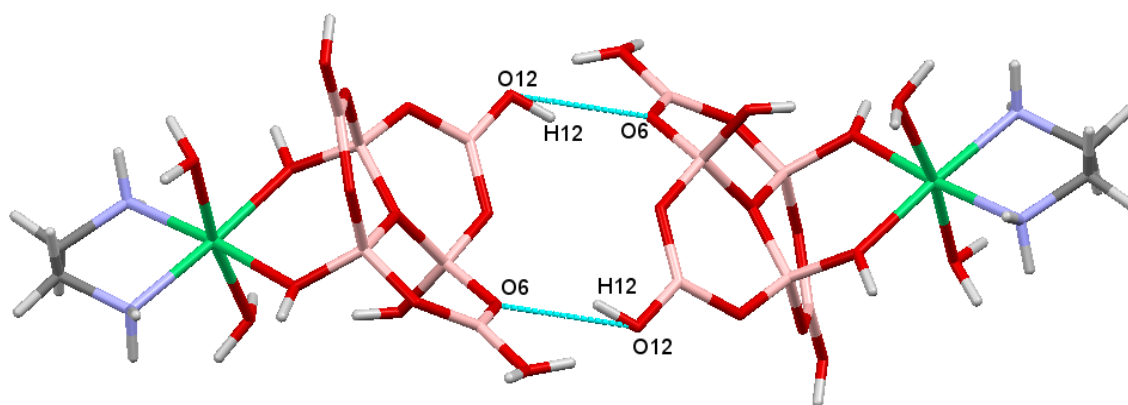


Figure 4.5 One of the five reciprocal $R_2^2(12)$ interactions in **37**.

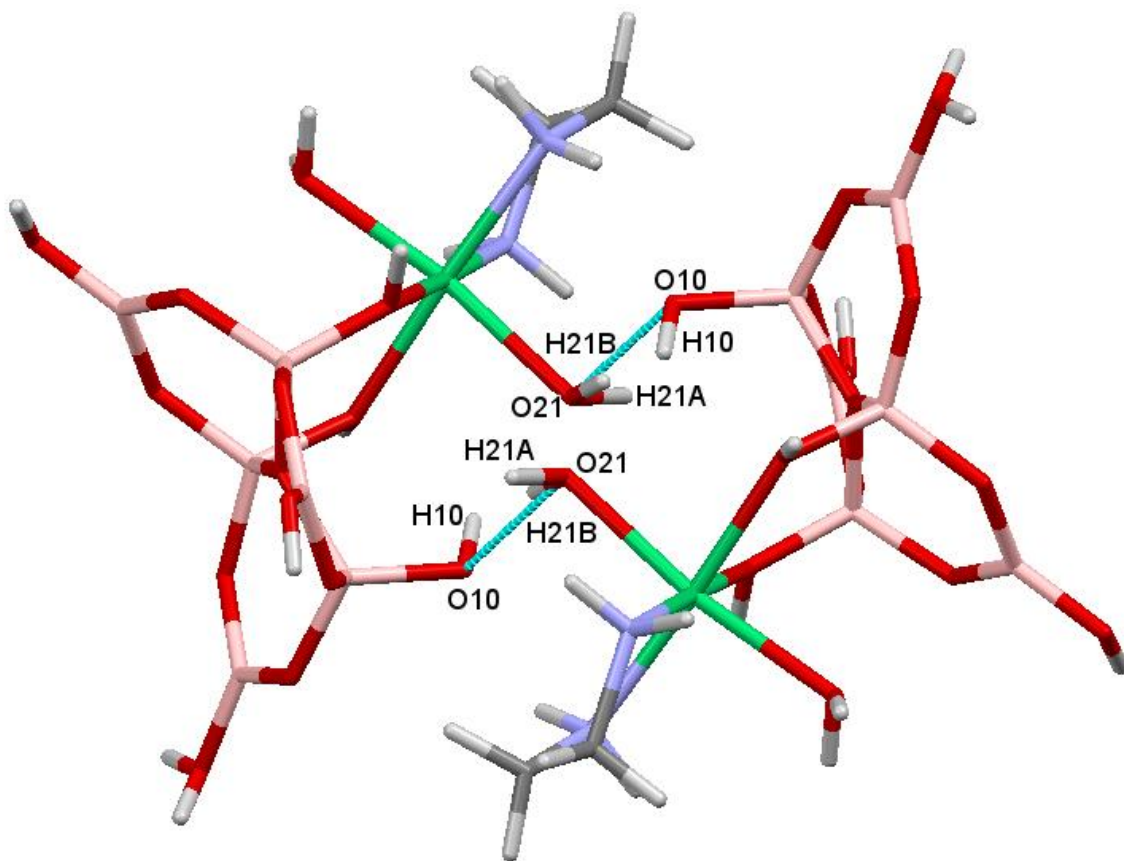


Figure 4.6 The reciprocal $R_2^2(16)$ H-bond interaction in **37**. Dished blue lines represent H-bonds.

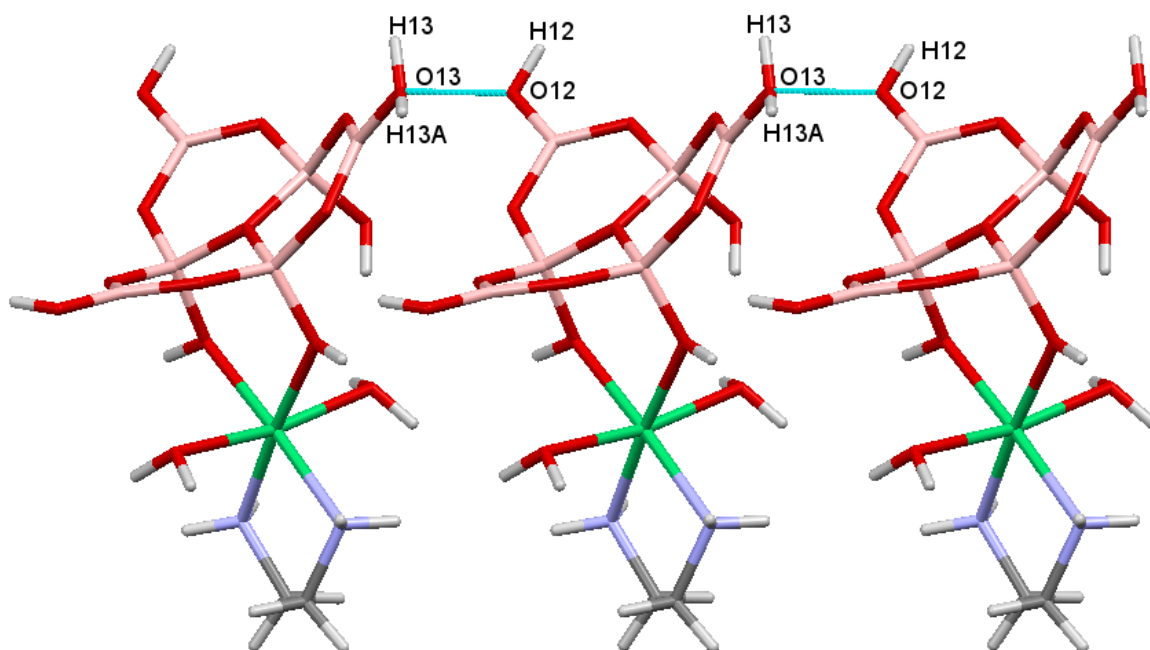


Figure 4.7 One of the two C(8) H-bonds connections in **37**.

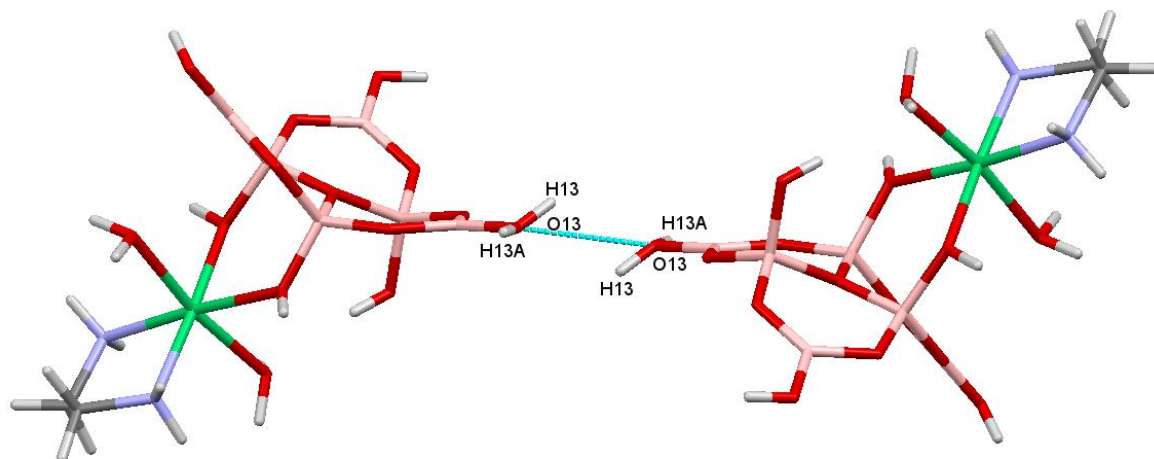


Figure 4.8 The dimer H-bond interaction in **37**.

The $[\text{Ni}(\text{H}_2\text{O})_2(\text{en})\{\text{B}_6\text{O}_7(\text{OH})_6\}]$, and H_2O molecules of **37** are connected through a complex series of H-bond interactions to produce the three-dimension network linking the hexaborates (Figure 4.9). The hexaborate(2-) anion in **37** are linked to three water molecules *via* three H-bond interactions $\text{O}21\text{-H}21\text{A}\cdots\text{O}31\text{B}^*$, $\text{O}31\text{B}\text{-H}31\text{D}\cdots\text{O}11^*$, and $\text{O}31\text{-H}31\text{A}\cdots\text{O}11^*$. Details of the H-bonding interactions are given in Table 4.8.

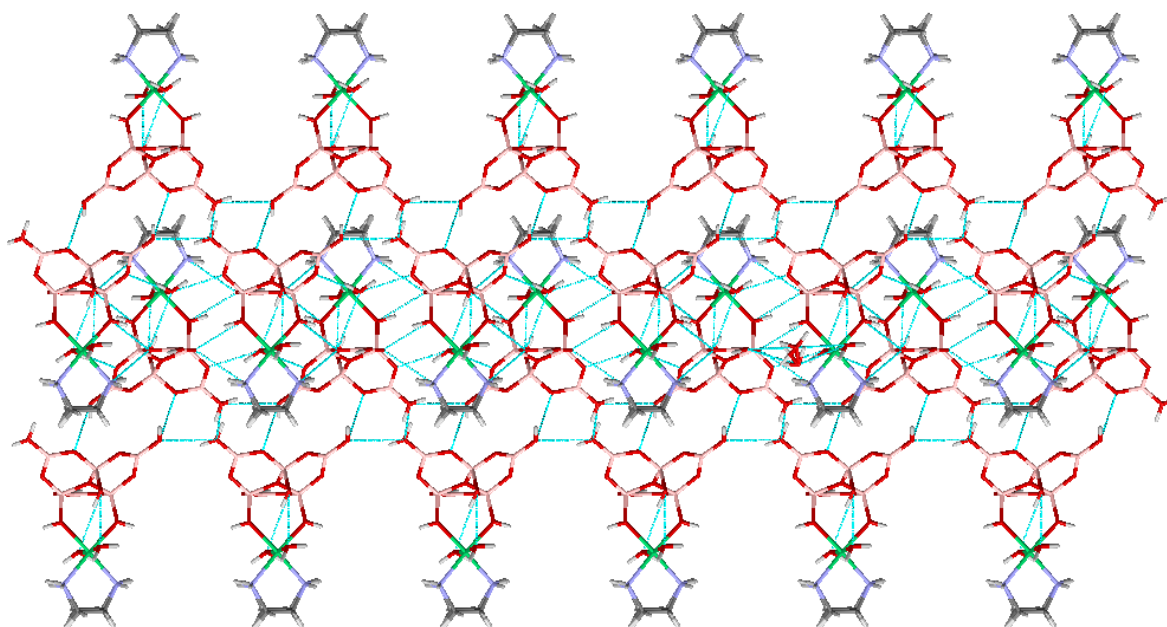


Figure 4.9 Diagram showing a 'plane' of $[\text{Ni}(\text{H}_2\text{O})_2(\text{en})\{\text{B}_6\text{O}_7(\text{OH})_6\}]$ (viewed along the a direction of the unit cell) and water molecule in **37**.

4.3.5.2 Structural characterisation of $[\text{Ni}(\text{EAN})][\text{B}_5\text{O}_6(\text{OH})_4]\cdot\text{H}_2\text{O}$ (**38**)

Crystallographic data of **38** are given in Table 4.9. The crystals of **38** are triclinic, $P\bar{1}$ and compound **38** is an ionic compound with one transition metal complex cation $[\text{Ni}(\text{EAN})]^+$ partnered with one $[\text{B}_5\text{O}_6(\text{OH})_4]^-$ anions and one water molecule as shown in Figure 4.10. The $[\text{Ni}(\text{EAN})]^+$ cation in **38** has Ni-N distances ranging from 1.8504(14) - 1.9284(16) Å. The Ni(II) complex cation in **38** is best considered as a 4-coordinate distorted square-planar geometry.

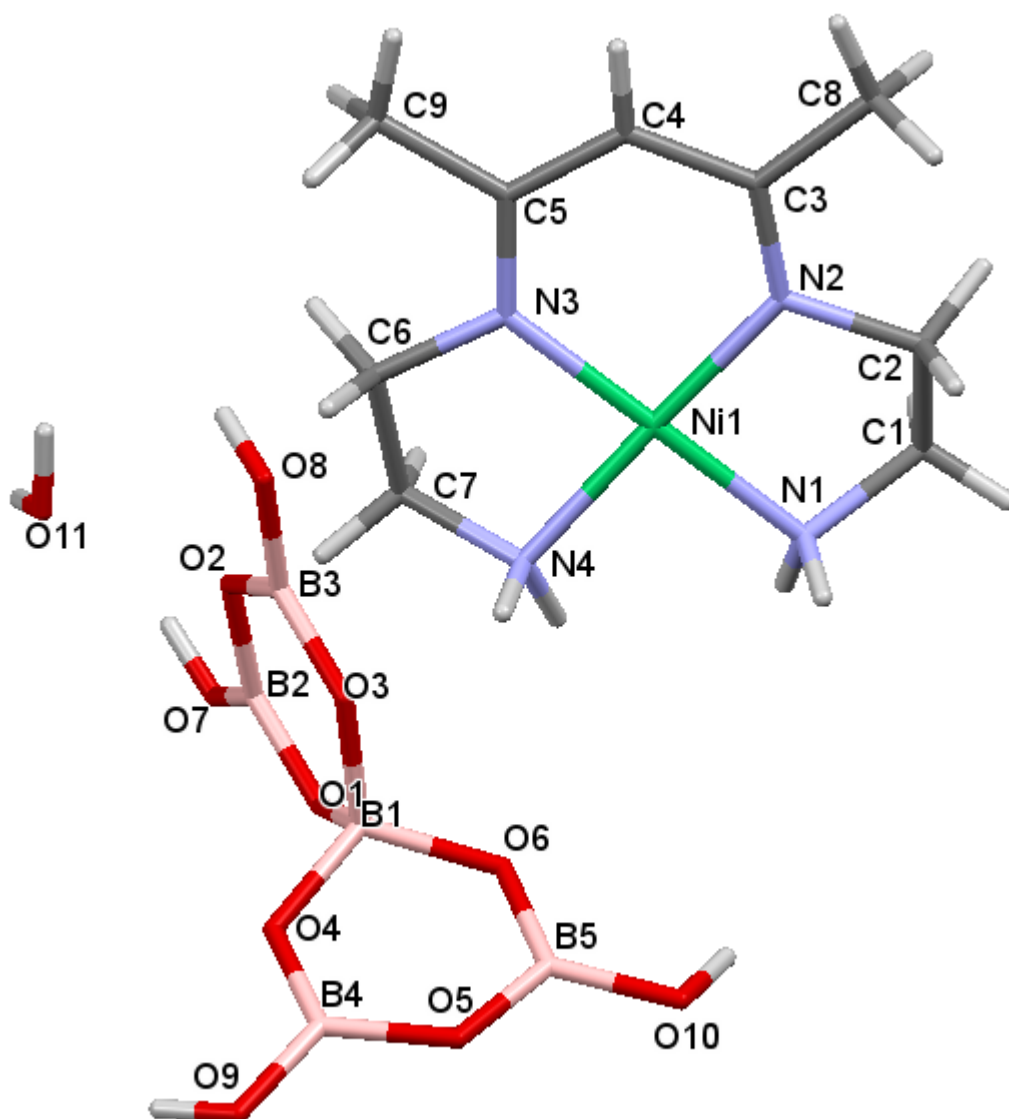


Figure 4.10 Diagram showing the complex cation, pentaborate anion and water molecule in **38** and the adopted numbering scheme.

Table 4.9 Crystal data and structure refinement of **38**.

Empirical formula	C ₉ H ₂₅ B ₅ N ₄ O ₁₁ Ni
Formula weight	478.09
Temperature	100(2) K
Wavelength	0.71073 Å
Crystal system	Triclinic
Space group	<i>P</i> -1
Unit cell dimensions	<i>a</i> = 8.5589(3) Å <i>α</i> = 115.895(3)°
	<i>b</i> = 11.3670(4) Å <i>β</i> = 101.639(3)°
	<i>c</i> = 11.9017(4) Å <i>γ</i> = 99.641(3)°
Volume	976.36(6) Å ³
<i>Z</i>	2
Density (calculated)	1.626 Mg / m ³
Absorption coefficient	1.057 mm ⁻¹
<i>F</i> (000)	496
Crystal	Block; Pink
Crystal size	0.050 × 0.040 × 0.040 mm ³
<i>θ</i> range for data collection	2.539 – 27.485°
Index ranges	-11 ≤ <i>h</i> ≤ 11, -14 ≤ <i>k</i> ≤ 11, -15 ≤ <i>l</i> ≤ 15
Reflections collected	16234
Independent reflections	4479 [<i>R</i> _{int} = 0.0256]
Completeness to <i>θ</i> = 25.242°	99.9%
Absorption correction	Semi-empirical from equivalents
Max. and min. transmission	1.000 and 0.797
Refinement method	Full-matrix least-squares on <i>F</i> ²
Data / restraints / parameters	4479 / 0 / 280
Goodness-of-fit on <i>F</i> ²	1.056
Final <i>R</i> indices [<i>F</i> ² > 2σ(<i>F</i> ²)]	<i>R</i> 1 = 0.0291, <i>wR</i> 2 = 0.0768
<i>R</i> indices (all data)	<i>R</i> 1 = 0.0329, <i>wR</i> 2 = 0.0788
Extinction coefficient	n/a
Largest diff. peak and hole	1.876 and -0.864 e Å ⁻³
Radiation source (wavelength)	Mo-Kα

The pentaborate anion is structurally similar to other pentaborate systems involving isolated [B₅O₆(OH)₄]⁻ anions.^{136,181} The B-O distances to the 4-coordinate tetrahedral B1 centre are 1.4595(18) - 1.4782(18) Å and they are significantly longer than those involving the trigonal boron centres which range from 1.3429(19) - 1.4049(19) Å. B-O bonds involving trigonal boron atoms and terminal OH groups are at the shorter end of this range [av. 1.356 Å] whilst B-O bonds involving trigonal boron atoms and distal (O2, O5) to the 4-coordinate B1 centre are at the longer end of this range [av. 1.3919 Å]. Bond angles at the B1 centre range from 108.42(12)° - 110.63(12)°, and angles at the other ring atoms range from 116.75(13)° - 122.77(14)° for boron centres consistent with sp³ and sp² hybridisation, respectively. The bond lengths and bond angles of **38** are listed in Appendix I (Table **23** and **24**).

In **38** the four H-bond donor sites of pentaborate(1-) anion are involved with H-bonds to α oxygen acceptor sites of two pentaborate anions (O9-H9⋯O4*, and O10-H10⋯O6*), a γ

oxygen acceptor site of a pentaborate(1-) anion (O8-H8...O2*), and one water molecule (O7-H7...O11*), so this molecule displays $\alpha\alpha\gamma\omega$ interactions.^{77,98} The direction of four donor sites in pentaborate anion are two 'in' and two 'out' (Figure 4.10). All the H-bonds data are given in Table 4.10.

Table 4.10 H-bonds [\AA and $^\circ$] of **38**.

<i>D-H...A</i>	<i>d(D...A)</i>	<i>D-H...A</i>	<i>d(D...A)</i>
N1-H1C...O5 ⁱ	2.9648(17)	O9-H9...O4 ^{iv}	2.7016(15)
N1-H1D...O1 ⁱⁱ	3.3848(18)	O10-H10...O6 ⁱ	2.7642(15)
N4-H4A...O1 ⁱⁱ	2.9598(17)	O11-H11A...O3 ^v	2.7460(15)
O7-H7...O11	2.6613(17)	O11-H11B...O8 ⁱⁱⁱ	2.7889(16)
O8-H8...O2 ⁱⁱⁱ	2.7994(15)		

(i) -x+2,-y+1,-z+1 (ii) -x+1,-y+1,-z+1 (iii) -x+1,-y+1,-z (iv) -x+2,-y+2,-z+1 (v) x-1,y,z

A view of part of the layered structure of $[\text{B}_5\text{O}_6(\text{OH})_4]^-$ anions in **38** is shown in Figure 4.11 illustrating a ribbon structure between adjacent pentaborate(1-) anions where each $[\text{B}_5\text{O}_6(\text{OH})_4]^-$ anion is connected *via* two reciprocal $R_2^2(8)$ connections. Each $R_2^2(8)$ connection is formed between neighbouring pentaborate(1-) anions as follows: O9-H9A...O4*/O9*-H9A*...O4 and O10*-H10*...O6/O10-H10...O6*. The other boroxyl (B_3O_3) rings of the pentaborate(1-) anion ribbon are linked to a further pentaborate(1-) anion, cross links the ribbons by a third reciprocal $R_2^2(8)$ interaction. This $R_2^2(8)$ connection is O8-H8...O2*/O8*-H8*...O2. The fourth donor hydroxyl group of each $[\text{B}_5\text{O}_6(\text{OH})_4]^-$ anion acts to crosslinks the planes *via* a $\beta \rightarrow \omega$ interaction with a water molecule O7-H7...O11*.

As shown in Figure 4.12 the supramolecular layered structure of **38** the water molecules and the $[\text{Ni}(\text{EAN})]^+$ cations connect pentaborate(1-) anion ribbons by complex series of H-bond interactions. This cation is involved in H-bonding to water molecules. The $[\text{Ni}(\text{EAN})]^+$ cation acts as H-bond donors to two pentaborate(1-) anions *via* three H-bond interactions N4-H4A...O1*, N1-H1C...O5*, and N1-H1D...O1*. All H-bonds data for **38** are listed in Table 4.10.

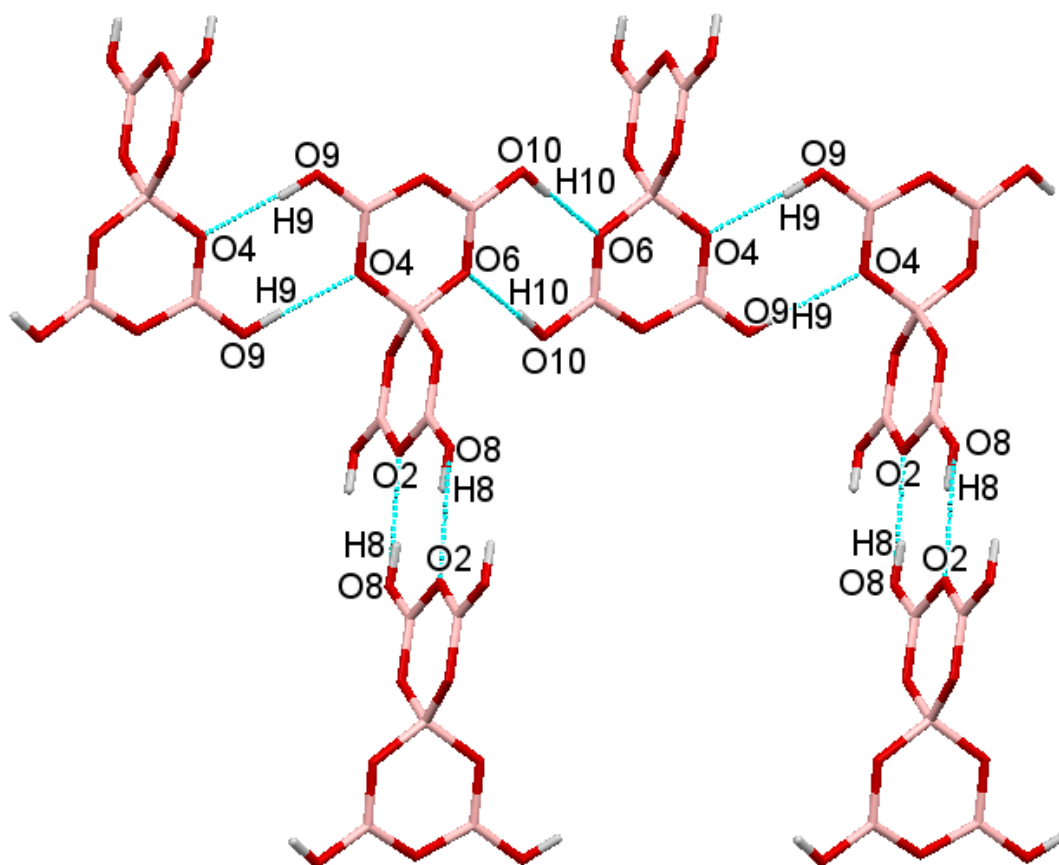


Figure 4.11 The three $R_2^2(8)$ H-bond motif connections in **38**. Dashed blue lines represent H-bonds.

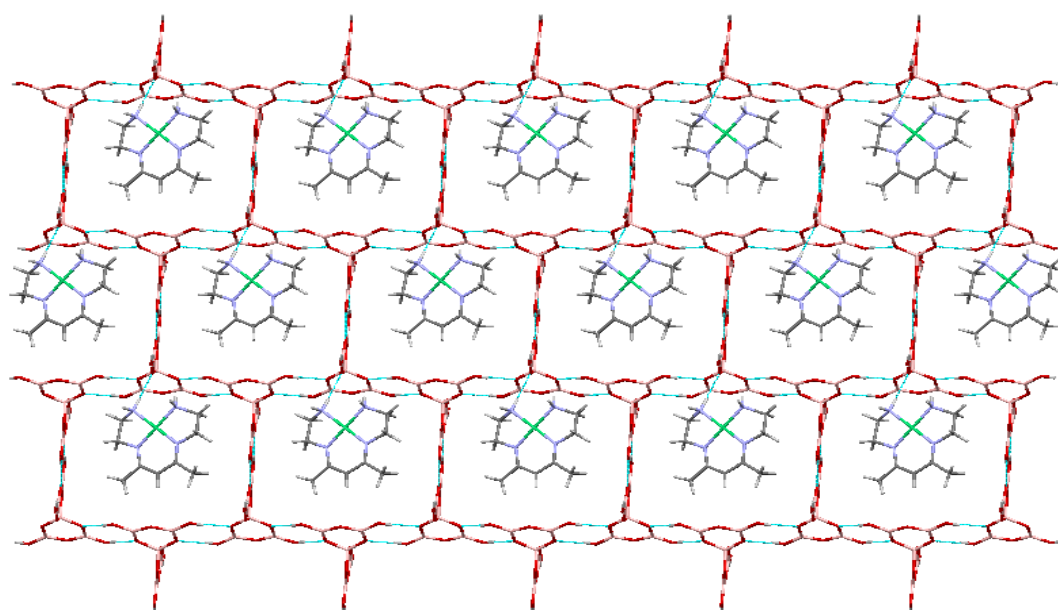


Figure 4.12 Diagram showing a 'plane' of polyborate anions (viewed along the a direction of the unit cell) and water molecule with $[\text{Ni}(\text{EAN})]^+$ cations in **38**.

4.3.5.3 Structural characterisation of $[\text{Ni}(\text{dach})_2(\text{H}_2\text{O})_2][\text{Ni}(\text{dach})_2][\text{B}_7\text{O}_9(\text{OH})_5]_2 \cdot 4\text{H}_2\text{O}$ (**39**)

Crystallographic data of **39** are listed in Table 4.11. The crystals of **39** are monoclinic, $C2/c$. The structure of **39** contains two different nickel(II) complex cations: $[\text{Ni}(\text{dach})_2]^{2+}$ and $[\text{Ni}(\text{dach})_2(\text{H}_2\text{O})_2]^{2+}$. Both of these cations contain one (1*S*,2*S*)-1,2-diaminocyclohexane (dach) and one (1*R*,2*R*)-1,2-diaminocyclohexane ligand in a distorted square-planar arrangement. One cation contains two mutually *trans* H_2O molecules yielding a 6-coordinate metal cation. Compound **39** has Ni-N distances of 2.113(9) Å (N1), 2.108(8) Å (N2), 2.036(15) Å (N1B), and 2.015(14) Å (N2B) [av. 2.068 Å], which are the same for both cations. The Ni-O axial distances are 2.1352(15) Å and 2.1353(15) Å [av. 2.1353 Å]. Each cation is partnered by a crystallographically identical $[\text{B}_7\text{O}_9(\text{OH})_5]^{2-}$ anion and an additional water of crystallization. The anions and cations in **39** are shown in Figure 4.13.

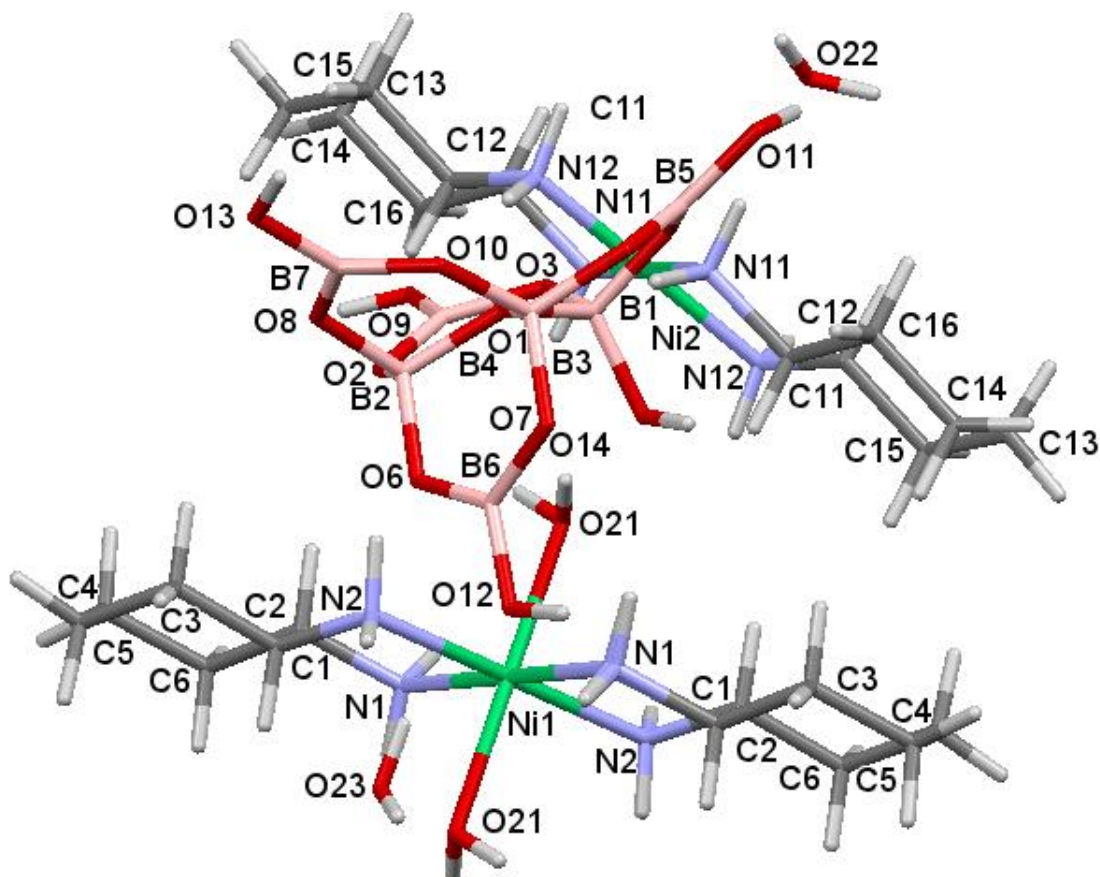


Figure 4.13 Diagram showing the complex cation, heptaborate(2-) anion and water molecule in **39** and the adopted numbering scheme.

Table 4.11 Crystal data and structure refinement of **39**.

Empirical formula	C ₂₄ H ₇₈ B ₁₄ N ₈ O ₃₄ Ni ₂	
Formula weight	1291.70	
Temperature	100(2) K	
Wavelength	0.71073 Å	
Crystal system	Monoclinic	
Space group	C2/c	
Unit cell dimensions	$a = 22.2909(7)$ Å	$\alpha = 90^\circ$
	$b = 10.9861(3)$ Å	$\beta = 107.744(3)^\circ$
	$c = 22.8446(7)$ Å	$\gamma = 90^\circ$
Volume	5328.3(3) Å ³	
Z	4	
Density (calculated)	1.610 Mg / m ³	
Absorption coefficient	0.812 mm ⁻¹	
$F(000)$	2704	
Crystal	Prism; Orange	
Crystal size	0.150 × 0.150 × 0.090 mm ³	
θ range for data collection	2.165 – 27.483°	
Index ranges	-27 ≤ h ≤ 28, -14 ≤ k ≤ 14, -29 ≤ l ≤ 29	
Reflections collected	33681	
Independent reflections	6102 [$R_{int} = 0.0275$]	
Completeness to $\theta = 25.242^\circ$	99.9%	
Absorption correction	Semi-empirical from equivalents	
Max. and min. transmission	1.000 and 0.921	
Refinement method	Full-matrix least-squares on F^2	
Data / restraints / parameters	6102 / 1165 / 525	
Goodness-of-fit on F^2	1.049	
Final R indices [$F^2 > 2\sigma(F^2)$]	$RI = 0.0391$, $wR2 = 0.1084$	
R indices (all data)	$RI = 0.0415$, $wR2 = 0.1099$	
Extinction coefficient	n/a	
Largest diff. peak and hole	0.851 and -0.727 e Å ⁻³	
Radiation source (wavelength)	Mo-K α	

Special details: Both the 1,2-diaminocyclohexane ligands were modelled as disordered over two positions and as a result various geometrical (SAME, SADI) and displacement (RIGU, SIMU) restraints were required.

The heptaborate(2-) anion contains four fused six-membered rings containing three tetrahedral boron centres and four trigonal boron centres (for more details see Section 3.3.5.4). The structure of the heptaborate(2-) anions in **39** is essentially the same as those reported for [H₃N(CH₂)₇NH₃][B₇O₉(OH)₅·H₂O],⁹⁷ [cyclo-C₆H₁₁NH₃]₂[B₇O₉(OH)₅·3H₂O·B(OH)₃], and [cyclo-C₇H₁₃NH₃]₂[B₇O₉(OH)₅·2H₂O·2B(OH)₃].⁷⁷ The B–O distances around the three-coordinate boron centres range from 1.356(2) – 1.374(2) Å [av. 1.366 Å], and B–O distances around the four-coordinate boron centres range from 1.435(2) – 1.512(2) Å [av. 1.468 Å]. The O–B–O angles for the three-coordinate boron centres range from 114.6(17) – 123.61(17)° [av. 119.99°] and O–B–O angles at the four-coordinate boron centres range from 106.06(14) – 112.17(15)° [av. 109.45°]. The ring B–O–B angles range from 110.72(13) – 123.15(15)° [av.

119.77°] indicating sp^2 hybridised oxygen atoms. The central three-coordinate oxygen centres is pyramidal (349.68° angle sum) and 0.283 Å out of the B1B2B3 plane, with B-O bond lengths, [av. 1.509 Å]. This distance is longer than typically expected for oxygen atoms bound to four-coordinate boron centres (~1.48 Å).⁷⁷ The three-coordinate oxygen centre, O1, are *trans-oid* relative to the OH group of B1. The bond lengths and angles are listed in Appendix I (Table 25 and Table 26).

In **39** the heptaborate(2-) anion has an opportunity to form many H-bond interactions. It has 5 potential H-bond donor sites and 14 potential H-bond acceptor sites. The labelling scheme of heptaborate(2-) anion is illustrated in Section 3.3.5.4. The BBFFG hydroxyl group donor sites of heptaborate(2-) anion form H-bond donor interactions to four different heptaborate(2-) anions. Whilst the G site is not involved in any donor H-bond interactions. These four interactions are O10-H10...O8*, O12-H12F...O9*, O13-H13...O7*, and O11-H11F...O5* (Figure 4.14). All the H-bonds data in **39** are listed in Table 4.12.

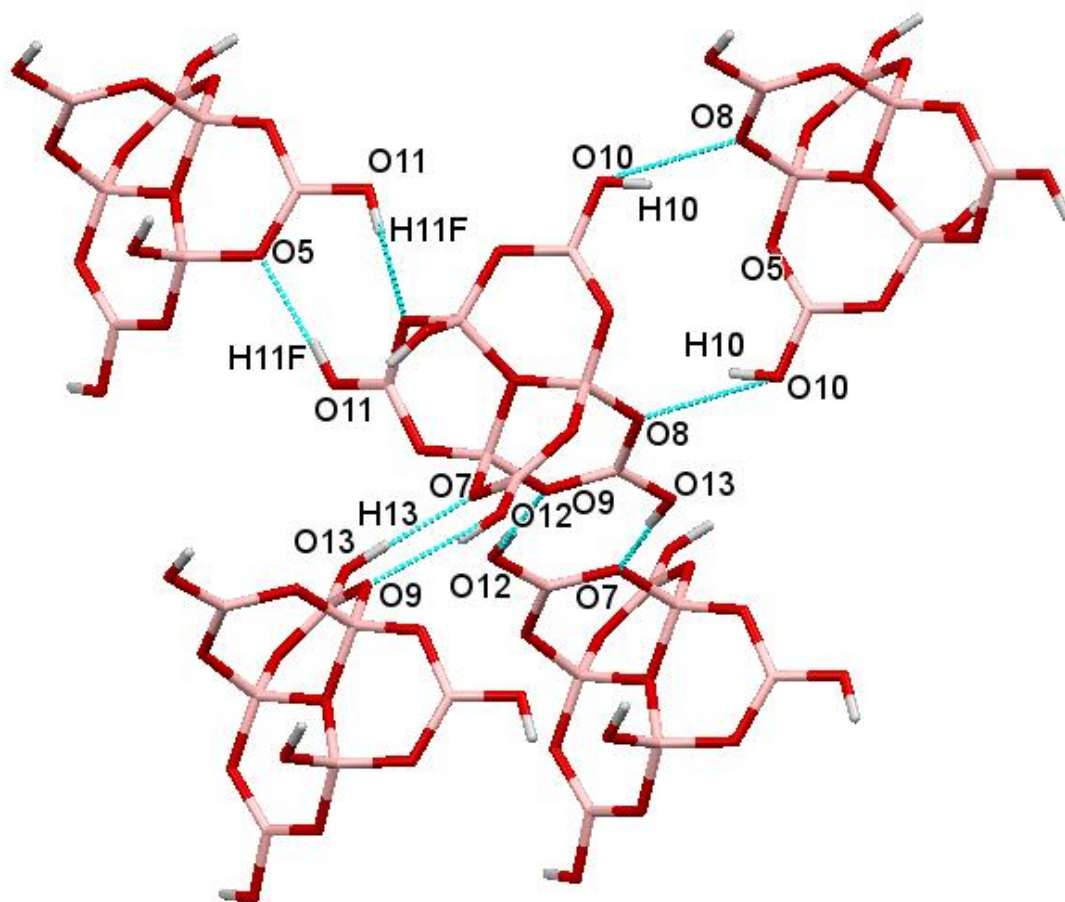


Figure 4.14 The four H-bond donor interactions of each heptaborate(2-) anion in **39**.

Table 4.12 H-bond interactions [\AA and $^\circ$] in **39**.

<i>D-H...A</i>	<i>d(D...A)</i>	<i>D-H...A</i>	<i>d(D...A)</i>
O21-H21A...O22 ⁱⁱⁱ	2.693(2)	N12-H12B...O23 ^v	3.10(2)
O21-H21B...O3 ⁱ	3.203(2)	N11B-H11C...O3 ⁱⁱ	2.98(2)
O21-H21B...O14 ⁱ	2.974(2)	N11B-H11D...O11 ^{iv}	3.08(2)
N1-H1A...O22 ⁱⁱ	3.251(18)	N12B-H12C...O10	2.99(2)
N1-H1B...O14 ⁱ	3.182(17)	N12B-H12D...O23 ^v	2.85(3)
N2-H2B...O2	3.098(13)	O10-H10...O8 ^{vi}	2.6854(19)
N2-H2B...O6	2.935(8)	O11-H11F...O5 ^{vii}	2.7034(19)
N1B-H1BA...O22 ⁱⁱ	3.25(3)	O12-H12F...O9 ^{viii}	2.7629(19)
N1B-H1BB...O14 ⁱ	3.19(3)	O13-H13...O7 ^{ix}	2.6831(18)
N2B-H2BB...O2	3.269(19)	O22-H22A...O23 ^v	2.829
N2B-H2BB...O6	2.976(13)	O22-H22B...O13 ^x	2.801(2)
N11-H11A...O3 ⁱⁱⁱ	2.970(8)	O23-H23A...O12	2.7857(19)
N11-H11B...O11 ^{iv}	2.992(8)	O23-H23B...O11 ^{viii}	2.806(2)
N12-H12A...O10	2.811(9)		

(i) $-x+3/2, -y+1/2, -z+1$ (ii) $-x+1, -y+1, -z+1$ (iii) $x+1/2, y-1/2, z$ (iv) $x, -y+1, z+1/2$ (v)
 $x-1/2, y+1/2, z$ (vi) $-x+3/2, -y+3/2, -z+1$ (vii) $-x+1, y, -z+1/2$ (viii) $-x+3/2, y-1/2, -z+1/2$ (xi)
 $-x+3/2, y+1/2, -z+1/2$ (x) $x-1/2, y-1/2, z$

Detailed inspection of Figure 4.15 shows that each $[\text{B}_7\text{O}_9(\text{OH})_5]^{2-}$ anion is connected by two $\text{R}_2^2(8)$ and one reciprocal $\text{R}_2^2(12)$ interaction. The two $\text{R}_2^2(8)$ connections are $\text{O11-H11F}\cdots\text{O5}^*/\text{O11}^*-\text{H11F}^*\cdots\text{O5}$ and $\text{O12-H12F}\cdots\text{O9}^*/\text{O13}^*-\text{H13}^*\cdots\text{O7}^*$, while the reciprocal $\text{R}_2^2(12)$ connection is $\text{O10-H10}\cdots\text{O8}^*/\text{O10}^*-\text{H10}^*\cdots\text{O8}$. All the H-bonds data in **39** are listed in Table 4.12.

A three-dimensional network is formed by connecting the plane shown in Figure 4.16 (part of which is shown in Figure 4.15) to the neighbouring planes by further H-bond interactions. The $[\text{Ni}(\text{dach})_2(\text{H}_2\text{O})_2]^{2+}$ and $[\text{Ni}(\text{dach})_2]^{2+}$ cations act as H-bond donors to two $[\text{B}_7\text{O}_9(\text{OH})_5]^{2-}$ anions and two water molecules. The connection of $[\text{Ni}(\text{dach})_2(\text{H}_2\text{O})_2]^{2+}$ and $[\text{Ni}(\text{dach})_2]^{2+}$ cations to the $[\text{B}_7\text{O}_9(\text{OH})_5]^{2-}$ anions occur by seven H-bond interactions $\text{N1-H1B}\cdots\text{O14}^*$, $\text{N2-H2B}\cdots\text{O2}^*$, $\text{N2B-H2BB}\cdots\text{O6}^*$, $\text{N11-H11A}\cdots\text{O3}^*$, $\text{N12-H12A}\cdots\text{O10}^*$, $\text{O21-H21B}\cdots\text{O14}^*$, and $\text{N11-H11D}\cdots\text{O11}^*$. The connection of the cations to the interstitial water molecules occur by three H-bond interactions: $\text{N12-H12D}\cdots\text{O23}^*$, $\text{N1B-H1BA}\cdots\text{O22}^*$, and $\text{O21-H21A}\cdots\text{O22}^*$. Details of the H-bonding interactions are given in Table 4.12.

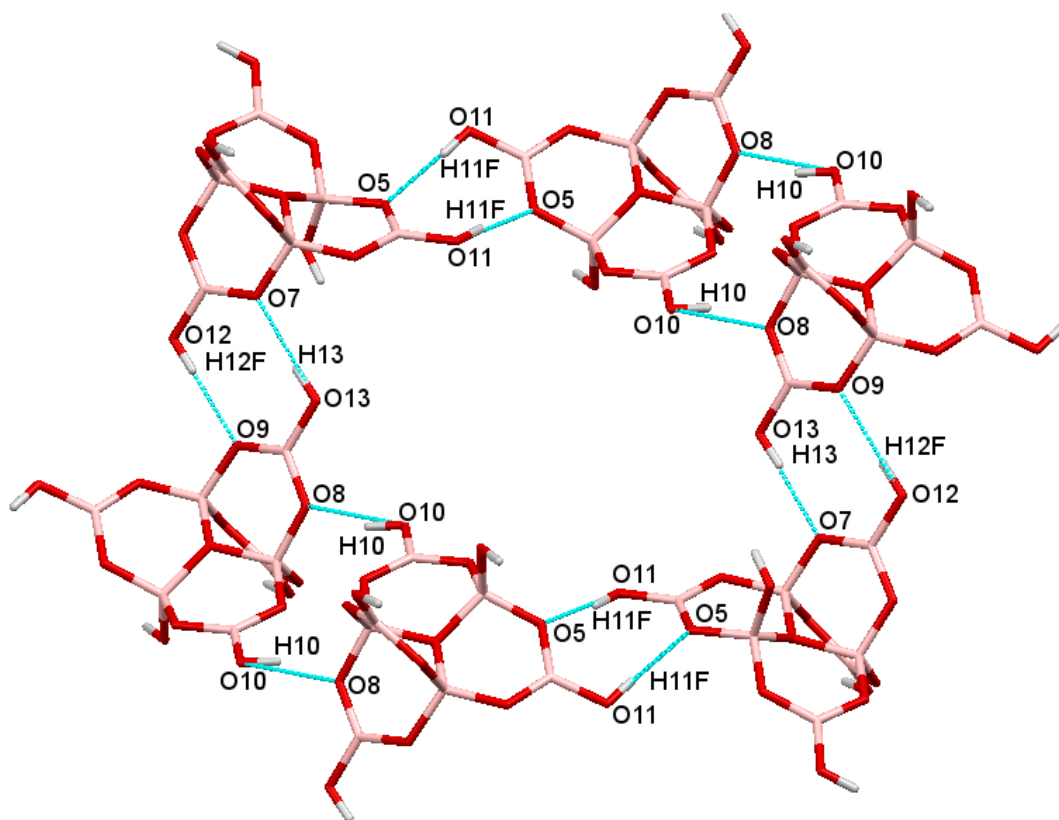


Figure 4.15 The $R_2^2(8)$ and $R_2^2(12)$ connections between heptaborate anions.

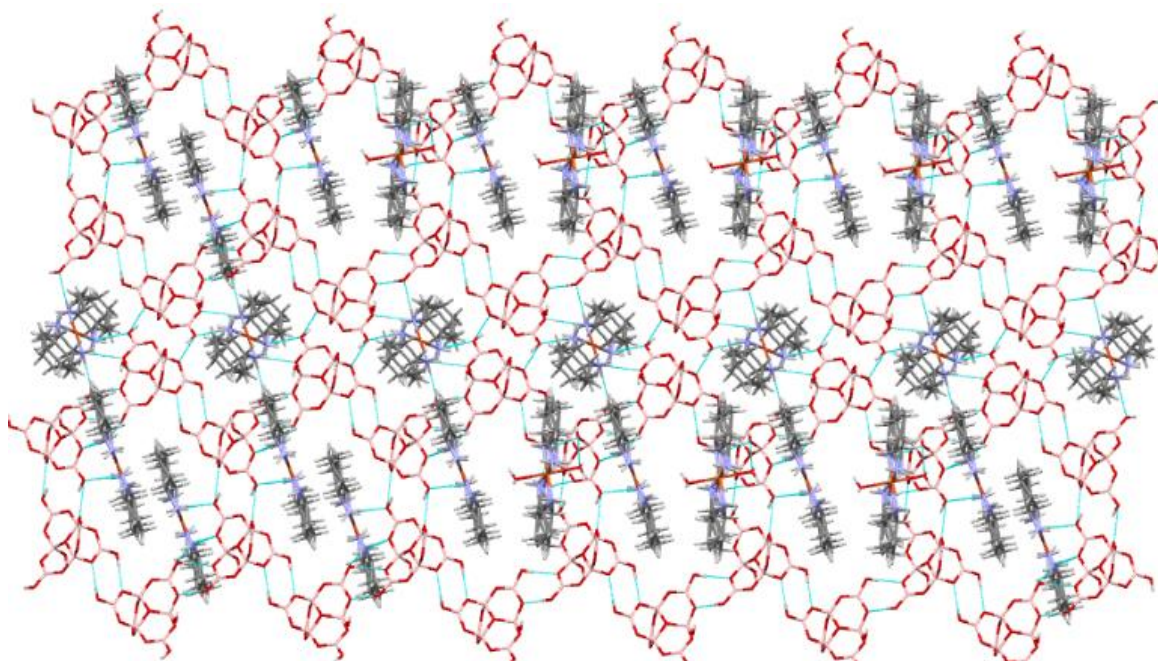


Figure 4.16 A plane of heptaborate anions and $[\text{Ni}(\text{dach})_2(\text{H}_2\text{O})_2]^{2+}$ and $[\text{Ni}(\text{dach})_2]^{2+}$ cations in plane H-bond interactions in **39**.

4.3.5.4 Structural characterisation of $[\text{Ni}(\text{hn})_2][\text{B}_5\text{O}_6(\text{OH})_4]_2$ (**40**)

Crystallographic data of **40** are listed in Table 4.13. The crystals of **40** are monoclinic, $P2_1/c$ and it is an ionic compound with one transition metal complex cation $[\text{Ni}(\text{hn})_2]^{+2}$ partnered with two crystallographically identical $[\text{B}_5\text{O}_6(\text{OH})_4]^-$ anions as shown in Figure 4.17. The $[\text{Ni}(\text{hn})_2]^{+2}$ in **40** has Ni-N distances ranging from 2.064(15) - 2.140(6) Å [av. 2.94 Å], whilst the Ni-O distances are 2.087(7) Å (O11) and 2.072(8) Å (O11B) [av. 2.080 Å]. The nickel(II) centre in **40** has a coordination number of six with a distorted octahedral geometry.

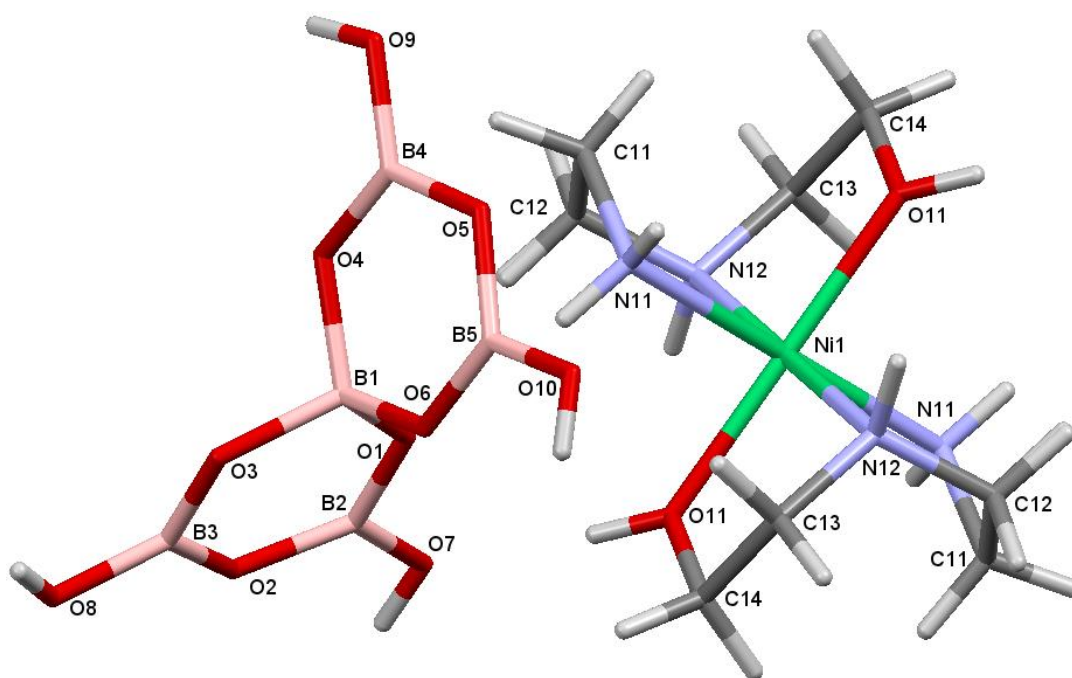


Figure 4.17 Diagram showing the complex cation and pentaborate(1-) anion in **40** and the adopted numbering scheme.

Table 4.13 Crystal data and structure refinement of **40**.

Empirical formula	$\text{C}_8\text{H}_{32}\text{B}_{10}\text{N}_4\text{O}_{22}\text{Ni}$	
Formula weight	703.18	
Temperature	100(2) K	
Wavelength	0.71073 Å	
Crystal system	Monoclinic	
Space group	$P2_1/c$	
Unit cell dimensions	$a = 8.3887(3)$ Å	$\alpha = 90^\circ$
	$b = 11.6644(4)$ Å	$\beta = 90.046(3)^\circ$
	$c = 14.3061(5)$ Å	$\gamma = 90^\circ$
Volume	$1399.84(8)$ Å ³	
Z	2	

Density (calculated)	1.668 Mg / m ³
Absorption coefficient	0.792 mm ⁻¹
<i>F</i> (000)	724
Crystal	Rod; Lilac
Crystal size	0.340 × 0.050 × 0.040 mm ³
θ range for data collection	2.848 – 27.499°
Index ranges	-10 ≤ <i>h</i> ≤ 10, -15 ≤ <i>k</i> ≤ 15, -18 ≤ <i>l</i> ≤ 18
Reflections collected	6244
Independent reflections	6244 [<i>R</i> _{int} = ?]
Completeness to $\theta = 25.242^\circ$	99.9%
Absorption correction	Semi-empirical from equivalents
Max. and min. transmission	1.000 and 0.798
Refinement method	Full-matrix least-squares on <i>F</i> ²
Data / restraints / parameters	6244 / 14 / 223
Goodness-of-fit on <i>F</i> ²	1.044
Final <i>R</i> indices [<i>F</i> ² > 2 σ (<i>F</i> ²)]	<i>R</i> 1 = 0.0444, <i>wR</i> 2 = 0.1113
<i>R</i> indices (all data)	<i>R</i> 1 = 0.0518, <i>wR</i> 2 = 0.1154
Extinction coefficient	n/a
Largest diff. peak and hole	1.018 and -0.468 e Å ⁻³
Radiation source (wavelength)	Mo-K α

Special details: This structure was refined as a two-component twin (Component two was rotated by -179.9835 ° around [-0.45 -0.00 0.89] (reciprocal) or [-0.83 -0.00 0.56] (direct) axis). The N-(2-hydroxyethyl)ethylenediamine ligand was successfully modelled as disordered over positions and as such various geometrical (SADI, DFIX, DANG) and displacement (EADP) restraints were applied.

The two pentaborate anions are structurally similar and are not notably different from other transition metal complex cation pentaborate anion structure systems involving isolated [B₅O₆(OH)₄]⁻ anions.^{136,181} The B-O distances to the four-coordinate tetrahedral B1 centres range from 1.462(3) - 1.476(3) Å [av. 1.47 Å] and these are significantly longer than those involving the trigonal boron centres which range from 1.348(3) - 1.389(3) Å [av. 1.365 Å]. B-O bonds involving trigonal boron atoms and terminal OH groups are at the shorter end of this range [av. 1.358(3) Å] whilst B-O bonds involving trigonal boron atoms and distal (O2, O5) to the 4-coordinate B1 centre are at the longer end of this range [av. 1.380 (3) Å]. Bond angles at the B1 range from 108.04(19)° - 111.66(18)°, and angles at the other ring atoms range from 116.1(2)° - 122.8(2)°. The bond lengths and bond angles of **40** are listed in Appendix I (Tables 27 and Table 28).

In **40** the four H-bond donor sites of pentaborate(1-) anion are involved with H-bonds to α oxygen acceptor sites of three different pentaborate(1-) anions (O8-H8...O3*, O9-H9...O6* and O10-H10...O4*) and an H-bond to a β oxygen acceptor site of the fourth pentaborate(1-) anion (O7-H7...O8*), so this molecule displays $\alpha\alpha\alpha\beta$ interactions to neighbouring pentaborate(1-) anions.^{77,98} The direction of four H-bond donor sites of pentaborate(1-) anion

in **40** are three 'in' and one 'out' (Figure 4.17). All the H-bond interactions data of **40** are listed in Table 4.14.

Table 4.14 H-bonds [\AA and $^\circ$] in **40**

$D-H\cdots A$	$d(D\cdots A)$	$D-H\cdots A$	$d(D\cdots A)$
O7–H7...O8 ⁱⁱ	2.804(2)	O11–H11...O7	2.767(8)
O8–H8...O3 ⁱⁱⁱ	2.678(2)	N11B–H11E...O7	2.867(15)
O9–H9...O6 ^{iv}	2.738(2)	N11B–H11F...O5 ^{vii}	2.977(12)
O10–H10...O4 ^v	2.725(2)	N11B–H11F...O10 ^{vii}	2.999(11)
N12–H12...O9 ^{vi}	2.974(3)	O11B–H11G...O5 ^{vii}	3.119(8)
N11–H11D...O1 ⁱ	2.976(7)	O11B–H11G...O10 ^{vii}	3.217(8)

(i) $-x,-y+1,-z+1$ (ii) $-x,-y+1,-z$ (iii) $-x+1,-y+1,-z$ (iv) $-x+1,y-1/2,-z+1/2$ (v) $-x+1,y+1/2,-z+1/2$ (vi) $-x+1,-y+1,-z+1$ (vii) $x-1,y,z$

Detailed inspection of Figure 4.18 shows that the $[\text{B}_5\text{O}_6(\text{OH})_4]^-$ ions are connected by two $R_2^2(8)$ interactions O9–H9...O6*/O10*–H10*...O4 and O9*–H9*...O6/O10–H10...O4* forming a chain. The pentaborate(1-) anion chains are linked to other pentaborate(1-) anion chains by two reciprocal H-bond interactions forming a three-dimensional network. The first reciprocal interaction is $R_2^2(8)$ O8–H8...O3*/O8*–H8*...O3. The second reciprocal interaction is $R_2^2(12)$ O7–H7...O8*/O7*–H7*...O8.

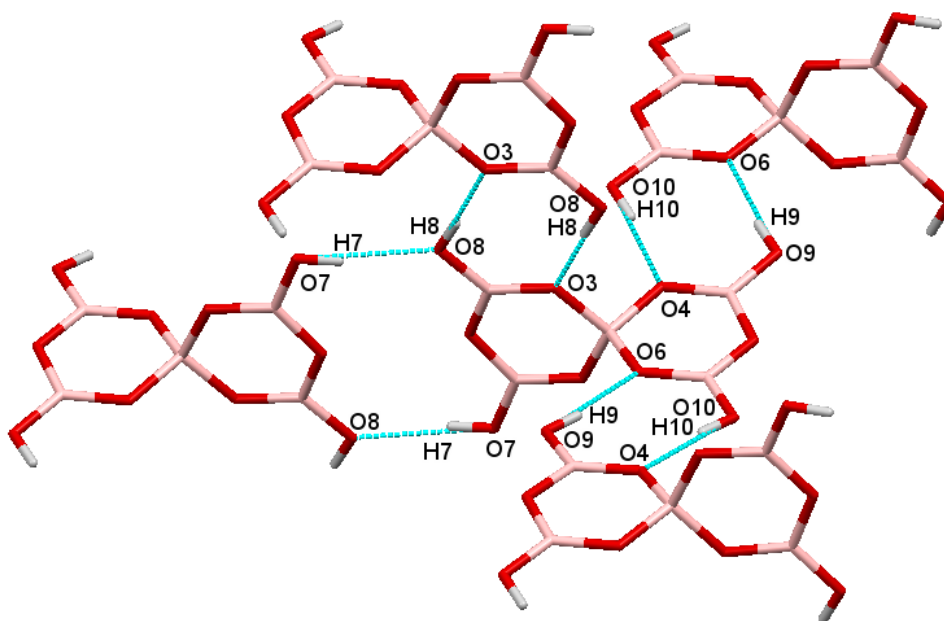


Figure 4.18 The $R_2^2(8)$ and $R_2^2(12)$ connections between two layers of pentaborate(1-) ion in **40**.

Two structural motifs that commonly occur in pentaborate giant structures containing the $\alpha\alpha\beta$ acceptor sites are called herringbone (HB) and brickwall (BW). However these motifs involve a C(8) chain β -interaction and structure **40** has a reciprocal-pair $R_2^2(12)$ β -interaction (Figure 4.19), and so it is neither of these structures. This motif is not as common as the other two but has been previously observed in a few examples [MeHN(CH₂CH₂)₂NMe][B₅O₆(OH)₄], [Me₂N(CH₂CH₂)₂NMe₂][B₅O₆(OH)₄]₂, 2-Et-4-MeC₃N₂H₃, and 2-ⁱPrC₃N₂H₄.^{170,192}

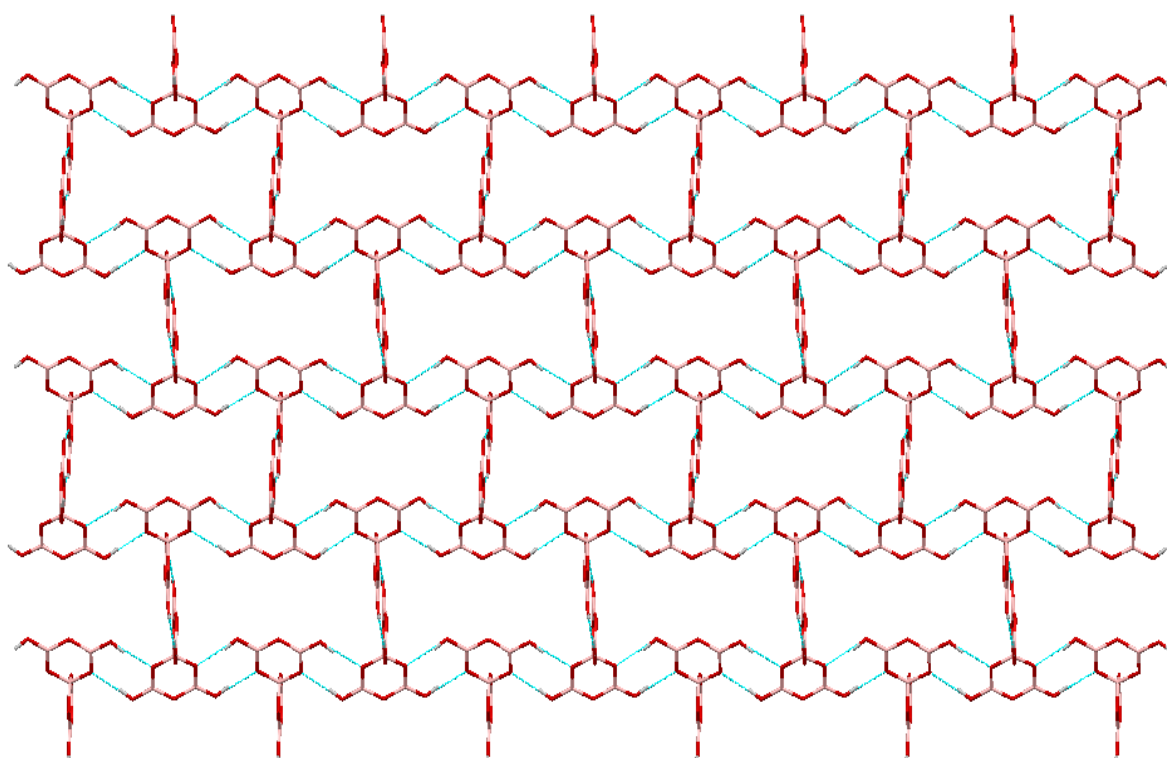


Figure 4.19 H-bonded [B₅O₆(OH)₄]⁻ network for **40** view perpendicular to the large channels (viewed along the *a* direction of the unit cell).

The solid-state structures of all transition metal complex polyborate compounds involve H-bonded supramolecular polyborate anion networks, with cavities and channels, which occlude the transition metal complex cations. The [Ni(hn)₂]²⁺ cations and [B₅O₆(OH)₄]⁻ anions of crystallisation of **40** are connected through a complex series of H-bond interactions (Figure 4.20), with the anion network templated by the cations.

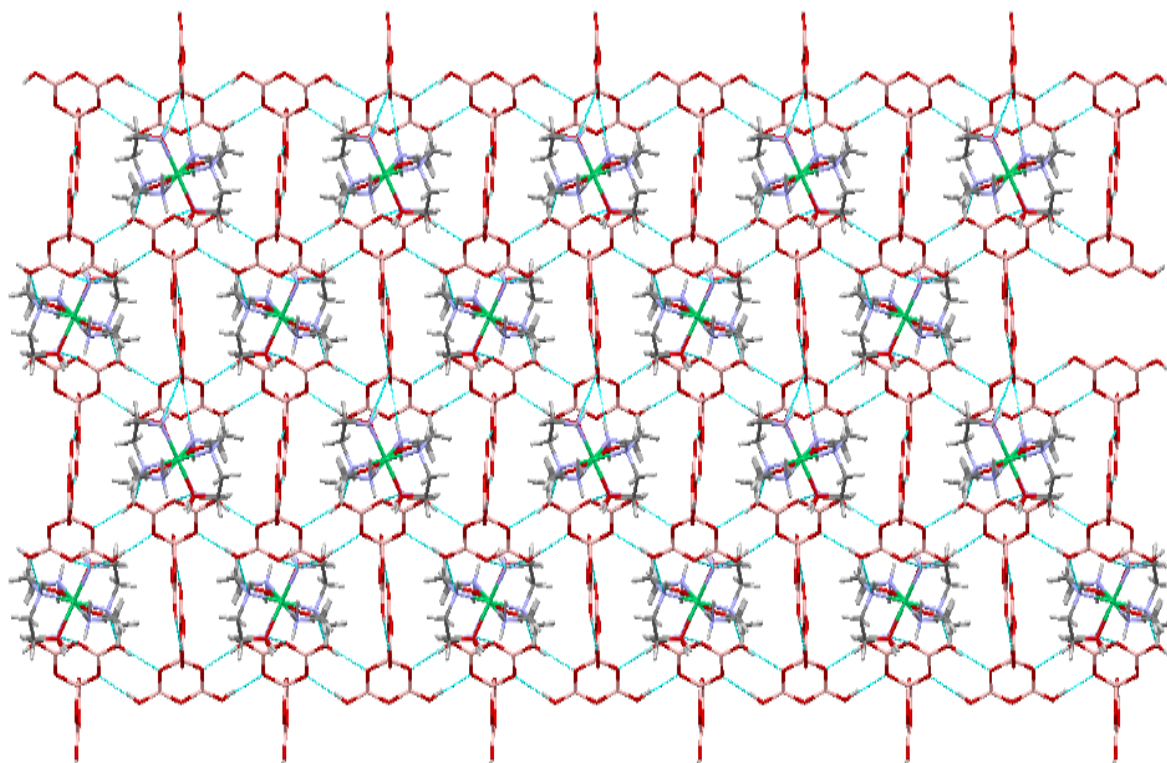


Figure 4.20 A plane of pentaborate(1-) anions and $[\text{Ni}(\text{hn})_2]^{2+}$ cations in plane of H-bond interactions in **40** (viewed along the a direction of the unit cell).

The $[\text{Ni}(\text{hn})_2]^{2+}$ cation acts as H-bond donors to four pentaborate(1-) anions *via* eight H-bond interactions N11-H11D \cdots O1*, O11-H11 \cdots O7*, N11B-H11E \cdots O7*, N12-H12 \cdots O9*, O11B-H11G \cdots O5*, N11B-H11B \cdots O5*, O11B-H11G \cdots O10*, and N11B-H11F \cdots O10*. Details of the H-bonding interactions are given in Table 4.14.

4.3.5.5 Structural characterisation of *s-fac*-[Ni(dien)₂][B₅O₆(OH)₄]₂ (41)

Crystallographic data of **41** are listed in Table 4.15. Crystals of **41** are triclinic, $P-1$ and compound **41** is an ionic compound with one transition metal complex cation $[\text{Ni}(\text{dien})_2]^{+2}$ partnered with two crystallographically identical $[\text{B}_5\text{O}_6(\text{OH})_4]^-$ anions as shown in Figure 4.21. The $[\text{Ni}(\text{dien})_2]^{+2}$ in **41** has Ni-N distances ranging from 2.095(8) - 2.161(8) Å [av. 2.142 Å]. The nickel(II) centre in **41** has a coordination number of six with a distorted octahedral geometry.

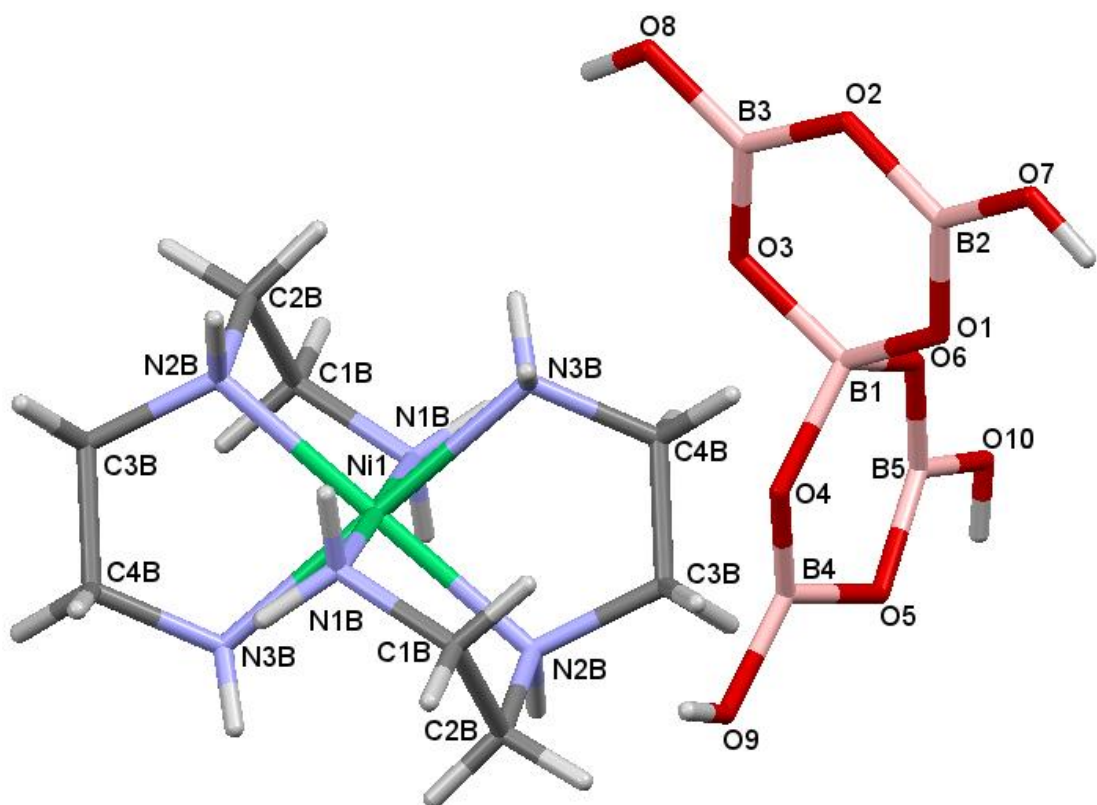


Figure 4.21 Diagram showing the complex cation and pentaborate(1-) anion in **41** and the adopted numbering scheme.

Table 4.15 Crystal data and structure refinement of **41**.

Empirical formula	C ₈ H ₃₄ B ₁₀ N ₆ O ₂₀ Ni	
Formula weight	701.22	
Temperature	100(2) K	
Wavelength	0.6889 Å	
Crystal system	Triclinic	
Space group	<i>P</i> -1	
Unit cell dimensions	<i>a</i> = 8.5579(11) Å	α = 78.099(10)°
	<i>b</i> = 9.2772(11) Å	β = 89.109(10)°
	<i>c</i> = 9.3422(10) Å	γ = 89.054(10)°
Volume	725.61(15) Å ³	
<i>Z</i>	1	
Density (calculated)	1.605 Mg / m ³	
Absorption coefficient	0.702 mm ⁻¹	
Crystal	Blade; orange	
Crystal size	0.020×0.020×0.010 mm ³	
θ range for data collection	2.160 - 26.572°	
Reflections collected	6369	
Independent reflections	3184 [<i>R</i> _{int} = 0.0479]	
Completeness to $\theta = 25.242^\circ$	99.9%	
Absorption correction	Semi-empirical from equivalents	
Max. and min. transmission	1.000 and 0.703	
Refinement method	Full-matrix least-squares on <i>F</i> ²	
Data / restraints / parameters	3184 / 278 / 282	

Goodness-of-fit on F^2	1.070
Final R indices [$F^2 > 2\sigma(F^2)$]	$RI = 0.0794$, $wR2 = 0.2215$
R indices (all data)	$RI = 0.0907$, $wR2 = 0.2358$
Extinction coefficient	n/a
Largest diff. peak and hole	1.188 and $-1.069 \text{ e } \text{\AA}^{-3}$
Radiation source (wavelength)	Mo-K α

The two pentaborate anions are structurally similar to other transition metal complex cation pentaborate anion structure systems involving isolated $[\text{B}_5\text{O}_6(\text{OH})_4]^-$ anions.^{136,181} The B-O distances to the 4-coordinate tetrahedral B1 centres range from 1.361(7) - 1.484(7) Å and these are significantly longer than those involving the trigonal boron centres which range from 1.343(5) - 1.407(16) Å. B-O bonds involving trigonal boron atoms and terminal OH groups are at the shorter end of this range [av. 1.365 Å] whilst B-O bonds involving trigonal boron atoms and distal (O2, O5) to the 4-coordinate B1 centre are at the longer end of this range [av. 1.39 Å]. Bond angles at the B1 range from $107.8(4)^\circ$ - $111.6(3)^\circ$, and angles at the other ring atoms range from $114.9(6)^\circ$ - $123.0(5)^\circ$. The bond lengths and bond angles of **41** are listed in Appendix I (Tables 29 and Table 30).

In **41** the four H-bond donor sites of pentaborate(1-) anion are involved with H-bonds to α oxygen acceptor sites of three different pentaborate(1-) anions (O8-H8 \cdots O3^{*}, O9-H9 \cdots O4^{*} and O7-H7 \cdots O1^{*}) and an H-bond to β oxygen acceptor site of the fourth pentaborate(1-) anion (O10-H10 \cdots O9^{*}).^{77,98} This compound displays $\alpha\alpha\alpha\beta$ interactions to neighbouring four different pentaborate(1-) anions (Figure 4.22). The hydrogen bonding motif is identical to that observed for compound **40**. The direction of four H-bond donor sites of pentaborate(1-) anion in **41** are three 'in' and one 'out' (Figure 4.21). All the H-bond interactions data of **41** are listed in Table 4.16.

Table 4.16 H-bonds [\AA and $^\circ$] in **41**.

$D\text{-H}\cdots A$	$d(D\cdots A)$	$D\text{-H}\cdots A$	$d(D\cdots A)$
O7-H7 \cdots O1 ⁱ	2.737(6)	N3A-H3AB \cdots O6 ^{vii}	3.280(9)
O8-H8 \cdots O3 ⁱⁱ	2.718(5)	N1B-H1BA \cdots O2 ⁱⁱ	3.360(12)
O9-H9 \cdots O4 ⁱⁱⁱ	2.683(3)	N1B-H1BB \cdots O6 ^v	3.300(11)
O10-H10 \cdots O9 ^{iv}	2.820(4)	N2B-H2B \cdots O7 ^{vi}	2.886(11)
N1A-H1AA \cdots O10 ^v	2.970(8)	N3B-H3BA \cdots O10 ^{vii}	2.926(11)
N1A-H1AB \cdots O7 ^{vi}	3.198(10)	N3B-H3BB \cdots O8 ⁱⁱ	3.209(11)
N2A-H2A \cdots O8 ⁱⁱ	2.910(9)		

i = -x,-y,2-z; ii = -x,1-y,1-z; iii = -x,-y,1-z; iv = 1-x,-y,1-z; v = +x,+y,-1+z; vi = 1+x,+y,-1+z; vii = 1-x,1-y,1-z

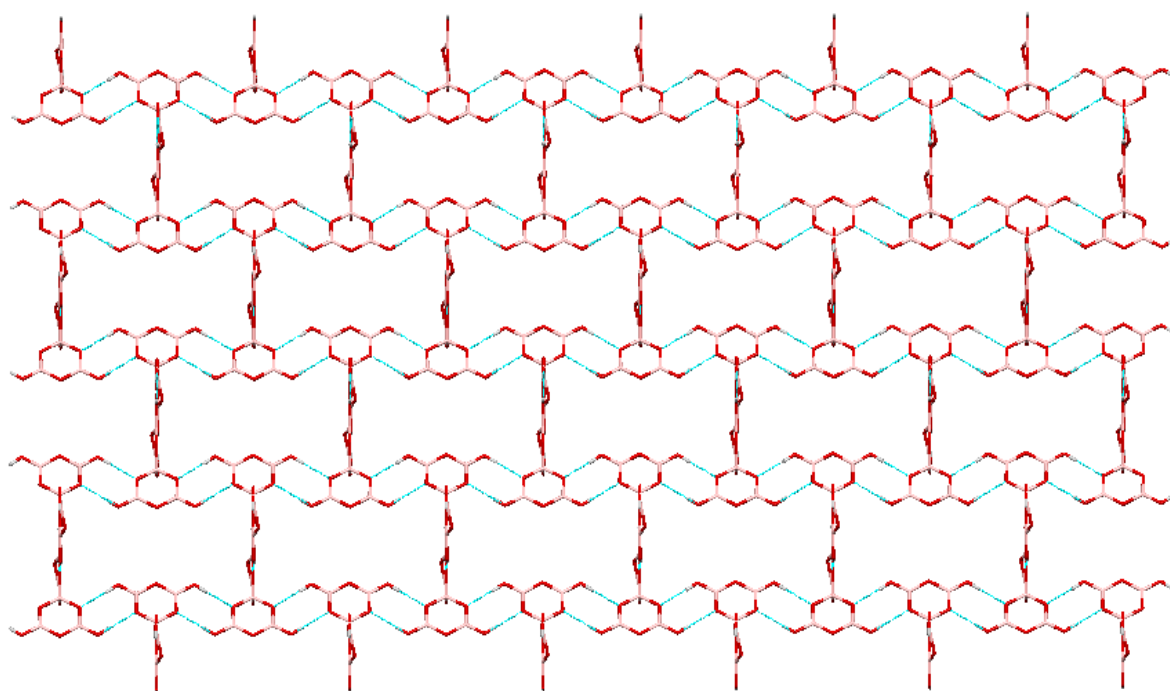


Figure **4.22** H-bonded $[\text{B}_5\text{O}_6(\text{OH})_4]^-$ network for **41** view perpendicular to the large channels (viewed along the a direction of the unit cell).

Detailed inspection of Figure **4.23** shows that the $[\text{B}_5\text{O}_6(\text{OH})_4]^-$ ions are connected by two reciprocal- α $R_2^2(8)$ interactions $\text{O}8\text{-H}8\cdots\text{O}3^*/\text{O}8^*\text{-H}8^*\cdots\text{O}3$ and $\text{O}7\text{-H}7\cdots\text{O}1^*/\text{O}7^*\text{-H}7^*\cdots\text{O}1$ forming a chain. The pentaborate(1-) anion chains are linked to other pentaborate(1-) anion chains by two reciprocal H-bond interactions forming a three-dimensional network. The first interaction is a reciprocal- α $R_2^2(8)$ $\text{O}9\text{-H}9\cdots\text{O}4^*/\text{O}9^*\text{-H}9^*\cdots\text{O}4$, while the second interaction is a reciprocal- β $R_2^2(12)$ $\text{O}10\text{-H}10\cdots\text{O}9^*/\text{O}10^*\text{-H}10^*\cdots\text{O}9$.

The $[\text{Ni}(\text{dien})_2]^{2+}$ cations and $[\text{B}_5\text{O}_6(\text{OH})_4]^-$ anions of crystallisation of **41** are connected through a complex series of H-bond interactions (Figure **4.24**), with the anion network templated by the cations. The $[\text{Ni}(\text{dien})_2]^{2+}$ cation acts as H-bond donors to four pentaborate(1-) anion molecules *via* nine H-bond interactions $\text{N}1\text{A-H}1\text{AA}\cdots\text{O}10^*$, $\text{N}1\text{A-H}1\text{AB}\cdots\text{O}7^*$, $\text{N}2\text{A-H}2\text{A}\cdots\text{O}8^*$, $\text{N}3\text{A-H}3\text{AB}\cdots\text{O}6^*$, $\text{N}1\text{B-H}1\text{BA}\cdots\text{O}2^*$, $\text{N}1\text{B-H}1\text{BB}\cdots\text{O}6^*$, $\text{N}2\text{B-H}2\text{B}\cdots\text{O}7^*$, $\text{N}3\text{B-H}3\text{BA}\cdots\text{O}10^*$, and $\text{N}3\text{B-H}3\text{BB}\cdots\text{O}8^*$. Details of the H-bonding interactions are given in Table **4.16**.

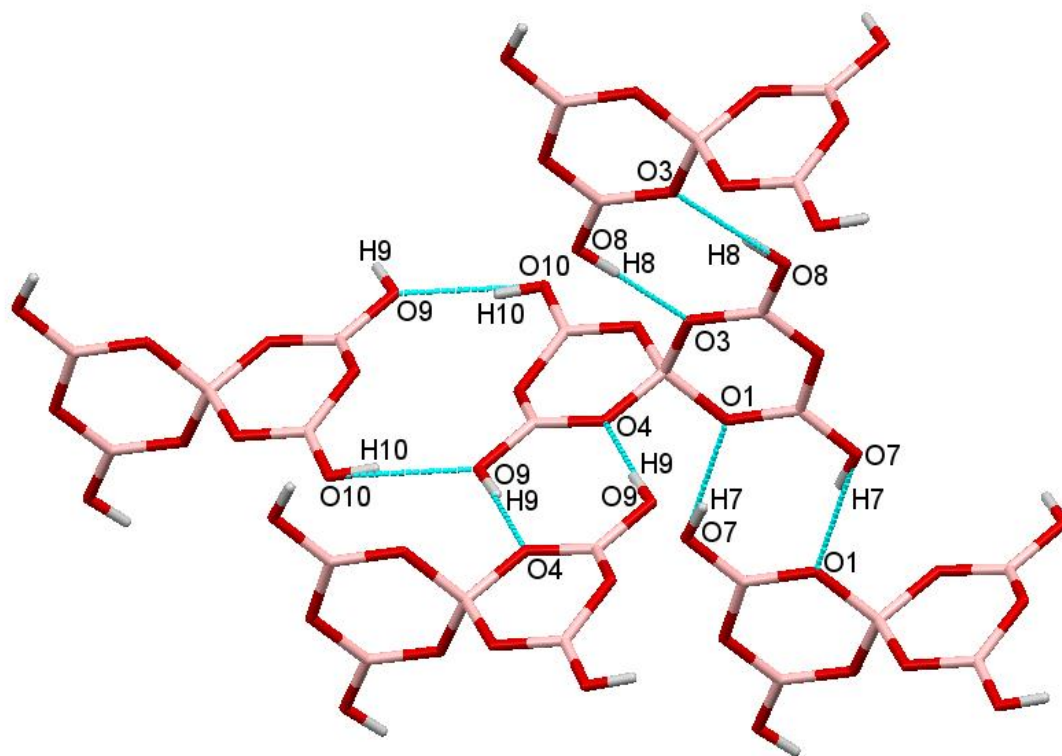


Figure 4.23 The $R_2^2(8)$ and $R_2^2(12)$ connections between two layers of pentaborate(1-) ion in **41**.

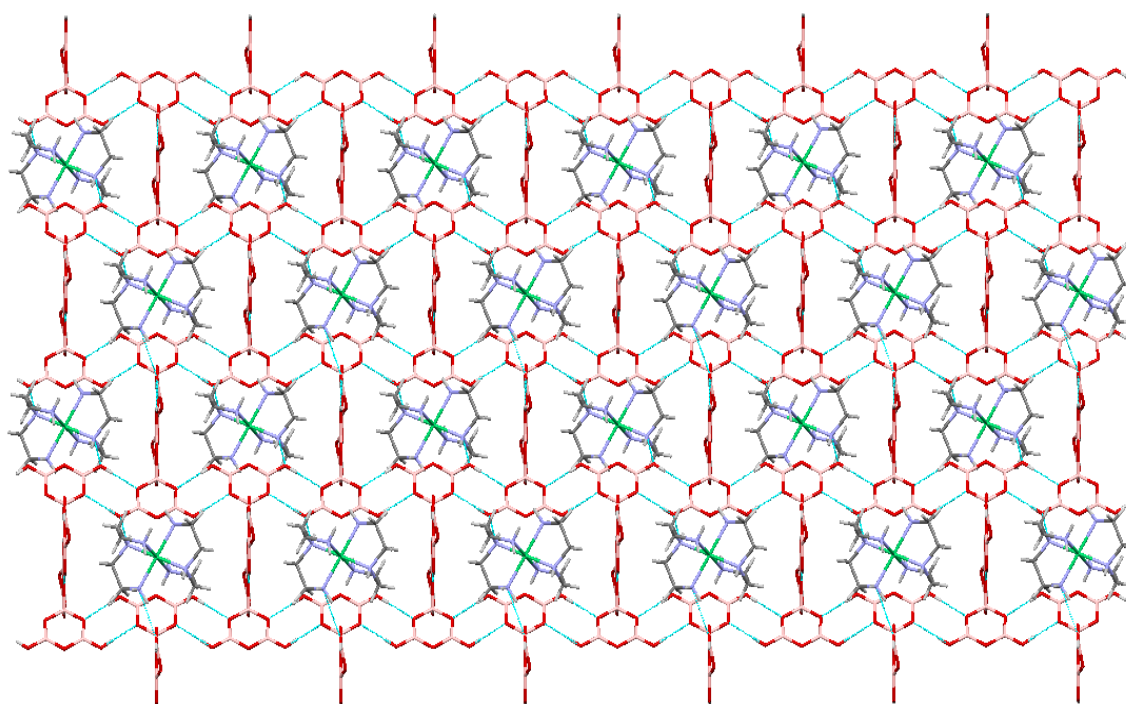


Figure 4.24 A plane of pentaborate(1-) anions and $[\text{Ni}(\text{dien})_2]^{2+}$ cations in plane of H-bond interactions in **41** (viewed along the a direction of the unit cell).

4.4 Conclusion and summary

The main aim of this chapter of the thesis was to prepare and investigate new polyborate compounds contains nickel(II) cations. Eight polyborate compounds **36-43** containing different polyborate anions (pentaborate(1-), hexaborate(2-), and heptaborate(2-) anions) have been prepared and templated from aqueous solution from boric acid using a series of nickel(II) complex cations. Five of these salts have been characterized by single-crystal XRD (**37-41**) studies.

New polyborate anion structural architecture has been identified within this Chapter. The hexaborate(2-) anion in **37** coordinates as a bidentate ligand with nickel(II) cation. Compound **39** is a rare example of a crystallographically characterized compound containing the isolated heptaborate(2-) anion.

Reaction of $[\text{Ni}(\text{en})_2]^{2+}$ with boric acid in a 1:10 ratio produced compounds containing the pentaborate(1-) anion (**36**), while the reaction in 1:7 ratio afforded a compound containing the hexaborate(2-) anion (**37**). These results show that the products obtained are also dependent upon the reaction stoichiometry.

Chapter Five

General Conclusion

And Future Work

5.1 General conclusion

This thesis has been concerned with the synthesis of polyborate salts partnered with transition metal cations. With non-metal cations, pentaborate(1-) salts are commonly observed. Each pentaborate(1-) anion has four H-bond donor sites. All of them are always used as an H-bond donor to other pentaborate anions and form supramolecular 3D frameworks. The cations in many of these structures are ‘innocent’, in that they interact weakly with the anions and do not significantly influence the structure, which is dominated by the anion-anion H-bond interactions.

The first aim of this study was to synthesise novel transition metal borate complexes with the synthesis of unique ‘isolated’ borate anions and anions other than the pentaborate(1-) anion. The second aim of this study was to investigate the structural feature of the transition metal complex polyborate compounds and evaluate the solid-state structure directing effects operating within these compounds. The strategy used to break the domination of pentaborate compounds and achieve these aims were:

- (i) The use of inert ‘non-innocent’ cations (*e.g.* multi-H-bond donor transition metal complexes such as $[\text{Co}(\text{NH}_3)_6]^{3+}$), to improve cation-anion H-bonds formation and reduce anion-anion H-bond interactions.
- (ii) The use of relatively high charged cations (*e.g.* Co^{3+} , Cu^{2+} , and Ni^{2+} complexes) with unusual or non-spherical shapes, in order to change the stoichiometry of the salt.
- (iii) The use of very large cations (*e.g.* $[\text{Co}(\text{diNOsar})]^{3+}$) to see how this influences the structures of the products.
- (iv) The use of different boric acid ratios to evaluate the effect of the ratio on reaction products.

The aims of this study were achieved as demonstrated by:

- (i) Two unique polyborate anions, $[\text{B}_7\text{O}_9(\text{OH})_6]^{3-}$ (**11**) and $[\text{B}_8\text{O}_{10}(\text{OH})_6]^{2-}$ (**6**) have been prepared by using inert transition metal cations $[\text{Co}(\text{dien})_2]^{3+}$ and $[\text{Co}(\text{en})_3]^{3+}$, respectively.
- (ii) Structures containing a variety of polyborate ions (*e.g.* triborate(1-) (**12**), tetraborate(2-) (**9**), pentaborate(1-) (**6**, **20**, **22**, **27**, **38**, **40**, **41**), hexaborate(2-) (**23**, **28**, **37**), and heptaborate(2-) (**24**, **39**)) have also been prepared and their structures have been investigated by single-crystal X-ray diffraction studies.

- (iii) The solid-state structures of transition metal complex polyborate compounds all display multiple cation-anion H-bond interactions and these undoubtedly play a major role in the energetics of engineering these structures. For instance, in compound **9**, all eighteen of the amino hydrogen atoms of the $[\text{Co}(\text{NH}_3)_6]^{3+}$ cation are involved in secondary coordination to anions *via* H-bonds.
- (iv) New polyborate anion structural architectures have been identified within this thesis. The hexaborate(2-) anion in **37** coordinates as a bidentate ligand with a Ni^{2+} cation, and in **23** and **28** it acts as a tridentate ligand with a Cu^{2+} cation. The pentaborate(1-) anion in (**22**) coordinates as a monodentate ligand with the copper(II) cation.
- (v) Reaction of transition metal complex cations with boric acid in different ratios produced compounds containing different polyborate anions, *e.g.* reaction of $[\text{Co}(\text{diNOsar})]^{3+} : \text{B}(\text{OH})_3$ in a 1:5 or 1:10 ratio gave rise to the triborate(1-) (**12**) or pentaborate(1-) salt (**13**), respectively.

5.2 Future work

This thesis has focused on structural aspects of transition metal polyborate compounds however their potential applications have not been investigated or explored. Such application may include fire retardant additives, wide band-gap semi-conductor, fluorescent, piezoelectric and SHG materials. Future work could investigate their physical properties and potential industrial applications.

Further synthetic work could focus on transition metal complexes with high oxidation state metals (*e.g.* Pt^{4+}) as templating cations and the inclusion of metals (*e.g.* Al^{3+}) in the polyborate framework. Work will also focus on employing larger and magnetically interesting polymetallic cages as the cationic counter parts to borate anions. Here we would be able to assess how cation size influences the type of borate obtained within the resultant salt.

Chapter six

Experimental

6.1 Material analysis

All material reagents were obtained commercially from Sigma-Aldrich (UK) or Lancaster Synthesis (UK) and unless specified were used without further purification. Solvents were standard reagent grade and were used as supplied unless otherwise stated.

NMR spectra were acquired using a Bruker Ultrashield™ plus 400, using the TopSpin™ 3.2 software package, operating at: 400 MHz for ^1H , 100 MHz for ^{13}C , and 128 MHz for ^{11}B , with $(\text{CH}_3)_4\text{Si}$ as an external standard for ^1H and ^{13}C , and $\text{BF}_3\cdot\text{OEt}_2$ for ^{11}B . All chemical shifts are given in ppm. Deuterium oxide was used as a solvent unless otherwise stated. Spectra were analysed using Master Re-Nova, version: 6.0.2-5475 software. Elemental analysis (C, H, and N) was carried out at external laboratories, OEA laboratories Ltd in Callington, Cornwall and Elemtex Ltd. Thermal gravimetric analysis (TGA) and differential scanning calorimetry (DSC) were obtained on an SDT Q600 V4.1 build 59 instruments. Samples were heated in an (Al_2O_3) alumina crucible at a temperature ramp rate of $10\text{ }^\circ\text{C}/\text{min}$ between $25\text{--}800\text{ }^\circ\text{C}$ under a flow air ($100\text{ mL}/\text{min}$). Fourier transform infra-red (FTIR) spectra were performed on a Perkin Elmer 100 FT-IR spectrometer over $4000\text{--}400\text{ cm}^{-1}$. Samples were analysed as KBr pellets. Powder X-ray diffraction (p-XRD) analyses were performed on an X-Pert PRO Phillips 3040/60 XRD diffractometer instrument. Spectra were analysed and recorded using the Phillips X' Pert Data Collector software package. UV/Vis spectra were performed on Perkin Elmer lambda 35 UV/Vis spectrophotometer. Samples were analysed at a concentration of $1\times 10^{-3}\text{ M}$. Molar magnetic susceptibility values of the prepared compounds were performed on a magnetic susceptibility balance, Johnson Matthey Equipment Limited. Melting point values were performed on a Stuart SMP10 melting point apparatus. Single-crystals were analysed by single-crystal X-ray diffraction at the EPSRC National Crystallography service centre at the University of Southampton (UK).

6.2 Preparation of cobalt(III) complexes

6.2.1 Preparation of $[\text{Co}(\text{en})_3]\text{Cl}_3\cdot 2\text{H}_2\text{O}$ (1)

Compound **1** was prepared using a modified version of a previously published procedure.¹⁵⁵ To an ice bath cooled solution of ethylenediamine (en) (20.00 g, 30%, 99.83 mmol) was added hydrochloric acid (5.7 mL, 6 M). The resulting mixture was poured into a solution of cobalt(III) chloride hexahydrate (8.00 g, 33.60 mmol) in distilled water (25 mL) and

activated charcoal (0.90 g). The cobalt(II) was oxidized to cobalt(III) by bubbling a vigorous stream of air through the solution for 7 hours. The resulting mixture was filtered to remove the charcoal. The mixture was heated in an evaporating dish on a steam bath until a crystalline crust began to form over the surface. After cooling, a solution of concentrated hydrochloric acid (5 mL) and ethanol (10 mL) were added. The orange crystals were collected by filtration, washed with ethanol until the washings were colourless before being dried in an oven at 90 °C for 24 hours to yield **1** (9.80 g, 76%). M.p. = 253-255 °C (dec.). $\chi_m = -155 \times 10^{-6} \text{ cm}^3 \text{ mol}^{-1}$. $^1\text{H/ppm}$: 2.9 (m, 12H, CH₂), 4.8 (s, 16H, NH₂, H₂O). $^{13}\text{C}\{^1\text{H}\}/\text{ppm}$: 44.5. IR (KBr/cm⁻¹): 3409(m), 3204(s), 3092(s), 1615(w), 1561(s), 1463(s), 1365(m), 1327(m), 1300(w), 1279(m), 1255(m), 1209(w), 1158(m), 1126(m), 1059(s), 1007(w), 895(w), 786(m), 740(w) 495(w), 466(w). [Lit. 3510-3440, 3195-3060, 1619, 1591-1563, 1466, 1366, 1325, 1302, 1277, 1251, 1215, 1163, 1122, 1057, 1002, 894, 782, 744, 490, 465].¹⁹³ [Lit. 3210, 3160, 3100].¹⁹⁴ UV-Vis $\lambda/\text{nm}(\epsilon/\text{M}^{-1}\text{cm}^{-1})$: 337 (72), 464 (80). [Lit. 338 (68), 466 (75)].¹⁶²

6.2.2 Preparation of [Co(NH₃)₆]Cl₃ (2)

Compound **2** was prepared by a modified version of a literature procedure.¹⁵⁶ To a hot solution of ammonium chloride (7.00 g, 130 mmol) in distilled water (14 mL) was added cobalt(III) chloride hexahydrate (10.00 g, 42 mmol). The reaction mixture was stirred to dissolve all the precipitate, and then activated charcoal (1.00 g) was added. The reaction mixture was cooled to room temperature, and then ammonium hydroxide solution (22 mL, 35%) was added. The oxidation of cobalt(II) to cobalt(III) was carried out by bubbling a stream of air through the solution for 4 hours. The mixture was carefully heated to 60 °C for 20 minutes. The product mixture was cooled in an ice bath, and the precipitate was collected by filtration. The product was dissolved in a hot solution of hydrochloric acid (80 mL, 0.5 M). The charcoal was removed by filtration of the hot solution and concentrated hydrochloric acid (12 mL) was added to the filtrate. The solution was cooled in an ice bath to yield orange crystals of **2** (8.20 g, 73%). M.p. = 237-240 °C (dec.). $\chi_m = -123 \times 10^{-6} \text{ cm}^3 \text{ mol}^{-1}$. IR (KBr/cm⁻¹): 3412(m), 3233(s), 3160(s), 1616(m), 1328(vs), 830(s), 620(m), 495(sh), 475(w). [Lit. 3240, 3170].¹⁹⁴ [Lit. 1610(m), 1330(vs), 830(s), 499(vw), 476(vw)].¹⁹⁵

6.2.3 Preparation of [Co(dien)₂]Cl₃·2H₂O (3)

Compound **3** was prepared by the method of Searle and Keene as described below.¹³ Diethylenetriamine (dien) (3.45 g, 30 mmol) and diethylenetriamine trihydrochloric acid (1.45 g, 60 mmol) were added to a solution of cobalt(II) chloride hexahydrate (4.76 g, 20 mmol) in distilled water (25 mL) and activated charcoal (2.50 g). A vigorous stream of air was passed through the solution for 24 hours, then the reaction mixture was filtered to remove charcoal. The filtrate volume was reduced to 5 mL using a rotary evaporator. The resulting mixture was cooled in an ice bath and a small amount of ethanol was then added to complete the precipitation of the crude product. The crude product was isolated by filtration, washed with ethanol, recrystallized from ethanol and acetone, and then dried in an oven at 60 °C for 60 minutes to yield orange crystals of **3** (6.90 g, 85%). M.p. = 224-225 °C (dec.). $\chi_m = -83 \times 10^{-6} \text{ cm}^3 \text{ mol}^{-1}$. ¹H/ppm: 3.0 (m, 16H, CH₂), 4.8 (s, 14H, NH₂, H₂O). [Lit. 3.0 (m, CH₂), 4.8 (s, NH₂, H₂O)].¹³ ¹³C{¹H}/ppm: 38.5, 42.2, 43.5, 45.9, 47.2, 50.4, 53.2, 54.9. IR (KBr/cm⁻¹): 3398(s), 3166(s), 3063(s), 2961(s), 2886(s), 1610(m), 1556(m), 1476(m), 1359(m), 1325(m), 1189(m), 1153(m), 1127(m), 1081(m), 1046(s), 896(w), 878(w), 777(m), 666(m), 570(m), 519(m).

6.2.4 Preparation of [Co(diNOsar)]Cl₃ (4)

Compound **4** was prepared following a previously published procedure.¹⁵⁷ To a stirred solution of **1** (2.45 g, 6.41 mmol) and anhydrous sodium carbonate Na₂CO₃ (1.20 g, 11.3 mmol) in distilled water (25 mL) was added formaldehyde (20 mL, 37%) followed by nitromethane (2.85 g, 37.0 mmol). The reaction mixture was placed in a water bath and the solution was maintained without stirring at 35-40 °C for 90 minutes. The colour rapidly changed from clear yellow to dark brown. The mixture was allowed to stand at 0 °C for 48 hours. The orange crystals of the “chloride carbonate” salt were filtered off. The resulting chloride carbonate solid was cautiously dissolved in hot hydrochloric acid (7 mL, 3 M). After cooling in an ice bath the fine crystals of **4** were isolated by filtration, air dried and placed in a vacuum desiccator to yield orange crystals (1.45 g, 42%). M.p. = 274-275 °C (dec.). $\chi_m = -167 \times 10^{-6} \text{ cm}^3 \text{ mol}^{-1}$. ¹H/ppm: 3.4, 3.9 (AB doublet of doublet, 12H, *J* = 12 Hz, CH₂ Caps), 3.0, 3.6 (complex AA'BB' coupling pattern, 12H, *J* = 8 Hz, CH₂ of en), 4.8 (s, 6H, NH₂). [Lit. two overlapping quartet, associated with AB or AA'BB' patterns of cap and en methylene groups, 3.4, 4.1, 3.1, and 3.6].¹⁶² ¹³C{¹H}/ppm: 51.2, 54.7, 87.4. IR (KBr/cm⁻¹): 3459(s), 3034(s), 2864(s), 1558(s), 1452(m), 1344(s), 1078(m), 1058(m), 812(m), 469(m). [Lit. 1555(s), 1353(s)].¹⁵⁷

6.2.5 Preparation of [Co(pn)₃]Cl₃ (5)

Compound **5** was prepared as described in the literature.¹⁵⁸ Cobalt(III) chloride hexahydrate (3.55 g, 14.9 mmol), hydrochloric acid (3 mL, 5 M), and 1,2-diaminopropane (pn) (3.70 g, 49.9 mmol) were mixed together and dissolved in distilled water (7.5 mL). Cobalt(II) was oxidized to cobalt(III) by passing a stream of air through the solution at room temperature for 24 hours. The resulting mixture was filtered to remove charcoal and the filtrate was acidified with a few drops of concentrated hydrochloric acid. The resulting solution was gently evaporated to dryness using a rotary evaporator to yield a dark green powder of **5** which was then recrystallized using ethanol (4.50 g, 78%). M.p. = 237-240 °C (dec.). $\chi_m = -133 \times 10^{-6} \text{ cm}^3 \text{ mol}^{-1}$. ¹H/ppm: 1.3 (m, 9H, CH₃ of pn), 2.5 (t, 3H, *J* = 13.2 Hz, *J* = 26.4 Hz, H_a of CH₂ of pn), 2.9 (m, 3H, H_b of CH₂ of pn), 3.0 (m, 3H, CH of pn), and 4.8 (s, 6H, NH₂). [Lit. 3.1 (m, 3H, CH of pn), 2.9 (dd, 3H, H_b of CH₂ of pn), 2.5 (t, 3H, H_a of CH₂ of pn), 1.4 (d, 9H, CH₃ of pn)]. ¹⁶⁰¹³C{¹H}/ppm: 16.5 (CH₃ of pn), 49.9 (CH of pn), and 53.9 (CH₂ of pn). IR (KBr/cm⁻¹): 3393(s), 3190(s), 3081(s), 2971(m), 1554(m), 1459(m), 1394(w), 1346(w), 1243(w), 1137(w), 1110(m), 1047(w), 1016(w), 917(w), 781(w).

6.3 Preparation of cobalt(III) complex polyborate compounds

6.3.1 Preparation of [Co(en)₃][B₅O₆(OH)₄][B₈O₁₀(OH)₆]·5H₂O (6)

A solution of compound **1** (1.00 g, 2.7 mmol) in water (10 mL) was added to an aqueous suspension solution of excess activated Dowex 550A (50 g) monosphere anion exchange resin in water (40 mL). The resulting mixture was stirred at room temperature for 24 hours. The Dowex 550A resin was separated by filtration with a Buchner funnel and washed four times with a distilled water (4 × 5 mL). The solution of [Co(en)₃](OH)₃ was reduced to a volume of 15 mL using a rotary evaporator. Methanol (15 mL) was added to the concentrated solution, followed by boric acid (2.46 g, 39.9 mmol). The reaction mixture was gently warmed for 3 hours. The solution volume was reduced to 5 mL using a rotary evaporator. The concentrated solution was left for 40 days in NMR tubes for crystallization to yield orange crystals of **6** (0.97 g, 41%). M.p. = 264-267 °C (dec.). $\chi_m = -101 \times 10^{-6} \text{ cm}^3 \text{ mol}^{-1}$. C₆H₄₄B₁₃CoN₆O₃₁. Anal. Calc.: C = 8.0%, H = 4.9%, N = 9.4%. Found: C = 8.2%, H = 5.0%, N = 9.6%. ¹H/ppm: 2.7 (m, 12H, CH₂ of en), 4.8 (s, 32 H, NH₂, H₂O, OH). ¹³C{¹H}/ppm: 44.6. ¹¹B/ppm: 13.4 (15%), 16.5 (85%). IR (KBr/cm⁻¹): 3461(s), 3265(s), 3149(s), 2960(w), 1611(w), 1394(s), 1324(s), 1170(s), 1059(s), 1033(m), 939(m), 863(m), 811(m), 779(m), 710(w). p-XRD d-spacing/Å (% rel. int.):

8.47 (53), 7.60 (54), 6.35 (73), 5.76 (100), 3.64 (370, 3.33 (53). TGA: 100-150 °C, loss of five interstitial H₂O: 9.7% (10.1% calc.); 150-250 °C, condensation of polyborate which loss of five further H₂O: 20.5% (20.1% calc.); 250-800 °C, oxidation of organic content 41.0% (40.3% calc.); residual CoB₁₃O₂₁ 59.0% (59.7% calc.).

6.3.2 Preparation of [Co(en)₃][B₅O₆(OH)₄]₂Cl·3H₂O (7)

The preparation of [Co(en)₃]Cl(OH)₂ was carried out using the same method as described above for the preparation of **6** from **1** (1.00 g, 2.66 mmol). Dowex (25 g), and boric acid (1.64 g, 26.6 mmol) was carefully added. The reaction mixture was gently warmed for 2 hours. The solution volume was reduced to (5 mL) using a rotary evaporator. The final mixture was sealed in an autoclave stainless steel reactor with a Teflon liner at 140 °C for 7 days before being cooled to ambient temperature to yield orange crystals of **7** (1.15 g, 57%). M.p. = 294-295 °C (dec.). $\chi_m = -230 \times 10^{-6} \text{ cm}^3 \text{ mol}^{-1}$. C₆H₃₈B₁₀ClCoN₆O₂₃. *Anal. Calc.*: C = 9.4%, H = 5.0%, N = 11.0%. Found: C = 9.7%, H = 4.8%, N = 10.5%. ¹H/ppm: 2.7 (m, 12H, CH₂ of en), 4.8 (s, 26H, NH₂, H₂O, OH). ¹³C{¹H}/ppm: 44.3. ¹¹B/ppm: 1.2 (8%), 12.9 (33%), and 17.4 (59%). IR (KBr/cm⁻¹): 3267(s), 3167(s), 2945(w) 1613(w), 1409(s), 1302(s), 1154(m), 1057(m), 1007(m), 986(m), 916(m), 895(m), 785(m), 709(m). UV-Vis, $\lambda/\text{nm}(\epsilon/\text{M}^{-1}\text{cm}^{-1})$: 337 (180), 462 (180). p-XRD d-spacing/Å (% rel. int.): 7.33 (55), 5.96 (100), 4.68 (11), 4.31 (20), 3.72 (5). TGA: 100-180 °C, loss of three interstitial H₂O: 7.8% (7.1% calc.); 180-280 °C, condensation of polyborate which loss of four further H₂O: 17.7% (16.5% calc.); 280-800 °C, oxidation of organic component 40.0% (40.1% calc.); residual CoB₁₀O₁₆Cl 60.0% (59.9% calc.).

6.3.3 Preparation of [Co(en)₃][B₇O₉(OH)₆]₆·6H₂O (8)

The preparation of [Co(en)₃](OH)₃ was carried out exactly in the same method as described above for the preparation of **6** from **1** (1.00 g, 2.66 mmol), Dowex (50 g), and boric acid (1.64 g, 26.6 mmol). The reaction mixture was gently warmed for 3 hours. The solution volume was reduced to 5 mL using a rotary evaporator. The final mixture was left for 7 days at room temperature for crystallization to yield orange crystals of **8** (0.80 g, 45%). M.p. = 242-244 °C (dec.). $\chi_m = -255 \times 10^{-6} \text{ cm}^3 \text{ mol}^{-1}$. C₆H₄₂B₇CoN₆O₂₁. *Anal. Calc.*: C = 10.8%, H = 6.4%, N = 12.3%. Found: C = 10.7%, H = 6.3%, N = 12.6%. ¹H/ppm: 2.7 (m, 12H, CH₂ of en), 4.8 (s, 30H, NH₂, H₂O, OH). ¹³C{¹H}/ppm: 44.2. ¹¹B/ppm: 13.0. IR (KBr/cm⁻¹): 3413(s), 3253(s), 2926(w), 2855(w), 1637(w), 1618(w), 1385(s), 1322(s), 1162(m), 1058(s), 1005(s), 930(m),

825(w), 757(w), 702(w). p-XRD d-spacing/Å (% rel. int.): 8.35 (74), 8.00 (31), 6.62 (100), 6.22 (31), 5.46 (39), 4.54 (39). TGA: 70-180 °C, loss three of six interstitial H₂O: 15.0% (16.1% calc.); 180-280 °C, condensation of polyborate which loss of three further H₂O: 23.2% (24.1% calc.); 280-800 °C, oxidation of organic component 49.8% (51.2% calc.); residual CoB₇O₁₂ 50.2% (48.8% calc.).

6.3.4 Preparation of [Co(NH₃)₆]₂[B₄O₅(OH)₄]₃·11H₂O (9)

The preparation of [Co(NH₃)₆](OH)₃ was carried out exactly in the same method as described previously for the preparation of **6** from **2** (0.71 g, 2.66 mmol) and Dowex (50 g). Boric acid (1.64 g, 26.6 mmol) was added to the solution, which was gently warmed with stirring for 2 hours. The solvent was evaporated to 5 mL using a rotary evaporator before being the product was crystallized from solution. The product was filtered off and allowed to dry for 3 hours in an oven at 40 °C to yield orange crystals of **9** (0.60 g, 41%). M.p. = 258-260 °C (dec.). $\chi_m = -330 \times 10^{-6} \text{ cm}^3 \text{ mol}^{-1}$. B₁₂Co₂H₇₀N₁₂O₃₈. *Anal.* Calc.: H = 6.4%, N = 15.4%. Found: H = 6.5%, N = 15.4%. ¹¹B/ppm: 10.4. IR (KBr/cm⁻¹): 3400(s), 3308(s), 1636(m), 1421(s), 1384(s), 1339(s), 1190(s), 1015(s), 995(s), 943(m), 809(m), 704(w). p-XRD d-spacing/Å (% rel. int.): 4.95 (99), 4.83 (100), 3.47 (34). TGA: 70-150 °C, condensation of polyborate which loss of eleven H₂O: 17.8% (18.1% calc.); 150-350 °C, oxidation of ammonia molecules 46.5% (46.7% calc.); residual Co₂B₁₂O₂₁ 53.5% (53.3% calc.).

6.3.5 Preparation of [Co(NH₃)₆][B₇O₉(OH)₅]Cl·5H₂O (10)

The preparation of [Co(NH₃)₆]Cl(OH)₂ was carried out exactly in the same method as described previously for the preparation of **6** from **2** (1.00 g, 3.73 mmol) and Dowex (30 g). Boric acid (2.30 g, 27.3 mmol) was added to the solution which was gently warmed with stirring for 2 hours. The solvent was evaporated to (5 mL) using a rotary evaporator. The product was isolated by filtration before being allowed to dry for 3 hours in an oven at 40 °C to yield orange crystals of **10** (0.80 g, 36%). M.p. = 249-251 °C (dec.). $\chi_m = -37 \times 10^{-6} \text{ cm}^3 \text{ mol}^{-1}$. B₇CoH₃₃N₆O₁₉Cl. *Anal.* Calc.: H = 5.6%, N = 14.2%. Found: H = 5.6%, N = 14.1%. ¹¹B/ppm: 13.4. IR (KBr/cm⁻¹): 3477(s), 3407(s), 3320(s), 1639(w), 1440(s), 1401(m), 1353.1(s), 1164(m), 1114(s), 1037(s), 954(m), 852(m), 800(m), 767(w), 732(w), 699(w), 653(w). p-XRD d-spacing/Å (% rel. int.): 8.04 (33), 6.20 (44), 5.84 (100), 5.24 (64), 4.11 (34), 2.03 (46). TGA: 70-150 °C, loss of five interstitial H₂O: 14.1% (15.2% calc.); 180-250 °C, condensation of

polyborate which loss of two and half further H₂O: 21.4% (22.8% calc.); 250-650 °C, oxidation of ammonia molecules 39.0% (40.0% calc.); residual CoB₇O_{11.5}Cl 61.0% (60.0% calc.).

6.3.6 Preparation of [Co(dien)₂][B₇O₉(OH)₆]·9H₂O (11)

The preparation of [Co(dien)₂](OH)₃ was carried out in the same method as described previously for the preparation of **6** from **3** (1.00 g, 2.45 mmol) and Dowex (50 g). Boric acid (1.51 g, 24.5 mmol) was added with stirring. The reaction mixture was stirred for 3 hours at room temperature. The solvents were evaporated to 5 mL using a rotary evaporator, then the concentrated solution was left for 25 days in several NMR tubes for crystallization to yield yellow crystals of **11** (0.65 g, 35%). M.p. = 238-240 °C (dec.). $\chi_m = -120 \times 10^{-6} \text{ cm}^3 \text{ mol}^{-1}$. C₈H₅₀B₇CoN₆O₂₄. *Anal. Calc.*: C = 12.8%, H = 6.7%, N = 11.2%. Found: C = 13.4%, H = 7.2%, N = 11.1%. ¹H/ppm: 3.0 (m, 12H, CH₂), 3.2 (m, 4H, CH₂), 4.8 (s, 34H, NH₂, H₂O, OH). ¹³C{¹H}/ppm: 43.3, 55.0, ¹¹B/ppm: 12.3. IR (KBr/cm⁻¹): 3432(s), 3201(s), 3095(s), 2950(m), 1631(w), 1415(s), 1385(s), 1331(s), 1134(m), 1084(s), 1047(s), 932(m), 861(m), 750(w), 656(w). p-XRD d-spacing/Å (% rel. int.): 3.87 (100), 2.02 (55), 1.43 (90), 1.22 (30). TGA: 70-200 °C, loss of nine interstitial H₂O: 19.5% (21.7% calc.); 200-280 °C, condensation of polyborate which loss of three further H₂O: 28.4% (28.9% calc.); 280-800 °C, oxidation of organic content 56.9% (56.5% calc.); residual CoB₇O₁₂ 43.1% (43.5% calc.).

6.3.7 Preparation of [Co(diNOsar)]₂[B₃O₃(OH)₄]Cl₅·4.75H₂O (12)

The preparation of [Co(diNOsar)]Cl₂OH was carried out in the same method as described previously in the preparation of **6** using **4** (1.00 g, 1.85 mmol) and Dowex (20 g). Boric acid (0.57 g, 9.25 mmol) was added to the aqueous solution which was stirred for 2 hours at room temperature. The solution volume was reduced in volume by gently evaporation at 45 °C to 5 mL before being left for 4 weeks in several NMR tubes for crystallization to yield orange needle crystals of **12** (0.12 g, 10%). M.p. = 283-285 °C (dec.). $\chi_m = -25 \times 10^{-6} \text{ cm}^3 \text{ mol}^{-1}$. C₂₈H_{73.5}B₃Cl₅Co₂N₁₆O_{19.75}. *Anal. Calc.*: C = 26.4%, H = 5.8%, N = 17.5%. Found: C = 25.6%, H = 6.5%, N = 16.7%. ¹H/ppm: 3.3, 3.9 (AB doublet of doublet, 12H, *J* = 12 Hz, CH₂ Caps), 2.9, 3.5 (complex AA'BB' coupling pattern, 12H, CH₂ of en), 4.8 (s, 19.5H, NH₂, H₂O, OH). ¹³C{¹H}/ppm: 51.4 (CH₂ group of the en), 55.1 (CH₂ group of the capping units), 87.9 (tertiary C-NO₂ of the caps). ¹¹B/ppm: 16.2. IR (KBr/cm⁻¹): 3552(s), 3475(s), 3413(s), 3236(m), 3014(m), 2866(m), 1617(s), 1559(s), 1432(m), 1343(m), 1179(w), 1134(w), 1076(m), 1018(w),

988(w), 952(w), 873(w), 847(w), 812(w), 780(w), and 620(m). p-XRD d-spacing/Å (% rel. int.): 8.81 (4), 8.21 (4), 7.85 (4), 7.25 (5), 4.86 (3), 3.17 (100). TGA: 70-150 °C, loss of five interstitial H₂O: 7.8% (6.7% calc.); 150-250 °C, condensation of polyborate which loss of two further H₂O: 11.0% (9.5% calc.); 250-800 °C, oxidation of organic content 68.8% (68.1% calc.); residual Co₂B₃O₅Cl₅ 31.3% (31.9% calc.).

6.3.8 Preparation of [Co(diNOsar)][B₅O₆(OH)₄]₂Cl·3H₂O (13)

The preparation of [Co(diNOsar)]Cl(OH)₂ was carried out in the same method as described previously in the preparation of **6** using **4** (1.00 g, 1.85 mmol) and Dowex (30 g). Boric acid (1.14 g, 18.5 mmol) was added to the aqueous solution which was gently warmed with stirring for 60 minutes. The solution volume was reduced using a rotary evaporator to 8 mL before being left for 3 weeks to yield orange crystals of **13** (0.95 g, 54%). M.p. = 283-285 °C (dec.). $\chi_m = -50 \times 10^{-6} \text{ cm}^3 \text{ mol}^{-1}$. C₁₄H₄₄B₁₀ClCoN₈O₂₇. *Anal.* Calc.: C = 18.4%, H = 5.1%, N = 12.3%. Found: C = 18.3%, H = 5.0%, N = 12.4%. ¹H/ppm: 3.4, 3.7 (AB doublet of doublet, 12H, *J* = 12 Hz, CH₂ Caps), 2.8, 3.6 (complex AA'BB' coupling pattern, 12H, CH₂ of en), 4.8 (s, 20H, NH₂, H₂O, OH). ¹³C{¹H}/ppm: 51.3 (CH₂ group of the en), 55.0 (CH₂ group of the capping units), 87.8 (tertiary C-NO₂ of the caps). ¹¹B/ppm: 15.9. IR (KBr/cm⁻¹): 3437(s), 3025(s), 2859(s), 1634(s), 1558(s), 1447(s), 1348(s), 1100(m), 1078(m), 925(m), 810(m), 696(w). p-XRD d-spacing/Å (% rel. int.): 8.66 (16), 7.36 (33), 6.04 (19), 4.88 (14), 3.19 (100). TGA: 70-150 °C, loss of four interstitial H₂O: 7.9% (7.9% calc.); 150-250 °C, condensation of polyborate which loss of four further H₂O: 15.0% (15.7% calc.); 250-800 °C, oxidation of organic content 59.1% (59.1% calc.); residual CoB₁₀O₁₆Cl 40.9% (40.9% calc.).

6.3.9 Preparation of [Co(pn)₃][B₅O₆(OH)₄]₂Cl·3H₂O (14)

The preparation of [Co(pn)₃]Cl(OH)₂ was carried out as described previously in the preparation of **6** using **5** (1.00 g, 2.58 mmol) and Dowex (30 g). Boric acid (1.59 g, 25.8 mmol) was added to the aqueous solution which was gently warmed with stirring for 2 hours. A rotary evaporator was used to reduce the solution volume to 5 mL. The final mixture was sealed in a Teflon lined stainless steel autoclave, and heated at 140 °C for 3 days. The product was isolated by filtration, and left overnight to dry in a desiccator. The crude result was recrystallized using mix-solvent H₂O:EtOH (2:8) to yield bright orange crystals of **14** (1.05 g, 50%). M.p. = 294-295 °C (dec.). $\chi_m = -200 \times 10^{-6} \text{ cm}^3 \text{ mol}^{-1}$. C₉H₄₄B₁₀ClCoN₆O₂₃. *Anal.* Calc.: C = 13.4%, H =

6.5%, N = 10.4%. Found: C = 13.6%, H = 6.3%, N = 10.4%. ^1H /ppm: 1.3 (m, 9H, CH_3 of pn), 2.5 (t, 3H, $J = 13.2$ Hz, $J = 26.4$ Hz, C_b of CH_2 of pn), 2.9 (m, 3H, H_a of CH_2 of pn), 3.0 (m, 3H, CH of pn), and 4.8 (s, 26H, NH_2 , H_2O , OH). $^{13}\text{C}\{^1\text{H}\}$ /ppm: 16.5 (CH_3 of pn), 49.9 (CH of pn), 53.9 (CH_2 of pn). ^{11}B /ppm: 1.2 (11%), 13.2 (33%), and 16.6 (56%). IR ($\text{KBr}/\text{cm}^{-1}$): 3437(s), 3249(m), 2925(m), 1638(w), 1435(s), 1352(s), 1238(w), 1091(m), 1023(m), 925(m), 780(w), 692(w). p-XRD d-spacing/Å (% rel. int.): 2.34 (93), 2.03 (98), 1.43 (60), 1.22 (100). TGA: 70-160 °C, loss of three interstitial H_2O : 7.2% (6.7% calc.); 160-250 °C, condensation of polyborate which loss of four further H_2O : 16.0% (15.6% calc.); 250-800 °C, oxidation of organic content 44.8% (43.2% calc.); residual $\text{CoB}_{10}\text{O}_{16}\text{Cl}$ 55.2% (56.8% calc.).

6.4 Preparation of copper(II) complexes

6.4.1 Preparation of $[\text{Cu}(\text{en})_2]\text{SO}_4$ (15)

Compound **15** was prepared as described in the literature.¹⁷⁴ A slight excess of the ethylenediamine (en) (2.10 g, 70%, 24.45 mmol) was added to an aqueous solution of copper(II) sulphate pentahydrate (4.00 g, 16.02 mmol) in distilled water (10 mL). The solution was concentrated by gentle evaporation on a warm water bath before being cooled in an ice bath to yield navy crystals of **15** (3.70 g, 83%). M.p. = 240-241 °C. $\chi_m = 1210 \times 10^{-6} \text{ cm}^3 \text{ mol}^{-1}$. IR ($\text{KBr}/\text{cm}^{-1}$): 3307(s), 3218(s), 3145(s), 2967(w), 2953(w), 2887(w), 1586(s), 1472(w), 1453(w), 1394(w), 1321(w), 1277(m), 1165(m), 1111(m), 1089(m), 1045(s), 1020(m), 988(m), 975(m), 671(m), 527(s), 469(m). [Lit. 968, 1050, 1062, 1120].¹⁷⁴

6.4.2 Preparation of $[\text{Cu}(\text{pn})_2]\text{SO}_4$ (16)

Compound **16** was prepared following a previously published procedure.¹⁷⁵ A solution of 1,2-propanediamine (pn) (2.37 g, 32.04 mmol) in distilled water (3 mL) was added to an aqueous solution of copper(II) sulphate pentahydrate (4.00 g, 16.02 mmol) in distilled water (10 mL). The solution volume was reduced to (4 mL) by gentle evaporation on a warm water bath before being cooled in an ice bath. The resulting product, which formed over the cooling period, was filtered, washed with $\text{H}_2\text{O}/\text{EtOH}$ and dried at 50 °C to yield purple crystals of **16** (3.80 g, 77%). M.p. = 232-235 °C (dec.). $\chi_m = 1380 \times 10^{-6} \text{ cm}^3 \text{ mol}^{-1}$. IR ($\text{KBr}/\text{cm}^{-1}$): 3431(s), 3248(s), 3134(s), 2933(w), 2879(w), 1592(s), 1460(w), 1394(w), 1280(w), 1125(sh), 1115(s),

1057(m), 1022(m), 912(w) 699(m), and 618(s). [Lit. 3431, 3214, 3130, 2940, 2886, 1582, 1466, 1401, 1281, 1121, 1027, 913, 619].¹⁷⁵

6.4.3 Preparation of [Cu(dach)₂(H₂O)₂]Cl₂ (17)

Compound **17** was prepared by a method as described by Pariya.¹⁷⁶ To a solution of copper(II) chloride di-hydrate (2.00 g, 11.73 mmol) in ethanol (100 mL) was added 1,2-diaminocyclohexane (dach) (2.68 g, 23.46 mmol). The solution volume was reduced by gentle evaporation on a warm water bath before being cooled in an ice bath. The resulting product, which formed over the cooling period, was isolated by filtration, washed with H₂O/EtOH and dried at 40 °C to yield pink crystals of **17** (3.00 g, 66%). M.p. = 238-240 °C (dec.). $\chi_m = 1270 \times 10^{-6} \text{ cm}^3 \text{ mol}^{-1}$. IR (KBr/cm⁻¹): 3470(s), 3360(s), 3256(s), 3222(s), 3135(s), 2930(s), 2857(s), 1591(s), 1447(s), 1399(m), 1184(m), 1168(m), 1132(s), 170(s), 156(s), 136(s), 987(s), 946(w), 912(w), 875(w), 859(w), 717(w). [Lit. 3270, 3230, 3150, 1592].¹⁹⁶

6.4.4 Preparation of [Cu(tn)₂]SO₄·0.5H₂O (18)

Compound **18** was prepared by the same procedure as was used for compound **15**.^{197,198} Copper(II) sulphate pentahydrate (3.00 g, 18.7 mmol) and 1,3-diaminopropane (tn) (2.78 g, 37.6 mmol) were added to water (10 mL) and then the addition of ethanol (25 mL) yielded purple crystals of **18** (4.10 g, 69%). M.p. = 264-265 °C (dec.). $\chi_m = 1170 \times 10^{-6} \text{ cm}^3 \text{ mol}^{-1}$. CuC₆H₂₁O_{4.5}N₄S. Anal. Calc.: C = 23.0%, H = 6.7%, N = 17.6%. Found: C = 23.0%, H = 6.7%, N = 17.1%. IR (KBr/cm⁻¹): 3427(s), 3212(s), 2938(m), 2884(m), 1575(s), 1441(w), 1401(w), 1321(w), 1282(w), 1179(s), 1115(s), 1025(w), 991(m), 912(m), 883(w), 688(w), and 618(s). [Lit. 3300-3200, 2920, 2890, 1580, 1450, 1400, 1320, 1270, 1160, 1010, 1000, 900, 870, 730, 670].¹⁹⁹

6.4.5 [Cu(N,N-dmen)₂]Cl₂ (19)

Compound **19** was prepared by a procedure modified from Cui *et al.*¹⁷⁷ Copper chloride dihydrate (4.00 g, 24 mmol) was dissolved in ethanol (40 mL) and gave a clear green solution. An ethanolic solution (10 mL) of *N,N*-dimethylethylenediamine (4.14 g, 47 mmol) was added dropwise to the green solution with stirring and was left to stir for a further 10 minutes and gave a dark blue solution. The solution was placed in an ice bath for 2 hours until a dark blue

precipitate had formed. Precipitate was collected by suction filtration and washed with 2 x 5 mL of diethyl ether and dried for 30 minutes in a desiccator. Crude yield: 75.6%. M.p.: 145-147 °C. $\chi_m = 960 \times 10^{-6} \text{ cm}^3 \text{ mol}^{-1}$, $\text{C}_8\text{H}_{24}\text{CuN}_4\text{Cl}_2$. *Anal. Calc.*: C = 30.9%, H = 7.8%, N = 18.0%. Found: C = 31.2%, H = 7.8%, N = 18.0%. IR (KBr/cm⁻¹): 3460 (m), 3407 (m), 3204 (s), 3112 (s), 3069 (m), 2969 (m), 2872 (m), 1635 (w), 1592 (m), 1472 (m), 1448 (m), 1397 (m), 1339 (w), 1319 (w), 1281 (w), 1224 (w), 1170 (s), 1131 (m), 1082 (m), 1066 (m), 1051 (m), 1025 (m), 995 (m), 901 (w), 830 (w), 792 (w), 735 (w), 681 (w), 583 (w), 550 (w), 471 (w).

6.5 Preparation of copper(II) complex polyborate salts

6.5.1 Preparation of $[\text{Cu}(\text{en})_2][\text{B}_5\text{O}_6(\text{OH})_4]_2 \cdot 2\text{H}_2\text{O}$ (20)

A stoichiometric amount of compound **15** (1.00 g, 3.57 mmol) and barium hydroxide octahydrate (1.13 g, 3.57 mmol) were dissolved in distilled water (25 mL). The mixture was rapidly stirred at room temperature for 10 minutes, then the white precipitate of barium sulphate was completely removed by gravity filtration (twice). Boric acid (2.20 g, 35.7 mmol) was added to the filtrate. After stirring for 30 minutes, volume of the solution was reduced to 5 mL by gentle evaporation on a warm water bath. The crude precipitate was collected by filtration and recrystallized using water/ethanol mixture 1:1. The product was carefully washed with ethanol then with acetone and dried at 50 °C for 5 hours to yield purple crystals of **20** (1.20 g, 52%). M.p. = 283-285 °C (dec.). $\chi_m = 1134 \times 10^{-6} \text{ cm}^3 \text{ mol}^{-1}$. $\text{C}_4\text{H}_{28}\text{CuB}_{10}\text{N}_4\text{O}_{22}$. *Anal. Calc.*: C = 7.5%, H = 4.1%, N = 8.8%. Found: C = 7.4%, H = 4.4%, N = 8.6%. ¹¹B/ppm 1.3 (2%), 13.4 (25%), 17.3 (72%). IR (KBr/cm⁻¹): 3459(s), 3328(s), 3282(s), 2956(w), 2904(w), 1614(m), 1416(s), 1314(s), 1139(s), 1094(s), 1041(s), 927(s), 776(s), 708(s), 549(m), 464(m). p-XRD d-spacing/Å (% rel. int.): 7.20 (62), 6.33 (64), 5.65 (66), 5.26 (75), 3.92 (100), 3.23 (41). TGA: 70-180 °C, loss of two interstitial H₂O: 6.0% (5.5% calc.); 180-280 °C, condensation of polyborate which loss of four further H₂O: 16% (16.5% calc.); 280-600 °C, oxidation of organic content 32.9% (34.9% calc.); residual CuB₁₀O₁₆ 67.1% (65.1% calc.).

6.5.2 Preparation of $[\text{Cu}(\text{en})_2][\text{B}_4\text{O}_5(\text{OH})_4] \cdot 2\text{B}(\text{OH})_3$ (21)

Compound **21** was prepared by a modified literature method.¹³⁷ The preparation of complex hydroxide solution was carried out in the same method as described previously in the preparation of **20** from **15** (1.00 g, 3.57 mmol) and barium hydroxide (1.12 g, 3.57 mmol). Boric acid (1.10 g, 17.85 mmol) was directly added to the filtrate. After stirring for 30 minutes the

solution volume was reduced to 5 mL using a rotary evaporator. The crude precipitate was collected by filtration. The product was recrystallized using H₂O/EtOH 1:1 mixture to yield navy crystals of **21** (1.05 g, 59%). M.p. = 275-276 °C (dec.). $\chi_m = 1007 \times 10^{-6} \text{ cm}^3 \text{ mol}^{-1}$. C₄H₂₆CuB₆N₄O₁₅. *Anal. Calc.*: C = 9.6%, H = 5.2%, N = 11.2%. Found: C = 9.7%, H = 5.4%, N = 11.4%. [Lit. C = 9.4%, H = 4.6%, N = 10.6%].¹³⁷ ¹¹B/ppm: 13.9. IR (KBr/cm⁻¹): 3513(s), 3346(s), 3252(s), 2960(s), 2920(m), 1612(w), 1466(s), 1432(s), 1363(s), 1219(m), 1147(m), 1042(s), 1005(s), 943(m), 882(m), 806(m), 707(m), 681(m), 524(m), 494(m), 461(m). p-XRD d-spacing/Å (% rel. int.): 7.26 (76), 6.37 (81), 5.67 (73), 5.28 (93), 4.21 (54), 3.92 (100). TGA: 100-200 °C, condensation of polyborate which loss of five H₂O: 18.9% (18.1% calc.); 200-550 °C, oxidation of organic content 41.2% (42.2% calc.); residual CuB₆O₁₀ 58.8% (57.8% calc.).

6.5.3 Preparation of [Cu(pn)₂{B₅O₆(OH)₄}] [B₅O₆(OH)₄]·4H₂O (22)

The preparation of [Cu(pn)₂](OH)₂ was carried out using the method described previously for the preparation of **20** from **16** (1.00 g, 3.24 mmol) and barium hydroxide (1.02 g, 3.24 mmol). Boric acid (2.00 g, 32.4 mmol) was added to the filtrate solution. After stirring for 30 minutes the solution volume was concentrated to 5 mL by gentle evaporation on a warm water bath. The crude precipitate was collected by filtration, and recrystallized by using water/ethanol. The product was carefully washed with ethanol and then acetone and then dried at 40 °C for 5 hours to yield purple crystals of **22** (1.30 g, 56%). M.p. = 296-298 °C (dec.). $\chi_m = 1094 \times 10^{-6} \text{ cm}^3 \text{ mol}^{-1}$. C₆H₃₆B₁₀CuN₄O₂₄. *Anal. Calc.*: C = 10.0%, H = 5.0%, N = 7.8%. Found: C = 10.1%, H = 5.4%, N = 7.6%. ¹¹B/ppm: 1.5 (2%), 13.2 (24%), 16.9 (74%). IR (KBr/cm⁻¹): 3405(s), 3305(s), 2974(s), 1615(w), 1423(s), 1380(s), 1336(s), 1305(s), 1121(m), 1061(s), 1019(s), 921(s), 778(s), 708(s). p-XRD d-spacing/Å (% rel. int.): 7.57 (33), 6.21 (17), 5.39 (18), 4.69 (100), 3.39 (51), 2.03 (20). TGA: 70-180 °C, loss of four interstitial H₂O: 9.1% (10% calc.); 180-250 °C, condensation of polyborate which loss of four further H₂O: 18.2% (20% calc.); 250-650 °C, oxidation of organic content 38.1% (40.6% calc.); residual CuB₁₀O₁₆ 61.9% (59.4% calc.).

6.5.4 Preparation of [Cu(TMEDA){B₆O₇(OH)₆}]·6H₂O (23)

A solution of *N,N,N',N'*-tetramethyl ethylenediamine (TMEDA) (3.72 g, 32.04 mmol) in water (3 mL) was added to an aqueous solution of copper(II) sulphate pentahydrate (4.00 g, 16.02 mmol) in distilled water (10 mL). The reaction mixture was stirred at room temperature

for 60 minutes, and then a solution of barium hydroxide octahydrate (5.05 g, 16.02 mmol) in water (15 mL) was added. The reaction mixture was stirred for a further 30 minutes and then filtered by gravity (twice). A solution of boric acid (9.90 g, 160.2 mmol) in water (10 mL) was added to the filtrate and the solution was stirred at room temperature for 3 hours. The volume of the solution was reduced to 20 mL by using a rotary evaporator. The solution was distributed over a few small vials and left for 10 days to yield bright blue crystals of **23** (4.80 g, 53%). M.p. = 243-245 °C (dec.). $\chi_m = 1320 \times 10^{-6} \text{ cm}^3 \text{ mol}^{-1}$. $\text{C}_6\text{H}_{34}\text{B}_6\text{CuN}_2\text{O}_{19}$. *Anal.* Calc.: C = 12.7%, H = 6.1%, N = 4.9%. Found: C = 12.8%, H = 6.2%, N = 5.0%. $^{11}\text{B/ppm}$: 15.3. IR (KBr/ cm^{-1}): 3399(s), 2926(w), 1638(w), 1470(m), 1419(s), 1366(s), 1133(s), 1086(s), 1037(s), 953(s), 902(m), 852(m), 809(s), 694(w), p-XRD d-spacing/Å (% rel. int.): 8.57 (100), 7.75 (66), 7.04 (28), 5.75 (75), 4.29 (28), 2.03 (48), 1.22 (30). TGA: 70-180 °C, loss of six interstitial H_2O : 19.4% (19.1% calc.); 180-250 °C, condensation of polyborate which loss of three further H_2O : 28.6% (28.6% calc.); 250-650 °C, oxidation of organic content 48.1% (49.2% calc.); residual $\text{CuB}_6\text{O}_{10}$ 51.9% (50.8% calc.).

6.5.5 Preparation of $[\text{Cu}(\text{dach})_2(\text{H}_2\text{O})_2][\text{Cu}(\text{dach})_2][\text{B}_7\text{O}_9(\text{OH})_5]_2 \cdot 4\text{H}_2\text{O}$ (24)

The preparation of $[\text{Cu}(\text{dach})_2(\text{H}_2\text{O})_2](\text{OH})_2$ was carried out following the same method as described previously in the preparation of **6** from **17** (1.00 g, 2.5 mmol) and Dowex (30 g). Boric acid (1.55 g, 25 mmol) was added to the $\text{H}_2\text{O}/\text{MeOH}$ solution which was gently warmed with stirring for 3 hours. The solution volume was reduced to 5 mL using a rotary evaporator. The product was collected by filtration and allowed to dry overnight in an oven at 40 °C to yield purple crystals of **24** (0.84 g, 52%). M.p. = 263-265 °C (dec.). $\chi_m = 1145 \times 10^{-6} \text{ cm}^3 \text{ mol}^{-1}$. $\text{C}_{12}\text{H}_{39}\text{B}_7\text{CuN}_4\text{O}_{17}$. *Anal.* Calc.: C = 22.2%, H = 6.0%, N = 8.6%. Found: C = 22.0%, H = 6.1%, N = 8.5%. $^{11}\text{B/ppm}$ 14.7. IR (KBr/ cm^{-1}): 3480(s), 3304(s), 3245(s), 2931(s), 2863(m), 1603(w), 1468(m), 1454(s), 1350(s), 1183(s), 1134(s), 1059(s), 987(w), 949(w), 919(w), 854(s), 815(s), 686(w). p-XRD d-spacing/Å (% rel. int.): 10.80 (71), 9.76 (100), 6.27 (45), 5.95 (36), 5.31 (36), 4.25 (40), 3.77 (41). TGA: 70-190 °C, loss of four interstitial H_2O : and two coordinate H_2O : 9.0% (8.3% calc.); 190-250 °C, condensation of polyborate which loss of five further H_2O : 16.0% (15.2% calc.); 250-650 °C, oxidation of organic content 51.0% (50.4% calc.); residual $\text{CuB}_7\text{O}_{11.5}$ 49.0% (49.6% calc.).

6.5.6 Preparation of [Cu(tn)₂][B₅O₆(OH)₄][B₃O₃(OH)₄]·2B(OH)₃·2H₂O (25)

The preparation of [Cu(tn)₂](OH)₂ was carried out following the same method as described previously in the preparation of **20** from **18** (1.10 g, 3.57 mmol) and barium hydroxide (1.13 g, 3.57 mmol). Boric acid (2.20 g, 35.7 mmol) was added to the filtrate solution. After stirring for 30 minutes the solution volume was concentrated to 5 mL by gentle evaporation on a warm water bath. The crude precipitate was collected by filtration and recrystallized using a water/ethanol solution. The product was collected by filtration and carefully washed with cold water and then acetone and then dried at 40 °C for 1 hour to yield blue crystals **25** (1.20 g, 52%). M.p. = 277-278 °C (dec.). $\chi_m = 1365 \times 10^{-6} \text{ cm}^3 \text{ mol}^{-1}$. CuC₆H₃₈O₂₅N₄B₁₀. *Anal. Calc.*: C = 10.1%, H = 5.4%, N = 7.6%. Found: C = 9.8%, H = 5.2%, N = 7.6%. ¹¹B/ppm: 16.7. IR (KBr/cm⁻¹): 3385(s), 3333(s), 2961(w), 1615(w), 1405(m), 1362(s), 1114(s), 1086(s), 1041(sh), 954(m), 911(w), 809(s), 696(w), 626(w). p-XRD d-spacing/Å (% rel. int.): 4.95 (99), 4.83 (100), 3.47 (34). TGA: 70-200 °C, loss of two interstitial H₂O: 5.8% (4.9% calc.); 200-250 °C, condensation of polyborate which loss of seven further H₂O: 21.8% (21.9% calc.); 250-850 °C, oxidation of organic content 42.5% (42.1% calc.); residual CuB₁₀O₁₆ 57.5% (57.9% calc.).

6.5.7 Preparation of [Cu(tn)₂][B₄O₅(OH)₄]·B(OH)₃·6H₂O (26)

The preparation of [Cu(tn)₂](OH)₂ was carried out exactly in the same method as described for the preparation of **20** from **18** (1.00 g, 3.57 mmol) and barium hydroxide (1.13 g, 3.57 mmol). Boric acid (1.10 g, 17.85 mmol) was added to the filtrate solution. After stirring for 30 minutes the solution volume was concentrated to 5 mL by gently evaporation on a warm water bath. The crude product was collected by filtration and recrystallized by using water/ethanol solution to yield navy crystals of **26** (0.45 g, 22%). M.p. = 270-272 °C (dec.). C₆H₃₉B₅CuN₄O₁₈. *Anal. Calc.*: C = 12.6%, H = 6.9%, N = 9.8%. Found: C = 12.9%, H = 6.8%, N = 9.5%. ¹¹B/ppm: 14.4. IR (KBr/cm⁻¹): 3429(s), 3350(s), 2961(s), 1626(w), 1450(s), 1403(s), 1380(m), 1164(m), 1112(m), 1027(s), 933(m), 873(w), 818(m), 708(w), 671(w). TGA: 70-200 °C, loss of six interstitial H₂O: 17.0% (18.8% calc.); 200-300 °C, condensation of polyborate which loss of seven further H₂O: 27.1% (29.8% calc.); 300-700 °C, oxidation of organic content 55.5% (55.8% calc.); residual CuB₅O_{8.5} 44.5% (44.2% calc.).

6.5.8 [Cu(N,N-dmen)₂(H₂O)]₂[B₅O₆(OH)₄]₂·3H₂O (27)

[Cu(N,N-dmen)₂]Cl₂ (1.00 g, 3 mmol), and Ag₂O (0.746 g, 3 mmol) were rapidly stirred in H₂O (25 mL) at room temperature for 30 minutes and the precipitate which had formed (AgCl) was removed by filtration. B(OH)₃ (1.99 g, 32 mmol) was added to the dark blue filtrate and left to stir for a further 30 mins. The reaction mixture was filtered twice by gravity and the filtrate was placed in small vials and left to allow for slow evaporation of solvent. After 12 h, purple crystals of **27** had formed and these were collected by filtration and dried in desiccator (1.19 g, 53%). M.p. = > 300 °C. $\chi_m = 820 \times 10^{-6} \text{ cm}^3 \text{ mol}^{-1}$. C₈H₄₀CuN₄B₁₀O₂₄. *Anal.* Calc.: C = 12.8%, H = 5.4%, N = 7.5%. Found: C = 13.0%, H = 5.3%, N = 7.3. ¹¹B/ppm 16.5. IR (KBr/cm⁻¹): 3587 (m), 3336 (m), 3271 (m), 1614 (w), 1421 (s), 1308 (s), 1158 (m), 1125 (m), 1065 (m), 1017 (m), 918 (m), 812 (w), 776 (m), 708 (m), 529 (w), 479 (w). P-XRD: d-spacing/Å (% rel. int.): 6.67 (15.82), 5.71 (100.00), 5.51 (12.12), 4.54 (24.80), 3.73 (40.37), 3.34 (11.56), 2.03 (13.06). TGA: 30-90 °C, loss of three interstitial and one coordinated H₂O: 9.8% (9.6% calc.); 90-250 °C, condensation of polyborate which loss of four further H₂O: 21.3% (19.2% calc.); 250-630 °C, oxidation of organic content 45.1% (42.7% calc.); residual CuB₁₀O₁₆ 54.9% (57.3% calc.).

6.5.9 [Cu(N,N-dmen){B₆O₇(OH)₆}]·4H₂O (28)

[Cu(N,N-dmen)₂]Cl₂ (1.00 g, 3 mmol) was dissolved in H₂O (25 ml) to a dark blue solution. Dowex monosphere 550A ion exchange resin (60 g) was added to the solution which was left to stir for 24 hours. The ion exchange resin was removed by filtration and B(OH)₃ (1.99 g, 30 mmol) was added to the filtrate which was then left to stir for 30 minutes. The dark blue reaction mixture was filtered into vials and left to allow for slow evaporation of H₂O to occur. After 1 week, the blue crystals of **28** which had formed and were collected filtration (0.61 g, 41%). M.p.= > 300 °C. $\chi_m = 880 \times 10^{-6} \text{ cm}^3 \text{ mol}^{-1}$. C₄H₂₆CuN₂B₆O₁₇. *Anal.* Calc.: C = 9.5%, H = 5.2%, N = 5.6%. Found: C = 9.7%, H = 5.2%, N = 5.5%. ¹¹B/ppm 16.9. IR (KBr/cm⁻¹): 3340 (b), 3254 (b), 2931 (w), 2859 (w), 2814 (w), 1641 (w), 1586 (w), 1467 (sh), 1423 (s), 1366 (s), 1269 (s), 1137 (s), 1091 (s), 1052 (s), 1007 (m), 958 (m), 892 (m), 859 (m), 808 (s), 784 (m), 694 (m), 574 (w). P-XRD d-spacing/Å (% rel. int.): 10.87 (100.00), 8.64 (24.76), 7.30 (27.96), 3.65 (22.86). TGA: 30-120 °C, loss of four interstitial H₂O: 14.2% (14.3% calc.); 120-250 °C, condensation of polyborate which loss of three further H₂O: 26.0% (25.0% calc.); 250-650 °C, oxidation of organic content 44.3% (22.5% calc.); residual CuB₆O₁₀ 55.7% (57.5% calc.).

6.6 Preparation of nickel(II) complexes

6.6.1 Preparation of [Ni(en)₃]Cl₂·2H₂O (29)

Compound **29** was prepared as described in the literature.¹⁸⁵ Nickel(II) chloride hexahydrate (5.75 g, 24.19 mmol) was dissolved in distilled water (25 mL) and then ethylenediamine (7.00 g, 70%, 81.25 mmol) was added to the nickel solution. The reaction mixture was stirred at room temperature for 2 hours, then gently evaporated on steam bath to 10 mL. Two drops of ethylene diamine were added. The solution was cooled in an ice bath and the crude product was collected by filtration and recrystallized from distilled water to yield purple crystals of **29** (6.50 g, 78%). M.p. = 243-245 °C (dec.). $\chi_m = 3390 \times 10^{-6} \text{ cm}^3 \text{ mol}^{-1}$. IR (KBr/cm⁻¹): 3294(s), 3246(s), 3158(s), 2960(m), 2878(m), 1588(m), 1457(m), 1369(m), 1331(m), 1273(m), 1155(m), 1102(m), 1029(s), 860, 668(s), 524(m), 501(m). [Lit. 3250, 2940-2875, 1587, 1457, 1369, 1330, 1275, 1140-1118-1100, 1026-974, 865, 662, 522].¹⁹³

6.6.2 Preparation of [Ni(AEN)]Cl·H₂O (30)

Compound **30** was prepared as described in the literature.¹⁸⁶ The 2,4-dimethyl-1-(3-azapropyl)-1,5,8-triazaocta-2,4-dienato (AEN) ligand was synthesized by dissolving ethylene diamine (12.00 g, 200 mmol) and acetyl acetone (10.00 g, 100 mmol) in acetic acid (400 mL, 20%). The reaction mixture was left for 24 hours and a solution of nickel(II) chloride hexahydrate (23.80 g, 100 mmol) in distilled water (100 mL) was added. The reaction mixture was stirred vigorously and during the stirring sodium hydroxide (175 g, 4.37 mol) was steadily added. The solution was left overnight, and then the reaction mixture was gently heated to redissolve the crude product. The hot solution was filtered and the solution was cooled for 24 hours at 0 °C to yield red crystals of **30** (8.40 g, 29%). M.p. = 242-244 °C (dec.). $\chi_m = -56 \times 10^{-6} \text{ cm}^3 \text{ mol}^{-1}$. NiC₉H₂₁ON₄Cl. Anal. Calc.: C = 36.5%, H = 7.1%, N = 18.9%. Found: C = 37.1%, H = 6.7%, N = 18.8%. ¹H/ppm: 2 (s, 6H, CH₃), 2.5 (s, 4H, CH₂ of en), 3.2 (s, 4H, CH₂ of en), and 4.8 (s, 7H, NH₂, H₂O, CH). ¹³C{¹H}/ppm: 20.1, 43.2, 53.6, 160.8. IR (KBr/cm⁻¹): 3447(s), 3250(m), 3172(s), 3080(s), 2983(m), 2945(m), 2888(w), 2822(s), 1613(w), 1558(s), 1527(s), 1475(s), 1439(s), 1420(s), 1330(s), 1276(s), 1149(s), 1089(s), 1031(s), 732(m), 570(w).

6.6.3 Preparation of [Ni(*trans*-dach)₂(H₂O)₂]Cl₂ (31)

Compound **31** was prepared as described in the literature¹⁸⁷ by adding excess amount of the mixture *cis* and *trans*-1,2-diaminocyclohexane (*dach*) ligand (2.88 g, 25.24 mmol) to a solution of nickel(II) chloride hexahydrate (2.00 g, 8.41 mmol) in water (15 mL). The solution was stirred for 2 hours and then cooled in an ice bath for two hours. The resulting crystals which formed over the cooling period were filtered, washed with cold distilled water and dried at 40 °C. The crude product was re-crystallized from hot water to yield violet crystals of **31** (1.30 g, 40%). M.p. = 253-255 °C (dec.). $\chi_m = 3040 \times 10^{-6} \text{ cm}^3 \text{ mol}^{-1}$. IR (KBr/cm⁻¹): 3459(s), 3342(s), 3278(s), 3262(sh), 3158(m), 2932(s), 2857(m), 1583(m), 1450(m), 1401(w), 1164(w), 1120(m), 1017(s), 985(m), 924(w), 860(w), 670(m), and 656(m). [Lit. 3340, 3260, 3180, 1605, 669, 661].¹⁹⁶

6.6.4 Preparation of [Ni(hn)₂]Cl₂ (32)

Compound **32** was synthesized by a method analogous to that described for [Ni(hn)₃]Br₂.¹⁸⁸ *N*-hydroxy ethyl ethylenediamine (*hn*) (2.63 g, 25.2 mmol) was added to an aqueous solution of nickel(II) chloride hexahydrate (3.00 g, 12.6 mmol) in distilled water (15 mL). The solution was stirred for 2 hours at room temperature. The solution volume was reduced by gently evaporation on a warm water bath and then cooled in an ice bath. The resulting crystals were filtered, washed with cold H₂O/EtOH and dried at 50 °C to yield purple crystals of **32** (4.40 g, 79%). M.p. = 174-175 °C (dec.). $\chi_m = 3200 \times 10^{-6} \text{ cm}^3 \text{ mol}^{-1}$. IR (KBr/cm⁻¹): 3390(s), 3304(s), 3275(s), 3237(s), 3188(s), 3166(s), 3050(sh), 2976(sh), 2921(s), 2874(s), 2807(m), 1596(s), 1470(s), 1457(s), 1442(s), 1408(m), 1397(m), 1357(m), 1330(s), 1313(s), 1281(w), 1237(w), 1201(w), 1107(s), 1090(s), 1063(s), 1041(s), 1024.7(s), 982(s), 907(m), 889(m), 881(m), 859(s), 820(m), 790.1(m), 671(m), 646(m), 631(m). [Lit. 3315(sh), 3232(s), 3160(s), 3070(m)].²⁰⁰

6.6.5 Preparation of [Ni(*dien*)₂]Cl₂·H₂O (33)

Compound **33** was prepared along a previously published procedure.¹⁸⁹ An aqueous solution of nickel(II) chloride hexahydrate (2.00 g, 8.4 mmol) in distilled water (10 mL) was added to an aqueous solution of diethylenetriamine (*dien*) (1.75 g, 17 mmol) in distilled water (10 mL). The reaction mixture was gently heated on water bath with stirring for 30 minutes and

then cooled in an ice bath. The resulting crystals were filtered, washed with cold water and dried at 50 °C. The product was re-crystallized from H₂O/EtOH to yield blue crystals of **33** (1.90 g, 64%). M.p. = 235-237 °C. [Lit. 232-232.5 °C].¹⁹⁴ $\chi_m = 2790 \times 10^{-6} \text{ cm}^3 \text{ mol}^{-1}$. IR (KBr/cm⁻¹): 3436(s), 3422(sh), 3378(sh), 3349(s), 3323(s), 3287(s), 3265(s), 3186(s), 3169(s), 2948(m), 2917(m), 2873(m), 1633(w), 1586(s), 1489(w), 1475(m), 1449(s), 1385(m), 1333(sh), 1322(s), 1315(m), 1282(w), 1252(m), 1145(m), 1093(s), 1060(s), 1027(sh), 1013(s), 980(s), 909(w), 890(s), 865(w), 825(w). [Lit. 3420(s), 3378(s), 3340(m), 3315(s), 3278(s), 3255(s), 3180(s), 3160(s), 1490(w), 1475(w), 1450(m), 1380(w), 1333(m), 1322(m), 1315(w), 1264(w), 1131(m), 1098(m), 1078(s), 1048(s), 1027(sh), 1014(s), 980(s), 910(w), 892(s), 867(w), 827(w)].²⁰¹

6.6.6 Preparation of [Ni(pn)₃]Cl₂·2H₂O (34)

Compound **34** was prepared as described in the literature.¹⁸⁵ To a solution of nickel(II) chloride hexahydrate (5.75 g, 24.19 mmol) in distilled water (25 mL) was added propylenediamine (pn) (6.00 g, 80.94 mmol). The reaction mixture was stirred at room temperature for 2 hours and then gently evaporated on a steam bath to (10 mL). Propylenediamine (1 mL) was added to the reaction mixture. The solution was cooled in an ice bath, and the crude product was collected by filtration and recrystallized by distilled water to yield purple crystals of **34** (7.10 g, 76%). M.p. = 247-248 °C (dec.). $\chi_m = 3010 \times 10^{-6} \text{ cm}^3 \text{ mol}^{-1}$. NiC₉H₃₄O₂N₆Cl₂. *Anal.* Calc.: C = 27.9%, H = 8.8%, N = 21.7%. Found: C = 28.1%, H = 8.9%, N = 21.7%. IR (KBr/cm⁻¹): 3725(sh), 3435(s), 3257(vs), 3165(s), 2965(s), 2940(s), 2878(s), 1598(s), 1461(s), 1394(s), 1375(s), 1307(m), 1269(w), 1202(m), 1158(s), 1074(m), 1047(s), 1019(vs), 934(m), 838(m), and 645(s). [Lit. 3743(w), 3449(w), 3256(vs), 3141(m), 2955(m), 2925(m), 2863(m), 1566(vs), 1450(m), 1381(vs), 1304(w), 1265(w), 1196(w), 1142(w), 1065(m), 1011(vs), 926(w), 825(w), and 640(m)].²⁰²

6.6.7 Preparation of [Ni₂(trien)₃]Cl₄·2H₂O (35)

Compound **35** was prepared as described in the literature.¹⁹⁰ To a solution of nickel(II) chloride hexahydrate (5.00 g, 21.04 mmol) in distilled water (25 mL) was added triethylenetetramine (trien) (6.14 g, 41.99 mmol). The solution mixture was stirred at room temperature for 2 hours, then the solution was evaporated on a steam bath to dryness. The crude product was collected and washed using a mixture of methanol (40 mL) and ether (20 mL). The

crude product was recrystallized by MeOH/ether mixture. The product was dried in an oven at 65 °C for 3 hours to yield light pink crystals of **35** (5.10 g, 66%). M.p. = 248-250 °C (dec.). $\chi_m = 2906 \times 10^{-6} \text{ cm}^3 \text{ mol}^{-1}$. $\text{NiC}_{18}\text{H}_{58}\text{O}_2\text{N}_{12}\text{Cl}_4$. *Anal.* Calc.: C = 29.5%, H = 8.0%, N = 22.9%. Found: C = 29.6%, H = 8.1%, N = 22.4%. IR (KBr/cm⁻¹): 3368(s), 3323(s), 3239(s), 3159(s), 2932(m), 2879(m), 1653(w), 1596(w), 1462(m), 1335(m), 1134(m), 1086(s), 1064(s), 1016(m), 966(s). UV-Vis λ/nm : 350, 540, 880. [Lit. 346, 539].²⁰³ [Lit. 353, 535, 877].²⁰⁴

6.7 Preparation of nickel(II) complex polyborate salts

6.7.1 Preparation of [Ni(en)₃] [B₅O₆(OH)₄]₂·2H₂O (36)

Compound **36** was prepared by a modified literature method.¹¹⁵ The preparation of [Ni(en)₃](OH)₂ was carried out as described previously for the preparation of **6** from **29** (0.92 g, 2.66 mmol) and Dowex (40 g). Boric acid (1.64 g, 26.6 mmol) was added to the aqueous solution which was then gently warmed with stirring for 3 hours. A rotary evaporator was used to reduce the volume of the solution to 5 mL and the resulting solution was sealed in a Teflon lined stainless steel autoclave, and heated at 140 °C for 3 days. The crystals were collected by filtration and left overnight to dry in a desiccator to yield light blue crystals of **36** (1.20 g, 63%). M.p. = 294-295 °C (dec.). $\chi_m = 2844 \times 10^{-6} \text{ cm}^3 \text{ mol}^{-1}$. ¹¹B/ppm: 13.4 (16%), 16.1 (84%). IR (KBr/cm⁻¹): 3344(s), 3297(s), 2947(w), 1607(w), 1407(s), 1314(s), 1168(m), 1026(s), 921(s), 851(w), 775(m), 706(w), 668(w), 484(w). [Lit. 3426, 3352, 3299, 2952, 1622, 1407, 1317, 923, 1168, 1025, 851, 775, 713, 478].¹¹⁵ p-XRD d-spacing/Å (% rel. int.): 6.12 (36), 5.75 (62), 5.55 (100), 4.30 (22), 3.93 (26), 3.86 (35), 3.71 (54). TGA: 70-180 °C, loss of two interstitial H₂O: 4.9% (5.1% calc.); 180-280 °C, condensation of polyborate which loss of four further H₂O: 15.0% (15.2% calc.); 280-800 °C, oxidation of organic content 38.1% (40.6% calc.); residual NiB₁₀O₁₆ 61.9% (59.4% calc.).

6.7.2 Preparation of [Ni(en){B₆O₇(OH)₆}(H₂O)₂]·H₂O (37)

An aqueous solution of ethylenediamine ligand (2.30 g, 70%, 26.79 mmol) was added to an aqueous solution of nickel(II) sulphate hexahydrate (2.12 g, 8.06 mmol) in water (10 mL). The reaction mixture was stirred for 5 minutes, then a solution of barium hydroxide octahydrate (2.54 g, 8.06 mmol) in water (10 mL) was added. The reaction mixture was stirred for 30 minutes and then filtered. A solution of boric acid (3.48 g, 56.42 mmol) in water (10 mL) was

added to the filtrate with stirring. The reaction mixture was stirred at room temperature for 2 hours. The solution was then distributed in several aliquots (vials) and left for 10 days to yield faint blue crystals of **37** (1.20 g, 33%). M.p. = 245-247 °C (dec.). $\chi_m = 2588 \times 10^{-6} \text{ cm}^3 \text{ mol}^{-1}$. $\text{C}_2\text{H}_{20}\text{B}_6\text{NiN}_2\text{O}_{16}$. *Anal. Calc.*: C = 5.3%, H = 4.5%, N = 6.2%. found: C = 5.4%, H = 4.5%, N = 6.2%. $^{11}\text{B/ppm}$: 17.7. IR (KBr/ cm^{-1}): 3400(s), 3350(s), 2924(w), 2854(w), 1600(w), 1420(m), 1380(s), 1360(s), 1133(s), 1095(s), 1044(s), 955(m), 908(m), 852(w), 809(s), 696(w), 537(w), 427(w). p-XRD d-spacing/Å (% rel. int.): 9.78 (100), 8.26 (24), 6.77 (53), 4.88 (48), 3.99 (34), 3.38 (30), 2.74 (47). TGA: 100-180 °C, loss of one interstitial H_2O : and two coordinated water molecules 0.8% (12% calc.); 180-280 °C, condensation of polyborate which loss of three further H_2O : 24.3% (23.9% calc.); 280-700 °C, oxidation of organic content 38.6% (37.2% calc.); residual $\text{NiB}_6\text{O}_{10}$ 61.4% (62.8% calc.).

6.7.3 Preparation of [Ni(AEN)] [B₅O₆(OH)₄]·H₂O (38)

The replacement of chloride in **38** with hydroxide was carried out as described previously in the preparation of **6** from **30** (2.10 g, 7.2 mmol) and Dowex (25 g). Boric acid (2.22 g, 36 mmol) was added to the aqueous solution which was gently warmed with stirring for 3 hours. A rotary evaporator was used to reduce the solution volume to 5 mL. The solution was then distributed in a few NMR tubes for crystallization and left for 10 days to yield dark red crystals of **38** (1.30 g, 38%). M.p. = 279-280 °C (dec.). $\chi_m = -170 \times 10^{-6} \text{ cm}^3 \text{ mol}^{-1}$. $\text{C}_9\text{H}_{25}\text{B}_5\text{NiN}_4\text{O}_{11}$. *Anal. Calc.*: C = 22.6%, H = 5.3%, N = 11.7%. Found: C = 22.7%, H = 5.4%, N = 11.7%. $^1\text{H/ppm}$: 2 (s, 6H, CH_3), 2.5 (t, 4H, $J = 6 \text{ Hz}$, CH_2 of en), 3.2 (t, 4H, $J = 6 \text{ Hz}$, CH_2 of en), 4.8 (s, 11H, NH_2 , H_2O , OH, CH), $^{13}\text{C}\{^1\text{H}\}/\text{ppm}$: 19.9, 43, 53.6, 160.5. $^{11}\text{B/ppm}$: 16.3. IR (KBr/ cm^{-1}): 3601(m), 3377(s), 3326(s), 3288(s), 3246(s), 3169(s), 2983(w), 2963(w), 1615(m), 1566(m), 1536(m), 1476(s), 1442(s), 1416(s), 1393(s), 1333(s), 1295(s), 1129(m), 1094(s), 1072(m), 1019(m), 924(s), 820(w), 778(m), 747(w), 725(w), 708(w). p-XRD d-spacing/Å (% rel. int.): 5.65 (69), 5.38 (100), 4.14 (46), 3.89 (33), 3.81 (53), 3.65 (58), 2.03 (41), 1.43 (33). TGA: 100-180 °C, loss of one interstitial H_2O : 2.5% (3.7% calc.); 180-280 °C, condensation of polyborate which loss of two further H_2O : 10.0% (11.3% calc.); 280-700 °C, oxidation of organic content 46.1% (48.0% calc.); residual $\text{NiB}_5\text{O}_{8.5}$ 53.9% (52.0% calc.).

6.7.4 Preparation of [Ni(dach)₂(H₂O)₂][Ni(dach)₂][B₇O₉(OH)₅]₂·4H₂O (39)

The replacement of chloride in **39** by hydroxide was carried out as described previously in the preparation of **6** from **31** (1.00 g, 2.53 mmol) and Dowex (40 g). Boric acid (1.56 g, 25.3 mmol) was added to the solution which was then gently warmed with stirring for 3 hours. The solution volume was reduced to 5 mL using a rotary evaporator. The product was isolated by filtration, and then allowed to dry in an oven at 40 °C for 3 hours to yield orange prismatic crystals of **39** (0.78 g, 47%). M.p. = 270-272 °C (dec.). $\chi_m = 3030 \times 10^{-6} \text{ cm}^3 \text{ mol}^{-1}$. C₂₄H₇₈B₁₄N₈Ni₂O₃₄. Anal. Calc.: C = 22.3%, H = 6.1%, N = 8.7%. Found: C = 21.8%, H = 6.3%, N = 8.4%. ¹¹B/ppm: 15.8. IR (KBr/cm⁻¹): 3663(s), 3271(s), 2929(m), 2863(m), 1603(w), 1468(m), 1453(s), 1350(s), 1180(s), 1125(m), 1066(s), 986(w), 948(w), 918(w), 854(m), 807(m), 716(w), 685(w). p-XRD d-spacing/Å (% rel. int.): 10.67 (100), 9.81 (89), 6.25 (58), 5.35 (70), 4.26 (48), 3.74 (55), 2.03(59). TGA: 100-190 °C, loss of four interstitial and two coordinated H₂O: 7.5% (8.4% calc.); 190-270 °C, condensation of polyborate which loss of five further H₂O: 15.0% (15.3% calc.); 270-720 °C, oxidation of organic content 48.2% (50.7% calc.); residual Ni₂B₁₄O₂₃ 51.8% (49.3% calc.).

6.7.5 Preparation of [Ni(hn)₂][B₅O₆(OH)₄]₂ (40)

The preparation of [Ni(hn)₂](OH)₂ was carried out as described previously in the preparation of **6** from **32** (1.00 g, 2.95 mmol) and Dowex (40 g). Boric acid (1.83 g, 29.6 mmol) was added with stirring. The reaction mixture was stirred for a further 2 hours at room temperature. The solvent was then evaporated to 5 mL using a rotary evaporator, then the resulting solution was left for 10 days in a few NMR tubes for crystallization to yield purple crystals of **40** (0.76 g, 37%). M.p. = 288-289 °C (dec.). $\chi_m = 3430 \times 10^{-6} \text{ cm}^3 \text{ mol}^{-1}$. C₈H₃₂B₁₀NiN₄O₂₂. Anal. Calc.: C = 13.7%, H = 4.6%, N = 8.0%. Found: C = 13.7%, H = 4.7%, N = 8.0%. ¹H/ppm: 2.8 (m, 4H, CH₂), 2.9 (m, 4H, CH₂), 3 (m, 4H, CH₂), 3.6 (m, 4H, CH₂) 4.8 (s, 16H, NH₂, OH). ¹³C{¹H}/ppm: 37.9, 46.1, 49.5, 58.9. ¹¹B/ppm: 1.2 (3%), 13.4 (23%), 18.0 (74%). IR (KBr/cm⁻¹): 3375(s), 3288(s), 3322(s), 2962(w), 1410(s), 1321(s), 1196(m), 1141(s), 1022(s), 980(w), 919(s), 846(w), 774(s), 722(w), 706(s), 669(w). p-XRD d-spacing/Å (% rel. int.): 6.18 (40), 5.88 (75), 5.50 (100), 3.94 (26), 3.78 (38), 3.66 (25). TGA: 230-290 °C, condensation of polyborate which loss of four H₂O: 10.3% (10.2% calc.); 290-700 °C, oxidation of organic content 37.9% (39.9% calc.); residual NiB₁₀O₁₆ 62.1% (60.1% calc.).

6.7.6 Preparation of *s-fac*-[Ni(dien)₂][B₅O₆(OH)₄]₂ (41)

The preparation of [Ni(dien)₂](OH)₂ was carried out as described previously for the preparation of **6** from **33** (1.05 g, 2.97 mmol) and Dowex (40 g). Boric acid (1.83 g, 29.7 mmol) was added to the H₂O/MeOH solution which was then gently warmed with stirring for 3 hours. The solution was concentrated to 5 mL using a rotary evaporator and the concentrated solution was left few days for crystallization. The produced crystals were carefully recovered by filtration and dried in air to yield purple crystals of **41** (0.70 g, 34%). M.p. = 287-289 °C (dec.). $\chi_m = 3516 \times 10^{-6} \text{ cm}^3 \text{ mol}^{-1}$. C₈H₃₄B₁₀NiN₆O₂₀. *Anal. Calc.*: C = 13.7%, H = 4.9%, N = 12.0%. Found: C = 14.0%, H = 5.4%, N = 12.1%. ¹¹B/ppm: 1.5 (1%), 13.3 (13%), 17.4 (86%). IR (KBr/cm⁻¹): 3362(s), 3333(s), 3297(s), 3263(s), 2988(w), 2950(w), 2903(w), 1615(w), 1594(w), 1412(s), 1330(s), 1303(s), 1186(w), 1135(m), 1059(m), 1042(m), 1028(m), 964(m), 931(m), 915(s), 809(w), 774(s), 772(m), 707(s), 677(w). p-XRD d-spacing/Å (% rel. int.): 6.22 (24), 5.88 (100), 5.57 (94), 4.27 (15), 3.79 (19), 3.71 (28), 2.94 (17). TGA: 100-200 °C, condensation of polyborate which loss of four H₂O: 14.9% (10.2% calc.); 200-650 °C, oxidation of organic content 40.3% (39.7% calc.); residual NiB₈O₁₃ 59.7% (60.3% calc.).

6.7.7 Preparation of [Ni(pn)₃][B₅O₆(OH)₄]₂·C₂H₅OH·5H₂O (42)

The preparation of [Ni(pn)₃](OH)₂ was carried out exactly in the same method as described previously for the preparation of **6** from **34** (1.55 g, 4 mmol) and Dowex (40 g). Boric acid (2.47 g, 40 mmol) was added to the aqueous solution which was gently warmed with stirring for 2 hours. A rotary evaporator was used to reduce the volume of the solution to 5 mL and the resulting mixture was sealed in a Teflon lined stainless steel autoclave, and heated at 140 °C for 5 days. The crystals which had formed were isolated by filtration, and left overnight to dry in a desiccator as yield light grey bluish crystals of **42** (1.60 g, 47%). M.p. = 289-290 °C (dec.). $\chi_m = 2810 \times 10^{-6} \text{ cm}^3 \text{ mol}^{-1}$. NiC₁₁H₅₄O₂₆N₆B₁₀. *Anal. Calc.*: C = 15.5%, H = 6.3%, N = 9.9%. Found: C = 15.5%, H = 6.6%, N = 10.0%. ¹H/ppm: 1.1 (m, 9H, CH₃ of pn), 1.2 (t, 3H, *J* = 1.2 Hz, *J* = 2.4 Hz, CH₃ of EtOH), 2.8 (m, 3H, CH of pn), 3.2 (m, 2H, CH₂ of EtOH), 3.6 (d, 6H, *J* = 6 Hz, CH₂ of pn), and 4.8 (s, 30H, NH₂, H₂O, OH). ¹³C{¹H}/ppm: 39.5. ¹¹B/ppm: 1.5 (2%), 13.8 (20%), and 16.8 (78%). IR (KBr/cm⁻¹): 3336(s), 3235(s), 2974(w), 1593(m), 1434(s), 1305(s), 1156(s), 1080(m), 1044(s), 1015(s), 916(s), 820(w), 777(s), 723(m), 708(m), 464(w). p-XRD d-spacing/Å (% rel. int.): 8.40 (39), 5.62 (48), 5.39 (43), 4.35 (40), 3.61 (100), 2.03 (66), 1.22 (36). TGA: 100-160 °C, loss of five interstitial H₂O: and C₂H₅OH 17.0% (16.0%

calc.); 160-260 °C, condensation of polyborate which loss of four further H₂O: 23.4% (24.3% calc.); 260-900 °C, oxidation of organic content 48.8% (50.5% calc.); residual NiB₁₀O₁₆ 51.2% (49.5% calc.).

6.7.8 Preparation of [Ni₂(trien)₃][B₅O₆(OH)₄]₂Cl₂·CH₃OH·6H₂O (43)

The preparation of [Ni(trien)₃](OH)₂ was carried out as described previously for the preparation of **6** from **35** (2.00 g, 2.72 mmol) and Dowex (20 g). Boric acid (1.68 g, 27.2 mmol) was added to the aqueous solution which was gently warmed with stirring for 3 hours. A rotary evaporator was used to reduce the volume of the solution to 5 mL and the final mixture was sealed in a Teflon lined stainless steel autoclave and heated at 140 °C for 4 days. The crystals which had formed were isolated by filtration, and left overnight to dry in a desiccator to afford light purple crystals of **43** (0.90 g, 28%). M.p. = 287-288 °C (dec.). $\chi_m = 3125 \times 10^{-6} \text{ cm}^3 \text{ mol}^{-1}$. NiC₁₃H₄₈O₂₁N₈B₁₀. *Anal.* Calc.: C = 19.0%, H = 6.5%, N = 14.0%. Found: C = 18.9%, H = 6.3%, N = 13.7%. ¹¹B/ppm: 1.2 (3%), 13.8 (30%), and 16.5 (67%). IR (KBr/cm⁻¹): 3290(s), 3238(s), 2951(w), 1410(s), 1313(s), 1163(m), 1057(m), 1022(m), 920(s), 822(w), 773(m), 705(m), 490(m). p-XRD d-spacing/Å (% rel. int.): 6.13 (20), 5.79 (100), 5.49 (12), 3.98 (14), 3.76 (22), 3.52 (13). TGA: 100-160 °C, loss of interstitial CH₃OH and six H₂O: 10.2% (11.6% calc.); 160-240 °C, condensation of polyborate which loss of four H₂O: 17.9% (17.6% calc.); 240-700 °C, oxidation of organic content 54.9% (54.1% calc.); residual Ni₂B₁₀O₁₆Cl₂ 45.2% (46.0% calc.).

References

- 1 M. A. Beckett, *Coord. Chem. Rev.*, 2016, **323**, 2–14.
- 2 S. Merlino and F. Sartori, *Science*, 1971, **171**, 377–379.
- 3 D. M. Schubert, M. Z. Visi and C. B. Knobler, *Inorg. Chem.*, 2000, **39**, 2250–2251.
- 4 M. A. Beckett, P. N. Horton, M. B. Hursthouse, D. A. Knox and J. L. Timmis, *Dalton Trans.*, 2010, **39**, 3944–3951.
- 5 M. A. Beckett, S. J. Coles, R. A. Davies, P. N. Horton and C. L. Jones, *Dalton Trans.*, 2015, **44**, 7032–7040.
- 6 M. A. Beckett, P. N. Horton, S. J. Coles and D. W. Martin, *Inorg. Chem.*, 2011, **50**, 12215–12218.
- 7 A. K. De, in *A Text book of Inorganic chemistry*, New Age International, 2007, pp. 88–104.
- 8 A. Hermann, M. Lein and P. Schwerdtfeger, *Angew. Chem. Int. Ed.*, 2007, **46**, 2444–2447.
- 9 H. A. Jahn and E. Teller, *Proc. Roy. Soc. A*, 1937, **161**, 220–235.
- 10 H. A. Jahn, *Proc. Roy. Soc. A*, 1937, **164**, 117–138.
- 11 D. Reinen, M. Atanasov and P. Kohler, *J. Mol. Struct.*, 2007, **838**, 151–156.
- 12 D. Reinen, M. Atanasov, P. Köhler and D. Babel, *Coord. Chem. Rev.*, 2010, **254**, 2703–2754.
- 13 G. H. Searle and F. R. Keene, *Inorg. Chem.*, 1972, **11**, 148–156.
- 14 F. R. Keene and G. H. Searle, *Inorg. Chem.*, 1974, **13**, 2173–2180.
- 15 A. Tatehata and A. Muraida, *Inorg. Chem. Commun.*, 1998, **1**, 392–394.
- 16 E. J. Corey and J. C. Bailar, *J. Am. Chem. Soc.*, 1959, **81**, 2620–2629.
- 17 G. E. Rodgers, in *Descriptive Inorganic Coordination and Solid-State Chemistry*, Cengage Learning, 3rd edn., 2011, pp. 377–378.
- 18 F. H. Nielsen, *J. Trace Elem. Med. Biol.*, 2014, **28**, 383–387.
- 19 F. H. Nielsen and S. L. Meacham, *J. Evid. Based. Complementary Altern. Med.*, 2011, **16**, 169–180.
- 20 C. D. Hunt and J. P. Idoso, *J. Trace Elem. Exp. Med.*, 1999, **12**, 221–233.
- 21 C. D. Hunt, *J. Trace Elem. Exp. Med.*, 2003, **16**, 291–306.
- 22 A. E. Newkirk, *Journal of the Franklin Institute*, 1967, **285**, 238–239.
- 23 P. C. Burns, J. D. Grice and F. C. Hawthorne, *Can. Mineral.*, 1995, **33**, 1131–1151.
- 24 P. C. Burns, *Can. Mineral.*, 1995, **33**, 1167–1176.
- 25 C. L. Christ and J. R. Clark, *Phys. Chem. Miner.*, 1977, **2**, 59–87.
- 26 J. D. Grice and P. C. Burns, *Can. Mineral.*, 1999, **37**, 731–762.
- 27 G. Heller, *Top. Curr. Chem.*, 1968, **131**, 39–89.
- 28 H. X. Liu, Y. X. Liang and X. Jiang, *J. Solid State Chem.*, 2008, **181**, 3243–3247.
- 29 F. Kong, S. P. Huang, Z. M. Sun, J. G. Mao and W. D. Cheng, *J. Am. Chem. Soc.*, 2006, **128**, 7750–7751.
- 30 C. Chen, Y. Wang, B. Wu, K. Wu, W. Zeng and L. Yu, *Nature*, 1995, **373**, 322–324.
- 31 P. Becker, *Adv. Mater.*, 1998, **10**, 979–992.
- 32 H. Lin, W. Qin, J. Zhang and C. Wu, *Solid State Commun.*, 2007, **141**, 436–439.
- 33 T. Justel, H. Nikol and C. Ronda, *Angew. Chem. Int. Ed.*, 1998, **37**, 3084–3103.
- 34 T. P. Hignett and G. H. McClellan, *Dev. Plant Soil Sci.*, 1985, **14**, 237–260.
- 35 J. J. Mortvedt, *Dev. Plant Soil Sci.*, 1985, **14**, 221–235.
- 36 J. A. Duffy, *Geochim. Cosmochim. Acta*, 1993, **57**, 3961–3970.
- 37 K. M. Davis, K. Miura, N. Sugimoto and K. Hirao, *Opt. Lett.*, 1996, **21**, 1729–1731.
- 38 Z. T. Yu, Z. Shi, Y. S. Jiang, H. M. Yuan, J. iH. Chen and C. A. Mater, *Chem. Mater.*, 2002, **14**, 1314–1318.
- 39 D. M. Schubert, F. Alam, M. Z. Visi and C. B. Knobler, *Chem. Mater.*, 2003, **15**, 866–871.

- 40 J. B. Farmer, *Adv. Inorg. Chem. Radiochem.*, 1982, **25**, 187–237.
- 41 Y. E. Anderson, S. K. Filatov, I. G. Polyakova and R. S. Bubnova, *Glas. Phys. Chem.*, 2004, **30**, 450–460.
- 42 P. Becker, P. Held and L. Bohaty, *Cryst. Res. Technol*, 2000, **35**, 1251–1262.
- 43 E. L. Belokoneva, T. A. Borisova and O. V. Dimitrova, *Crystallogr. Reports*, 2003, **48**, 583–590.
- 44 E. L. Belokoneva, O. V. Dimitrova and N. N. Mochenova, *Crystallogr. Reports*, 2009, **54**, 6–12.
- 45 X. Chen, M. Li, J. Zuo, X. Chang, H. Zang and W. Xiao, *Solid State Sci.*, 2007, **9**, 678–685.
- 46 X. Chen, C. Yang, X. Chang, H. Zang and W. Xiao, *J. Alloy. Comp.*, 2010, **492**, 543–547.
- 47 X. Chen, C. Yang, Z. Chu, X. Chang, H. Zang and W. Xiao, *J. Chem. Crystallogr.*, 2011, **41**, 816–822.
- 48 W. A. Harrison, T. E. Gier and G. D. Stucky, *Angew. Chem. Int. Ed. Engl.*, 1993, **32**, 724–726.
- 49 A. G. Ivanova, E. L. Belokoneva, O. V. Dimitrova and N. N. Mochenova, *Crystallogr. Reports*, 2006, **51**, 584–588.
- 50 J. G. Jesudurai, K. Prabha, P. D. Christy, J. Madhavan and P. Sagayaraj, *Spectrochim. Acta. A. Mol. Biomol. Spectrosc.*, 2008, **71**, 1371–1378.
- 51 C. C. Li and J. H. Jean, *J. Am. Ceram. Soc.*, 2002, **85**, 1441–1448.
- 52 L. Li, X. Jin, G. Li, Y. Wang, F. Liao, G. Yao and J. Lin, *Chem. Mater.*, 2003, **15**, 2253–2260.
- 53 L. Li, P. Lu, Y. Wang, X. Jin, G. Li, Y. Wang, L. You and J. Lin, *Chem. Mater.*, 2002, **14**, 4963–4968.
- 54 Z. H. Liu and L. Q. Li, *Cryst. Growth Des.*, 2006, **6**, 1247–1249.
- 55 Z. H. Liu, L. Q. Li and M. Z. Wang, *J. Alloy. Comp.*, 2006, **407**, 334–339.
- 56 C. D. Mcmillen, H. G. Giesber and J. W. Kolis, *J. Cryst. Growth*, 2008, **310**, 299–305.
- 57 P. A. Nagpure, N. S. Bajaj, R. P. Sonekar and S. K. Omanwar, *Indian J. Pure Appl. Phys.*, 2011, **49**, 799–802.
- 58 N. Penin, L. Seguin, B. Gerand, M. Touboul and G. Nowogrocki, *J. Alloy. Comp.*, 2002, **334**, 97–109.
- 59 N. Penin, M. Touboul and G. Nowogrocki, *J. Solid State Chem.*, 2005, **178**, 671–679.
- 60 M. J. Polinski, S. Wang, E. V. Alekseev, J. N. Cross, W. Depmeier and T. A. Schmitt, *Inorg. Chem.*, 2012, **51**, 11541–11548.
- 61 C. G. Salentine, *Inorg. Chem.*, 1987, **26**, 128–132.
- 62 M. Touboul, N. Penin and G. Nowogrocki, *J. Solid State Chem.*, 1999, **143**, 260–265.
- 63 N. A. Yamnova, Y. E. Tismenko, N. V. Zubkova, O. V. Dimitrova and A. P. Kantor, *Crystallogr. Reports*, 2003, **48**, 557–562.
- 64 T. Yang, J. Sun, L. Eriksson, G. Li, X. Zou, F. Liao and J. Lin, *Inorg. Chem.*, 2008, **47**, 3228–3233.
- 65 H. Yu, S. Pan, H. Wu, J. Han, X. Dong and Z. Zhou, *J. Solid State Chem.*, 2011, **184**, 1644–1648.
- 66 W. H. Zachariasen and H. A. Plettinger, *Acta Cryst.*, 1963, **16**, 376–379.
- 67 M. Zhang, S. Pan, J. Han and Z. Zhou, *J. Solid State Chem.*, 2011, **184**, 825–829.
- 68 L. Zhou, S. Pan, X. Su, Z. Yang, H. Wu, H. Yu, F. Zhang, S. Cui and Z. Zhou, *J. Mol. Struct.*, 2013, **1049**, 473–478.
- 69 M. Schindler and F. C. Hawthorne, *Can. Mineral.*, 2001, **39**, 1243–1256.
- 70 D. M. Schubert, R. A. Smith and M. Z. Visi, *Glas. Technol.*, 2003, **44**, 63–70.
- 71 T. Balakrishnan, G. Bhagavannarayana and K. Ramamurthi, *Spectroch*, 2008, **71**, 578–

- 583.
- 72 M. A. Beckett, E. L. Bennett, P. N. Horton and M. B. Hursthouse, *J. Organomet. Chem.*, 2010, **695**, 1080–1083.
- 73 M. A. Beckett, C. C. Bland, P. N. Horton, M. B. Hursthouse and K. S. Varma, *J. Organomet. Chem.*, 2007, **692**, 2832–2838.
- 74 M. A. Beckett, C. C. Bland, P. N. Horton, M. B. Hursthouse and K. S. Varma, *Inorg. Chem.*, 2007, **46**, 3801–3803.
- 75 M. A. Beckett, S. J. Coles, M. E. Light, L. Fischer, B. M. Thomas and K. S. Varma, *Polyhedron*, 2006, **25**, 1011–1016.
- 76 M. A. Beckett, P. N. Horton, S. J. Coles, D. A. Kose and A. M. Kreuziger, *Polyhedron*, 2012, **38**, 157–161.
- 77 M. A. Beckett, P. N. Horton, M. B. Hursthouse, J. L. Timmis and K. S. Varma, *Dalton Trans.*, 2012, **41**, 4396–4403.
- 78 M. A. Beckett, P. N. Horton, M. B. Hursthouse, J. L. Timmis and K. S. Varma, *Inorg. Chim. Acta*, 2012, **383**, 199–203.
- 79 M. A. Beckett, P. N. Horton, M. B. Hursthouse, J. L. Timmis and K. S. Varma, *Collect. Czech. Chem. Commun.*, 2010, **75**, 971–980.
- 80 M. A. Beckett, G. C. Strickland, K. S. Varma, D. E. Hibbs, M. B. Hursthouse and K. A. M. Malik, *J. Organomet. Chem.*, 1997, **535**, 33–41.
- 81 A. T. Colak, Y. Sahin, O. Z. Yeşilel, F. Colak, F. Yilmaz and M. Taş, *Inorg. Chim. Acta*, 2012, **383**, 169–177.
- 82 C. C. Freyhardt and M. Wiebcke, *J. Chem. Soc., Chem. Commun.*, 1994, **14**, 1675–1676.
- 83 C. C. Freyhardt, M. Wiebcke and G. Engelhardt, *J. Inclusion Phenom. Mol. Recognit. Chem.*, 1994, **18**, 161–175.
- 84 R. Janda, G. Heller and J. Pickardt, *Zeitschrift für Krist.*, 1981, **154**, 1–9.
- 85 D. A. Kose, M. A. Beckett and N. Colak, *J. Biol. Chem.*, 2012, **40**, 219–225.
- 86 M. Li, J. Chang, Z. Wang and H. Shi, *J. Solid State Chem.*, 2006, **179**, 3265–3269.
- 87 Q. Li, F. Xue, T. Mak, N. Territories and H. Kong, *Inorg. Chem.*, 1999, **38**, 4142–4145.
- 88 Z. E. Lin and G. Y. Yang, *Eur. J. Inorg. Chem.*, 2011, **26**, 3857–3867.
- 89 Z. H. Liu, L. Q. Li and W. J. Zhang, *Inorg. Chem.*, 2006, **45**, 1430–1432.
- 90 Z. H. Liu, W. J. Zhang and J. J. Zhang, *Thermochim. Acta*, 2005, **439**, 151–153.
- 91 Y. Miao, Z. Zhang, D. Hong and Y. L. Ji, *Chem. Res. Chinese Universities*, 2010, **26**, 335–338.
- 92 M. Wiebcke, C. Freyhardt, J. Felsche and G. Engelhardt, *Z. Naturforsch.*, 1993, **48B**, 978–985.
- 93 C. Y. Pan, G. M. Wang, S. T. Zheng and G. Y. Yang, *J. Solid State Chem.*, 2007, **180**, 1553–1558.
- 94 C. Y. Pan, G. M. Wang, S. T. Zheng and G. Y. Yang, *Z. Anorg. Allg. Chem.*, 2007, **633**, 336–340.
- 95 P. Press, G. Britain and A. Chemie, *J. Inorg. Nucl. Chem.*, 1968, **30**, 2743–2754.
- 96 A. Rosenheim and F. Leyser, *Z. Anorg. Allg. Chem.*, 1921, **119**, 1–38.
- 97 D. M. Schubert, M. Z. Visi, S. Khan and C. B. Knobler, *Inorg. Chem.*, 2008, **47**, 4740–4745.
- 98 M. Z. Visi, C. B. Knobler, J. J. Owen, M. I. Khan and D. M. Schubert, *Cryst. Growth Des.*, 2006, **6**, 538–545.
- 99 G. M. Wang, C. Y. Pan, S. T. Zheng and G. Y. Yang, *Acta Cryst.*, 2007, **E63**, o1101–o1103.
- 100 G. M. Wang, C. Y. Pan, S. T. Zheng and G. Y. Yang, *Acta Cryst.*, 2007, **E63**, o1104–o1105.

- 101 G. M. Wang, Y. Q. Sun and G. Y. Yang, *J. Solid State Chem.*, 2004, **177**, 4648–4654.
- 102 T. J. Weakley, *Acta Cryst.*, 1985, **C41**, 377–379.
- 103 H. X. Yang, W. J. Zhang, X. L. Liu and Z. H. Liu, *Acta Cryst.*, 2006, **E62**, o4877–o4879.
- 104 S. Yang, G. Li, S. Tian, F. Liao and J. Lin, *Cryst. Growth Des.*, 2007, **7**, 1246–1250.
- 105 S. Yang, G. Li, S. Tian, F. Liao, M. Xiong and J. Lin, *J. Solid State Chem.*, 2007, **180**, 2225–2232.
- 106 Y. Yang, D. Fu, G. Li and Y. Zhang, *Z. Anorg. Allg. Chem.*, 2013, **639**, 722–727.
- 107 Y. Yang, J. B. Sun, M. Cui, R. Bin Liu, Y. Wang and C. G. Meng, *J. Solid State Chem.*, 2011, **184**, 1666–1670.
- 108 Z. L. Yang, S. H. Yang, G. B. Li and J. H. Lin, *Acta Physico-Chimica Sinica*, 2007, **23**, 285–288.
- 109 H. X. Zhang, S. T. Zheng and G. Y. Yang, *Acta Cryst.*, 2004, **C60**, 545–546.
- 110 M. Wiebcke, C. C. Freyhardt, J. Felsche and G. Engelhardt, *Z. Naturforsch.*, 1993, **48b**, 978–985.
- 111 G. M. Wang, Y. Q. Sun and G. Y. Yang, *J. Solid State Chem.*, 2006, **179**, 1545–1553.
- 112 G. M. Wang, Y. Q. Sun and G. Y. Yang, *J. Solid State Chem.*, 2005, **178**, 729–735.
- 113 Z. H. Liu, J. J. Zhang and W. J. Zhang, *Inorg. Chim. Acta*, 2006, **359**, 519–524.
- 114 H. X. Zhang, S. T. Zheng and G. Y. Yang, *Acta Cryst.*, 2004, **C60**, m241–243.
- 115 Z. Lijuan, Z. Jianjian and L. Zhihong, *Chinese J. Chem.*, 2009, **27**, 494–500.
- 116 H. H. Sung, M. Wu and I. D. Williams, *Inorg. Chem. Commun.*, 2000, **3**, 401–404.
- 117 L. Zhao, P. Li and B. Cao, *Acta Cryst.*, 2009, **E65**, m368–368.
- 118 Y. Q. Sun, G. M. Li and Y. P. Chen, *Dalton. Trans.*, 2012, **41**, 5774–5777.
- 119 A. K. Paul, K. Sachidananda and S. Natarajan, *Cryst. Growth Des.*, 2010, **10**, 456–464.
- 120 G. Y. Yang and S. C. Sevov, *Inorg. Chem.*, 2001, **40**, 2214–2215.
- 121 Q. Meng, G. M. Wang, H. He, B. F. Yang and G. Y. Yang, *J. Clust. Sci.*, 2014, **25**, 1295–1305.
- 122 Y. Yang, D. Fu, Y. Zhang and C. Meng, *Z. Anorg. Allg. Chem.*, 2014, **640**, 1443–1448.
- 123 Y. Yang, Y. Wang, J. Zhu, R. Liu, J. Xu and C. Meng, *Inorg. Chim. Acta*, 2011, **376**, 401–407.
- 124 Y. Yang, Y. Wang, J. Sun, M. Cui and C. Meng, *Z. Anorg. Allg. Chem.*, 2011, **637**, 729–734.
- 125 G. M. Wang, J. H. Li, Z. X. Li, P. Wang and H. Li, *Z. Anorg. Allg. Chem.*, 2008, **634**, 1192–1196.
- 126 S. M. Lan, W. J. Di, Z. D. Shao and Y. X. Liang, *Acta Cryst.*, 2011, **C67**, m338–341.
- 127 Y. Yang, Y. Wang, J. Zhu, R. Liu, J. Xu and C. Meng, *Z. Anorg. Allg. Chem.*, 2011, **637**, 735–740.
- 128 P. Zhao, L. Cheng and G. Y. Yang, *Inorg. Chem. Commun.*, 2012, **20**, 138–141.
- 129 C. Rong, J. Jiang and L. Q. Lu, *Chinese J. Inorg. Chem.*, 2012, **28**, 2217–2222.
- 130 J. Zhou, S. T. Zheng, M. Zhang, G. Z. Liu and G. Y. Yang, *CrystEngComm*, 2009, **11**, 2597–2600.
- 131 L. Dan, Y. Xiaoyan and L. Zhu, *Chinese J. Chem.*, 2011, **29**, 463–467.
- 132 H. Li, S. Pan, H. Wu, J. P. Smit and K. R. Poepfelmeier, *J. Alloys Compd.*, 2011, **509**, 3310–3313.
- 133 X. Chen, Y. Zhao, X. Chang, J. Zuo, H. Zang and W. Xiao, *J. Solid State Chem.*, 2006, **179**, 3911–3918.
- 134 H. X. Zhang, J. Zhang, S. T. Zheng and G. Y. Yang, *Inorg. Chem. Commun.*, 2004, **7**, 781–783.
- 135 N. Jemai, M. Rzaigui and S. Akriche, *J. Clust. Sci.*, 2015, **26**, 2051–2064.
- 136 X. Li, G. Li, L. Wang, M. Shang, D. Zhang, Y. Liu, H. Yuan and S. Feng, *Inorg.*

- Chem. Commun.*, 2015, **58**, 31–34.
- 137 M. S. Moghadam, U. Timper and G. Heller, *Z. Naturforsch.*, 1994, **49b**, 627–634.
- 138 M. A. Altahan, M. A. Beckett, S. J. Coles and P. N. Horton, *Inorg. Chem. Commun.*, 2015, **59**, 95–98.
- 139 M. A. Altahan, M. A. Beckett, S. J. Coles and P. N. Horton, *Inorg. Chem.*, 2015, **52**, 412–414.
- 140 L. Jun, X. Shuping and G. Shiyang, *Spectrochim. Acta*, 1995, **51A**, 519–532.
- 141 F. A. Cotton and G. Wilkinson, in *Advanced Inorganic Chemistry*, Fourth ed., 1972, pp. 657–669.
- 142 G. A. Bain and J. F. Berry, *J. Chem. Educ.*, 2008, **85**, 532–536.
- 143 F. Bloch, *Phys. Rev.*, 1946, **70**, 460.
- 144 E. M. Purcell, H. C. Torrey and R. V. Pound, *Phys. Rev.*, 1946, **69**, 37.
- 145 F. A. Bovey, P. A. Mirau and H. S. Gutowsky, in *Nuclear magnetic resonance spectroscopy*, Elsevier, 2nd edn., 1988, pp. 1–36.
- 146 R. K. Harris and B. E. Mann, in *NMR and the periodic table*, Academic Press, 1978, pp. 15–18.
- 147 R. R. Ernst, G. Bodenhausen and A. Wokaun, in *Principles of Nuclear Magnetic Resonance in One and Two Dimensions*, 1987, vol. 14, pp. 50–60.
- 148 Z. Gabelica, J. B. Nagy, P. Bodart and G. Debras, *Chem. Lett.*, 1984, 1059–1062.
- 149 C. G. Salentine, *Inorg. Chem.*, 1983, **22**, 3920–3924.
- 150 H. Smith and R. J. Wiersema, *Inorg. Chem.*, 1972, **11**, 1959–1961.
- 151 R. K. Momii and N. H. Nachtrieb, *Inorg. Chem.*, 1967, **6**, 1189–1192.
- 152 Z. Liu, J. Zhang and W. Zhang, *Z. Krist. NCS*, 2005, **220**, 555–556.
- 153 Y. Tao, Z. Lixia, X. Shuping, G. Shiyang and Y. Kaibei, *J. Alloy. Comp.*, 2003, **358**, 87–92.
- 154 N. Jamai, M. Rzaigui and S. Akriche, *Acta Cryst.*, 2014, **E70**, m167–m168.
- 155 J. A. Broomhead, F. P. Dwyer and J. W. Hogarth, *Inorg. Synth.*, 1960, **6**, 183–186.
- 156 J. Bjerrum and J. McCreynolds, *Inorg. Synth.*, 1946, **2**, 217–218.
- 157 R. J. Geue, T. W. Hambley, J. M. Harrowfield, A. M. Sargeson and M. R. Snow, *J. Am. Chem. Soc.*, 1984, **106**, 5478–5488.
- 158 F. P. Dwyer, A. M. Sargeson and L. B. James, *J. Am. Chem. Soc.*, 1964, **86**, 590–592.
- 159 D. Kahn, *AMP J. Technol.*, 1991, **1**, 43–54.
- 160 J. L. Sudmeier, I. G. Blackmer, C. H. Bradley and F. L. Anet, *J. Am. Chem. Soc.*, 1972, **94**, 757–761.
- 161 R. Bala, A. Kaur, M. Kashyap and D. E. Janzen, *J. Mol. Struct.*, 2014, **1063**, 203–212.
- 162 J. M. Harrowfield, G. A. Lawrance and A. M. Sargeson, *J. Chem. Educ.*, 1985, **62**, 804–806.
- 163 C. L. Christ and J. R. Clark, *Phys. Chem. Min.*, 1977, **2**, 59–87.
- 164 M. C. Etter, *Acc. Chem. Res.*, 1990, **23**, 120–126.
- 165 H. A. Levy and G. C. Lisensky, *Acta Crystallogr.*, 1978, **B34**, 3502–3510.
- 166 C. Y. Pan, G. M. Wang, S. T. Zheng and G. Y. Yang, *Z. Anorg. Allg. Chem.*, 2007, **633**, 336–340.
- 167 P. C. Burns and F. C. Hawthorne, *Can. Mineral.*, 1993, **31**, 305–312.
- 168 A. D. Negro, J. M. Pozaz and L. Ungaretti, *Am. Mineral.*, 1975, **60**, 897–883.
- 169 D. M. Schubert, M. Z. Visi and C. B. Knobler, *Inorg. Chem.*, 2008, **47**, 2017–2023.
- 170 M. A. Beckett, P. N. Horton, M. B. Hursthouse and J. L. Timmis, *RSC Adv.*, 2013, **3**, 15185–15191.
- 171 A. A. Achilleos, L. R. Gahan, T. W. Hambley, P. C. Healy and D. M. Weedon, *Inorg. Chim. Acta*, 1989, **157**, 209–214.
- 172 B. J. Hathaway and P. G. Hodgson, *J. Inorg. Nucl. Chem.*, 1973, **35**, 4071–4081.

- 173 G. Heller and J. Pickardt, *Z. Naturforsch.*, 1985, **40b**, 462–466.
- 174 I. M. Procter, B. J. Hathaway and P. Nicholls, *J. Chem. Soc.*, 1968, 1678–1684.
- 175 S. M. Hosseinpour-Mashkani, F. Mohandes, M. Salavati-Niasari and K. Venkateswara-Rao, *Mater. Res. Bull.*, 2012, **47**, 3148–3159.
- 176 C. Pariya, F. L. Liao, S. L. Wang and C. S. Chung, *Polyhedron*, 1998, **17**, 547–554.
- 177 A. Cui, X. Chen, L. Sun, J. Wei, J. Yang and H. Kou, *J. Chem. Educ.*, 2011, **88**, 311–312.
- 178 W. B. Bruce and E. C. Lingafelter, *Acta Cryst.*, 1964, **17**, 254–259.
- 179 Y. Inada, K. Ozutsumi, S. Funahashi, J. S. Soyama, T. Kawashima and M. Tanakal, *Inorg. Chem.*, 1993, **32**, 3010–3014.
- 180 U. S. Yadav and B. K. Rai, *Orient. J. Chem. Chem.*, 2013, **29**, 1203–1207.
- 181 C. Y. Pan, S. Hu, D. G. Li, P. Ouyang, F. H. Zhao and Y. Y. Zheng, *Dalton. Trans.*, 2010, **39**, 5772–5773.
- 182 A. W. Addison, T. N. Rao, J. Reedijk, J. V. Rijn and G. C. Verschoor, *J. Chem. Soc. Dalt. Trans.*, 1984, **7**, 1349–1356.
- 183 Z. Liu, L. Li, J. Li and M. Hu, *J. Alloy. Comp.*, 2005, **394**, 277–281.
- 184 S. Natarajan, W. Klein, M. Panthöfer, L. Van Wüllen, M. Jansen, I. Die and R. V. Zinkacetat, *Z. Anorg. Allg. Chem.*, 2003, **629**, 959–962.
- 185 H. M. Slate, F. P. Dwyer, I. K. Reid and W. J. Hogarth, *Inorg. Synth.*, McGraw-Hill, 8th edn., 1960.
- 186 W. H. Elfring and N. J. Rose, *Inorg. Chem.*, 1975, **14**, 2759–2768.
- 187 R. Saito and Y. Kidani, *Chem. Lett.*, 1976, **5**, 123–126.
- 188 R. N. Keller and L. J. Edwards, *J. Am. Chem. Soc.*, 1952, **74**, 215–219.
- 189 J. G. Breckenridge, *Can. J. Res.*, 1948, **26**, 11–19.
- 190 H. B. Jonassen and B. E. Douglas, *J. Am. Chem. Soc.*, 1949, **71**, 4094–4097.
- 191 G. Wilkinson, P. L. Pauson and F. A. Cotton, *J. Am. Chem. Soc.*, 1953, **76**, 1970–1974.
- 192 M. A. Beckett, P. N. Horton, M. B. Hursthouse and J. L. Timmis, *Polyhedron*, 2014, **77**, 96–102.
- 193 D. B. Powell and N. Sheppard, *J. Chem. Soc.*, 1959, 791–795.
- 194 G. F. Svator, C. Curran and J. V. Quagliano, *J. Am. Chem. Soc.*, 1955, **77**, 6159–1963.
- 195 L. Sacconi, A. Sabatini and P. Gans, *Inorg. Chem.*, 1964, **3**, 1772–1774.
- 196 R. Saito and Y. Kidani, *Bull. Chem. Soc. Jpn.*, 1978, **51**, 159–163.
- 197 G. Gordon and R. K. Birdwhistell, *J. Am. Chem. Soc.*, 1958, **81**, 3567–3569.
- 198 W. W. Wendlandt, *J. Inorg. Nucl. Chem.*, 1963, **25**, 833–842.
- 199 G. Diazfleming and R. E. Shepherd, *Spectrochim. Acta A*, 1987, **43A**, 1141–1146.
- 200 J. Bassett, R. Grzeskowiak and B. L. O'leary, *J. Inorg. Nucl. Chem.*, 1970, **32**, 3861–3866.
- 201 N. F. Curtis and H. K. Powell, *J. Chem. Soc.*, 1968, 3069–3073.
- 202 J. Zhou, G. Q. Bian, Y. Zhang, J. Dai and N. Cheng, *Z. Anorg. Allg. Chem.*, 2007, **633**, 2701–2705.
- 203 C. K. Jorgensen, *Acta Chem. Scand.*, 1957, **11**, 399–400.
- 204 N. F. Curtis and D. A. House, *J. Am. Chem. Soc.*, 1965, **11**, 6194–6197.

Appendix I

Crystallographic details

Diffractometer: Rigaku AFC12 goniometer equipped with an enhanced sensitivity (HG) Saturn724+ detector mounted at the window of an FR-E+ SuperBright molybdenum rotating anode generator with HF Varimax optics (100µm focus). **Cell determination and data collection:** CrystalClear-SM Expert 3.1 b27 (Rigaku, 2013). **Data reduction, cell refinement and absorption correction:** CrystalClear-SM Expert 3.1 b27 (Rigaku, 2012). **Structure solution :** SUPERFLIP (Palatinus, L. & Chapuis, G. (2007). J. Appl. Cryst. 40, 786-790.) **Structure refinement:** SHELXL-2013 (G Sheldrick, G.M. (2008). Acta Cryst. A64, 112-122.). **Graphics:** ORTEP3 for Windows (L. J. Farrugia, J. Appl. Crystallogr. 1997, 30, 565).

Table 1 Bond lengths [Å] in **6**.

Co1–N6	1.869(19)	C11–C12	1.507(5)	C26–H26B	0.9900	B12–O11	1.543(3)
Co1–N26	1.937(17)	C11–H11A	0.9900	C27–N27	1.485(15)	B13–O21	1.423(3)
Co1–N16	1.945(16)	C11–H11B	0.9900	C27–H27A	0.9900	B13–O17	1.453(3)
Co1–N22	1.961(2)	C12–N12	1.501(4)	C27–H27B	0.9900	B13–O15	1.475(3)
Co1–N12	1.966(3)	C12–H12A	0.9900	N26–H26C	0.9900	B13–O11	1.565(3)
Co1–N17	1.966(15)	C12–H12B	0.9900	N26–H26D	0.9900	B14–O13	1.354(3)
Co1–N2	1.969(3)	N11–H11C	0.9900	N27–H27C	0.9900	B14–O12	1.372(3)
Co1–N21	1.977(3)	N11–H11D	0.9900	N27–H27D	0.9900	B14–O22	1.385(3)
Co1–N1	1.979(2)	N12–H12C	0.9900	B1–O4	1.459(4)	B15–O15	1.366(3)
Co1–N11	1.981(3)	N12–H12D	0.9900	B1–O1	1.467(4)	B15–O23	1.368(3)
Co1–N7	1.993(18)	C16–C17	1.490(15)	B1–O3	1.468(4)	B15–O14	1.373(3)
Co1–N27	2.028(16)	C16–N16	1.501(14)	B1–O6	1.491(4)	B16–O17	1.368(3)
C1–N1	1.494(4)	C16–H16A	0.9900	B2–O1	1.359(4)	B16–O24	1.375(3)
C1–C2	1.511(5)	C16–H16B	0.9900	B2–O7	1.363(4)	B16–O16	1.379(3)
C1–H1A	0.9900	C17–N17	1.466(14)	B2–O2	1.374(4)	B17–O25	1.357(4)
C1–H1B	0.9900	C17–H17A	0.9900	B3–O3	1.357(4)	B17–O18	1.359(4)
C2–N2	1.492(4)	C17–H17B	0.9900	B3–O8	1.363(4)	B17–O19	1.388(4)
C2–H2A	0.9900	N16–H16C	0.9900	B3–O2	1.388(4)	B18–O26	1.344(4)
C2–H2B	0.9900	N16–H16D	0.9900	B4–O4	1.354(4)	B18–O20	1.369(4)
N1–H1C	0.9900	N17–H17C	0.9900	B4–O9	1.358(4)	B18–O19	1.398(4)
N1–H1D	0.9900	N17–H17D	0.9900	B4–O5	1.376(4)	O21–H21	0.8400
N2–H2C	0.9900	C21–N21	1.499(6)	B5–O6	1.354(4)	O22–H22	0.8400
N2–H2D	0.9900	C21–C22	1.506(6)	B5–O10	1.365(4)	O23–H23	0.8400
C6–C7	1.480(15)	C21–H21A	0.9900	B5–O5	1.391(4)	O24–H24	0.8400
C6–N6	1.503(14)	C21–H21B	0.9900	O7–H7	0.8400	O25–H25	0.8400
C6–H6A	0.9900	C22–N22	1.469(6)	O8–H8	0.8400	O26–H26	0.8400
C6–H6B	0.9900	C22–H22A	0.9900	O9–H9	0.8400	O41–H41A	0.8501
C7–N7	1.481(15)	C22–H22B	0.9900	O10–H10	0.8400	O41–H41B	0.8501
C7–H7A	0.9900	N21–H21C	0.9900	B11–O20	1.439(4)	O42–H42A	0.8497
C7–H7B	0.9900	N21–H21D	0.9900	B11–O12	1.446(3)	O42–H42B	0.8500
N6–H6C	0.9900	N22–H22C	0.9900	B11–O18	1.472(4)	O43–H43A	0.8497
N6–H6D	0.9900	N22–H22D	0.9900	B11–O11	1.554(3)	O43–H43B	0.8500
N7–H7C	0.9900	C26–N26	1.491(15)	B12–O13	1.443(3)	O44–H44A	0.8499
N7–H7D	0.9900	C26–C27	1.495(16)	B12–O14	1.469(3)	O44–H44B	0.8498
C11–N11	1.494(4)	C26–H26A	0.9900	B12–O16	1.472(3)	O51–H51A	0.8500
						O51–H51B	0.8500

Table 2 Bond angles [°] in 6.

N6–Co1–N26	91.5(8)	C11–C12–H12A	110.4	Co1–N27–H27D	109.3
N6–Co1–N16	96.8(7)	N12–C12–H12B	110.4	H27C–N27–H27D	108.0
N26–Co1–N16	92.1(7)	C11–C12–H12B	110.4	O4–B1–O1	108.0(2)
N22–Co1–N12	92.28(11)	H12A–C12–H12B	108.6	O4–B1–O3	109.6(2)
N6–Co1–N17	95.8(8)	C11–N11–Co1	109.14(19)	O1–B1–O3	112.2(2)
N26–Co1–N17	172.5(7)	C11–N11–H11C	109.9	O4–B1–O6	112.4(2)
N16–Co1–N17	85.2(6)	Co1–N11–H11C	109.9	O1–B1–O6	107.1(2)
N22–Co1–N2	89.36(11)	C11–N11–H11D	109.9	O3–B1–O6	107.7(2)
N12–Co1–N2	91.40(11)	Co1–N11–H11D	109.9	O1–B2–O7	120.8(3)
N22–Co1–N21	85.69(10)	H11C–N11–H11D	108.3	O1–B–O2	122.0(3)
N12–Co1–N21	91.74(11)	C12–N12–Co1	109.61(19)	O7–B2–O2	117.1(3)
N2–Co1–N21	174.24(11)	C12–N12–H12C	109.7	O3–B3–O8	122.6(2)
N22–Co1–N1	92.30(11)	Co1–N12–H12C	109.7	O3–B3–O2	121.2(2)
N12–Co1–N1	174.45(11)	C12–N12–H12D	109.7	O8–B3–O2	116.1(2)
N2–Co1–N1	85.52(10)	Co1–N12–H12D	109.7	O4–B4–O9	119.0(3)
N21–Co1–N1	91.72(10)	H12C–N12–H12D	108.2	O4–B4–O5	121.5(3)
N22–Co1–N11	175.88(11)	C17–C16–N16	107.6(14)	O9–B4–O5	119.5(3)
N12–Co1–N11	85.32(11)	C17–C16–H16A	110.2	O6–B5–O10	120.9(3)
N2–Co1–N11	94.04(11)	N16–C16–H16A	110.2	O6–B5–O5	121.2(3)
N21–Co1–N11	91.02(11)	C17–C16–H16B	110.2	O10–B5–O5	117.9(3)
N1–Co1–N11	90.28(11)	N16–C16–H16B	110.2	B2–O1–B1	122.5(2)
N6–Co1–N7	87.3(6)	H16A–C16–H16B	108.5	B2–O2–B3	119.0(2)
N26–Co1–N7	92.6(8)	N17–C17–C16	108.5(13)	B3–O3–B1	122.9(2)
N16–Co1–N7	173.7(7)	N17–C17–H17A	110.0	B4–O4–B1	122.4(2)
N17–Co1–N7	89.7(7)	C16–C17–H17A	110.0	B4–O5–B5	119.6(2)
N6–Co1–N27	172.0(7)	N17–C17–H17B	110.0	B5–O6–B1	121.5(2)
N26–Co1–N27	84.1(6)	C16–C17–H17B	110.0	B2–O7–H7	109.5
N16–Co1–N27	90.0(7)	H17A–C17–H17B	108.4	B3–O8–H8	109.5
N17–Co1–N27	88.9(7)	C16–N16–Co1	108.4(11)	B4–O9–H9	109.5
N7–Co1–N27	86.3(7)	C16–N16–H16C	110.0	B5–O10–H10	109.5
N1–C1–C2	107.5(2)	Co1–N16–H16C	110.0	O20–B11–O12	109.3(2)
N1–C1–H1A	110.2	C16–N16–H16D	110.0	O20–B11–O18	112.2(2)
C2–C1–H1A	110.2	Co1–N16–H16D	110.0	O12–B11–O18	108.7(2)
N1–C1–H1B	110.2	H16C–N16–H16D	108.4	O20–B11–O11	110.3(2)
C2–C1–H1B	110.2	C17–N17–Co1	111.5(10)	O12–B11–O11	107.0(2)
H1A–C1–H1B	108.5	C17–N17–H17C	109.3	O18–B11–O11	109.1(2)
N2–C2–C1	106.9(3)	Co1–N17–H17C	109.3	O13–B12–O14	108.8(2)
N2–C2–H2A	110.3	C17–N17–H17D	109.3	O13–B12–O16	111.3(2)
C1–C2–H2A	110.3	Co1–N17–H17D	109.3	O14–B12–O16	110.0(2)
N2–C2–H2B	110.3	H17C–N17–H17D	108.0	O13–B12–O11	111.1(2)
C1–C2–H2B	110.3	N21–C21–C22	107.5(4)	O14–B12–O11	108.46(19)
H2A–C2–H2B	108.6	N21–C21–H21A	110.2	O16–B12–O11	107.12(19)
C1–N1–Co1	109.27(19)	C22–C21–H21A	110.2	O21–B13–O17	109.0(2)
C1–N1–H1C	109.8	N21–C21–H21B	110.2	O21–B13–O15	111.2(2)
Co1–N1–H1C	109.8	C22–C21–H21B	110.2	O17–B13–O15	111.0(2)
C1–N1–H1D	109.8	H21A–C21–H21B	108.5	O21–B13–O11	112.3(2)
Co1–N1–H1D	109.8	N22–C22–C21	107.0(4)	O17–B13–O11	107.92(19)
H1C–N1–H1D	108.3	N22–C22–H22A	110.3	O15–B13–O11	105.34(19)
C2–N2–Co1	109.6(2)	C21–C22–H22A	110.3	O13–B14–O12	122.3(2)
C2–N2–H2C	109.8	N22–C22–H22B	110.3	O13–B14–O22	119.2(2)
Co1–N2–H2C	109.8	C21–C22–H22B	110.3	O12–B14–O22	118.5(2)
C2–N2–H2D	109.8	H22A–C22–H22B	108.6	O15–B15–O23	121.1(2)
Co1–N2–H2D	109.8	C21–N21–Co1	108.3(3)	O15–B15–O14	121.3(2)
H2C–N2–H2D	108.2	C21–N21–H21C	110.0	O23–B15–O14	117.6(2)
C7–C6–N6	107.0(13)	Co1–N21–H21C	110.0	O17–B16–O24	117.7(2)
C7–C6–H6A	110.3	C21–N21–H21D	110.0	O17–B16–O16	122.3(2)
N6–C6–H6A	110.3	Co1–N21–H21D	110.0	O24–B16–O16	120.0(2)
C7–C6–H6B	110.3	H21C–N21–H21D	108.4	O25–B17–O18	121.7(3)
N6–C6–H6B	110.3	C22–N22–Co1	109.8(3)	O25–B17–O19	117.6(2)
H6A–C6–H6B	108.6	C22–N22–H22C	109.7	O18–B17–O19	120.7(3)
C6–C7–N7	108.1(15)	Co1–N22–H22C	109.7	O26–B18–O20	122.5(3)

C6–C7–H7A	110.1	C22–N22–H22D	109.7	O26–B18–O19	116.6(2)
N7–C7–H7A	110.1	Co1–N22–H22D	109.7	O20–B18–O19	120.8(3)
C6–C7–H7B	110.1	H22C–N22–H22D	108.2	B12–O11–B11	115.79(19)
N7–C7–H7B	110.1	N26–C26–C27	109.2(19)	B12–O11–B13	108.60(18)
H7A–C7–H7B	108.4	N26–C26–H26A	109.8	B11–O11–B13	120.15(19)
C6–N6–Co1	110.4(12)	C27–C26–H26A	109.8	B14–O12–B11	122.8(2)
C6–N6–H6C	109.6	N26–C26–H26B	109.8	B14–O13–B12	123.2(2)
Co1–N6–H6C	109.6	C27–C26–H26B	109.8	B15–O14–B12	118.6(2)
C6–N6–H6D	109.6	H26A–C26–H26B	108.3	B15–O15–B13	124.1(2)
Co1–N6–H6D	109.6	N27–C27–C26	107.7(19)	B16–O16–B12	122.5(2)
H6C–N6–H6D	108.1	N27–C27–H27A	110.2	B16–O17–B13	119.8(2)
C7–N7–Co1	106.1(10)	C26–C27–H27A	110.2	B17–O18–B11	122.1(2)
C7–N7–H7C	110.5	N27–C27–H27B	110.2	B17–O19–B18	118.6(2)
Co1–N7–H7C	110.5	C26–C27–H27B	110.2	B18–O20–B11	121.3(2)
C7–N7–H7D	110.5	H27A–C27–H27B	108.5	B13–O21–H21	109.5
Co1–N7–H7D	110.5	C26–N26–Co1	108.9(19)	B14–O22–H22	109.5
H7C–N7–H7D	108.7	C26–N26–H26C	109.9	B15–O23–H23	109.5
N11–C11–C12	106.8(3)	Co1–N26–H26C	109.9	B16–O24–H24	109.5
N11–C11–H11A	110.4	C26–N26–H26D	109.9	B17–O25–H25	109.5
C12–C11–H11A	110.4	Co1–N26–H26D	109.9	B18–O26–H26	109.5
N11–C11–H11B	110.4	H26C–N26–H26D	108.3	H41A–O41–H41B	109.5
C12–C11–H11B	110.4	C27–N27–Co1	111.5(13)	H42A–O42–H42B	109.5
H11A–C11–H11B	108.6	C27–N27–H27C	109.3	H43A–O43–H43B	109.5
N12–C12–C11	106.6(3)	Co1–N27–H27C	109.3	H44A–O44–H44B	109.5
N12–C12–H12A	110.4	C27–N27–H27D	109.3	H51A–O51–H51B	109.5

Table 3 Bond lengths [Å] in **9**.

B1–O6	1.4469(19)	O17–H17	0.8400	N3–H3A	0.9100	N21–H21A	0.9100
B1–O5	1.455(2)	O18–H18	0.8400	N3–H3B	0.9100	N21–H21B	0.9100
B1–O4	1.500(2)	O19–H19	0.8400	N3–H3C	0.9100	N21–H21C	0.9100
B1–O1	1.5104(19)	B21–O26	1.437(2)	N4–H4A	0.9100	N22–H22A	0.9100
B2–O1	1.367(2)	B21–O25	1.470(2)	N4–H4B	0.9100	N22–H22B	0.9100
B2–O2	1.376(2)	B21–O21	1.498(2)	N4–H4C	0.9100	N22–H22C	0.9100
B2–O7	1.378(2)	B21–O24	1.5042(19)	N5–H5A	0.9100	N23–H23A	0.9100
B3–O8	1.452(2)	B22–O22	1.364(2)	N5–H5B	0.9100	N23–H23B	0.9100
B3–O5	1.4648(19)	B22–O21	1.374(2)	N5–H5C	0.9100	N23–H23C	0.9100
B3–O3	1.494(2)	B22–O27	1.376(2)	N6–H6A	0.9100	O41–H41A	0.848(9)
B3–O2	1.5011(19)	B23–O28	1.452(2)	N6–H6B	0.9100	O41–H41B	0.852(9)
B4–O3	1.370(2)	B23–O25	1.469(2)	N6–H6C	0.9100	O42–H42A	0.856(9)
B4–O9	1.372(2)	B23–O22	1.486(2)	Co11–N13 ⁱ	1.9625(14)	O42–H42B	0.854(9)
B4–O4	1.377(2)	B23–O23	1.512(2)	Co11–N13	1.9625(14)	O43–H43A	0.846(9)
O6–H6	0.8400	B24–O23	1.366(2)	Co11–N11	1.9705(14)	O43–H43B	0.848(9)
O7–H7	0.8400	B24–O24	1.375(2)	Co11–N11 ⁱ	1.9706(14)	O44–H44A	0.849(9)
O8–H8	0.8400	B24–O29	1.376(2)	Co11–N12 ⁱ	1.9820(14)	O44–H44B	0.851(9)
O9–H9	0.8400	O26–H26	0.8400	Co11–N12	1.9820(14)	O45–H45A	0.857(9)
B11–O16	1.4519(19)	O27–H27	0.8400	N11–H11A	0.9100	O45–H45B	0.850(9)
B11–O15	1.471(2)	O28–H38	0.8400	N11–H11B	0.9100	O46–H46A	0.853(9)
B11–O14	1.485(2)	O29–H29	0.8400	N11–H11C	0.9100	O46–H46B	0.846(9)
B11–O11	1.507(2)	Co1–N5	1.9625(13)	N12–H12A	0.9100	O47–H47A	0.858(9)
B12–O12	1.364(2)	Co1–N6	1.9646(14)	N12–H12B	0.9100	O47–H47B	0.830(9)
B12–O11	1.366(2)	Co1–N1	1.9679(13)	N12–H12C	0.9100	O48–H48A	0.858(9)
B12–O17	1.383(2)	Co1–N4	1.9681(14)	N13–H13A	0.9100	O48–H48B	0.858(9)
B13–O18	1.438(2)	Co1–N2	1.9720(14)	N13–H13B	0.9100	O49–H49A	0.850(9)
B13–O15	1.4770(19)	Co1–N3	1.9738(13)	N13–H13C	0.9100	O49–H49B	0.856(9)
B13–O12	1.486(2)	N1–H1A	0.9100	Co21–N23	1.9646(13)	O50–H50A	0.853(9)
B13–O13	1.512(2)	N1–H1B	0.9100	Co21–N23 ⁱⁱ	1.9646(13)	O50–H50B	0.849(9)
B14–O13	1.373(2)	N1–H1C	0.9100	Co21–N21	1.9680(13)	O51–H51A	0.844(9)
B14–O14	1.374(2)	N2–H2A	0.9100	Co21–N21 ⁱⁱ	1.9680(13)	O51–H51B	0.844(9)
B14–O19	1.376(2)	N2–H2B	0.9100	Co21–N22	1.9759(14)		
O16–H16	0.8400	N2–H2C	0.9100	Co21–N22 ⁱⁱ	1.9760(14)		

Table 4 Bond angles [°] in **9**.

O6–B1–O5	113.76(13)	O23–B24–O29	117.02(15)	N11–Co11–N12 ⁱ	92.42(6)
O6–B1–O4	106.19(13)	O24–B24–O29	120.90(15)	N11 ⁱ –Co11–N12 ⁱ	87.58(6)
O5–B1–O4	111.11(13)	B22–O21–B21	121.26(13)	N13 ⁱ –Co11–N12	88.48(6)
O6–B1–O1	112.01(13)	B22–O22–B23	115.77(13)	N13–Co11–N12	91.52(6)
O5–B1–O1	107.89(12)	B24–O23–B23	121.40(13)	N11–Co11–N12	87.58(6)
O4–B1–O1	105.61(12)	B24–O24–B21	116.45(13)	N11 ⁱ –Co11–N12	92.42(6)
O1–B2–O2	122.91(14)	B23–O25–B21	110.55(12)	N12 ⁱ –Co11–N12	180.0
O1–B2–O7	120.43(15)	B21–O26–H26	109.5	Co11–N11–H11A	109.5
O2–B2–O7	116.66(14)	B22–O27–H27	109.5	Co11–N11–H11B	109.5
O8–B3–O5	112.18(12)	B23–O28–H38	109.5	H11A–N11–H11B	109.5
O8–B3–O3	109.67(13)	B24–O29–H29	109.5	Co11–N11–H11C	109.5
O5–B3–O3	109.21(12)	N5–Co1–N6	91.56(6)	H11A–N11–H11C	109.5
O8–B3–O2	108.12(12)	N5–Co1–N1	89.12(5)	H11B–N11–H11C	109.5
O5–B3–O2	109.11(13)	N6–Co1–N1	179.19(5)	Co11–N12–H12A	109.5
O3–B3–O2	108.49(12)	N5–Co1–N4	89.93(6)	Co11–N12–H12B	109.5
O3–B4–O9	117.15(15)	N6–Co1–N4	88.85(6)	H12A–N12–H12B	109.5
O3–B4–O4	122.08(14)	N1–Co1–N4	90.72(6)	Co11–N12–H12C	109.5
O9–B4–O4	120.77(15)	N5–Co1–N2	88.65(6)	H12A–N12–H12C	109.5
B2–O1–B1	119.43(13)	N6–Co1–N2	89.92(6)	H12B–N12–H12C	109.5
B2–O2–B3	117.90(12)	N1–Co1–N2	90.52(6)	Co11–N13–H13A	109.5
B4–O3–B3	119.58(13)	N4–Co1–N2	178.10(6)	Co11–N13–H13B	109.5
B4–O4–B1	118.55(13)	N5–Co1–N3	177.72(6)	H13A–N13–H13B	109.5
B1–O5–B3	111.66(12)	N6–Co1–N3	89.19(6)	Co11–N13–H13C	109.5
B1–O6–H6	109.5	N1–Co1–N3	90.14(6)	H13A–N13–H13C	109.5
B2–O7–H7	109.5	N4–Co1–N3	92.24(6)	H13B–N13–H13C	109.5
B3–O8–H8	109.5	N2–Co1–N3	89.19(6)	N23–Co21–N23 ⁱⁱ	180.00(3)
B4–O9–H9	109.5	Co1–N1–H1A	109.5	N23–Co21–N21	90.08(6)
O16–B11–O15	112.64(13)	Co1–N1–H1B	109.5	N23 ⁱⁱ –Co21–N21	89.92(6)
O16–B11–O14	108.57(13)	H1A–N1–H1B	109.5	N23–Co21–N21 ⁱⁱ	89.92(6)
O15–B11–O14	108.68(13)	Co1–N1–H1C	109.5	N23 ⁱⁱ –Co21–N21 ⁱⁱ	90.08(6)
O16–B11–O11	108.41(13)	H1A–N1–H1C	109.5	N21–Co21–N21 ⁱⁱ	180.0
O15–B11–O11	109.90(13)	H1B–N1–H1C	109.5	N23–Co21–N22	89.26(6)
O14–B11–O11	108.56(13)	Co1–N2–H2A	109.5	N23 ⁱⁱ –Co21–N22	90.74(6)
O12–B12–O11	122.95(15)	Co1–N2–H2B	109.5	N21–Co21–N22	87.91(6)
O12–B12–O17	116.31(14)	H2A–N2–H2B	109.5	N21 ⁱⁱ –Co21–N22	92.09(6)
O11–B12–O17	120.74(14)	Co1–N2–H2C	109.5	N23–Co21–N22 ⁱⁱ	90.74(6)
O18–B13–O15	113.40(13)	H2A–N2–H2C	109.5	N23 ⁱⁱ –Co21–N22 ⁱⁱ	89.26(6)
O18–B13–O12	106.85(13)	H2B–N2–H2C	109.5	N21–Co21–N22 ⁱⁱ	92.09(6)
O15–B13–O12	109.13(13)	Co1–N3–H3A	109.5	N21 ⁱⁱ –Co21–N22 ⁱⁱ	87.91(6)
O18–B13–O13	111.02(13)	Co1–N3–H3B	109.5	N22–Co21–N22 ⁱⁱ	180.0
O15–B13–O13	107.54(13)	H3A–N3–H3B	109.5	Co21–N21–H21A	109.5
O12–B13–O13	108.81(13)	Co1–N3–H3C	109.5	Co21–N21–H21B	109.5
O13–B14–O14	122.78(16)	H3A–N3–H3C	109.5	H21A–N21–H21B	109.5
O13–B14–O19	121.51(15)	H3B–N3–H3C	109.5	Co21–N21–H21C	109.5
O14–B14–O19	115.71(15)	Co1–N4–H4A	109.5	H21A–N21–H21C	109.5
B12–O11–B11	118.07(12)	Co1–N4–H4B	109.5	H21B–N21–H21C	109.5
B12–O12–B13	120.22(12)	H4A–N4–H4B	109.5	Co21–N22–H22A	109.5
B14–O13–B13	118.62(13)	Co1–N4–H4C	109.5	Co21–N22–H22B	109.5
B14–O14–B11	119.11(13)	H4A–N4–H4C	109.5	H22A–N22–H22B	109.5
B11–O15–B13	111.10(12)	H4B–N4–H4C	109.5	Co21–N22–H22C	109.5
B11–O16–H16	109.5	Co1–N5–H5A	109.5	H22A–N22–H22C	109.5
B12–O17–H17	109.5	Co1–N5–H5B	109.5	H22B–N22–H22C	109.5
B13–O18–H18	109.5	H5A–N5–H5B	109.5	Co21–N23–H23A	109.5
B14–O19–H19	109.5	Co1–N5–H5C	109.5	Co21–N23–H23B	109.5
O26–B21–O25	113.87(13)	H5A–N5–H5C	109.5	H23A–N23–H23B	109.5
O26–B21–O21	107.12(13)	H5B–N5–H5C	109.5	Co21–N23–H23C	109.5
O25–B21–O21	109.23(13)	Co1–N6–H6A	109.5	H23A–N23–H23C	109.5
O26–B21–O24	110.35(13)	Co1–N6–H6B	109.5	H23B–N23–H23C	109.5
O25–B21–O24	108.64(13)	H6A–N6–H6B	109.5	H41A–O41–H41B	107.0(14)
O21–B21–O24	107.43(12)	Co1–N6–H6C	109.5	H42A–O42–H42B	106.5(14)
O22–B22–O21	122.49(15)	H6A–N6–H6C	109.5	H43A–O43–H43B	108.8(14)

O22–B22–O27	118.02(15)	H6B–N6–H6C	109.5	H44A–O44–H44B	106.8(14)
O21–B22–O27	119.49(15)	N13 ⁱ –Co11–N13	180.0	H45A–O45–H45B	106.2(12)
O28–B23–O25	113.02(13)	N13 ⁱ –Co11–N11	91.02(6)	H46A–O46–H46B	106.1(13)
O28–B23–O22	108.24(13)	N13–Co11–N11	88.98(6)	H47A–O47–H47B	106.7(14)
O25–B23–O22	109.42(13)	N13 ⁱ –Co11–N11 ⁱ	88.98(6)	H48A–O48–H48B	106.0(14)
O28–B23–O23	109.15(13)	N13–Co11–N11 ⁱ	91.02(6)	H49A–O49–H49B	106.9(14)
O25–B23–O23	108.99(13)	N11–Co11–N11 ⁱ	180.0	H50A–O50–H50B	106.2(14)
O22–B23–O23	107.89(12)	N13 ⁱ –Co11–N12 ⁱ	91.52(6)	H51A–O51–H51B	108.1(13)
O23–B24–O24	122.07(14)	N13–Co11–N12 ⁱ	88.48(6)		

Table 5 Bond lengths [Å] in **11**.

Co1–N23	1.956(2)	O10–H10	0.8400	C32–H32A	0.9900	C34–H34A	0.9900
Co1–N32	1.957(2)	O11–H11	0.8400	C32–H32B	0.9900	C34–H34B	0.9900
Co1–N22	1.960(2)	O12–H12	0.8400	C33–N32	1.489(3)	N31–H31C	0.9900
Co1–N21	1.963(2)	O13–H13	0.8400	C33–C34	1.515(4)	N31–H31D	0.9900
Co1–N31	1.967(2)	O14–H14	0.8400	C33–H33A	0.9900	N32–H32	1.0000
Co1–N33	1.969(2)	O15–H15	0.8400	C33–H33B	0.9900	N33–H33C	0.9900
B1–O1	1.424(3)	C21–N21	1.493(3)	C34–N33	1.491(4)	N33–H33D	0.9900
B1–O3	1.473(4)	C21–C22	1.518(3)	C34–H34A	0.9900	O51–H51A	0.8706
B1–O4	1.486(3)	C21–H21A	0.9900	C34–H34B	0.9900	O51–H51B	0.8702
B1–O6	1.507(3)	C21–H21B	0.9900	N31–H31C	0.9900	O52–H52A	0.8701
B2–O9	1.444(3)	C22–N22	1.490(3)	N31–H31D	0.9900	O52–H52B	0.8703
B2–O1	1.453(3)	C22–H22A	0.9900	N32–H32	1.0000	O53–H53A	0.8700
B2–O7	1.492(3)	C22–H22B	0.9900	N33–H33C	0.9900	O53–H53B	0.8704
B2–O2	1.508(4)	C23–N22	1.497(3)	N33–H33D	0.9900	O54–H54A	0.8698
B3–O2	1.356(3)	C23–C24	1.515(3)	N21–H21D	0.9900	O54–H54B	0.8703
B3–O3	1.367(3)	C23–H23A	0.9900	N22–H22	1.0000	O55–H55A	0.8696
B3–O10	1.371(4)	C23–H23B	0.9900	N23–H23C	0.9900	O55–H55B	0.8703
B4–O11	1.348(3)	C24–N23	1.483(4)	N23–H23D	0.9900	O56–H56A	0.8706
B4–O4	1.357(3)	C24–H24A	0.9900	C31–N31	1.489(4)	O56–H56	0.8702
B4–O5	1.400(3)	C24–H24B	0.9900	C31–C32	1.516(3)	O57–H57A	0.8704
B5–O6	1.347(3)	N21–H21C	0.9900	C31–H31A	0.9900	O57–H57B	0.8701
B5–O12	1.361(3)	N21–H21D	0.9900	C31–H31B	0.9900	O58–H58A	0.8699
B5–O5	1.385(3)	N22–H22	1.0000	C32–N32	1.497(3)	O58–H58B	0.8702
B6–O7	1.354(3)	N23–H23C	0.9900	C32–H32A	0.9900	O88–H88A	0.8699
B6–O8	1.365(3)	N23–H23D	0.9900	C32–H32B	0.9900	O88–H88B	0.8699
B6–O13	1.366(3)	C31–N31	1.489(4)	C33–N32	1.489(3)	O59–H59A	0.8699
B7–O9	1.448(3)	C31–C32	1.516(3)	C33–C34	1.515(4)	O59–H59B	0.8704
B7–O15	1.464(4)	C31–H31A	0.9900	C33–H33A	0.9900	O89–H89A	0.8698
B7–O14	1.471(3)	C31–H31B	0.9900	C33–H33B	0.9900	O89–H89B	0.8702
B7–O8	1.516(3)	C32–N32	1.497(3)	C34–N33	1.491(4)		

Table 6 Bond angles [°] in **11**.

N23–Co1–N33	177.72(9)	B7–O15–H15	109.5	H31A–C31–H31B	108.3
N32–Co1–N33	86.65(9)	N21–C21–C22	109.2(2)	N32–C32–C31	110.2(2)
N22–Co1–N33	95.19(9)	N21–C21–H21A	109.8	N32–C32–H32A	109.6
N21–Co1–N33	90.38(9)	C22–C21–H21A	109.8	C31–C32–H32A	109.6
N31–Co1–N33	88.56(9)	N21–C21–H21B	109.8	N32–C32–H32B	109.6
O1–B1–O3	113.0(2)	C22–C21–H21B	109.8	C31–C32–H32B	109.6
O1–B1–O4	113.7(2)	H21A–C21–H21B	108.3	H32A–C32–H32B	108.1
O3–B1–O4	108.5(2)	N22–C22–C21	109.4(2)	N32–C33–C34	109.7(2)
O1–B1–O6	108.0(2)	N22–C22–H22A	109.8	N32–C33–H33A	109.7
O3–B1–O6	105.42(19)	C21–C22–H22A	109.8	C34–C33–H33A	109.7
O4–B1–O6	107.77(18)	N22–C22–H22B	109.8	N32–C33–H33B	109.7
O9–B2–O1	111.7(2)	C21–C22–H22B	109.8	C34–C33–H33B	109.7
O9–B2–O7	110.52(19)	H22A–C22–H22B	108.2	H33A–C33–H33B	108.2
O1–B2–O7	110.13(19)	N22–C23–C24	109.6(2)	N33–C34–C33	108.1(2)
O9–B2–O2	109.6(2)	N22–C23–H23A	109.8	N33–C34–H34A	110.1
O1–B2–O2	109.80(19)	C24–C23–H23A	109.8	C33–C34–H34A	110.1

O7-B2-O2	104.9(2)	N22-C23-H23B	109.8	N33-C34-H34B	110.1
O2-B3-O3	122.9(3)	C24-C23-H23B	109.8	C33-C34-H34B	110.1
O2-B3-O10	117.5(2)	H23A-C23-H23B	108.2	H34A-C34-H34B	108.4
O3-B3-O10	119.6(2)	N23-C24-C23	107.0(2)	C31-N31-Co1	111.75(15)
O11-B4-O4	118.3(2)	N23-C24-H24A	110.3	C31-N31-H31C	109.3
O11-B4-O5	120.5(2)	C23-C24-H24A	110.3	Co1-N31-H31C	109.3
O4-B4-O5	121.2(2)	C22-N22-C23	114.9(2)	C31-N31-H31D	109.3
O6-B5-O12	123.2(2)	N23-C24-H24B	110.3	Co1-N31-H31D	109.3
O6-B5-O5	120.8(2)	C23-C24-H24B	110.3	H31C-N31-H31D	107.9
O12-B5-O5	116.0(2)	H24A-C24-H24B	108.6	C33-N32-C32	116.0(2)
O7-B6-O8	124.3(2)	C21-N21-Co1	112.58(14)	C33-N32-Co1	108.63(16)
O7-B6-O13	115.1(2)	C21-N21-H21C	109.1	C32-N32-Co1	108.24(16)
O8-B6-O13	120.7(2)	Co1-N21-H21C	109.1	C33-N32-H32	107.9
O9-B7-O15	110.6(2)	C21-N21-H21D	109.1	C32-N32-H32	107.9
O9-B7-O14	112.0(2)	Co1-N21-H21D	109.1	Co1-N32-H32	107.9
O15-B7-O14	104.40(19)	H21C-N21-H21D	107.8	C34-N33-Co1	110.75(15)
O9-B7-O8	111.29(19)	C22-N22-Co1	108.76(16)	C34-N33-H33C	109.5
O15-B7-O8	109.2(2)	C23-N22-Co1	108.30(15)	Co1-N33-H33C	109.5
O14-B7-O8	109.04(19)	C22-N22-H22	108.3	C34-N33-H33D	109.5
B1-O1-B2	125.1(2)	C23-N22-H22	108.3	Co1-N33-H33D	109.5
B3-O2-B2	122.5(2)	Co1-N22-H22	108.3	H33C-N33-H33D	108.1
B3-O3-B1	120.7(2)	C24-N23-Co1	110.15(15)	H51A-O51-H51B	109.4
B4-O4-B1	124.41(18)	C24-N23-H23C	109.6	H52A-O52-H52B	109.4
B5-O5-B4	118.79(19)	Co1-N23-H23C	109.6	H53A-O53-H53B	109.5
B5-O6-B1	124.81(19)	C24-N23-H23D	109.6	H54A-O54-H54B	109.5
B6-O7-B2	123.01(19)	Co1-N23-H23D	109.6	H55A-O55-H55B	109.5
B6-O8-B7	120.71(19)	H23C-N23-H23D	108.1	H56A-O56-H56B	109.5
B2-O9-B7	129.20(18)	N31-C31-C32	109.2(2)	H57A-O57-H57B	109.5
B3-O10-H10	109.5	N31-C31-H31A	109.8	H58A-O58-H58B	109.5
B4-O11-H11	109.5	C32-C31-H31A	109.8	H88A-O88-H88B	109.5
B5-O12-H12	109.5	N31-C31-H31B	109.8	H59A-O59-H59B	109.5
B6-O13-H13	109.5	C32-C31-H31B	109.8	H89A-O89-H89B	109.5
B7-O14-H14	109.5				

Table 7 Bond lengths [\AA] in **12**.

Co1-N15	1.966(2)	N18-O1	1.212(3)	C42-N35	1.496(3)	C18-H18B	0.9900
Co1-N16	1.969(2)	N18-O13	1.226(3)	C42-C43	1.504(4)	C19-N14	1.487(3)
Co1-N12	1.970(2)	C31-C41	1.518(4)	C42-H42A	0.9900	C19-H19A	0.9900
Co1-N11	1.972(2)	C31-C33	1.526(4)	C42-H42B	0.9900	C19-H19B	0.9900
Co1-N13	1.972(2)	C31-C37	1.528(3)	C43-N36	1.486(3)	C20-N14	1.487(3)
Co1-N14	1.975(2)	C31-N37	1.529(3)	C43-H43A	0.9900	C20-H20A	0.9900
Co2-N31	1.963(2)	C32-C40	1.518(4)	C43-H43B	0.9900	C20-H20B	0.9900
Co2-N36	1.965(2)	C32-C44	1.526(4)	C44-N36	1.486(3)	C21-N15	1.490(3)
Co2-N35	1.967(2)	C32-C36	1.528(3)	C44-H44A	0.9900	C21-H21A	0.9900
Co2-N33	1.970(2)	C32-N38	1.531(3)	C44-H44B	0.9900	C21-H21B	0.9900
Co2-N34	1.971(2)	C33-N31	1.478(3)	N31-H31	1.0000	C22-N15	1.493(3)
Co2-N32	1.973(2)	C33-H33A	0.9900	N32-H32	1.0000	C22-C23	1.495(4)
B1-O1	1.466(4)	C33-H33B	0.9900	N33-H33	1.0000	C22-H22A	0.9900
B1-O5	1.467(3)	C34-N31	1.489(3)	N34-H34	1.0000	C22-H22B	0.9900
B1-O4	1.468(3)	C34-C35	1.510(4)	N35-H35	1.0000	C23-N16	1.486(3)
B1-O3	1.471(4)	C34-H34A	0.9900	N36-H36	1.0000	C23-H23A	0.9900
B2-O1	1.351(3)	C34-H34B	0.9900	N37-O31	1.211(3)	C23-H23B	0.9900
B2-O6	1.359(4)	C35-N32	1.481(3)	N37-O32	1.226(3)	C24-N16	1.484(3)
B2-O2	1.380(4)	C35-H35A	0.9900	N38-O33	1.209(3)	C24-H24A	0.9900
B3-O3	1.347(4)	C35-H35B	0.9900	N38-O34	1.219(3)	C24-H24B	0.9900
B3-O7	1.357(4)	C36-N32	1.491(3)	O51-H51A	0.8496	N11-H11	1.0000
B3-O2	1.386(4)	C36-H36A	0.9900	O51-H51A	0.8496	N12-H12	1.0000
O4-H4	0.8400	C36-H36B	0.9900	C13-H13B	0.9900	N13-H13	1.0000
O5-H5	0.8400	C37-N33	1.493(3)	C14-N11	1.495(3)	N14-H14	1.0000
O6-H6	0.8400	C37-H37A	0.9900	C14-C15	1.503(4)	N15-H15	1.0000
O7-H7	0.8400	C37-H37B	0.9900	C14-H14A	0.9900	O51-H51B	0.8495

C11–C17	1.519(4)	C38–N33	1.486(3)	C14–H14B	0.9900	O52–H52A	0.8496
C11–C21	1.522(4)	C38–C39	1.500(4)	C15–N12	1.492(3)	O52–H52B	0.8502
C11–C13	1.525(3)	C38–H38A	0.9900	C15–H15A	0.9900	O53–H53A	0.8496
C11–N17	1.527(3)	C38–H38B	0.9900	C15–H15B	0.9900	O53–H53B	0.8505
C12–C16	1.505(4)	C39–N34	1.495(3)	C16–N12	1.493(3)	O54–H54A	0.8501
C12–C24	1.528(3)	C39–H39A	0.9900	C16–H16A	0.9900	O54–H54B	0.8501
C12–C20	1.531(3)	C39–H39B	0.9900	C16–H16B	0.9900	O55–H55A	0.8500
C12–N18	1.531(3)	C40–N34	1.485(3)	C17–N13	1.494(3)	O55–H55B	0.8494
C13–N11	1.487(3)	C40–H40A	0.9900	C17–H17A	0.9900	O61–H61A	0.8500
C13–H13A	0.9900	C40–H40B	0.9900	C17–H17B	0.9900	O61–H61B	0.8499
N16–H16	1.0000	C41–N35	1.495(3)	C18–N13	1.492(3)		
N17–O12	1.212(3)	C41–H41A	0.9900	C18–C19	1.502(4)		
N17–O11	1.223(3)	C41–H41B	0.9900	C18–H18A	0.9900		

Table 8 Bond angles [°] in 12.

N15–Co1–N16	86.43(9)	N14–C20–C12	110.6(2)	N32–C36–C32	111.5(2)
N15–Co1–N12	92.58(9)	N14–C20–H20A	109.5	N32–C36–H36A	109.3
N16–Co1–N12	90.39(9)	C12–C20–H20A	109.5	C32–C36–H36A	109.3
N15–Co1–N11	90.78(9)	N14–C20–H20B	109.5	N32–C36–H36B	109.3
N16–Co1–N11	175.79(9)	C12–C20–H20B	109.5	C32–C36–H36B	109.3
N12–Co1–N11	86.58(9)	H20A–C20–H20B	108.1	H36A–C36–H36B	108.0
N15–Co1–N13	90.32(9)	N15–C21–C11	111.8(2)	N33–C37–C31	111.0(2)
N16–Co1–N13	92.05(9)	N15–C21–H21A	109.3	N33–C37–H37A	109.4
N12–Co1–N13	176.33(9)	C11–C21–H21A	109.3	C31–C37–H37A	109.4
N11–Co1–N13	91.12(9)	N15–C21–H21B	109.3	N33–C37–H37B	109.4
N15–Co1–N14	176.54(9)	C11–C21–H21B	109.3	C31–C37–H37B	109.4
N16–Co1–N14	91.25(9)	H21A–C21–H21B	107.9	H37A–C37–H37B	108.0
N12–Co1–N14	90.00(9)	N15–C22–C23	106.4(2)	N33–C38–C39	107.8(2)
N11–Co1–N14	91.67(9)	N15–C22–H22A	110.5	N33–C38–H38A	110.2
N13–Co1–N14	87.20(9)	C23–C22–H22A	110.5	C39–C38–H38A	110.2
N31–Co2–N36	176.86(9)	N15–C22–H22B	110.5	N33–C38–H38B	110.2
N31–Co2–N35	90.61(9)	C23–C22–H22B	110.5	C39–C38–H38B	110.2
N36–Co2–N35	87.52(9)	H22A–C22–H22B	108.6	H38A–C38–H38B	108.5
N31–Co2–N33	91.96(9)	N16–C23–C22	106.9(2)	N34–C39–C38	106.4(2)
N36–Co2–N33	90.56(9)	N16–C23–H23A	110.4	N34–C39–H39A	110.4
N35–Co2–N33	90.24(9)	C22–C23–H23A	110.4	C38–C39–H39A	110.4
N31–Co2–N34	91.98(9)	N16–C23–H23B	110.4	N34–C39–H39B	110.4
N36–Co2–N34	90.02(9)	C22–C23–H23B	110.4	C38–C39–H39B	110.4
N35–Co2–N34	176.12(8)	H23A–C23–H23B	108.6	H39A–C39–H39B	108.6
N33–Co2–N34	86.78(9)	N16–C24–C12	112.3(2)	N34–C40–C32	111.7(2)
N31–Co2–N32	86.84(9)	N16–C24–H24A	109.1	N34–C40–H40A	109.3
N36–Co2–N32	90.69(9)	C12–C24–H24A	109.1	C32–C40–H40A	109.3
N35–Co2–N32	91.21(9)	N16–C24–H24B	109.1	N34–C40–H40B	109.3
N33–Co2–N32	178.12(10)	C12–C24–H24B	109.1	C32–C40–H40B	109.3
N34–Co2–N32	91.82(9)	H24A–C24–H24B	107.9	H40A–C40–H40B	107.9
O1–B1–O5	109.8(2)	C13–N11–C14	112.5(2)	N35–C41–C31	111.7(2)
O1–B1–O4	108.3(2)	C13–N11–Co1	118.41(16)	N35–C41–H41A	109.3
O5–B1–O4	108.3(2)	C14–N11–Co1	106.96(15)	C31–C41–H41A	109.3
O1–B1–O3	112.3(2)	C13–N11–H11	106.0	N35–C41–H41B	109.3
O5–B1–O3	108.8(2)	C14–N11–H11	106.0	C31–C41–H41B	109.3
O4–B1–O3	109.2(2)	Co1–N11–H11	106.0	H41A–C41–H41B	107.9
O1–B2–O6	122.9(3)	C15–N12–C16	112.5(2)	N35–C42–C43	107.0(2)
O1–B2–O2	121.6(3)	C15–N12–Co1	107.50(16)	N35–C42–H42A	110.3
O6–B2–O2	115.5(2)	C16–N12–Co1	118.58(16)	C43–C42–H42A	110.3
O3–B3–O7	123.7(3)	C15–N12–H12	105.8	N35–C42–H42B	110.3
O3–B3–O2	121.6(3)	C16–N12–H12	105.8	C43–C42–H42B	110.3
O7–B3–O2	114.7(2)	Co1–N12–H12	105.8	H42A–C42–H42B	108.6
B2–O1–B1	122.2(2)	C18–N13–C17	112.02(19)	N36–C43–C42	107.1(2)
B2–O2–B3	118.8(2)	C18–N13–Co1	106.79(15)	N36–C43–H43A	110.3
B3–O3–B1	122.4(2)	C17–N13–Co1	118.35(16)	C42–C43–H43A	110.3
B1–O4–H4	109.5	C18–N13–H13	106.3	N36–C43–H43B	110.3

B1-O5-H5	109.5	C17-N13-H13	106.3	C42-C43-H43B	110.3
B2-O6-H6	109.5	Co1-N13-H13	106.3	H43A-C43-H43B	108.5
B3-O7-H7	109.5	C19-N14-C20	112.0(2)	N36-C44-C32	111.3(2)
C17-C11-C21	112.4(2)	C19-N14-Co1	106.89(15)	N36-C44-H44A	109.4
C17-C11-C13	112.3(2)	C20-N14-Co1	119.12(16)	C32-C44-H44A	109.4
C21-C11-C13	113.3(2)	C19-N14-H14	106.0	N36-C44-H44B	109.4
C17-C11-N17	108.1(2)	C20-N14-H14	106.0	C32-C44-H44B	109.4
C21-C11-N17	105.3(2)	Co1-N14-H14	106.0	H44A-C44-H44B	108.0
C13-C11-N17	104.8(2)	C21-N15-C22	113.1(2)	C33-N31-C34	113.33(19)
C16-C12-C24	113.3(2)	C21-N15-Co1	118.40(16)	C33-N31-Co2	118.36(16)
C16-C12-C20	112.9(2)	C22-N15-Co1	107.74(16)	C34-N31-Co2	107.43(16)
C24-C12-C20	112.1(2)	C21-N15-H15	105.5	C33-N31-H31	105.6
C16-C12-N18	108.1(2)	C22-N15-H15	105.5	C34-N31-H31	105.6
C24-C12-N18	103.8(2)	Co1-N15-H15	105.5	Co2-N31-H31	105.6
C20-C12-N18	105.8(2)	C24-N16-C23	113.6(2)	C35-N32-C36	113.03(19)
N11-C13-C11	111.6(2)	C24-N16-Co1	117.49(15)	C35-N32-Co2	106.92(16)
N11-C13-H13A	109.3	C23-N16-Co1	106.97(16)	C36-N32-Co2	117.78(15)
C11-C13-H13A	109.3	C24-N16-H16	106.0	C35-N32-H32	106.1
N11-C13-H13B	109.3	C23-N16-H16	106.0	C36-N32-H32	106.1
C11-C13-H13B	109.3	Co1-N16-H16	106.0	Co2-N32-H32	106.1
H13A-C13-H13B	108.0	O12-N17-O11	124.1(2)	C38-N33-C37	113.2(2)
N11-C14-C15	106.5(2)	O12-N17-C11	119.3(2)	C38-N33-Co2	107.63(15)
N11-C14-H14A	110.4	O11-N17-C11	116.6(2)	C37-N33-Co2	118.47(15)
C15-C14-H14A	110.4	O14-N18-O13	124.5(2)	C38-N33-H33	105.5
N11-C14-H14B	110.4	O14-N18-C12	117.5(2)	C37-N33-H33	105.5
C15-C14-H14B	110.4	O13-N18-C12	117.9(2)	Co2-N33-H33	105.5
H14A-C14-H14B	108.6	C41-C31-C33	112.7(2)	C40-N34-C39	113.00(19)
N12-C15-C14	106.4(2)	C41-C31-C37	112.7(2)	C40-N34-Co2	117.52(16)
N12-C15-H15A	110.5	C33-C31-C37	113.1(2)	C39-N34-Co2	106.91(15)
C14-C15-H15A	110.5	C41-C31-N37	107.9(2)	C40-N34-H34	106.2
N12-C15-H15B	110.5	C33-C31-N37	104.6(2)	C39-N34-H34	106.2
C14-C15-H15B	110.5	C37-C31-N37	105.2(2)	Co2-N34-H34	106.2
H15A-C15-H15B	108.6	C40-C32-C44	113.7(2)	C41-N35-C42	113.05(19)
N12-C16-C12	111.3(2)	C40-C32-C36	112.8(2)	C41-N35-Co2	117.75(16)
N12-C16-H16A	109.4	C44-C32-C36	111.3(2)	C42-N35-Co2	106.41(15)
C12-C16-H16A	109.4	C40-C32-N38	107.0(2)	C41-N35-H35	106.3
N12-C16-H16B	109.4	C44-C32-N38	106.5(2)	C42-N35-H35	106.3
C12-C16-H16B	109.4	C36-C32-N38	104.8(2)	Co2-N35-H35	106.3
H16A-C16-H16B	108.0	N31-C33-C31	111.5(2)	C44-N36-C43	113.1(2)
N13-C17-C11	111.7(2)	N31-C33-H33A	109.3	C44-N36-Co2	118.52(16)
N13-C17-H17A	109.3	C31-C33-H33A	109.3	C43-N36-Co2	106.96(15)
C11-C17-H17A	109.3	N31-C33-H33B	109.3	C44-N36-H36	105.8
N13-C17-H17B	109.3	C31-C33-H33B	109.3	C43-N36-H36	105.8
C11-C17-H17B	109.3	H33A-C33-H33B	108.0	Co2-N36-H36	105.8
H17A-C17-H17B	107.9	N31-C34-C35	106.4(2)	O31-N37-O32	124.3(2)
N13-C18-C19	107.6(2)	N31-C34-H34A	110.4	O31-N37-C31	119.1(2)
N13-C18-H18A	110.2	C35-C34-H34A	110.4	O32-N37-C31	116.5(2)
C19-C18-H18A	110.2	N31-C34-H34B	110.4	O33-N38-O34	123.6(2)
N13-C18-H18B	110.2	C35-C34-H34B	110.4	O33-N38-C32	118.6(2)
C19-C18-H18B	110.2	H34A-C34-H34B	108.6	O34-N38-C32	117.6(2)
H18A-C18-H18B	108.5	N32-C35-C34	106.9(2)	H51A-O51-H51B	109.5
N14-C19-C18	107.1(2)	N32-C35-H35A	110.3	H52A-O52-H52B	109.5
N14-C19-H19A	110.3	C34-C35-H35A	110.3	H53A-O53-H53B	109.5
C18-C19-H19A	110.3	N32-C35-H35B	110.3	H54A-O54-H54B	109.5
N14-C19-H19B	110.3	C34-C35-H35B	110.3	H55A-O55-H55B	109.4
C18-C19-H19B	110.3	H35A-C35-H35B	108.6	H61A-O61-H61B	109.5
H19A-C19-H19B	108.5				

Table 9 Bond lengths [\AA] in **20**.

Cu1–N2	2.0044(14)	B2–O7	1.356(2)	B5–O10	1.365(2)	C1–H1B	0.9900
Cu1–N2 ⁱ	2.0044(14)	B2–O2	1.393(2)	B5–O5	1.388(2)	C2–N2	1.487(2)
Cu1–N1	2.0195(14)	B3–O8	1.366(2)	O7–H7	0.8400	C2–H2	0.9900
Cu1–N1	2.0195(14)	B3–O3	1.370(2)	O8–H8	0.8400	C2–H2	0.9900
B1–O1	1.455(2)	B3–O2	1.377(2)	O9–H9	0.8400	N1–H1C	0.9900
B1–O6	1.463(2)	B4–O9	1.359(2)	O10–H10	0.8400	N1–H1D	0.9900
B1–O4	1.4725(19)	B4–O4	1.360(2)	C1–N1	1.487(2)	N2–H2C	0.9900
B1–O3	1.487(2)	B4–O5	1.384(2)	C1–C2	1.519(2)	N2–H2D	0.9900
B2–O1	1.355(2)	B5–O6	1.360(2)	C1–H1A	0.9900	O21–H21A	0.8500
						O21–H21B	0.8501

Table 10 Bond angles [$^{\circ}$] in **20**.

N2–Cu1–N2 ⁱ	180.0	O4–B4–O5	120.77(14)	N2–C2–C1	107.59(13)
N2–Cu1–N1	84.80(6)	O6–B5–O10	122.71(14)	N2–C2–H2A	110.2
N2 ⁱ –Cu1–N1	95.20(6)	O6–B5–O5	121.31(15)	C1–C2–H2A	110.2
N2–Cu1–N1 ⁱ	95.20(6)	O10–B5–O5	115.96(15)	N2–C2–H2B	110.2
N2 ⁱ –Cu1–N1 ⁱ	84.80(6)	B2–O1–B1	125.52(13)	C1–C2–H2B	110.2
N1–Cu1–N1 ⁱ	180.0	B3–O2–B2	119.10(14)	H2A–C2–H2B	108.5
O1–B1–O6	109.30(13)	B3–O3–B1	122.03(13)	C1–N1–Cu1	107.07(10)
O1–B1–O4	108.70(12)	B4–O4–B1	123.68(13)	C1–N1–H1C	110.3
O6–B1–O4	111.51(13)	B4–O5–B5	119.34(14)	Cu1–N1–H1C	110.3
O1–B1–O3	110.56(13)	B5–O6–B1	123.30(12)	C1–N1–H1D	110.3
O6–B1–O3	109.02(12)	B2–O7–H7	109.5	Cu1–N1–H1D	110.3
O4–B1–O3	107.74(13)	B3–O8–H8	109.5	H1C–N1–H1D	108.6
O1–B2–O7	118.31(15)	B4–O9–H9	109.5	C2–N2–Cu1	110.10(10)
O1–B2–O2	119.97(15)	B5–O10–H10	109.5	C2–N2–H2C	109.6
O7–B2–O2	121.68(16)	N1–C1–C2	107.37(13)	Cu1–N2–H2C	109.6
O8–B3–O3	120.77(15)	N1–C1–H1A	110.2	C2–N2–H2D	109.6
O8–B3–O2	117.12(15)	C2–C1–H1A	110.2	Cu1–N2–H2D	109.6
O3–B3–O2	122.09(15)	N1–C1–H1B	110.2	H2C–N2–H2D	108.2
O9–B4–O4	122.10(15)	C2–C1–H1B	110.2	H21A–O21–H21B	109.5
O9–B4–O5	117.12(15)	H1A–C1–H1B	108.5		

Table 11 Bond lengths [\AA] in **22**.

Cu1–N2B	1.9714(11)	N12–H12B	0.9100	C11B–C12B	1.492(12)	O11–B12	1.3419(17)
Cu1–N2	1.9714(11)	N12B–C12B	1.525(10)	C11B–H11G	0.9900	O11–B11	1.4666(16)
Cu1–N12B	1.9832(11)	N12B–H12C	0.9100	C11B–H11H	0.9900	O12–B13	1.3794(16)
Cu1–N12	1.9832(11)	N12B–H12D	0.9100	C12B–C13B	1.511(18)	O12–B12	1.3848(17)
Cu1–N11B	2.0084(11)	C1–C2	1.509(2)	C12B–H12E	1.0000	O13–B13	1.3440(16)
Cu1–N11	2.0084(11)	C1–H1C	0.9900	C13B–H13D	0.9800	O13–B11	1.4609(16)
Cu1–N1B	2.0115(12)	C1–H1D	0.9900	C13B–H13E	0.9800	O14–B14	1.3494(17)
Cu1–N1	2.0115(12)	C2–C3	1.498(3)	C13B–H13F	0.9800	O14–B11	1.4474(16)
N1–C1	1.498(2)	C2–H2	1.0000	O1–B2	1.3535(17)	O15–B15	1.3692(16)
N1–H1A	0.9100	C3–H3A	0.9800	O1–B1	1.4645(15)	O15–B14	1.3818(17)
N1–H1B	0.9100	C3–H3B	0.9800	O2–B3	1.3764(16)	O16–B15	1.3501(16)
N1B–C1B	1.366(11)	C3–H3C	0.9800	O2–B2	1.3824(17)	O16–B11	1.4590(16)
N1B–H1BA	0.9100	C11–C12	1.512(2)	O3–B3	1.3501(16)	O17–B12	1.3484(17)
N1B–H1BB	0.9100	C11–H11E	0.9900	O3–B1	1.4628(15)	O17–H17	0.8400
N2–C2	1.4890(19)	C11–H11F	0.9900	O4–B4	1.3474(16)	O18–B13	1.3545(16)
N2–H2A	0.9100	C12–C13	1.515(5)	O4–B1	1.4640(16)	O18–H18	0.8400
N2–H2B	0.9100	C12–H12	1.0000	O5–B4	1.3662(16)	O19–B14	1.3465(17)
N2B–C2B	1.467(13)	C13–H13A	0.9800	O5–B5	1.3800(16)	O19–H19	0.8400
N2B–H2BA	0.9100	C13–H13B	0.9800	O6–B5	1.3497(16)	O20–B15	1.3522(17)
N2B–H2BB	0.9100	C13–H13C	0.9800	O6–B1	1.4547(16)	O20–H20	0.8400
N11–C11	1.4778(19)	C1B–C2B	1.537(13)	O7–B2	1.3447(17)	O21–H21A	0.8695
N11–H11A	0.9100	C1B–H1BC	0.9900	O7–H7	0.8400	O21–H21B	0.8700
N11–H11B	0.9100	C1B–H1BD	0.9900	O8–B3	1.3551(16)	O23–H23A	0.8699
N11B–C11B	1.483(10)	C2B–C3B	1.482(17)	O8–H8	0.8400	O23–H23B	0.8700

N11B–H11C	0.9100	C2B–H2BC	1.0000	O9–B4	1.3548(16)	O22–H22A	0.8699
N11B–H11D	0.9100	C3B–H3BA	0.9800	O9–H9	0.8400	O22–H22B	0.8701
N12–C12	1.4799(19)	C3B–H3BB	0.9800	O10–B5	1.3502(17)	O24–H24A	0.8703
N12–H12A	0.9100	C3B–H3BC	0.9800	O10–H10	0.8400	O24–H24B	0.8698

Table 12 Bond angles [°] in 22.

N2B–Cu1–N12B	175.36(5)	C2–C1–H1D	110.3	H13D–C13B–H13E	109.5
N2–Cu1–N12	175.36(5)	H1C–C1–H1D	108.5	C12B–C13B–H13F	109.5
N2B–Cu1–N11B	95.19(4)	N2–C2–C3	112.14(14)	H13D–C13B–H13F	109.5
N12B–Cu1–N11B	84.75(5)	N2–C2–C1	106.23(14)	H13E–C13B–H13F	109.5
N2–Cu1–N11	95.19(4)	C3–C2–C1	112.35(16)	B2–O1–B1	122.37(10)
N12–Cu1–N11	84.75(5)	N2–C2–H2	108.7	B3–O2–B2	119.38(11)
N2B–Cu1–N1B	85.56(5)	C3–C2–H2	108.7	B3–O3–B1	121.64(10)
N12B–Cu1–N1B	94.14(5)	C1–C2–H2	108.7	B4–O4–B1	122.98(10)
N11B–Cu1–N1B	175.44(5)	C2–C3–H3A	109.5	B4–O5–B5	119.17(10)
N2–Cu1–N1	85.56(5)	C2–C3–H3B	109.5	B5–O6–B1	122.85(10)
N12–Cu1–N1	94.14(5)	H3A–C3–H3B	109.5	B2–O7–H7	109.5
N11–Cu1–N1	175.44(5)	C2–C3–H3C	109.5	B3–O8–H8	109.5
C1–N1–Cu1	106.85(9)	H3A–C3–H3C	109.5	B4–O9–H9	109.5
C1–N1–H1A	110.4	H3B–C3–H3C	109.5	B5–O10–H10	109.5
Cu1–N1–H1A	110.4	N11–C11–C12	108.20(14)	O6–B1–O3	108.66(10)
C1–N1–H1B	110.4	N11–C11–H11E	110.1	O6–B1–O4	111.91(10)
Cu1–N1–H1B	110.4	C12–C11–H11E	110.1	O3–B1–O4	108.24(10)
H1A–N1–H1B	108.6	N11–C11–H11F	110.1	O6–B1–O1	109.21(10)
C1B–N1B–Cu1	105.1(5)	C12–C11–H11F	110.1	O3–B1–O1	110.99(10)
C1B–N1B–H1BA	110.7	H11E–C11–H11F	108.4	O4–B1–O1	107.84(10)
Cu1–N1B–H1BA	110.7	N12–C12–C11	106.78(13)	O7–B2–O1	122.49(12)
C1B–N1B–H1BB	110.7	N12–C12–C13	111.8(3)	O7–B2–O2	117.07(12)
Cu1–N1B–H1BB	110.7	C11–C12–C13	112.0(3)	O1–B2–O2	120.44(12)
H1BA–N1B–H1BB	108.8	N12–C12–H12	108.7	O3–B3–O8	122.43(12)
C2–N2–Cu1	109.24(9)	C11–C12–H12	108.7	O3–B3–O2	121.05(11)
C2–N2–H2A	109.8	C13–C12–H12	108.7	O8–B3–O2	116.41(11)
Cu1–N2–H2A	109.8	C12–C13–H13A	109.5	O4–B4–O9	117.86(11)
C2–N2–H2B	109.8	C12–C13–H13B	109.5	O4–B4–O5	121.31(11)
Cu1–N2–H2B	109.8	H13A–C13–H13B	109.5	O9–B4–O5	120.82(11)
H2A–N2–H2B	108.3	C12–C13–H13C	109.5	O6–B5–O10	119.29(11)
C2B–N2B–Cu1	106.6(5)	H13A–C13–H13C	109.5	O6–B5–O5	121.41(12)
C2B–N2B–H2BA	110.4	H13B–C13–H13C	109.5	O10–B5–O5	119.30(11)
Cu1–N2B–H2BA	110.4	N1B–C1B–C2B	107.2(9)	B12–O11–B11	124.11(10)
C2B–N2B–H2BB	110.4	N1B–C1B–H1BC	110.3	B13–O12–B12	118.68(11)
Cu1–N2B–H2BB	110.4	C2B–C1B–H1BC	110.3	B13–O13–B11	123.84(10)
H2BA–N2B–H2BB	108.6	N1B–C1B–H1BD	110.3	B14–O14–B11	123.18(10)
C11–N11–Cu1	107.41(9)	C2B–C1B–H1BD	110.3	B15–O15–B14	119.22(10)
C11–N11–H11A	110.2	H1BC–C1B–H1BD	108.5	B15–O16–B11	121.47(10)
Cu1–N11–H11A	110.2	N2B–C2B–C3B	105.5(16)	B12–O17–H17	109.5
C11–N11–H11B	110.2	N2B–C2B–C1B	105.2(9)	B13–O18–H18	109.5
Cu1–N11–H11B	110.2	C3B–C2B–C1B	108.3(15)	B14–O19–H19	109.5
H11A–N11–H11B	108.5	N2B–C2B–H2BC	112.5	B15–O20–H20	109.5
C11B–N11B–Cu1	108.3(4)	C3B–C2B–H2BC	112.5	O14–B11–O16	111.31(10)
C11B–N11B–H11C	110.0	C1B–C2B–H2BC	112.5	O14–B11–O13	109.53(10)
Cu1–N11B–H11C	110.0	C2B–C3B–H3BA	109.5	O16–B11–O13	107.60(10)
C11B–N11B–H11D	110.0	C2B–C3B–H3BB	109.5	O14–B11–O11	109.45(10)
Cu1–N11B–H11D	110.0	H3BA–C3B–H3BB	109.5	O16–B11–O11	108.23(10)
H11C–N11B–H11D	108.4	C2B–C3B–H3BC	109.5	O13–B11–O11	110.71(10)
C12–N12–Cu1	110.88(9)	H3BA–C3B–H3BC	109.5	O11–B12–O17	122.66(12)
C12–N12–H12A	109.5	H3BB–C3B–H3BC	109.5	O11–B12–O12	120.91(12)
Cu1–N12–H12A	109.5	N11B–C11B–C12B	109.4(8)	O17–B12–O12	116.43(12)
C12–N12–H12B	109.5	N11B–C11B–H11G	109.8	O13–B13–O18	121.68(12)
Cu1–N12–H12B	109.5	C12B–C11B–H11G	109.8	O13–B13–O12	121.34(11)
H12A–N12–H12B	108.1	N11B–C11B–H11H	109.8	O18–B13–O12	116.94(11)
C12B–N12B–Cu1	108.2(3)	C12B–C11B–H11H	109.8	O19–B14–O14	118.94(12)

C12B–N12B–H12C	110.1	H11G–C11B–H11H	108.2	O19–B14–O15	120.62(12)
Cu1–N12B–H12C	110.1	C11B–C12B–C13B	112.3(17)	O14–B14–O15	120.44(12)
C12B–N12B–H12D	110.1	C11B–C12B–N12B	103.7(8)	O16–B15–O20	121.50(12)
Cu1–N12B–H12D	110.1	C13B–C12B–N12B	107(2)	O16–B15–O15	121.16(12)
H12C–N12B–H12D	108.4	C11B–C12B–H12E	111.1	O20–B15–O15	117.34(11)
N1–C1–C2	107.11(13)	C13B–C12B–H12E	111.1	H21A–O21–H21B	109.5
N1–C1–H1C	110.3	N12B–C12B–H12E	111.1	H23A–O23–H23B	109.4
C2–C1–H1C	110.3	C12B–C13B–H13D	109.5	H22A–O22–H22B	109.4
N1–C1–H1D	110.3	C12B–C13B–H13E	109.5	H24A–O24–H24B	109.5

Table 13 Bond lengths [\AA] in **23**.

Cu1–N2A	1.99(2)	O8–B3	1.453(3)	C3–H3B	0.9800	C3A–H3AB	0.9800
Cu1–O2	1.9802(16)	O9–B6	1.360(3)	C3–H3C	0.9800	C3A–H3AC	0.9800
Cu1–O3	1.9934(16)	O9–B3	1.455(3)	C4–H4A	0.9800	C4A–H4AA	0.9800
Cu1–N1	2.035(6)	O10–B6	1.365(3)	C4–H4B	0.9800	C4A–H4AB	0.9800
Cu1–N1A	2.037(10)	O10–B1	1.453(3)	C4–H4C	0.9800	C4A–H4AC	0.9800
Cu1–N2	2.069(10)	O11–B4	1.375(3)	C5–H5A	0.9800	C5A–H5AA	0.9800
Cu1–O4	2.1871(16)	O11–H11	0.8400	C5–H5B	0.9800	C5A–H5AB	0.9800
O1–B1	1.513(3)	O12–B5	1.368(3)	C5–H5C	0.9800	C5A–H5AC	0.9800
O1–B2	1.513(3)	O12–H12	0.8400	C6–H6A	0.9800	C6A–H6AA	0.9800
O1–B3	1.516(3)	O13–B6	1.368(3)	C6–H6B	0.9800	C6A–H6AB	0.9800
O2–B1	1.483(3)	O13–H13	0.8400	C6–H6C	0.9800	C6A–H6AC	0.9800
O2–H2	0.872(9)	N1–C3	1.485(7)	N1A–C3A	1.478(12)	O21–H21A	0.8697
O3–B2	1.482(3)	N1–C1	1.481(7)	N1A–C4A	1.496(12)	O21–H21B	0.8706
O3–H3	0.8880	N1–C4	1.498(7)	N1A–C1A	1.496(11)	O24–H24A	0.8699
O4–B3	1.455(3)	N2–C6	1.466(8)	N2A–C6A	1.472(16)	O24–H24B	0.8699
O4–H4	0.8683	N2–C5	1.485(8)	N2A–C5A	1.471(14)	O22–H22A	0.8701
O5–B4	1.358(3)	N2–C2	1.496(8)	N2A–C2A	1.507(14)	O22–H22B	0.8702
O5–B1	1.436(3)	C1–C2	1.512(6)	C1A–C2A	1.488(11)	O23–H23A	0.8695
O6–B4	1.362(3)	C1–H1A	0.9900	C1A–H1AA	0.9900	O23–H23B	0.8704
O6–B2	1.436(3)	C1–H1B	0.9900	C1A–H1AB	0.9900	O25–H25A	0.8699
O7–B5	1.367(3)	C2–H2A	0.9900	C2A–H2AA	0.9900	O25–H25B	0.8701
O7–B2	1.451(3)	C2–H2B	0.9900	C2A–H2AB	0.9900	O26–H26A	0.8696
O8–B5	1.359(3)	C3–H3A	0.9800	C3A–H3AA	0.9800	O26–H26B	0.8699

Table 14 Bond angles [$^\circ$] in **23**.

N2A–Cu1–O2	90.0(4)	O5–B4–O6	123.3(2)	H6B–C6–H6C	109.5
N2A–Cu1–O3	175.7(4)	O5–B4–O11	117.9(2)	C3A–N1A–C4A	108.8(9)
O2–Cu1–O3	89.72(7)	O6–B4–O11	118.8(2)	C3A–N1A–C1A	109.7(9)
O2–Cu1–N1	176.69(17)	O8–B5–O7	123.2(2)	C4A–N1A–C1A	109.8(8)
O3–Cu1–N1	91.90(17)	O8–B5–O12	117.6(2)	C3A–N1A–Cu1	107.9(7)
N2A–Cu1–N1A	87.4(5)	O7–B5–O12	119.1(2)	C4A–N1A–Cu1	113.1(7)
O2–Cu1–N1A	163.1(3)	O9–B6–O10	122.5(2)	C1A–N1A–Cu1	107.4(6)
O3–Cu1–N1A	91.6(3)	O9–B6–O13	118.0(2)	C6A–N2A–C5A	108.6(14)
O2–Cu1–N2	92.3(2)	O10–B6–O13	119.4(2)	C6A–N2A–C2A	108.7(12)
O3–Cu1–N2	166.8(2)	C3–N1–C1	109.7(5)	C5A–N2A–C2A	108.7(12)
N1–Cu1–N2	85.4(3)	C3–N1–C4	108.7(5)	C6A–N2A–Cu1	114.0(13)
N2A–Cu1–O4	94.4(4)	C1–N1–C4	111.8(5)	C5A–N2A–Cu1	112.9(10)
O2–Cu1–O4	91.08(6)	C3–N1–Cu1	114.5(4)	C2A–N2A–Cu1	103.8(9)
O3–Cu1–O4	89.97(6)	C1–N1–Cu1	104.5(4)	C2A–C1A–N1A	109.3(7)
N1–Cu1–O4	91.80(17)	C4–N1–Cu1	107.7(4)	C2A–C1A–H1AA	109.8
N1A–Cu1–O4	105.8(3)	C6–N2–C5	109.7(7)	N1A–C1A–H1AA	109.8
N2–Cu1–O4	103.1(2)	C6–N2–C2	109.6(6)	C2A–C1A–H1AB	109.8
B1–O1–B2	114.76(16)	C5–N2–C2	109.9(7)	N1A–C1A–H1AB	109.8
B1–O1–B3	119.46(17)	C6–N2–Cu1	110.7(7)	H1AA–C1A–H1AB	108.3
B2–O1–B3	118.68(17)	C5–N2–Cu1	108.6(5)	C1A–C2A–N2A	110.4(9)
B1–O2–Cu1	118.98(14)	C2–N2–Cu1	108.4(5)	C1A–C2A–H2AA	109.6
B1–O2–H2	108.2(14)	N1–C1–C2	110.2(4)	N2A–C2A–H2AA	109.6
Cu1–O2–H2	124.8(13)	N1–C1–H1A	109.6	C1A–C2A–H2AB	109.6

B2-O3-Cu1	118.09(14)	C2-C1-H1A	109.6	N2A-C2A-H2AB	109.6
B2-O3-H3	107.3	N1-C1-H1B	109.6	H2AA-C2A-H2AB	108.1
Cu1-O3-H3	127.9	C2-C1-H1B	109.6	N1A-C3A-H3AA	109.5
B3-O4-Cu1	116.32(13)	H1A-C1-H1B	108.1	N1A-C3A-H3AB	109.5
B3-O4-H4	112.9	N2-C2-C1	108.8(5)	H3AA-C3A-H3AB	109.5
Cu1-O4-H4	130.4	N2-C2-H2A	109.9	N1A-C3A-H3AC	109.5
B4-O5-B1	121.34(19)	C1-C2-H2A	109.9	H3AA-C3A-H3AC	109.5
B4-O6-B2	121.45(19)	N2-C2-H2B	109.9	H3AB-C3A-H3AC	109.5
B5-O7-B2	123.67(19)	C1-C2-H2B	109.9	N1A-C4A-H4AA	109.5
B5-O8-B3	120.99(18)	H2A-C2-H2B	108.3	N1A-C4A-H4AB	109.5
B6-O9-B3	122.69(18)	N1-C3-H3A	109.5	H4AA-C4A-H4AB	109.5
B6-O10-B1	123.55(18)	N1-C3-H3B	109.5	N1A-C4A-H4AC	109.5
B4-O11-H11	109.5	H3A-C3-H3B	109.5	H4AA-C4A-H4AC	109.5
B5-O12-H12	109.5	N1-C3-H3C	109.5	H4AB-C4A-H4AC	109.5
B6-O13-H13	109.5	H3A-C3-H3C	109.5	N2A-C5A-H5AA	109.5
O5-B1-O10	109.79(18)	H3B-C3-H3C	109.5	N2A-C5A-H5AB	109.5
O5-B1-O2	112.08(18)	N1-C4-H4A	109.5	H5AA-C5A-H5AB	109.5
O10-B1-O2	110.43(19)	N1-C4-H4B	109.5	N2A-C5A-H5AC	109.5
O5-B1-O1	109.75(18)	H4A-C4-H4B	109.5	H5AA-C5A-H5AC	109.5
O10-B1-O1	108.49(18)	N1-C4-H4C	109.5	H5AB-C5A-H5AC	109.5
O2-B1-O1	106.18(17)	H4A-C4-H4C	109.5	N2A-C6A-H6AA	109.5
O6-B2-O7	109.61(18)	H4B-C4-H4C	109.5	N2A-C6A-H6AB	109.5
O6-B2-O3	111.55(18)	N2-C5-H5A	109.5	H6AA-C6A-H6AB	109.5
O7-B2-O3	111.09(18)	N2-C5-H5B	109.5	N2A-C6A-H6AC	109.5
O6-B2-O1	109.47(18)	H5A-C5-H5B	109.5	H6AA-C6A-H6AC	109.5
O7-B2-O1	108.11(18)	N2-C5-H5C	109.5	H6AB-C6A-H6AC	109.5
O3-B2-O1	106.91(17)	H5A-C5-H5C	109.5	H21A-O21-H21B	109.5
O8-B3-O9	109.32(17)	H5B-C5-H5C	109.5	H24A-O24-H24B	109.5
O8-B3-O4	112.42(19)	N2-C6-H6A	109.5	H22A-O22-H22B	109.4
O9-B3-O4	112.49(19)	N2-C6-H6B	109.5	H23A-O23-H23B	109.5
O8-B3-O1	108.72(18)	H6A-C6-H6B	109.5	H25A-O25-H25B	109.5
O9-B3-O1	108.06(17)	N2-C6-H6C	109.5	H26A-O26-H26B	109.4
O4-B3-O1	105.61(16)	H6A-C6-H6C	109.5		

Table 15 Bond lengths [\AA] in **24**.

Cu1-N1B ⁱ	1.910(13)	N1B-H1BA	0.9100	C11-C16	1.518(6)	C15B-H15D	0.9900
Cu1-N1B	1.910(13)	N1B-H1BB	0.9100	C11-C12	1.524(5)	C16B-H16C	0.9900
Cu1-N2B ⁱ	1.923(11)	N2B-C2B	1.496(7)	C11-H11	1.0000	C16B-H16D	0.9900
Cu1-N2B	1.923(11)	N2B-H2BA	0.9100	C12-C13	1.516(6)	O1-B2	1.505(3)
Cu1-N2	2.073(6)	N2B-H2BB	0.9100	C12-H12	1.0000	O1-B1	1.511(3)
Cu1-N2 ⁱ	2.073(6)	C1B-C6B	1.510(8)	C13-C14	1.530(7)	O1-B3	1.512(3)
Cu1-N1	2.076(7)	C1B-C2B	1.521(8)	C13-H13A	0.9900	O2-B4	1.373(3)
Cu1-N1 ⁱ	2.076(7)	C1B-H1BC	1.0000	C13-H13B	0.9900	O2-B1	1.464(3)
Cu1-O21 ⁱ	2.381(3)	C2B-C3B	1.516(8)	C14-C15	1.509(6)	O3-B4	1.355(4)
Cu1-O21	2.381(3)	C2B-H2BC	1.0000	C14-H14A	0.9900	O3-B2	1.436(3)
O21-H21A	0.8681	C3B-C4B	1.529(9)	C14-H14B	0.9900	O4-B6	1.367(3)
O21-H21B	0.8685	C3B-H3BA	0.9900	C15-C16	1.537(6)	O4-B2	1.467(3)
N1-C1	1.475(6)	C3B-H3BB	0.9900	C15-H15A	0.9900	O5-B6	1.366(3)
N1-H1A	0.9100	C4B-C5B	1.514(8)	C15-H15B	0.9900	O5-B3	1.468(3)
N1-H1B	0.9100	C4B-H4BA	0.9900	C16-H16A	0.9900	O6-B5	1.376(3)
N2-C2	1.480(6)	C4B-H4BB	0.9900	C16-H16B	0.9900	O6-B2	1.471(3)
N2-H2A	0.9100	C5B-C6B	1.547(9)	N11B-C11B	1.485(8)	O7-B5	1.359(3)
N2-H2B	0.9100	C5B-H5BA	0.9900	N11B-H11C	0.9100	O7-B3	1.461(3)
C1-C6	1.511(6)	C5B-H5BB	0.9900	N11B-H11D	0.9100	O8-B7	1.360(4)
C1-C2	1.516(6)	C6B-H6BA	0.9900	N12B-C12B	1.483(8)	O8-B3	1.437(3)
C1-H1	1.0000	C6B-H6BB	0.9900	N12B-H12C	0.9100	O9-B7	1.371(4)
C2-C3	1.512(6)	Cu2-N11 ⁱⁱ	1.963(7)	N12B-H12D	0.9100	O9-B1	1.439(3)
C2-H2	1.0000	Cu2-N11	1.963(7)	C11B-C16B	1.520(9)	O10-B4	1.373(4)
C3-C4	1.523(7)	Cu2-N12B ⁱⁱ	1.999(19)	C11B-C12B	1.524(8)	O10-H10	0.8400
C3-H3A	0.9900	Cu2-N12B	1.999(19)	C11B-H11E	1.0000	O11-B6	1.370(3)
C3-H3B	0.9900	Cu2-N12	2.013(8)	C12B-C13B	1.516(9)	O11-H11F	0.8400

C4–C5	1.510(7)	Cu2–N12 ⁱⁱ	2.013(8)	C12B–H12E	1.0000	O12–B5	1.372(3)
C4–H4A	0.9900	Cu2–N11B ⁱⁱ	2.070(18)	C13B–C14B	1.528(9)	O12–H12F	0.8400
C4–H4B	0.9900	Cu2–N11B	2.070(18)	C13B–H13C	0.9900	O13–B7	1.364(4)
C5–C6	1.528(7)	N11–C11	1.483(6)	C13B–H13D	0.9900	O13–H13	0.8400
C5–H5A	0.9900	N11–H11A	0.9100	C14B–C15B	1.509(9)	O14–B1	1.461(4)
C5–H5B	0.9900	N11–H11B	0.9100	C14B–H14C	0.9900	O14–H14	0.8400
C6–H6A	0.9900	N12–C12	1.481(6)	C14B–H14D	0.9900	O22–H22A	0.8495
C6–H6B	0.9900	N12–H12A	0.9100	C15B–C16B	1.540(9)	O22–H22B	0.8500
N1B–C1B	1.478(7)	N12–H12B	0.9100	C15B–H15C	0.9900	O23–H23A	0.8490
						O23–H23B	0.8518

Table 16 Bond angles [°] in 24.

N1B ⁱ –Cu1–N1B	180.0	N1B–C1B–H1BC	107.0	Cu2–N11B–H11C	110.5
N1B ⁱ –Cu1–N2B ⁱ	89.8(4)	C6B–C1B–H1BC	107.0	C11B–N11B–H11D	110.5
N1B–Cu1–N2B ⁱ	90.2(4)	C2B–C1B–H1BC	107.0	Cu2–N11B–H11D	110.5
N1B ⁱ –Cu1–N2B	90.2(4)	N2B–C2B–C3B	112.8(8)	H11C–N11B–H11D	108.6
N1B–Cu1–N2B	89.8(4)	N2B–C2B–C1B	105.8(7)	C12B–N12B–Cu2	112.3(9)
N2B ⁱ –Cu1–N2B	180.0(5)	C3B–C2B–C1B	110.2(8)	C12B–N12B–H12C	109.1
N2–Cu1–N2 ⁱ	180.0	N2B–C2B–H2BC	109.3	Cu2–N12B–H12C	109.1
N2–Cu1–N1	81.3(2)	C3B–C2B–H2BC	109.3	C12B–N12B–H12D	109.1
N2 ⁱ –Cu1–N1	98.7(2)	C1B–C2B–H2BC	109.3	Cu2–N12B–H12D	109.1
N2–Cu1–N1 ⁱ	98.7(2)	C2B–C3B–C4B	110.2(8)	H12C–N12B–H12D	107.9
N2 ⁱ –Cu1–N1 ⁱ	81.3(2)	C2B–C3B–H3BA	109.6	N11B–C11B–C16B	112.6(9)
N1–Cu1–N1 ⁱ	180.0	C4B–C3B–H3BA	109.6	N11B–C11B–C12B	108.1(9)
N1B ⁱ –Cu1–O21 ⁱ	101.4(5)	C2B–C3B–H3BB	109.6	C16B–C11B–C12B	109.8(9)
N1B–Cu1–O21 ⁱ	78.6(5)	C4B–C3B–H3BB	109.6	N11B–C11B–H11E	108.8
N2B ⁱ –Cu1–O21 ⁱ	105.1(4)	H3BA–C3B–H3BB	108.1	C16B–C11B–H11E	108.8
N2B–Cu1–O21 ⁱ	74.9(4)	C5B–C4B–C3B	112.5(9)	C12B–C11B–H11E	108.8
N2–Cu1–O21 ⁱ	85.33(18)	C5B–C4B–H4BA	109.1	N12B–C12B–C13B	114.0(10)
N2 ⁱ –Cu1–O21 ⁱ	94.67(18)	C3B–C4B–H4BA	109.1	N12B–C12B–C11B	107.0(10)
N1–Cu1–O21 ⁱ	86.6(3)	C5B–C4B–H4BB	109.1	C13B–C12B–C11B	110.2(9)
N1 ⁱ –Cu1–O21 ⁱ	93.4(3)	C3B–C4B–H4BB	109.1	N12B–C12B–H12E	108.5
N1B ⁱ –Cu1–O21	78.6(5)	H4BA–C4B–H4BB	107.8	C13B–C12B–H12E	108.5
N1B–Cu1–O21	101.4(5)	C4B–C5B–C6B	109.5(8)	C11B–C12B–H12E	108.5
N2B ⁱ –Cu1–O21	74.9(4)	C4B–C5B–H5BA	109.8	C12B–C13B–C14B	109.9(10)
N2B–Cu1–O21	105.1(4)	C6B–C5B–H5BA	109.8	C12B–C13B–H13C	109.7
N2–Cu1–O21	94.67(18)	C4B–C5B–H5BB	109.8	C14B–C13B–H13C	109.7
N2 ⁱ –Cu1–O21	85.33(18)	C6B–C5B–H5BB	109.8	C12B–C13B–H13D	109.7
N1–Cu1–O21	93.4(3)	H5BA–C5B–H5BB	108.2	C14B–C13B–H13D	109.7
N1 ⁱ –Cu1–O21	86.6(3)	C1B–C6B–C5B	110.3(8)	H13C–C13B–H13D	108.2
O21 ⁱ –Cu1–O21	180.0	C1B–C6B–H6BA	109.6	C15B–C14B–C13B	111.9(10)
Cu1–O21–H21A	110.3	C5B–C6B–H6BA	109.6	C15B–C14B–H14C	109.2
Cu1–O21–H21B	110.0	C1B–C6B–H6BB	109.6	C13B–C14B–H14C	109.2
H21A–O21–H21B	108.5	C5B–C6B–H6BB	109.6	C15B–C14B–H14D	109.2
C1–N1–Cu1	111.5(4)	H6BA–C6B–H6BB	108.1	C13B–C14B–H14D	109.2
C1–N1–H1A	109.3	N11 ⁱⁱ –Cu2–N11	180.0	H14C–C14B–H14D	107.9
Cu1–N1–H1A	109.3	N12B ⁱⁱ –Cu2–N12B	180.0	C14B–C15B–C16B	110.3(9)
C1–N1–H1B	109.3	N11 ⁱⁱ –Cu2–N12	94.00(17)	C14B–C15B–H15C	109.6
Cu1–N1–H1B	109.3	N11–Cu2–N12	86.01(17)	C16B–C15B–H15C	109.6
H1A–N1–H1B	108.0	N11 ⁱⁱ –Cu2–N12 ⁱⁱ	86.01(17)	C14B–C15B–H15D	109.6
C2–N2–Cu1	109.5(3)	N11–Cu2–N12 ⁱⁱ	93.99(17)	C16B–C15B–H15D	109.6
C2–N2–H2A	109.8	N12–Cu2–N12 ⁱⁱ	180.0	H15C–C15B–H15D	108.1
Cu1–N2–H2A	109.8	N12B ⁱⁱ –Cu2–N11B ⁱⁱ	83.5(4)	C11B–C16B–C15B	108.7(9)
C2–N2–H2B	109.8	N12B–Cu2–N11B ⁱⁱ	96.5(4)	C11B–C16B–H16C	110.0
Cu1–N2–H2B	109.8	N12B ⁱⁱ –Cu2–N11B	96.5(4)	C15B–C16B–H16C	110.0
H2A–N2–H2B	108.2	N12B–Cu2–N11B	83.5(4)	C11B–C16B–H16D	110.0
N1–C1–C6	114.8(5)	N11B ⁱⁱ –Cu2–N11B	180.0	C15B–C16B–H16D	110.0
N1–C1–C2	109.0(5)	C11–N11–Cu2	110.3(4)	H16C–C16B–H16D	108.3
C6–C1–C2	110.7(5)	C11–N11–H11A	109.6	B2–O1–B1	119.42(19)
N1–C1–H1	107.3	Cu2–N11–H11A	109.6	B2–O1–B3	110.7(2)
C6–C1–H1	107.3	C11–N11–H11B	109.6	B1–O1–B3	119.13(19)

C2-C1-H1	107.3	Cu2-N11-H11B	109.6	B4-O2-B1	120.3(2)
N2-C2-C3	113.5(5)	H11A-N11-H11B	108.1	B4-O3-B2	122.7(2)
N2-C2-C1	107.0(4)	C12-N12-Cu2	107.2(4)	B6-O4-B2	121.3(2)
C3-C2-C1	111.4(5)	C12-N12-H12A	110.3	B6-O5-B3	120.3(2)
N2-C2-H2	108.3	Cu2-N12-H12A	110.3	B5-O6-B2	119.0(2)
C3-C2-H2	108.3	C12-N12-H12B	110.3	B5-O7-B3	120.8(2)
C1-C2-H2	108.3	Cu2-N12-H12B	110.3	B7-O8-B3	122.8(2)
C2-C3-C4	111.4(6)	H12A-N12-H12B	108.5	B7-O9-B1	120.7(2)
C2-C3-H3A	109.3	N11-C11-C16	113.3(5)	B4-O10-H10	109.5
C4-C3-H3A	109.3	N11-C11-C12	107.8(5)	B6-O11-H11F	109.5
C2-C3-H3B	109.3	C16-C11-C12	109.9(4)	B5-O12-H12F	109.5
C4-C3-H3B	109.3	N11-C11-H11	108.5	B7-O13-H13	109.5
H3A-C3-H3B	108.0	C16-C11-H11	108.5	B1-O14-H14	109.5
C5-C4-C3	111.1(6)	C12-C11-H11	108.5	O9-B1-O14	108.4(2)
C5-C4-H4A	109.4	N12-C12-C13	114.6(5)	O9-B1-O2	111.3(2)
C3-C4-H4A	109.4	N12-C12-C11	108.2(5)	O14-B1-O2	111.5(2)
C5-C4-H4B	109.4	C13-C12-C11	111.1(4)	O9-B1-O1	107.5(2)
C3-C4-H4B	109.4	N12-C12-H12	107.6	O14-B1-O1	112.1(2)
H4A-C4-H4B	108.0	C13-C12-H12	107.6	O2-B1-O1	106.0(2)
C4-C5-C6	113.4(6)	C11-C12-H12	107.6	O3-B2-O4	110.2(2)
C4-C5-H5A	108.9	C12-C13-C14	110.2(5)	O3-B2-O6	111.0(2)
C6-C5-H5A	108.9	C12-C13-H13A	109.6	O4-B2-O6	111.4(2)
C4-C5-H5B	108.9	C14-C13-H13A	109.6	O3-B2-O1	109.7(2)
C6-C5-H5B	108.9	C12-C13-H13B	109.6	O4-B2-O1	107.1(2)
H5A-C5-H5B	107.7	C14-C13-H13B	109.6	O6-B2-O1	107.3(2)
C1-C6-C5	109.9(5)	H13A-C13-H13B	108.1	O8-B3-O7	112.0(2)
C1-C6-H6A	109.7	C15-C14-C13	111.4(5)	O8-B3-O5	109.8(2)
C5-C6-H6A	109.7	C15-C14-H14A	109.4	O7-B3-O5	111.0(2)
C1-C6-H6B	109.7	C13-C14-H14A	109.4	O8-B3-O1	109.5(2)
C5-C6-H6B	109.7	C15-C14-H14B	109.4	O7-B3-O1	108.1(2)
H6A-C6-H6B	108.2	C13-C14-H14B	109.4	O5-B3-O1	106.3(2)
C1B-N1B-Cu1	107.6(6)	H14A-C14-H14B	108.0	O3-B4-O10	117.0(2)
C1B-N1B-H1BA	110.2	C14-C15-C16	111.5(5)	O3-B4-O2	123.4(2)
Cu1-N1B-H1BA	110.2	C14-C15-H15A	109.3	O10-B4-O2	119.5(3)
C1B-N1B-H1BB	110.2	C16-C15-H15A	109.3	O7-B5-O12	116.9(2)
Cu1-N1B-H1BB	110.2	C14-C15-H15B	109.3	O7-B5-O6	123.0(2)
H1BA-N1B-H1BB	108.5	C16-C15-H15B	109.3	O12-B5-O6	120.1(2)
C2B-N2B-Cu1	103.8(6)	H15A-C15-H15B	108.0	O5-B6-O4	121.9(2)
C2B-N2B-H2BA	111.0	C11-C16-C15	109.0(4)	O5-B6-O11	117.2(2)
Cu1-N2B-H2BA	111.0	C11-C16-H16A	109.9	O4-B6-O11	121.0(2)
C2B-N2B-H2BB	111.0	C15-C16-H16A	109.9	O8-B7-O13	122.4(2)
Cu1-N2B-H2BB	111.0	C11-C16-H16B	109.9	O8-B7-O9	122.8(2)
H2BA-N2B-H2BB	109.0	C15-C16-H16B	109.9	O13-B7-O9	114.8(3)
N1B-C1B-C6B	115.4(8)	H16A-C16-H16B	108.3	H22A-O22-H22B	109.5
N1B-C1B-C2B	109.9(7)	C11B-N11B-Cu2	106.4(9)	H23A-O23-H23B	109.5
C6B-C1B-C2B	110.1(7)	C11B-N11B-H11C	110.5		

Table 17 Bond lengths [\AA] in 27.

Cu1-O21	2.3368(10)	N12-C14	1.4819(16)	O5-B5	1.3771(18)	O13-B13	1.3619(15)
Cu1-N1	1.9998(11)	C1-C2	1.5077(18)	O6-B1	1.4596(15)	O14-B11	1.4715(15)
Cu1-N2	2.0781(11)	C11-C12	1.5173(18)	O6-B5	1.3570(16)	O14-B14	1.3606(15)
Cu1-N11	1.9937(11)	O1-B1	1.4859(15)	O7-B2	1.3629(16)	O15-B14	1.3842(16)
Cu1-N12	2.0755(11)	O1-B2	1.3586(15)	O8-B3	1.3502(16)	O15-B15	1.3844(16)
N1-C1	1.4822(17)	O2-B2	1.3813(16)	O9-B4	1.3519(18)	O16-B11	1.4728(15)
N2-C2	1.4854(15)	O2-B3	1.3915(16)	O10-B5	1.3703(17)	O16-B15	1.3615(15)
N2-C3	1.4811(16)	O3-B1	1.4773(15)	O11-B11	1.4712(15)	O17-B12	1.3609(15)
N2-C4	1.4810(16)	O3-B3	1.3586(15)	O11-B12	1.3599(15)	O18-B13	1.3533(16)
N11-C11	1.4864(17)	O4-B1	1.4620(16)	O12-B12	1.3829(15)	O19-B14	1.3590(16)
N12-C12	1.4903(16)	O4-B4	1.3608(16)	O12-B13	1.3870(15)	O20-B15	1.3607(16)
N12-C13	1.4806(16)	O5-B4	1.3866(17)	O13-B11	1.4763(15)		

Table 18 Bond angles [°] in 27.

N1-Cu1-O21	94.53(4)	N11-C11-C12	108.35(10)	O10-B5-O5	120.30(12)
N1-Cu1-N2	85.96(4)	N12-C12-C11	109.81(10)	B12-O11-B11	123.29(10)
N1-Cu1-N12	93.87(4)	B2-O1-B1	122.41(10)	B12-O12-B13	119.25(10)
N2-Cu1-O21	90.55(4)	B2-O2-B3	119.98(10)	B13-O13-B11	124.20(9)
N11-Cu1-O21	94.35(4)	B3-O3-B1	123.04(10)	B14-O14-B11	123.70(10)
N11-Cu1-N1	171.11(5)	B4-O4-B1	124.01(10)	B14-O15-B15	119.02(10)
N11-Cu1-N2	94.23(4)	B5-O5-B4	118.58(10)	B15-O16-B11	123.18(9)
N11-Cu1-N12	85.65(4)	B5-O6-B1	122.24(10)	O11-B11-O13	110.64(9)
N12-Cu1-O21	91.37(4)	O3-B1-O1	110.12(9)	O11-B11-O14	109.31(10)
N12-Cu1-N2	178.08(4)	O4-B1-O1	107.69(10)	O11-B11-O16	108.62(9)
C1-N1-Cu1	109.19(8)	O4-B1-O3	109.15(10)	O14-B11-O13	108.17(9)
C2-N2-Cu1	103.59(7)	O6-B1-O1	109.64(10)	O14-B11-O16	110.39(9)
C3-N2-Cu1	111.18(8)	O6-B1-O3	108.43(10)	O16-B11-O13	109.72(10)
C3-N2-C2	110.40(10)	O6-B1-O4	111.80(10)	O11-B12-O12	121.67(11)
C4-N2-Cu1	115.25(8)	O1-B2-O2	120.54(11)	O11-B12-O17	122.70(11)
C4-N2-C2	108.45(10)	O1-B2-O7	123.58(11)	O17-B12-O12	115.63(10)
C4-N2-C3	107.87(10)	O7-B2-O2	115.86(11)	O13-B13-O12	120.20(11)
C11-N11-Cu1	110.72(8)	O3-B3-O2	120.54(11)	O18-B13-O12	116.01(11)
C12-N12-Cu1	103.84(8)	O8-B3-O2	115.72(11)	O18-B13-O13	123.78(11)
C13-N12-Cu1	110.43(8)	O8-B3-O3	123.72(11)	O14-B14-O15	120.87(11)
C13-N12-C12	110.66(10)	O4-B4-O5	120.46(12)	O19-B14-O14	122.36(11)
C13-N12-C14	107.63(10)	O9-B4-O4	117.52(12)	O19-B14-O15	116.75(11)
C14-N12-Cu1	114.99(8)	O9-B4--O5	122.01(12)	O16-B15-O15	121.41(11)
C14-N12-C12	109.27(10)	O6-B5-O5	122.75(12)	O20-B15-O15	115.07(11)
N1-C1-C2	107.67(10)	O6-B5-O10	116.95(12)	O20-B15-O16	123.51(11)
N2-C2-C1	110.03(10)				

Table 19 Bond lengths [Å] in 28.

Cu1-O8	2.0052(9)	O2-B1	1.4381(16)	O6-B3	1.4529(16)	O12-B5	1.3750(17)
Cu1-O9	2.2481(9)	O2-B4	1.3582(17)	O6-B6	1.3619(17)	O13-B6	1.3756(17)
Cu1-O10	1.9566(9)	O3-B2	1.4778(16)	O7-B1	1.4531(16)	N1-C1	1.4829(18)
Cu1-N1	2.0011(11)	O3-B4	1.3770(17)	O7-B6	1.3653(17)	N2-C2	1.4880(17)
Cu1-N2	2.0478(11)	O4-B2	1.4623(16)	O8-B1	1.4818(16)	N2-C3	1.4785(18)
O1-B1	1.5161(16)	O4-B5	1.3733(17)	O9-B2	1.4437(17)	N2-C4	1.4796(18)
O1-B2	1.5142(16)	O5-B3	1.4409(16)	O10-B3	1.4674(16)	C1-C2	1.5115(19)
O1-B3	1.5199(15)	O5-B5	1.3561(17)	O11-B4	1.3713(17)		

Table 20 Bond angles [°] in 28.

O8-Cu1-O9	83.58(4)	B2-O9-Cu1	116.51(7)	O9-B2-O1	106.07(10)
O8-Cu1-N2	177.94(4)	B3-O10-Cu1	121.92(7)	O9-B2-O3	112.36(10)
O10-Cu1-O8	90.76(4)	C1-N1-Cu1	110.26(8)	O9-B2-O4	113.30(11)
O10-Cu1-O9	91.63(4)	C2-N2-Cu1	104.20(8)	O5-B3-O1	108.59(10)
O10-Cu1-N1	166.49(4)	C3-N2-Cu1	109.86(8)	O5-B3-O6	110.22(10)
O10-Cu1-N2	90.90(4)	C3-N2-C2	110.83(11)	O5-B3-O10	112.11(10)
N1-Cu1-O8	92.91(4)	C3-N2-C4	108.87(11)	O6-B3-O1	108.78(10)
N1-Cu1-O9	101.69(4)	C4-N2-Cu1	113.83(9)	O6-B3-O10	110.74(10)
N1-Cu1-N2	85.74(5)	C4-N2-C2	109.19(11)	O10-B3-O1	106.25(10)
N2-Cu1-O9	95.15(4)	N1-C1-C2	108.58(11)	O2-B4-O3	122.97(12)
B1-O1-B3	115.85(9)	N2-C2-C1	109.65(11)	O2-B4-O11	119.83(12)
B2-O1-B1	116.15(9)	O2-B1-O1	108.79(10)	O11-B4-O3	117.21(12)
B2-O1-B3	119.11(9)	O2-B1-O7	109.46(11)	O4-B5-O12	120.12(12)
B4-O2-B1	123.69(11)	O2-B1-O8	111.18(10)	O5-B5-O4	123.92(12)
B4-O3-B2	119.53(10)	O7-B1-O1	107.95(10)	O5-B5-O12	115.95(12)
B5-O4-B2	121.43(10)	O7-B1-O8	110.82(10)	O6-B6-O7	122.69(12)
B5-O5-B3	122.73(11)	O8-B1-O1	108.55(10)	O6-B6-O13	117.20(12)
B6-O6-B3	121.48(10)	O3-B2-O1	107.46(10)	O7-B6-O13	120.09(12)

B6-O7-B1	122.90(10)	O4-B2-O1	108.92(10)	
B1-O8-Cu1	118.29(7)	O4-B2-O3	108.51(10)	

Table 21 Bond lengths [Å] in 37

Ni-O8	2.065(3)	O2-B1	1.468(7)	O6-B3	1.460(6)	O12-B5	1.367(7)
Ni1-O9	2.065(3)	O2-B4	1.391(7)	O6-B6	1.365(7)	O13-B6	1.370(7)
Ni1-O21	2.096(3)	O3-B2	1.464(7)	O7-B1	1.460(6)	N1-C1	1.464(13)
Ni1-O22	2.082(3)	O3-B4	1.382(7)	O7-B6	1.358(6)	N1-C1B	1.518(12)
Ni1-N1	2.086(4)	O4-B2	1.441(6)	O8-B1	1.468(6)	N2-C2	1.483(13)
Ni1-N2	2.085(4)	O4-B5	1.364(6)	O9-B2	1.470(6)	N2-C2B	1.454(12)
O1-B1	1.498(6)	O5-B3	1.439(6)	O10-B3	1.455(6)	C1-C2	1.52(2)
O1-B2	1.515(6)	O5-B5	1.360(7)	O11-B4	1.327(6)	C1B-C2B	1.52(2)
O1-B3	1.538(6)						

Table 22 Bond angles [°] in 37

O8-Ni1-O9	90.48(12)	B5-O5-B3	124.4(4)	O9-B2-O1	106.3(4)
O8-Ni1-O21	84.84(13)	B6-O6-B3	122.3(4)	O5-B3-O1	108.4(4)
O8-Ni1-O22	89.04(14)	B6-O7-B1	124.1(4)	O5-B3-O6	109.0(4)
O8-Ni1-N1	93.51(14)	B1-O8-Ni1	124.8(3)	O5-B3-O10	109.9(4)
O8-Ni1-N2	175.70(14)	B2-O9-Ni1	124.8(3)	O6-B3-O1	108.1(4)
O9-Ni1-O21	85.55(14)	C1-N1-Ni1	107.7(5)	O10-B3-O1	109.7(3)
O9-Ni1-O22	88.86(14)	C1B-N1-Ni1	109.2(5)	O10-B3-O6	111.7(4)
O9-Ni1-N1	176.01(14)	C2-N2-Ni1	110.0(5)	O3-B4-O2	118.6(4)
O9-Ni1-N2	93.21(14)	C2B-N2-Ni1	108.2(5)	O11-B4-O2	122.1(5)
O22-Ni1-O2	171.67(12)	O2-B1-O1	108.9(4)	O11-B4-O3	119.3(5)
O22-Ni1-N1	91.38(16)	O7-B1-O	110.2(4)	O4-B5-O12	114.8(5)
O22-Ni1-N2	93.24(16)	O7-B1-O2	107.8(4)	O5-B5-O4	122.3(5)
N1-Ni1-O21	94.62(16)	O7-B1-O8	111.0(4)	O5-B5-O12	122.9(5)
N2-Ni1-O21	93.23(16)	O8-B1-O1	107.6(4)	O6-B6-O13	120.1(4)
N2-Ni1-N1	82.80(14)	O8-B1-O2	111.2(4)	O7-B6-O6	122.2(5)
B1-O1-B2	117.7(3)	O3-B2-O1	108.6(4)	O7-B6-O13	117.8(5)
B1-O1-B3	119.1(4)	O3-B2-O9	112.2(4)	N1-C1-C2	109.3(14)
B2-O1-B3	120.1(4)	O4-B2-O1	110.0(4)	N2-C2-C1	109.4(13)
B4-O2-B1	124.1(4)	O4-B2-O3	108.4(4)	N1-C1B-C2B	108.7(12)
B4-O3-B2	124.9(4)	O4-B2-O9	111.4(4)	N2-C2B-C1B	108.2(12)
B5-O4-B2	123.6(4)				

Table 23 Bond lengths [Å] in 38.

C1-N1	1.481(2)	C6-N3	1.473(2)	B1-O6	1.4643(18)	B5-O5	1.386(2)
C1-C2	1.511(2)	C6-C7	1.513(2)	B1-O4	1.4713(19)	N1-Ni1	1.9214(14)
C1-H1A	0.9900	C6-H6A	0.9900	B1-O3	1.4782(18)	N1-H1C	0.9100
C1-H1B	0.9900	C6-H6B	0.9900	B2-O7	1.3445(19)	N1-H1D	0.9100
C2-N2	1.472(2)	C7-N4	1.474(3)	B2-O1	1.353(2)	N2-Ni1	1.8506(14)
C2-H2A	0.9900	C7-H7A	0.9900	B2-O2	1.4049(19)	N3-Ni1	1.8504(14)
C2-H2B	0.9900	C7-H7B	0.9900	B3-O3	1.3429(19)	N4-Ni1	1.9284(16)
C3-N2	1.328(2)	C8-H8A	0.9800	B3-O8	1.3689(19)	N4-H4A	0.9100
C3-C4	1.397(2)	C8-H8B	0.9800	B3-O2	1.3921(18)	N4-H4B	0.9100
C3-C8	1.507(2)	C8-H8C	0.9800	B4-O9	1.355(2)	O7-H7	0.8400
C4-C5	1.391(2)	C9-H9A	0.9800	B4-O4	1.3597(19)	O8-H8	0.8400
C4-H4	0.9500	C9-H9B	0.9800	B4-O5	1.3846(19)	O9-H9	0.8400
C5-N3	1.329(2)	C9-H9C	0.9800	B5-O10	1.3557(19)	O10-H10	0.8400
C5-C9	1.510(2)	B1-O1	1.4595(18)	B5-O6	1.3644(19)	O11-H11A	0.8702
						O11-H11B	0.8700

Table 24 Bond angles [°] in **38**.

N1–C1–C2	106.36(14)	N4–C7–H7B	110.3	O10–B5–O6	122.73(14)
N1–C1–H1A	110.5	C6–C7–H7B	110.3	O10–B5–O5	116.75(13)
C2–C1–H1A	110.5	H7A–C7–H7B	108.6	O6–B5–O5	120.51(13)
N1–C1–H1B	110.5	C3–C8–H8A	109.5	C1–N1–Ni1	107.98(10)
C2–C1–H1B	110.5	C3–C8–H8B	109.5	C1–N1–H1C	110.1
H1A–C1–H1B	108.6	H8A–C8–H8B	109.5	Ni1–N1–H1C	110.1
N2–C2–C1	106.92(14)	C3–C8–H8C	109.5	C1–N1–H1D	110.1
N2–C2–H2A	110.3	H8A–C8–H8C	109.5	Ni1–N1–H1D	110.1
C1–C2–H2A	110.3	H8B–C8–H8C	109.5	H1C–N1–H1D	108.4
N2–C2–H2B	110.3	C5–C9–H9A	109.5	C3–N2–C2	119.26(14)
C1–C2–H2B	110.3	C5–C9–H9B	109.5	C3–N2–Ni1	126.48(12)
H2A–C2–H2B	108.6	H9A–C9–H9B	109.5	C2–N2–Ni1	113.74(11)
N2–C3–C4	122.55(15)	C5–C9–H9C	109.5	C5–N3–C6	118.52(15)
N2–C3–C8	119.90(15)	O1–B1–O4	108.42(12)	Ni1–N4–H4B	110.3
C4–C3–C8	117.54(14)	O6–B1–O4	110.63(12)	H4A–N4–H4B	108.6
C5–C4–C3	125.63(15)	O1–B1–O3	110.38(12)	B2–O1–B1	124.63(12)
C5–C4–H4	117.2	O6–B1–O3	109.28(12)	B3–O2–B2	118.05(12)
C3–C4–H4	117.2	O4–B1–O3	108.91(12)	B3–O3–B1	123.40(12)
N3–C5–C4	122.64(15)	O7–B2–O1	117.85(14)	B4–O4–B1	122.81(12)
N3–C5–C9	119.62(15)	O7–B2–O2	121.68(14)	B4–O5–B5	119.62(12)
C4–C5–C9	117.75(14)	O1–B2–O2	120.46(13)	B5–O6–B1	122.43(12)
N3–C6–C7	107.40(15)	O3–B3–O8	118.34(13)	B2–O7–H7	109.5
N3–C6–H6A	110.2	O3–B3–O2	122.05(13)	B3–O8–H8	109.5
C7–C6–H6A	110.2	O8–B3–O2	119.61(13)	B4–O9–H9	109.5
N3–C6–H6B	110.2	O9–B4–O4	122.77(14)	B5–O10–H10	109.5
C7–C6–H6B	110.2	O9–B4–O5	117.14(13)	H11A–O11–H11B	109.5
H6A–C6–H6B	108.5	O4–B4–O5	120.07(14)	N3–Ni1–N2	95.19(6)
N4–C7–C6	107.02(16)	C5–N3–Ni1	126.73(12)	N3–Ni1–N1	175.84(6)
N4–C7–H7A	110.3	C6–N3–Ni1	114.62(11)	N2–Ni1–N1	86.46(6)
C6–C7–H7A	110.3	C7–N4–Ni1	107.05(11)	N3–Ni1–N4	85.81(6)
H9A–C9–H9C	109.5	C7–N4–H4A	110.3	N2–Ni1–N4	175.94(6)
H9B–C9–H9C	109.5	Ni1–N4–H4A	110.3	N1–Ni1–N4	92.81(7)
O1–B1–O6	109.21(12)	C7–N4–H4B	110.3		

Table 25 Bond lengths [\AA] in **39**.

Ni1–N2B	2.015(14)	N1B–H1BA	0.9100	C11–C12	1.518(4)	C15B–H15D	0.9900
Ni1–N2B ⁱ	2.015(14)	N1B–H1BB	0.9100	C11–C16	1.529(5)	C16B–H16C	0.9900
Ni1–N1B ⁱ	2.036(15)	N2B–C2B	1.485(7)	C11–H11	1.0000	C16B–H16D	0.9900
Ni1–N1B	2.036(15)	N2B–H2BA	0.9100	C12–C13	1.525(5)	O1–B3	1.505(2)
Ni1–N2 ⁱ	2.108(8)	N2B–H2BB	0.9100	C12–H12	1.0000	O1–B2	1.511(2)
Ni1–N2	2.108(8)	C1B–C6B	1.517(7)	C13–C14	1.528(5)	O1–B1	1.512(2)
Ni1–N1 ⁱ	2.113(9)	C1B–C2B	1.530(6)	C13–H13A	0.9900	O2–B4	1.357(2)
Ni1–N1	2.113(9)	C1B–H1BC	1.0000	C13–H13B	0.9900	O2–B2	1.439(2)
Ni1–O21 ⁱ	2.1352(15)	C2B–C3B	1.524(7)	C14–C15	1.516(5)	O3–B4	1.372(2)
Ni1–O21	2.1353(15)	C2B–H2BC	1.0000	C14–H14A	0.9900	O3–B1	1.443(2)
O21–H21A	0.8542	C3B–C4B	1.522(7)	C14–H14B	0.9900	O4–B5	1.356(2)
O21–H21B	0.8546	C3B–H3BA	0.9900	C15–C16	1.531(5)	O4–B3	1.435(2)
N1–C1	1.484(6)	C3B–H3BB	0.9900	C15–H15A	0.9900	O5–B5	1.370(2)
N1–H1A	0.9100	C4B–C5B	1.522(6)	C15–H15B	0.9900	O5–B1	1.461(2)
N1–H1B	0.9100	C4B–H4BA	0.9900	C16–H16A	0.9900	O6–B6	1.357(2)
N2–C2	1.475(6)	C4B–H4BB	0.9900	C16–H16B	0.9900	O6–B2	1.459(2)
N2–H2A	0.9100	C5B–C6B	1.528(7)	N11B–C11B	1.479(8)	O7–B6	1.373(2)
N2–H2B	0.9100	C5B–H5BA	0.9900	N11B–H11C	0.9100	O7–B3	1.471(2)
C1–C6	1.521(6)	C5B–H5BB	0.9900	N11B–H11D	0.9100	O8–B7	1.360(2)
C1–C2	1.525(5)	C6B–H6BA	0.9900	N12B–C12B	1.482(7)	O8–B2	1.464(2)
C1–H1	1.0000	C6B–H6BB	0.9900	N12B–H12C	0.9100	O9–B7	1.368(2)
C2–C3	1.522(6)	Ni2–N11	1.897(7)	N12B–H12D	0.9100	O9–B3	1.465(2)
C2–H2	1.0000	Ni2–N11 ⁱⁱ	1.897(7)	C11B–C16B	1.521(7)	O10–B4	1.364(2)
C3–C4	1.520(6)	Ni2–N12 ⁱⁱ	1.900(6)	C11B–C12B	1.523(7)	O10–H10	0.8400
C3–H3A	0.9900	Ni2–N12	1.900(6)	C11B–H11E	1.0000	O11–B5	1.374(2)
C3–H3B	0.9900	Ni2–N11B	1.965(17)	C12B–C13B	1.531(7)	O11–H11F	0.8400
C4–C5	1.516(6)	Ni2–N11B ⁱⁱ	1.965(17)	C12B–H12E	1.0000	O12–B6	1.373(2)
C4–H4A	0.9900	Ni2–N12B ⁱⁱ	1.971(16)	C13B–C14B	1.521(7)	O12–H12F	0.8400
C4–H4B	0.9900	Ni2–N12B	1.971(16)	C13B–H13C	0.9900	O13–B7	1.373(2)
C5–C6	1.526(6)	N11–C11	1.491(5)	C13B–H13D	0.9900	O13–H13	0.8400
C5–H5A	0.9900	N11–H11A	0.9100	C14B–C15B	1.515(7)	O14–B1	1.456(3)
C5–H5B	0.9900	N11–H11B	0.9100	C14B–H14C	0.9900	O14–H14	0.8400
C6–H6A	0.9900	N12–C12	1.479(5)	C14B–H14D	0.9900	O22–H22A	0.8507
C6–H6B	0.9900	N12–H12A	0.9100	C15B–C16B	1.527(7)	O22–H22B	0.8507
N1B–C1B	1.484(7)	N12–H12B	0.9100	C15B–H15C	0.9900	O23–H23A	0.8497
						O23–H23B	0.8487

Table 26 Bond angles [$^\circ$] in **39**.

N2B–Ni1–N2B ⁱ	180.0	N1B–C1B–H1BC	108.0	Ni2–N11B–H11C	110.3
N2B–Ni1–N1B ⁱ	95.2(3)	C6B–C1B–H1BC	108.0	C11B–N11B–H11D	110.3
N2B ⁱ –Ni1–N1B ⁱ	84.8(3)	C2B–C1B–H1BC	108.0	Ni2–N11B–H11D	110.3
N2B–Ni1–N1B	84.8(3)	N2B–C2B–C3B	112.8(8)	H11C–N11B–H11D	108.6
N2B ⁱ –Ni1–N1B	95.2(3)	N2B–C2B–C1B	106.4(7)	C12B–N12B–Ni2	111.3(8)
N1B ⁱ –Ni1–N1B	180.0	C3B–C2B–C1B	109.9(6)	C12B–N12B–H12C	109.4
N2 ⁱ –Ni1–N2	180.0	N2B–C2B–H2BC	109.2	Ni2–N12B–H12C	109.4
N2 ⁱ –Ni1–N1 ⁱ	81.50(18)	C3B–C2B–H2BC	109.2	C12B–N12B–H12D	109.4
N2–Ni1–N1 ⁱ	98.50(18)	C1B–C2B–H2BC	109.2	Ni2–N12B–H12D	109.4
N2 ⁱ –Ni1–N1	98.50(18)	C4B–C3B–C2B	110.9(7)	H12C–N12B–H12D	108.0
N2–Ni1–N1	81.50(18)	C4B–C3B–H3BA	109.5	N11B–C11B–C16B	114.6(9)
N1 ⁱ –Ni1–N1	180.0	C2B–C3B–H3BA	109.5	N11B–C11B–C12B	108.0(8)
N2B–Ni1–O21 ⁱ	96.6(6)	C4B–C3B–H3BB	109.5	C16B–C11B–C12B	111.9(8)
N2B ⁱ –Ni1–O21 ⁱ	83.4(6)	C2B–C3B–H3BB	109.5	N11B–C11B–H11E	107.4
N1B ⁱ –Ni1–O21 ⁱ	87.2(8)	H3BA–C3B–H3BB	108.1	C16B–C11B–H11E	107.4
N1B–Ni1–O21 ⁱ	92.8(8)	C3B–C4B–C5B	111.3(7)	C12B–C11B–H11E	107.4
N2 ⁱ –Ni1–O21 ⁱ	88.0(4)	C3B–C4B–H4BA	109.4	N12B–C12B–C11B	107.0(7)
N2–Ni1–O21 ⁱ	92.0(4)	C5B–C4B–H4BA	109.4	N12B–C12B–C13B	113.6(8)
N1 ⁱ –Ni1–O21 ⁱ	87.1(5)	C3B–C4B–H4BB	109.4	C11B–C12B–C13B	109.4(8)
N1–Ni1–O21 ⁱ	92.9(5)	C5B–C4B–H4BB	109.4	N12B–C12B–H12E	108.9
N2B–Ni1–O21	83.4(6)	H4BA–C4B–H4BB	108.0	C11B–C12B–H12E	108.9

N2B ⁱ -Ni1-O21	96.6(6)	C4B-C5B-C6B	111.3(7)	C13B-C12B-H12E	108.9
N1B ⁱ -Ni1-O21	92.8(8)	C4B-C5B-H5BA	109.4	C14B-C13B-C12B	108.3(8)
N1B-Ni1-O21	87.2(8)	C6B-C5B-H5BA	109.4	C14B-C13B-H13C	110.0
N2 ⁱ -Ni1-O21	92.0(4)	C4B-C5B-H5BB	109.4	C12B-C13B-H13C	110.0
N2-Ni1-O21	88.0(4)	C6B-C5B-H5BB	109.4	C14B-C13B-H13D	110.0
N1 ⁱ -Ni1-O21	92.9(5)	H5BA-C5B-H5BB	108.0	C12B-C13B-H13D	110.0
N1-Ni1-O21	87.1(5)	C1B-C6B-C5B	111.2(7)	H13C-C13B-H13D	108.4
O21 ⁱ -Ni1-O21	180.0	C1B-C6B-H6BA	109.4	C15B-C14B-C13B	112.5(9)
Ni1-O21-H21A	109.3	C5B-C6B-H6BA	109.4	C15B-C14B-H14C	109.1
Ni1-O21-H21B	109.6	C1B-C6B-H6BB	109.4	C13B-C14B-H14C	109.1
H21A-O21-H21B	109.2	C5B-C6B-H6BB	109.4	C15B-C14B-H14D	109.1
C1-N1-Ni1	110.2(4)	H6BA-C6B-H6BB	108.0	C13B-C14B-H14D	109.1
C1-N1-H1A	109.6	N11-Ni2-N11 ⁱⁱ	180.0(3)	H14C-C14B-H14D	107.8
Ni1-N1-H1A	109.6	N11-Ni2-N12 ⁱⁱ	92.05(16)	C14B-C15B-C16B	112.1(8)
C1-N1-H1B	109.6	N11 ⁱⁱ -Ni2-N12 ⁱⁱ	87.95(16)	C14B-C15B-H15C	109.2
Ni1-N1-H1B	109.6	N11-Ni2-N12	87.95(16)	C16B-C15B-H15C	109.2
H1A-N1-H1B	108.1	N11 ⁱⁱ -Ni2-N12	92.05(16)	C14B-C15B-H15D	109.2
C2-N2-Ni1	108.7(4)	N12 ⁱⁱ -Ni2-N12	180.0	C16B-C15B-H15D	109.2
C2-N2-H2A	109.9	N11B-Ni2-N11B ⁱⁱ	180.0	H15C-C15B-H15D	107.9
Ni1-N2-H2A	109.9	N11B-Ni2-N12B ⁱⁱ	94.4(4)	C11B-C16B-C15B	108.6(8)
C2-N2-H2B	109.9	N11B ⁱⁱ -Ni2-N12B ⁱⁱ	85.6(4)	C11B-C16B-H16C	110.0
Ni1-N2-H2B	109.9	N11B-Ni2-N12B	85.6(4)	C15B-C16B-H16C	110.0
H2A-N2-H2B	108.3	N11B ⁱⁱ -Ni2-N12B	94.4(4)	C11B-C16B-H16D	110.0
N1-C1-C6	113.1(5)	N12B ⁱⁱ -Ni2-N12B	180.0	C15B-C16B-H16D	110.0
N1-C1-C2	108.5(5)	C11-N11-Ni2	110.0(4)	H16C-C16B-H16D	108.3
C6-C1-C2	109.8(5)	C11-N11-H11A	109.7	B3-O1-B2	110.72(13)
N1-C1-H1	108.4	Ni2-N11-H11A	109.7	B3-O1-B1	119.72(13)
C6-C1-H1	108.4	C11-N11-H11B	109.7	B2-O1-B1	119.24(13)
C2-C1-H1	108.4	Ni2-N11-H11B	109.7	B4-O2-B2	123.15(15)
N2-C2-C3	113.5(5)	H11A-N11-H11B	108.2	B4-O3-B1	120.25(15)
N2-C2-C1	108.3(5)	C12-N12-Ni2	108.4(3)	B5-O4-B3	122.19(15)
C3-C2-C1	110.9(5)	C12-N12-H12A	110.0	B5-O5-B1	120.87(15)
N2-C2-H2	108.0	Ni2-N12-H12A	110.0	B6-O6-B2	120.93(15)
C3-C2-H2	108.0	C12-N12-H12B	110.0	B6-O7-B3	119.12(14)
C1-C2-H2	108.0	Ni2-N12-H12B	110.0	B7-O8-B2	120.21(15)
C4-C3-C2	111.1(5)	H12A-N12-H12B	108.4	B7-O9-B3	121.08(14)
C4-C3-H3A	109.4	N11-C11-C12	105.3(4)	B4-O10-H10	109.5
C2-C3-H3A	109.4	N11-C11-C16	112.3(4)	B5-O11-H11F	109.5
C4-C3-H3B	109.4	C12-C11-C16	109.8(4)	B6-O12-H12F	109.5
C2-C3-H3B	109.4	N11-C11-H11	109.7	B7-O13-H13	109.5
H3A-C3-H3B	108.0	C12-C11-H11	109.7	B1-O14-H14	109.5
C5-C4-C3	110.8(5)	C16-C11-H11	109.7	O3-B1-O14	107.86(15)
C5-C4-H4A	109.5	N12-C12-C11	107.5(4)	O3-B1-O5	111.44(16)
C3-C4-H4A	109.5	N12-C12-C13	115.9(4)	O14-B1-O5	111.96(15)
C5-C4-H4B	109.5	C11-C12-C13	110.9(4)	O3-B1-O1	107.29(15)
C3-C4-H4B	109.5	N12-C12-H12	107.4	O14-B1-O1	112.17(15)
H4A-C4-H4B	108.1	C11-C12-H12	107.4	O5-B1-O1	106.06(14)
C4-C5-C6	112.3(5)	C13-C12-H12	107.4	O2-B2-O6	112.08(15)
C4-C5-H5A	109.1	C12-C13-C14	108.5(4)	O2-B2-O8	110.02(15)
C6-C5-H5A	109.1	C12-C13-H13A	110.0	O6-B2-O8	110.99(15)
C4-C5-H5B	109.1	C14-C13-H13A	110.0	O2-B2-O1	109.17(14)
C6-C5-H5B	109.1	C12-C13-H13B	110.0	O6-B2-O1	108.03(14)
H5A-C5-H5B	107.9	C14-C13-H13B	110.0	O8-B2-O1	106.34(14)
C1-C6-C5	111.1(5)	H13A-C13-H13B	108.4	O4-B3-O9	110.11(15)
C1-C6-H6A	109.4	C15-C14-C13	112.4(4)	O4-B3-O7	110.78(15)
C5-C6-H6A	109.4	C15-C14-H14A	109.1	O9-B3-O7	111.52(15)
C1-C6-H6B	109.4	C13-C14-H14A	109.1	O4-B3-O1	110.07(14)
C5-C6-H6B	109.4	C15-C14-H14B	109.1	O9-B3-O1	107.11(14)
H6A-C6-H6B	108.0	C13-C14-H14B	109.1	O7-B3-O1	107.13(14)
C1B-N1B-Ni1	107.5(8)	H14A-C14-H14B	107.9	O2-B4-O10	122.62(17)
C1B-N1B-H1BA	110.2	C14-C15-C16	111.3(4)	O2-B4-O3	122.72(17)
Ni1-N1B-H1BA	110.2	C14-C15-H15A	109.4	O10-B4-O3	114.60(17)
C1B-N1B-H1BB	110.2	C16-C15-H15A	109.4	O4-B5-O5	123.61(17)

Ni1–N1B–H1BB	110.2	C14–C15–H15B	109.4	O4–B5–O11	116.65(16)
H1BA–N1B–H1BB	108.5	C16–C15–H15B	109.4	O5–B5–O11	119.73(17)
C2B–N2B–Ni1	108.7(7)	H15A–C15–H15B	108.0	O6–B6–O7	122.91(17)
C2B–N2B–H2BA	109.9	C11–C16–C15	108.0(4)	O6–B6–O12	117.23(17)
Ni1–N2B–H2BA	109.9	C11–C16–H16A	110.1	O7–B6–O12	119.86(17)
C2B–N2B–H2BB	109.9	C15–C16–H16A	110.1	O8–B7–O9	122.23(17)
Ni1–N2B–H2BB	109.9	C11–C16–H16B	110.1	O8–B7–O13	117.28(17)
H2BA–N2B–H2BB	108.3	C15–C16–H16B	110.1	O9–B7–O13	120.49(17)
N1B–C1B–C6B	113.7(8)	H16A–C16–H16B	108.4	H22A–O22–H22B	109.4
N1B–C1B–C2B	107.8(8)	C11B–N11B–Ni2	107.1(9)	H23A–O23–H23B	109.6
C6B–C1B–C2B	111.0(7)	C11B–N11B–H11C	110.3		

Table 27 Bond lengths [Å] in 40.

O1–B2	1.348(3)	O9–B4	1.357(3)	O11B–H11	0.883(14)	C11–H11B	0.9900
O1–B1	1.462(3)	O9–H9	0.8400	N12–H12	1.0000	C14–O11	1.41(2)
O2–B3	1.372(3)	O10–B5	1.350(3)	C12–C11	1.514(7)	C14–H14A	0.9900
O2–B2	1.379(3)	O10–H10	0.8400	C12–C11B	1.514(10)	C14–H14B	0.9900
O3–B3	1.357(3)	Ni1–N11B	2.064(15)	C12–H12A	0.9900	N11–H11C	0.9100
O3–B1	1.472(3)	Ni1–N11B ⁱ	2.064(15)	C12–H12B	0.9900	N11–H11D	0.9100
O4–B4	1.350(3)	Ni1–O11B	2.072(8)	C12–H12C	0.9900	O11–H11	0.865(13)
O4–B1	1.476(3)	Ni1–O11B ⁱ	2.072(8)	C12–H12D	0.9900	C11B–O11B	1.42(3)
O5–B4	1.382(3)	Ni1–N12	2.080(2)	C13–C14	1.498(7)	C11B–H11H	0.9900
O5–B5	1.389(3)	Ni1–N12 ⁱ	2.080(2)	C13–C14B	1.501(10)	C11B–H11I	0.9900
O6–B5	1.352(3)	Ni1–O11 ⁱ	2.087(7)	C13–H13A	0.9900	C14B–N11B	1.51(3)
O6–B1	1.472(3)	Ni1–O11	2.087(7)	C13–H13B	0.9900	C14B–H14C	0.9900
O7–B2	1.364(3)	Ni1–N11	2.140(6)	C13–H13C	0.9900	C14B–H14D	0.9900
O7–H7	0.8400	Ni1–N11 ⁱ	2.140(6)	C13–H13D	0.9900	N11B–H11E	0.9100
O8–B3	1.363(3)	N12–C12	1.466(4)	C11–N11	1.51(2)	N11B–H11F	0.9100
O8–H8	0.8400	N12–C13	1.497(4)	C11–H11A	0.9900		

Table 28 Bond angles [°] in 40.

B2–O1–B1	122.92(19)	N12–Ni1–O11 ⁱ	99.43(17)	H13C–C13–H13D	108.3
B3–O2–B2	119.58(19)	N12 ⁱ –Ni1–O11 ⁱ	80.57(17)	N11–C11–C12	101.8(13)
B3–O3–B1	123.24(19)	N12–Ni1–O11	80.57(17)	N11–C11–H11A	111.4
B4–O4–B1	123.44(19)	N12 ⁱ –Ni1–O11	99.43(17)	C12–C11–H11A	111.4
B4–O5–B5	119.0(2)	O11 ⁱ –Ni1–O11	180.0	N11–C11–H11B	111.4
B5–O6–B1	123.68(19)	N12–Ni1–N11	81.18(15)	C12–C11–H11B	111.4
B2–O7–H7	109.5	N12 ⁱ –Ni1–N11	98.82(15)	H11A–C11–H11B	109.3
B3–O8–H8	109.5	O11 ⁱ –Ni1–N11	82.6(3)	O11–C14–C13	107.4(12)
B4–O9–H9	109.5	O11–Ni1–N11	97.4(3)	O11–C14–H14A	110.2
B5–O10–H10	109.5	N12–Ni1–N11 ⁱ	98.82(15)	C13–C14–H14A	110.2
O1–B1–O6	109.32(19)	N12 ⁱ –Ni1–N11 ⁱ	81.18(15)	O11–C14–H14B	110.2
O1–B1–O3	111.66(18)	O11 ⁱ –Ni1–N11 ⁱ	97.4(3)	C13–C14–H14B	110.2
O6–B1–O3	108.15(18)	O11–Ni1–N11 ⁱ	82.6(3)	H14A–C14–H14B	108.5
O1–B1–O4	109.46(18)	N11–Ni1–N11 ⁱ	180.0	C11–N11–Ni1	109.0(12)
O6–B1–O4	110.20(18)	C12–N12–C13	116.1(2)	C11–N11–H11C	109.9
O3–B1–O4	108.04(19)	C12–N12–Ni1	108.9(2)	Ni1–N11–H11C	109.9
O1–B2–O7	119.4(2)	C13–N12–Ni1	106.40(18)	C11–N11–H11D	109.9
O1–B2–O2	121.5(2)	C12–N12–H12	108.4	Ni1–N11–H11D	109.9
O7–B2–O2	119.0(2)	C13–N12–H12	108.4	H11C–N11–H11D	108.3
O3–B3–O8	122.6(2)	Ni1–N12–H12	108.4	C14–O11–Ni1	116.3(10)
O3–B3–O2	120.8(2)	N12–C12–C11	114.4(11)	C14–O11–H11	111(2)
O8–B3–O2	116.7(2)	N12–C12–C11B	108.7(17)	Ni1–O11–H11	131(2)
O4–B4–O9	122.8(2)	N12–C12–H12A	108.7	O11B–C11B–C12	120.3(18)
O4–B4–O5	121.1(2)	C11–C12–H12A	108.7	O11B–C11B–H11H	107.3
O9–B4–O5	116.1(2)	N12–C12–H12B	108.7	C12–C11B–H11H	107.3
O10–B5–O6	123.1(2)	C11–C12–H12B	108.7	O11B–C11B–H11I	107.3
O10–B5–O5	116.1(2)	H12A–C12–H12B	107.6	C12–C11B–H11I	107.3
O6–B5–O5	120.7(2)	N12–C12–H12C	110.0	H11H–C11B–H11I	106.9

N11B–Ni1–N11B ⁱ	180.0	C11B–C12–H12C	110.0	C13–C14B–N11B	113(2)
N11B–Ni1–O11B	76.1(4)	N12–C12–H12D	110.0	C13–C14B–H14C	108.9
N11B ⁱ –Ni1–O11B	103.9(4)	C11B–C12–H12D	110.0	N11B–C14B–H14C	108.9
N11B–Ni1–O11B ⁱ	103.9(4)	H12C–C12–H12D	108.3	C13–C14B–H14D	108.9
N11B ⁱ –Ni1–O11B ⁱ	76.1(4)	N12–C13–C14	113.1(14)	N11B–C14B–H14D	108.9
O11B–Ni1–O11B ⁱ	180.0(2)	N12–C13–C14B	109(2)	H14C–C14B–H14D	107.7
N11B–Ni1–N12	82.9(3)	N12–C13–H13A	109.0	C14B–N11B–Ni1	110.1(12)
N11B ⁱ –Ni1–N12	97.1(3)	C14–C13–H13A	109.0	C14B–N11B–H11E	109.6
O11B–Ni1–N12	85.69(19)	N12–C13–H13B	109.0	Ni1–N11B–H11E	109.6
O11B ⁱ –Ni1–N12	94.31(19)	C14–C13–H13B	109.0	C14B–N11B–H11F	109.6
N11B–Ni1–N12 ⁱ	97.1(3)	H13A–C13–H13B	107.8	Ni1–N11B–H11F	109.6
N11B ⁱ –Ni1–N12 ⁱ	82.9(3)	N12–C13–H13C	109.9	H11E–N11B–H11F	108.1
O11B–Ni1–N12 ⁱ	94.31(19)	C14B–C13–H13C	109.9	C11B–O11B–Ni1	106.3(13)
O11B ⁱ –Ni1–N12 ⁱ	85.69(19)	N12–C13–H13D	109.9	C11B–O11B–H11G	100(3)
N12–Ni1–N12 ⁱ	180.0	C14B–C13–H13D	109.9	Ni1–O11B–H11G	130(3)

Table 29 Bond lengths [Å] in **41**.

O1–B1	1.476(7)	O6–B1	1.466(5)	Ni1–N3A	2.161(8)	C3A–C4A	1.527(13)
O1–B2	1.361(7)	O6–B5	1.352(5)	Ni1–N1B	2.152(10)	N1B–C1B	1.496(15)
O2–B2	1.382(8)	O7–B2	1.359(7)	Ni1–N1	2.152(10)	N2B–C2B	1.476(15)
O2–B3	1.386(8)	O8–B3	1.358(8)	Ni1–N2B	2.105(11)	N2B–C3B	1.495(15)
O3–B1	1.484(7)	O9–B4	1.377(5)	Ni1–N2B	2.105(11)	N3B–C4B	1.490(16)
O3–B3	1.356(6)	O10–B5	1.364(5)	Ni1–N3B	2.130(10)	C1B–C2B	1.503(15)
O4–B1	1.484(4)	Ni1–N1A	2.103(8)	Ni1–N3B	2.130(10)	C3B–C4B	1.497(16)
O4–B4	1.343(5)	Ni1–N1A ¹	2.103(8)	N1A–C1A	1.507(15)		
O5–B4	1.392(14)	Ni1–N2A ¹	2.095(8)	N2A–C2A	1.498(13)		
O5–B5	1.404(17)	Ni1–N2A	2.095(8)	N2A–C3A	1.464(13)		
O5A–B4	1.406(13)	Ni1–N3A	2.161(8)	N3A–C4	1.472(13)		
O5A–B5	1.407(16)			C1A–C2	1.460(14)		

Table 30 Bond angles [°] in **41**.

B2–O1–B1	123.4(4)	O3–B3–O8	123.0(5)	N2A ¹ –Ni1–N1A	99.8(3)
B2–O2–B3	119.5(3)	O8–B3–O2	116.0(4)	N2A ¹ –Ni1–N1A ¹	80.2(3)
B3–O3–B1	123.3(4)	O4–B4–O5	119.5(10)	N2A–Ni1–N1A ¹	99.8(3)
B4–O4–B1	123.1(3)	O4–B4–O5A	121.4(6)	N2A–Ni1–N1A	80.2(3)
B4–O5–B5	116.7(13)	O4–B4–O9	122.9(3)	N2A ¹ –Ni1–N2A	180.0
B4–O5A–B5	115.5(15)	O9–B4–O5	115.9(7)	N2A–Ni1–N3A	82.4(3)
B5–O6–B1	122.7(3)	O9–B4–O5A	114.9(6)	N2A ¹ –Ni1–N3A ¹	82.4(3)
O1–B1–O3	110.6(3)	O6–B5–O5	119.9(11)	N2A ¹ –Ni1–N3A	97.6(3)
O1–B1–O4	108.0(4)	O6–B5–O5A	121.8(7)	N2A–Ni1–N3A ¹	97.6(3)
O3–B1–O4	107.8(4)	O6–B5–O10	118.8(4)	N3A ¹ –Ni1–N3A	180.0
O6–B1–O1	109.8(4)	O10–B5–O5	120.0(8)	N1B–Ni1–N1B ¹	180.0
O6–B1–O3	109.0(4)	O10–B5–O5A	118.0(6)	N2B–Ni1–N1B	82.2(4)
O6–B1–O4	111.6(3)	N1A–Ni1–N1A ¹	180.0	N2B–Ni1–N1B ¹	97.8(4)
O1–B2–O2	121.0(5)	N1A ¹ –Ni1–N3A	89.1(3)	N2B ¹ –Ni1–N1B ¹	82.2(4)
O7–B2–O1	122.4(6)	N1A ¹ –Ni1–N3A ¹	90.9(3)	N2B ¹ –Ni1–N1B	97.8(4)
O7–B2–O2	116.6(5)	N1A–Ni1–N3A ¹	89.1(3)	N2B ¹ –Ni1–N2B	180.0
O3–B3–O2	121.0(5)	N1A–Ni1–N3A	90.9(3)	N2B ¹ –Ni1–N3B	99.5(4)
				N2B ¹ –Ni1–N3B ¹	80.5(4)